UNIVERSITY OF NOTTINGHAM

Department of Civil Engineering

Unbound Pavement Materials and Analytical Design

by

Michael Mundy B.E. (Hons), B.Sc.

Thesis submitted to the University of Nottingham, U.K.
for the degree of Doctor of Philosophy

July 2002

"The question is not whether you agree or disagree with someone's' point of view, but whether it provides food for thought"

Michael Mundy, 2000

CONTENTS

ABSTRACT

Increasing constraints on infrastructure construction and maintenance budgets are causing road authorities to seek greater efficiencies in the design of road pavements. As a result, there is a continuing requirement for the more efficient use of materials and the application of cost-effective design methods which accurately model predicted vehicle loadings and state conditions.

Many analytical pavement design modelling procedures have remained virtually unchanged since their inception in the late 1980s. Improved analytical modelling of pavements is now seen as a priority in order to accurately calculate critical stresses and strains and thereby reduce the likelihood of poor pavement performance. The procedure should require designers to adequately examine the dependence of a material's performance linked to *in-situ* state conditions, particularly moisture saturation levels, and apply sound mechanistic modelling principals. It was found that virtually all the methods used around the world did not achieve this. As a result, key factors have been highlighted which should be incorporated in a new design procedure.

The research study clearly illustrates the influence of the controlling parameters (resilient modulus, permanent strain rate, shear strength, permeability, durability) and properties that affect the successful use of granular materials in flexible pavements. The extensive use of functional performance-based testing has allowed limiting values to be established for the controlling parameters, which has lead to the development of a proposed performance-based specification for the supply of unbound granular materials. Following an extensive materials characterisation program, a set of outcomes is specified which will aid in optimising the performance of unbound granular materials. In addition, a new system has been developed to classify the shear strength of a material to determine its suitability for use within a pavement layer.

A wide range of pavements, subjected to applied design standard axle traffic loadings, have been modelled in order to derive a stress locus which encompassed all stress combinations expected within the UGMs of any loaded pavement configuration. From this information, the Author has derived a new set of stress conditions that can be applied to the RLT test to determine moduli for design purposes. The benefits of the new stress levels include their separation into those encountered in basecourse (high quality material) and sub-base/fill (marginal/poor quality material) layers. In addition, the test sequence employs small stress increments to improve the continuity of modulus test results for graphical presentation or modelling purposes. On applying the new stress sequence to testing a material, it was found that the variation in resilient modulus for repeat testing was 4% or less for the basecourse stress sequence.

Given that granular materials are most stress dependent, materials must be assessed at stress conditions representative of those *in-situ*, under applied design traffic loadings. This is particularly important given that resilient modulus and permanent strain rate are very sensitive to the applied stress conditions experienced by a material element (ie, stress-dependent).

Case studies, examining the use of a range of unbound granular materials in various pavements, are presented as a means of establishing performance relationships between laboratory assessment and observed and measured performance of existing pavements. From these studies it appears that relationships *do* exist between key material performance indicators, MPIs (resilient modulus, permanent strain rate and shear strength parameters) measured from laboratory RLT test results and observed field pavement performance (stiffness and deflection curvature).

This study's developments should provide engineers with increased confidence in the ability to characterise material quality and determine layer suitability. It is expected that a more structured approach to material assessment and pavement design, will provide the basis for guiding the designer through a decision-making process, with a clear level of risk determined at the conclusion of the assessment. This should allow

alternative materials to be more widely trialed for use in pavements with clear environmental benefits.

PREFACE

The work presented in this thesis draws largely on the Author's technical work, performed since 1989, when Transport SA undertook studies into the performance assessment of unbound granular materials to diagnose the possible causes associated with their lack of field performance when used in several major road construction projects.

An extensive study was established under the Agency's Materials Technology Research and Development (MTRD) program, MTRD 8. Under this program, the Author developed RLT equipment specifications and testing procedures for use initially by laboratory staff and broadened them to practitioner application. Others were to contribute at a later stage, through a national working committee, in order to advance the development of the documents into national standards. From the Author's initial equipment specification was developed the first commercial RLT system for Australian pavement materials research.

Another study program aimed at materials characterisation was devised with the Author undertaking all of the initial testing activities associated with MTRD 16, Stage 1 to ensure that techniques were adopted which provided the level of repeatability aimed for. Without this, it was seen as little value to embark on a substantial and relatively costly characterisation program to "rank" the materials in terms of perceived quality. Once these techniques had been 'perfected' for Stage 1 and 2 using two different crushed rock materials, the Author took more of an operator training, data analysis, testing management and technical advisory role to monitor the work of the 'new' testing operators and provide a service to clients. Before the 'hand-over phase' of the project to these 'new' operators, the Author wrote a number of work instructions to supplement the test procedure. These documents assisted in the training role provided by the Author to ensure results of consistent quality were produced by different operators. The MTRD series of reports written by the Author, MTRD 16-1 to 3 were subsequently published by Transport

SA and distributed widely to Stakeholders (State Road Authorities, Universities, ARRB and private Organisations, both nationally and overseas).

The Author also initiated a project, MTRD 79, which was aimed at incorporating the test data derived from the MTRD 16 materials study into mechanistic pavement modelling in order to develop an improved design procedure. This report has been distributed nationally and internationally and has been widely used for training purposes.

Finally, within the MTRD 66 project, the Author has developed the equipment, test procedure and material evaluation for resilient modulus determination of subgrade materials.

LIST OF TABLES

LIST OF FIGURES

Figure **Description**

ACKNOWLEDGEMENTS

The Author wishes to acknowledge the assistance of the professional and technical staff within Transport SA, ARRB TR and other State Road Authorities who either contributed to the work at the national level or assisted with the provision of some data referred to in the research. Bob Andrews and Mike Butcher of Transport SA for their support and interest in pavement materials and the pursuit of 'best practice'. To Rodney Brimble, Neville Gray, Daryl Chatfield and Doug Wright for their commitment toward quality materials testing.

Gratitude is also expressed toward the University of Nottingham, which has greatly encouraged and supported this research, and in particular to Andrew Dawson, Prof. Stephen Brown and Dr Ban Seng Choo. To Andrew especially, I thank you for providing the opportunity for myself to travel to the United Kingdom and Europe to project manage the COURAGE project and for sharing together our experiences of research and life in general. His and Steve Brown's passion for this field of engineering has helped to maintain its momentum within the European Community. Thanks also to the COURAGE team members, from many different countries, for their professionalism and dedication toward their research and support of myself and family during our stay in Europe in 1999. Also, sincere gratitude is expressed toward John Statton and Paul Taylor for their encouragement prior to, and during, our venture to Europe.

To my family, Ingrid, Michaela and Stefan, thank you for your tolerance and understanding whilst I worked through such a large work-project. To my parents Grantley and Margaret, I thank you for the importance you have placed on educating the mind.

ABBREVIATIONS

AADT	Annual Average Daily Traffic
A/C	Asphaltic Concrete
AIM	Asphalt Institute Method
AMADEUS	Advanced Models for Analytical Design of European Pavement Structures
APRG	Austroads Pavement Reference Group (formerly the Australian Pavement Research Group)
AASHO	American Association of State Highway Officials
AASHTO	American Association of State Highway and Transportation Officials
AUSTROADS	Association of Australian and New Zealand Road Transport and Traffic Authorities
AWGRU	Australian Working Group of Repeated load triaxial Users
BISAR	BItumen Stress Analysis in Roads
BST	Bituminous Surface Treatment
CAM	Coefficient of Aggressiveness
CBR	Californian Bearing Ratio
CCP	Constant Confining Pressure
CEN	European Committee for Standardisation
Ch.	Chainage
COST	COoperation in Science and Technology
COURAGE	COnstruction with Unbound Road AGgregates in Europe
C/R	Crushed Rock
CRB	Crushed Rock Base
CSIRO	Commonwealth Scientific and Industrial Research Organisation
CTQR	Cement Treated Quarry Rubble
DDR	Dry Density Ratio
DoT-Tas	Department of Transport - Tasmania
EC	European Commission

EF	Equivalence Factor for equating pavement damage from one load system to another
E_qF	Equivalence Factor for equating layers of different pavement materials
ESA	Equivalent Standard Axle
ESALs	Equivalent Standard Axle Loadings
FWD	Falling Weight Deflectometer
GAM	Gross Axle Mass
GVM	Gross Vehicle Mass
HA	Highway Agency
IAM	Individual Axle Mass
IST	Instituto Superior Téchnico, Portugal
LA	Los Angeles abrasion
LCPC	Laboratoire Central des Ponts et Chausées (Nantes, France)
LVDT	Linear Variable Differential Transducer
MC	Moisture Content
MDD	Maximum Dry Density
MM	Maintenance Marker
MPI	Material Performance Indicator
MRD-WA	Main Roads Department – Western Australia
MSWI	Municipal Solid Waste Incineration ash
MTRD	Materials Technology Research and Development
$N_{10\,(20)}$	predicted ten (or twenty)-year design traffic loading of ESAs
NAASRA	National Association of Australian State Road Authorities
NE	Number of Equivalent Axles (French)
NRA	National Roads Authority (Ireland)
OGFC	Open Graded Friction Course asphalt
OMC	Optimum Moisture Content
PM	Pavement Material
PRA	Public Roads Administration (Iceland)
Q/R	Quarry Rubble
RLT	Repeated Load Triaxial
RMC	Relative Moisture Content

RRD	Road Running Distance
RTD	Road Transport Development
SAMI	Strain Alleviating Membrane Interlayer
S/G	Subgrade
SHRP	Strategic Highway Research Programme
SPDM	Shell Pavement Design Manual
SRA	(Australian) State Road Authorities
STXL	Static Triaxial
TDR	Time Domain Reflectometry
TSA	Transport SA (South Australia, Australia), formerly Department of Road Transport
UGM	Unbound Granular Material
UK	United Kingdom
UMATTA	Unbound Materials Testing Apparatus
USA	United States of America
VCP	Variable Confining Pressure
WIM	Weigh In Motion
ZAG	

SYMBOLS

a	radius of plate or loaded area (mm)
a_i	structural layer coefficient of layer I
a_2	base coefficient
a_3	sub-base coefficient
A	aggressiveness of an axle or coefficient
A_1	permanent strain rate parameter
A_{1c}	characteristic permanent strain rate parameter
B	parameter or coefficient or pressure cell thickness (mm)
c	cohesion (kPa)
C	pressure cell aspect ratio
Cr	pressure cell registration ratio
CV	Coefficient of Variation
d	diameter of pressure cell diaphragm (mm)
d_{max}	maximum surface deflection
D	diameter of pressure cell (mm)
D_i	thickness of layer i
D_o	central deflection (mm)
D_{200}	deflection at a horizontal distance of 200mm from the central deflection (mm)
E	elastic modulus or modulus of elasticity (MPa)
E_{calc}	calculated modulus of elasticity, assuming linearity and isotropy, determined from measured stresses and computed strains (MPa)
E_{meas}	measured modulus of elasticity, assuming linearity and isotropy, determined from measured stresses and measured strains (MPa)
E_{BS}	elastic modulus of base (MPa)
E_h	horizontal resilient modulus (MPa)
E_N	elastic modulus of alternative material (MPa)
E_qF	equivalency factor
E_r	resilient modulus (MPa)
E_S	elastic modulus of subgrade (MPa)

E_{SB}	elastic modulus of sub-base (MPa)
$E_{subgrade}$	elastic modulus at the top of the subgrade (MPa)
$E_{top\ of\ base}$	elastic modulus at the top of the base layer (MPa)
E_v	vertical resilient modulus (MPa)
E_2	elastic modulus of the unbound layer (MPa)
E_3	elastic modulus of the subgrade (MPa)
$F_{dynamic}$	dynamic force imparted by a vibratory roller (kN)
G_a	Boyce parameter
G_s	specific gravity
h_2	thickness of the unbound layer
I_θ	influence factor for vertical stress determination under a pressure pad
k	coefficient of permeability (m/s)
k_1	material model constant
k_2	material model exponent
K	factor which accounts for the axle type
K_a	active earth pressure coefficient or Boyce parameter
K_o	earth pressure coefficient, at rest value
K_{or}	lateral earth pressure coefficient considered as residual stress
K_p	passive earth pressure coefficient
n	Boyce parameter
N	number of pavement sub-layers
N	number of cycles
N_{ESA}	Number of design ESAs
P	axle load considered or total wheel load (kN)
P_o	reference isolated axle load (if distance to next axle is greater than 2m)
p	mean normal stress (kPa)
p_{max}	maximum mean normal stress (kPa)
p	uniform pressure (kPa)
q	deviatoric stress or pressure in cell liquid (kPa)
$\frac{q}{p}$	stress ratio
r	radius of applied surface load or radial distance from the centre of the plate (mm)

R	modular ratio, being the ratio of the vertical moduli of each pavement sub-layer
s_x	standard deviation
SN	structural number
S_r	degree of saturation (%)
t	thickness of pressure cell diaphragm (mm)
T_N	thickness of alternative material
T_S	thickness of standard (asphalt) material
w	moisture content of material (% by mass)
$\bar{x}$	statistical mean
z	depth into pavement layer (mm)
α	damage power
α	modelling coefficient for describing permanent deformation behaviour
Δq	change in deviatoric stress or pressure in cell liquid (kPa)
$\frac{d\varepsilon_{1p}}{dN}$	permanent strain rate parameter (% / cycle)
ε_v	horizontal tensile strain
ε_p	permanent strain
ε_q	shear strain
ε_t	tensile strain
ε_v	volumetric strain or vertical resilient compressive strain
$\varepsilon_{z,\,ad}$	working vertical compressive strain
$\varepsilon_{1,\,2,\,3}$	principal strains
ε_{1p}	axial permanent strain
$\varepsilon_{1p(100)}$	axial permanent strain after 100 cycles
ε_{1p}*	corrected axial permanent strain after N cycles
ε_{1r}	resilient axial strain
ε_{3r}	resilient lateral strain
γ	unit weight of soil or granular material (kN/m^3)
μ	modelling coefficient for describing permanent deformation behaviour
ν	Poisson's ratio

ν_N	Poisson's ratio of alternative material
ν_s	Poisson's ratio of subgrade
ϕ	angle of shearing resistance or angle of internal friction, commonly referred to as the 'friction angle' (degrees)
ρ_d	dry density of material (kg/m^3)
ρ_w	wet density of material (kg/m^3)
ρ_{water}	density of water = 1000kg/m^3 at 20°C
σ_h	horizontal normal stress (kPa)
σ_{ho}	horizontal at-rest normal stress (kPa)
σ_{hr}	horizontal residual stress (kPa)
$\sigma_{h\ total}$	total unloaded horizontal normal stress (kPa)
σ_n	total normal stress on the failure plane (kPa)
σ_o	mean stress level under loading plate or uniform normal contact stress (kPa)
σ_v	vertical stress (kPa)
$\sigma_{v\ compaction}$	vertical stress due to compaction loading (kPa)
σ_{vo}	vertical overburden or geostatic stress (kPa)
σ_x	lateral stress transverse to the direction of movement of the vehicle (kPa)
σ_y	lateral stress longitudinal to the direction of movement of the vehicle (kPa)
σ_z	vertical stress normal to the pavement surface (kPa)
σ_1	total vertical stress (kPa)
$\sigma_{1\ max}$	maximum principal vertical stress (kPa)
$\sigma_{1\ min}$	minimum principal vertical stress (kPa)
σ_3	lateral or confining stress (kPa)
$\sigma_{3\ max}$	maximum principal lateral stress (kPa)
$\sigma_{3\ min}$	minimum principal lateral stress (kPa)
σ_3/σ_1	inverse stress ratio
τ_f	shear stress at failure or shear strength (kPa)

GLOSSARY OF TERMS

C.F. $= D_0 - D_{200}$ (mm)

DDR $= \frac{\rho_d}{MDD}(\%)$

$E_r = \frac{\Delta(\sigma_1 - \sigma_3)}{\varepsilon_{1r}}$ CCP

$= \frac{(\Delta\sigma_1 - 2\nu\Delta\sigma_3)}{\varepsilon_{1r}}$

$= \frac{(\Delta\sigma_1 - \Delta\sigma_3)(\Delta\sigma_1 + 2\Delta\sigma_3)}{\varepsilon_{1r}(\Delta\sigma_1 + \Delta\sigma_3) - 2\varepsilon_{3r}\Delta\sigma_3}$ VCP

$K_o = 1 - \sin\phi$

$p = \frac{(\sigma_1 + 2\sigma_3)}{3}$ (kPa) for laboratory triaxial condition

$= \frac{(\sigma_x + \sigma_y + \sigma_z)}{3}$ (kPa) for field condition

$q = \sigma_1 - \sigma_3$ (kPa) for laboratory triaxial condition

$= \sigma_z - \frac{(\sigma_x + \sigma_y)}{2}$ (kPa) for field condition

$S_r = \frac{w}{\left(\frac{\rho_{water}}{\rho_d} - \frac{1}{G_s}\right)}$ (%)

$\nu_r = \frac{-\varepsilon_{3r}}{\varepsilon_{1r}}$ CCP

$= \frac{(\Delta\sigma_1\varepsilon_{3r} - \Delta\sigma_3\varepsilon_{1r})}{(2\Delta\sigma_3\varepsilon_{3r} - \varepsilon_{1r}\Delta(\sigma_1 + \sigma_3))}$ VCP

$\varepsilon_{1p}^* = \varepsilon_{1\,p} - \varepsilon_{1\,p\,(100)}$

$\varepsilon_{1r} = \frac{(\Delta\sigma_1 - 2\nu\Delta\sigma_3)}{E_r}$ VCP

$\varepsilon_{3r} = \frac{(\Delta\sigma_3(1-\nu) - \nu\Delta\sigma_1)}{E_r}$ VCP

$$\rho_d = \frac{\rho_w}{1 + \frac{w}{100}} \ (kg/m^3)$$

$\Delta\sigma_1 = \sigma_{1\,max} - \sigma_{1\,min}$

$\Delta\sigma_3 = \sigma_{3\,max} - \sigma_{3\,min}$

CHAPTER 1
INTRODUCTION

The strong need for roads has been apparent right back to the days of the Romans, where the road network was developed to support trade and travel, in addition to enabling soldiers to be transported across the countryside to defend the Empire.

The Romans built over 85,000km of roads across their Empire - 8,000km in Britain alone. The Romans built their road network with the following considerations. The roads:

- generally took the shortest, straightest route between two places
- were built to move troops quickly
- were used to encourage trade and allowed the spread of new ideas and fashions to all parts of the Empire
- made it easier to collect taxes

These considerations are still very important in today's society. The Roman's recognised that the fundamentals of good road construction were to provide good drainage, quality materials and workmanship. The early Roman roads (see Figure 1.1) generally consisted of four layers of materials overlying the natural soil, viz:

- stone slabs - wearing course layer
- crushed stone - base layer
- stone blocks made of cement - sub-base layer
- sand layer - levelling layer

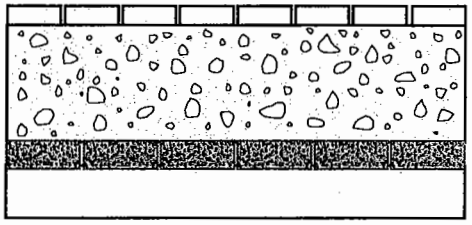

FIGURE 1.1: CROSS-SECTION OF AN EARLY ROMAN PAVEMENT

Information source: Ancient Romans Display, British Museum, London (1999)

Today's flexible pavements are also multi-layered systems often comprising an asphaltic concrete surfacing, an unbound granular or bituminous bound base and an unbound granular sub-base. These pavements necessitate using high quality materials in the upper part of the structure where stress intensities from applied wheel loads are high. Materials are selected based upon their engineering properties to suit *in-situ* conditions, due to both traffic and climate.

Roads are an essential part of modern everyday life, since they provide a platform for freight haulage in addition to satisfying the diverse range of business and recreational commuting needs. The road network has enormous economic and social impact, generates substantial employment and contributes significantly to Gross Domestic Product (GDP).

The design of pavement structures must take into account the many uncertainties that exist. Some of these include predicting traffic volumes (present, future and their distributions, day and night), varying vehicle axle mass configurations, constituent material properties, seasonal effects (which may cause variation in *in-situ* conditions such as moisture content and freeze/thaw periods) and drainage ability. The design of roads has not been one of engineering's exact sciences, having been more an "art", principally based on a designer's experience and knowledge. A principal means to improvement is by developing a more scientific understanding of the materials by which some of the inefficiencies of empiricism could be addressed.

The economic importance of roads worldwide could largely be linked to the reliance of the freight industry on a highly productive network that can deliver to the depot or the retail door. The quantities of freight goods transported by road are compared with rail to illustrate the proportional level of use of the two asset networks (see Table 1.1).

The data in Table 1.1 illustrate that the road network carries between 1.5 to just over 3 times the quantity of freight transported by rail in Germany, France and Australia. For the United Kingdom, however, the factor is as high as nearly 11.

Country	Road Freight (tonnes-km) [3]	Road Freight (% of all freight modes)	Rail Freight (tonnes-km) [3]	Rail Freight (% of all freight modes)	Ratio Road : Rail
Germany [1]	216 billion	64	70 billion	17	3.1
UK [1]	152 billion	65	14 billion	7	10.9
France [1]	122 billion	63	49 billion	25	2.5
Australia [2]	119 billion	34	81 billion	23	1.5

TABLE 1.1: QUANTITIES OF FREIGHT TRANSPORTED BY ROAD IN SELECTED COUNTRIES

(1) Figures at 1994, Reference: ECMT, 1998
(2) Figures at 1995, Reference: ABS, 2000
(3) Total tonne-kilometres are the product of the reported average load and total business kilometres travelled while laden

The road system in Australia alone consists of 800,000km of public roads from unformed tracks to local roads, arterials, highways and major freeways. The total value of the network, including land, is reported to be more than $AUD100 billion (Austroads, 2000) or circa £40 billion.

1.1 Pavement Structures

Pavements are designed and constructed to carry a range of vehicular traffic types and volumes.

A pavement is a multi-layer structure (see Figure 1.2) composed of a surfacing layer (composing the wearing course and/or levelling course and a bonding layer [1] (usually a bituminous chip seal), base layer, sub-base layer and capping or 'select fill' layer. The natural foundation upon which the pavement is constructed is referred to as the subgrade, which may in itself be layered due to material or moisture variations.

The surfacing layer provides a smooth riding surface, adequate resistance to skidding of vehicular traffic and low tyre noise. In addition, it is a means to suppress dust (thereby preventing loss of fines) and provide drainage of surface water to the side drains of a properly cambered road. This 'layer' may actually consist of two separate layers in some pavements, namely a wearing course and a levelling (or intermediate) course. In both cases the material used is normally asphalt. The levelling course is

[1] bonding layer consists of a primer seal, which penetrates into the top of the granular material basecourse, followed by a further spray application of bitumen binder and bituminous chip seal subsequently rolled in. This layer allows subsequent asphaltic layers to bond to it as a result of the

sometimes used directly above the base layer to provide better levelling control before placing the wearing course.

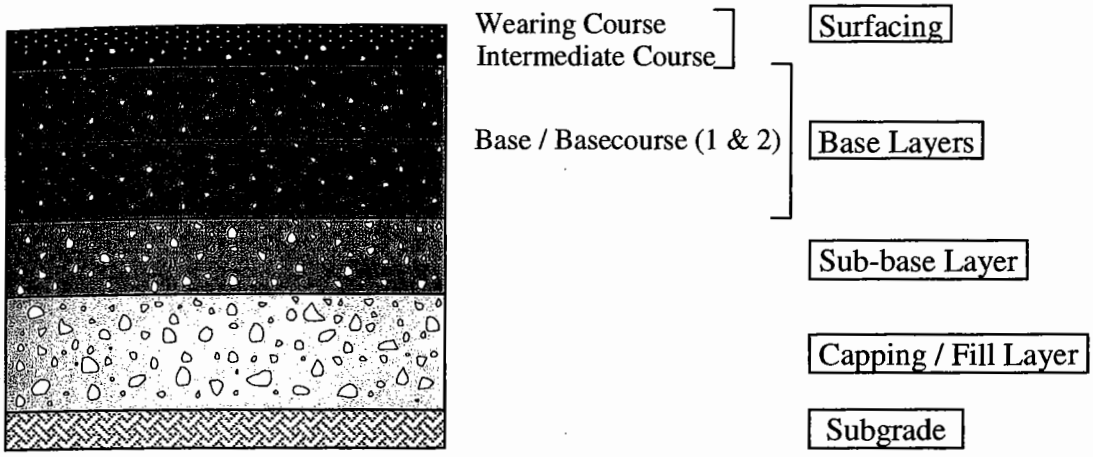

FIGURE 1.2: VIEW OF A GRANULAR PAVEMENT

The base layer is the main structural layer of the pavement, which generally consists of high quality materials, used to distribute the surface wheel loads to the foundation. The sub-base also allows for distribution of wheel loads, albeit to a lesser extent. This layer provides a total pavement thickness such that strain levels experienced at the top of the subgrade, due to surface loadings, are acceptable given the anticipated design life of the pavement. An additional granular layer is often used below the sub-base (directly on top of the subgrade) if the bearing capacity of the subgrade is low. This layer is referred to in Europe as a capping layer, whilst in Australia it may just be termed a select fill material. The capping layer protects the subgrade against frost and establishes a level, stronger foundation upon which construction traffic may move and subsequent pavement layers may be successfully placed and compacted.

1.1.1 Pavement Description and Structural Types in Australia

The pavement structure types, ***employing unbound granular materials***, used in Australia are:

Flexible Pavements: which consist of bituminous spray seal wearing course (for low trafficked or rural roads) or an asphaltic wearing course (typically between 35mm to

rough interface formed.

125mm in thickness) placed upon one or two basecourse layers of unbound granular crushed rock material of between 125mm to 150mm in thickness (see Figure 1.3). This material overlays two or one sub-base layers of unbound quarry rubble granular materials (125 to 150mm thick) giving a total overall thickness of between 300 to 575mm. The difference between crushed rock and quarry rubble products is described in Chapter 8.

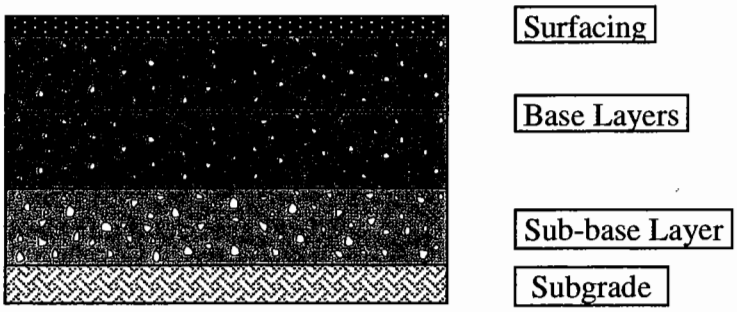

FIGURE 1.3: FLEXIBLE PAVEMENT IN AUSTRALIA

Inverted Pavements: which consist of an asphaltic wearing course placed upon an unbound or semi-bound (with 1-2% for both cement or bitumen binder) granular material of approximately 125mm to 175mm in thickness. This layer in turn rests upon a sub-base layer of materials, generally treated with 4% cement binder (275 to 300mm thick) giving a total overall thickness of between 460 to 575mm. In Australia, these pavements have historically been referred to as "upside-down pavements" as the structurally weaker layer of UGM is placed higher up in the pavement than the strong cement-treated layer (see Figure 1.4).

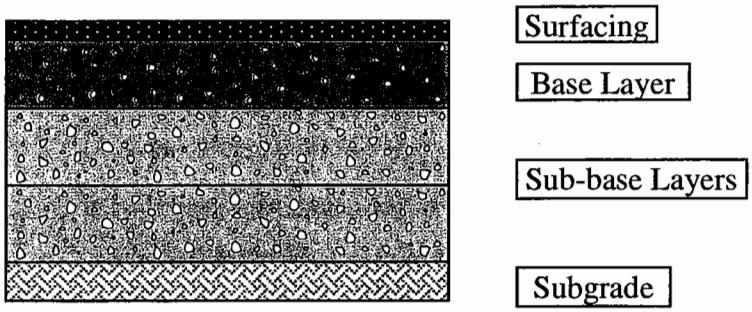

FIGURE 1.4: INVERTED PAVEMENT IN AUSTRALIA

Other pavement types such as fully bound (for example, full depth asphalt) or composite pavements (asphalt and cement-treated materials) are not presented here as discussion is centred around only those containing unbound granular materials.

1.1.2 Pavement Description and Structural Types in Europe

The structural pavement types employing unbound granular materials in Europe are:

Flexible Pavements: which consist of a bituminous surface course, or a surface dressing (on very light traffic pavements) and a base layer of bituminous materials of up to 300mm (on heavily trafficked roads). This material overlays one or more layers of unbound granular materials (150 to 750mm thick) giving a total overall thickness of between 250 to 1000mm (see Figure 1.5).

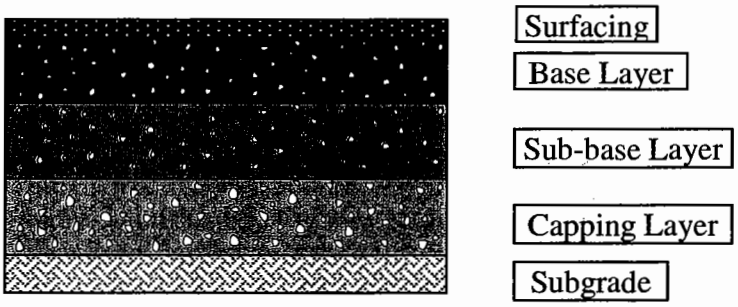

FIGURE 1.5: FLEXIBLE PAVEMENT IN EUROPE

Inverted Pavements: which consist of bituminous surface course and a base layer of bituminous materials of approximately 100mm to 200mm in thickness. This material overlays a layer of unbound granular material of approximately 120mm in thickness. This layer in turn rests upon a sub-base layer of materials treated with hydraulic binders (300 to 500mm thick) giving a total overall thickness of between 600 to 800mm (see Figure 1.6). These pavements are specified in the French Pavement Design Manual (Corte et al, 1997).

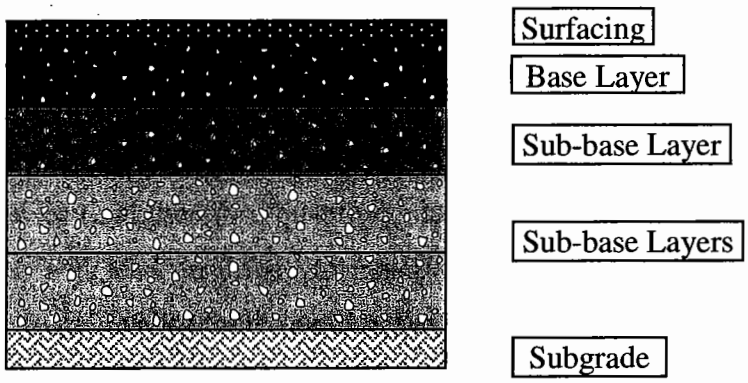

FIGURE 1.6: INVERTED PAVEMENT IN EUROPE

1.2 Pavement Materials

The behaviour of unbound granular materials (UGMs) in the pavement is not well understood and only in relatively recent years (since the 1970s) has any serious research effort been committed to better understanding their properties and performance. It is known that the performance of such materials is strongly influenced by the geological material characteristics and by the *in-situ* conditions which they experience during their life in the pavement structure. Both of these aspects vary widely across many countries due to large geological and environmental variations.

As a result, granular pavement layers have a much less predictable performance than, say, bituminous layers. At the same time, testing methods for aggregates and granular materials have been largely empirically based, only giving indirect indices on which to predict behaviour. While this approach may function reasonably within a local (national) context, the geological and climate factors severely limit the current assessment methods. This is now exacerbated by the increasing need to use waste, recycled and by-product aggregates in road construction for which relevant testing experience, or field performance data, does not exist. These difficulties lead to inefficient and/or unreliable pavements, or to the exclusion of suitable materials due to an adversity to risk-taking. In the latter case, unnecessary quarrying and/or material dumping may occur leading to undesirable environmental impacts.

1.3 Analytical Pavement Design

In most pavement construction projects, the use of aggregates is largely determined by the design of the pavement. The design specifies the quality of the materials to be used and the layer thicknesses (and therefore quantity). Over-design of individual pavement layer thicknesses will lead, in effect, to material wastage. In addition, over-specification of aggregate quality will lead to the wastage of high-grade materials, which should be reserved for more demanding road requirements.

A number of techniques have been used over the years for designing pavements. This information has been well summarised in the European Commission funded **COST 333** and Advanced Models for Analytical Design of European Pavement Structures (or **AMADEUS**) Projects (European Commission, 2000). These projects undertook a comprehensive survey of many European countries to determine the approaches used to design pavements and the sources from which material design data is derived. In addition, a simple design example was presented to each participating country's road agency to investigate the variability in design expected using these wide range of techniques and materials data sources. The results proved to be highly variable in individual layer thicknesses and hence total pavement thickness.

The 'technique' or method used for pavement design over the years has generally been one of the following approaches[2]:

- ***experienced-based*** (or prescription or catalogue) ***methods*** which provide a catalogue of standard designs and materials based on past successful practice. This technique *has been* used in countries such as Singapore where "standard" designs based on Swedish codes of practice have generally been used, as reported by the Singapore Department of Works in 1992. This approach is often best applied when the effects of variation in local materials, layer thicknesses, traffic loadings/volumes and climate is well understood. Pavement failures have often resulted, however, when this approach, established in one locality, has been transferred and applied in another country which may have totally different

[2] Country-by country review by COST 333 project.

conditions (eg, subgrade soils or climate). Alternatively, it may lead to the design of very conservative pavements, which are uneconomical.

- ***empirical methods*** where design is calculated from measured or estimated material properties from laboratory or field testing such as CBR or deflection, and is related to past successful experience. An example of this method is the determination of the total pavement thickness for bituminous surfacing flexible structures, based on subgrade CBR and traffic volume (Austroads, 1996)
- ***mechanistic or analytical or rational methods*** where the response, and subsequent performance, of different pavement types to traffic loadings depends solely on the measured performance properties of the material components which comprise the pavement. This method of analysis relies on the designer selecting a 'trial pavement' cross-section with consideration given to the number and thicknesses of each layer, the material types, material state conditions, material performance properties from laboratory or field tests and estimating load levels throughout the design life. The designer then analyses the stresses and strains caused by the applied traffic loadings on this 'trial pavement' (using a response model) and then determines the 'critical life' for selected layers, based on established performance prediction models. If necessary, the pavement design is then revised and a further iteration of the cycle is conducted.
- ***semi-empirical methods*** use a combination of empirical and mechanistic methods.

It should be remembered that aggregates have to meet specifications to achieve their required performance. Two types of specification generally exist. The one most often used is an **empirical specification**, which utilises the results of laboratory classification test properties and the historical experience gathered from field performance observations or data. The other type is a **performance specification**, based upon laboratory performance-type tests which characterise the materials over a wide range of geological types, loadings and environmental conditions. Again, this specification should assess laboratory characteristics against field performance to ensure appropriate limits are adopted for the chosen parameters. The difference is that the laboratory performance-based tests provide the opportunity to better simulate

expected *in-situ* conditions and investigate the effects of new loadings, materials and climate conditions.

At present, few specifications world-wide for unbound granular materials are truly performance-based, rather being empirically-based, despite the fact that most countries employ some form of mechanistic analysis in their pavement design procedures. Given that pavement material performance data derived from laboratory and/or field testing is critical to the mechanistic design processes mentioned above, it is essential that these properties be measured.

1.4 Overview of Mechanistic Pavement Design Requirements

In order to utilise a mechanistic pavement design technique, which requires the development of a pavement 'response' model for analysing the structure, certain information is required pertaining to the constituent material properties. Linear-elastic modelling requires knowledge of elastic resilient modulus and Poisson's ratio of the constituent pavement and subgrade materials for their given state conditions (of density and moisture content).

It shall be illustrated in §2.4.6 that the resilient modulus of a granular material is functionally very dependent upon the stress state conditions under which it is assessed (hence, it is stress-dependent). This, coupled with the fact that vertical and lateral stresses change rapidly with depth into unbound granular materials (UGMs) beneath thin asphalt surfacings, suggests that each sub-layer of material within the pavement can be characterised by a "unique value of resilient modulus". This value is based upon the average traffic-imposed stress conditions to which it is subjected. Knowledge of the "correct" *in-situ* stresses is also vital for the rational approach to pavement design and diagnostic investigation. The pavement design response models can be used in an iterative sense (see Figure 1.7) until the agreement between the resilient modulus used and the resilient modulus predicted from the calculated stresses is satisfied to within certain tolerances (Mundy, September 1992). This iteration can be achieved manually if simplified procedures are adopted (Mundy, September 1992) or automatically with more advanced non-linear response models,

as constructed using finite element code. The latter generally rely upon more complex material models (and model parameters) to predict resilient modulus and Poisson's ratio.

These models need to model well the resilient axial and radial strains (or volumetric and shear strains) as measured in laboratory testing systems in order to account for non-linearity and material behaviour under varying stress and state conditions. Such material models do exist, such as the Boyce model (Boyce, 1980), but their parameters *must* be determined using quality material data, which is derived by testing at a range of expected *in-situ* conditions and takes into account equipment strain measuring limitations. It has been found, however, that even with complex models used in design, quite low and unrealistic moduli have been determined when used in pavement analysis (Uzan, 1985). "Neither the material model nor the analysis is at fault; it appears that the state of stress prevailing in the field is not re-produced in the analysis"

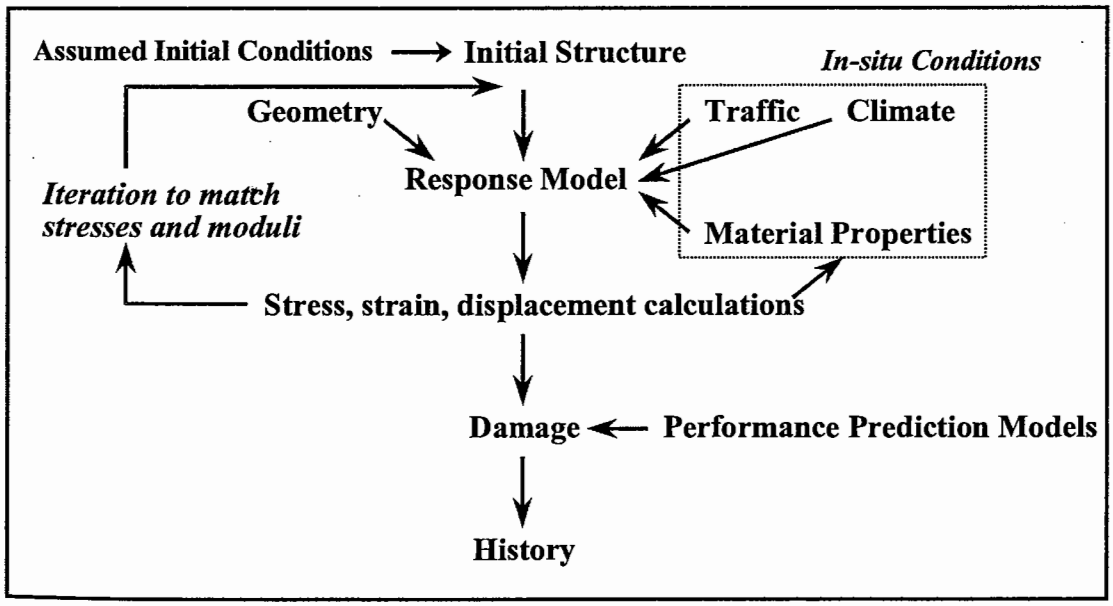

FIGURE 1.7: FLOW CHART OF ITERATIVE PAVEMENT DESIGN PROCEDURE

Thus, three challenges exist:

i)to know the loading, environmental and material conditions *in-situ* within the pavement structure so that laboratory testing may be performed using the same conditions

ii) to measure material response in the laboratory well

iii) to have good quality analytical tools so that *in-situ* performance can be reliably predicted from the laboratory data

Once a harmonised set of resilient modulus values and stresses have been developed, the stresses and strains in the pavement can be calculated and compared to those which are known to be permissible for acceptable pavement performance. Generally, there will be different stress or strain criteria to limit fatigue in bound layers, rutting of different granular layers, localise shear failure, etc.

1.5 Research Aims

The main area for research described here is the study of the properties of pavement materials and their application to analytical pavement design modelling.

A summary of the research aims is to:

(a) highlight the key unbound granular material performance indicators (MPIs) and illustrate the large quantitative variations which can result within each by testing the materials under a range of state and property conditions (such as density, moisture, grading, shape, etc).

(b) examine the shortcomings in current knowledge and design practice concerning UGMs and identify improvements to incorporate in analytical pavement design methodologies. A select number of methods from various countries shall be used for this study.

(c) determine, theoretically, stress regimes expected to be experienced by UGMs in a wide range of flexible pavement types, subjected to applied design standard axle traffic loadings.

(d) compare the theoretically computed stress regimes with the results of any practical field studies.

(e) recommend a newly proposed shear strength classification system for UGMs located beneath thinly surfaced (< 40mm) bituminous layers as means of controlling permanent deformation (and hence rut) development.

(f) recommend changes to repeated load triaxial testing stresses levels and sequences for UGMs of varying quality such that they be more closely

aligned with pavement generated stresses, resulting from applied standard axle loadings.

(g) recommend changes to existing RLT testing procedures, based upon research undertaken, in order to achieve repeatable design parameters over a targeted range of predicted *in-situ* stress conditions.

(h) critically examine the performance of a number of materials tested under a range of state conditions (of density and moisture content), as would be experienced *in-situ*. Suggest limits for key material performance indicators (MPIs) determined from the materials tested, which could in turn be embodied in a proposed performance-based specification.

(i) demonstrate the applicability and value of the improvements by highlighting the relationships which do exist between key material performance indicators (measured from laboratory RLT tests) and observed / measured field pavement performance.

1.6 Contents of Thesis

This thesis contains a further nine technical Chapters which investigate the behaviour of unbound granular materials, as assessed through laboratory performance-based testing, and examines a number of existing pavement structures which have been assessed for condition both visually and through non-destructive testing to establish whether relationships exist between the two. In addition, a Chapter discussing the conclusions of this study and another Chapter presenting further work which should be undertaken to further progress the alignment of testing, design and field performance assessment are presented.

Chapter 2 proposes that material performance can be assessed in the laboratory using both repeated load and static triaxial testing by looking at 'key' material performance indicators (MPIs) as proposed by the Author. The influence that material properties and *in-situ* conditions (climate and traffic based) have upon the MPIs is discussed.

Chapter 3 reviews a select group of existing design procedures for pavements with thick UGM layers in order to highlight the limitations of current design practice, particularly after considering the findings of Chapter 2. Methods and approaches

used in a select range of countries, such as America, Australia, UK, France and Sweden. As a result of this study, subsequent improvements to analytical pavement design methods are proposed at the conclusion of Chapter 3. These recommendations are used to feed back into design practice.

In order to recommend changes to repeated load triaxial testing stress levels and sequences for varying quality UGMs, such that they be more closely aligned with pavement generated stresses, Chapter 4 will investigate research studies undertaken world-wide to practically measure stress levels within unbound granular material pavement layers.

Chapter 5 provides a theoretical study of *in-situ* pavement stress conditions to determine stress regimes experienced by UGMs in a range of different flexible pavement types and utilising varying material quality performance properties. The effect of non-linearity is clearly shown for thinly surfaced pavements, which has a direct impact on how these types of pavements should be modelled analytically. Additionally, since repeated load triaxial testing is now becoming more widely used as a tool to assess the performance of unbound granular materials (UGMs), with the view to 'ranking' materials and providing data for pavement design, this study also reviews a range of testing procedures used.

Having determined the likely range of *in-situ* pavement stress conditions experienced by UGMs in a range of different flexible pavement types, and hence, the stress regimes, Chapter 6 reviews the stress levels and sequences applied in current testing procedures. This Chapter also provides a discussion of the development of the RLT test equipment and associated procedure, highlighting the effort of the Author. Finally, some key aspects of material modelling are presented.

Chapter 7 discusses a test program for the characterisation of materials to enable laboratory-based performance indicators of resilient modulus and strain rate to be determined. In addition, some data is analysed to examine the statistical variations of these MPIs, which could be expected from testing and how they conform to generally accepted limits. A limited number of practical tests were performed, using

the new modified test procedure proposed, in order to demonstrate the improvements consequent upon the recommendations of Chapter 6.

A detailed analysis of a range of materials tested in a laboratory based test program, as proposed in Chapter 7, will be developed in Chapter 8. It is anticipated that materials could be successfully placed in one of the quality 'Class' categories proposed by the Author, depending on their state conditions. To achieve this, the materials will be performed assessed according to proposed limits based on four of the critical MPIs.

In Chapter 9 it will be discussed how the results of this work could be translated into improved practice in the form of a 'performance-based specification' and by use of Clauses within Pavement Construction (road-builder) Specifications.

Next, a number of case studies will be discussed in Chapter 10 to highlight the merits of functional-type testing to characterise constituent pavement materials according to their field state and stress range conditions. It is anticipated that the value of laboratory-based performance testing will be strengthened by highlighting the relationships that are expected to exist between key material performance indicators (measured from laboratory RLT tests) and observed / measured field pavement performance.

Finally, the conclusions (Chapter 11) and suggestions for further work (Chapter 12) are given.

CHAPTER 2
BACKGROUND TO MATERIAL BEHAVIOUR

2.1 Introduction

The performance of UGMs is most critical for moderately trafficked, thinly surfaced pavements. Here the materials range from being highly stressed at the top of the base layer to low stress levels much deeper into the structure. The principal concerns to designers are ensuring that the materials possess adequate resistance to permanent deformation (to minimise rutting) and exhibit satisfactory levels of stiffness when loaded. Adequate stiffness will ensure that tensile strains in the surfacing layer are at acceptable levels to resist tensile fatigue and that good load spreading to the foundation layers occurs (to minimise vertical compressive strains at the surface of the subgrade).

This Chapter provides a discussion concerning what the Author considers are critical material performance indicators (MPIs) which are directly linked to pavement performance resulting from *loaded* pavement structures. In turn the MPIs are influenced strongly by the material properties themselves, of which some of the more important properties will be discussed.

2.2 Performance Tests

2.2.1 Repeated Load Triaxial Test

This test is used to characterise pavement material behaviour in terms of permanent deformation and resilient modulus. The repeated load triaxial (RLT) test closely resembles the loading experienced in an unbound material under traffic loading. The test is conducted on a cylindrical specimen 'element' of material. The vertical load is dynamically applied, with a magnitude to represent the vertical traffic load. A uniformly distributed pressure is applied to the curved surface of the cylinder. It represents the horizontal compressive stresses induced by the restraint that the remainder of the pavement structure applied to the attempted horizontal expansion of the cylinder under the vertically applied load.

2.2.2 Static Triaxial Test

This test is used to determine the resistance to shear of a material under stress conditions likely to be experienced by the material *in-situ* within the pavement. The static peak (or failure) stress is determined for different confining stresses which cover a range expected within the granular material of the loaded pavement structure. The static triaxial (STXL) test can be used to determine the Mohr-Coulomb failure envelope for the resulting Mohr's circles, from which the material's cohesion and angle of shearing resistance can be determined.

2.3 Key Material Performance Indicators

Performance related properties of unbound granular materials require that the materials have an ability to withstand imposed traffic loading conditions whilst the materials operate under a range of environmental conditions during their service life.

The key MPIs which directly influence material, and consequently pavement behaviour, are resilient modulus, permanent deformation (or strain rate), durability, permeability, cohesion and angle of shearing resistance. These MPIs need to be established in relation to a materials' predicted state conditions (density, moisture content, grading, etc) under the imposed traffic loading regime and the influence of local climate conditions (refer to Figure 2.1).

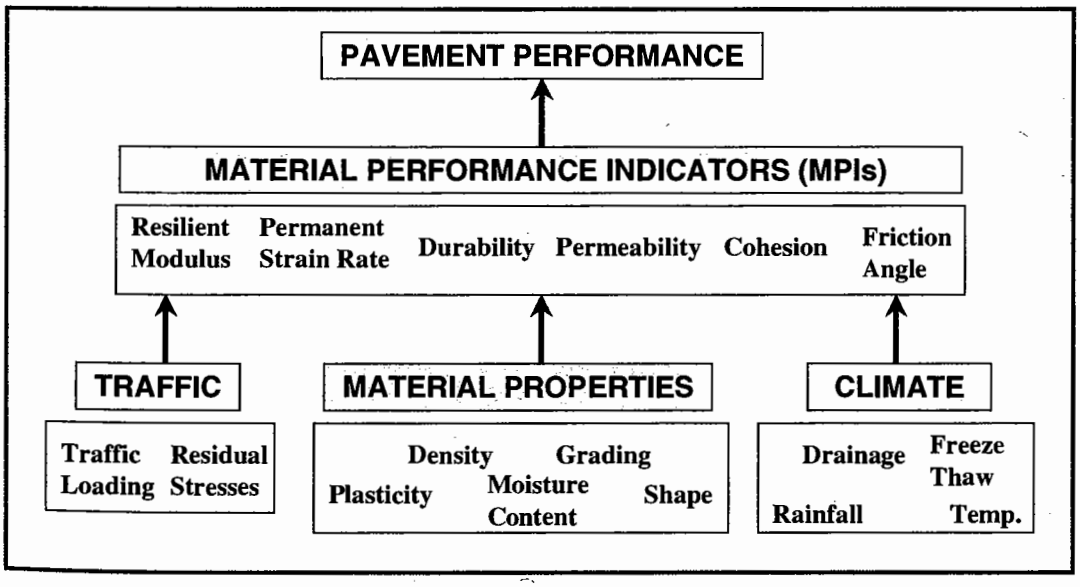

FIGURE 2.1: COMPONENTS WHICH EFFECT PAVEMENT PERFORMANCE

2.3.1 Resilient Modulus

Resilient modulus, E_r , is defined as the ratio of the applied vertical deviator or dynamic stress divided by the recoverable (reversible or elastic unloading) vertical strain, ε_{1r} , measured as a result of the applied stress.

By definition for constant confining pressure tests,

$$E_r = \frac{\Delta(\sigma_1 - \sigma_3)}{\varepsilon_{1r}} \quad \ldots (2.1)$$

This parameter needs to be determined for analytical structural modelling purposes. Satisfactory levels of resilient modulus are required for materials used in pavement sub-layers within a given pavement configuration in order to reduce strains imposed by traffic loadings in not only the overlying and underlying material layers, but also in the granular layer itself.

Unbound granular materials of higher quality with higher resilient modulus levels (for any given stress condition) tend to work more effectively in distributing vertical stresses over a broader plan area within a loaded pavement structure. The "bridging" effect reduces vertical elastic compressive strains deeper within the pavement materials and subgrade directly under the load (see Figure 2.2).

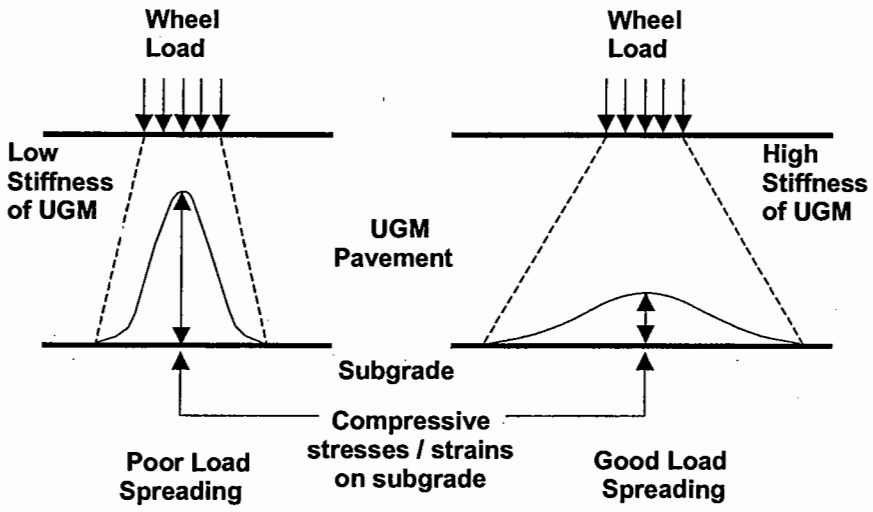

FIGURE 2.2: LOAD SPREADING ABILITY OF UGMS

This action has been verified by load transmission tests (Herner, 1955) where materials of different quality were used as a 'standard thickness' layer within a loaded pavement. Stress levels measured at the base of the layer varied greatly, depending on the geological nature, grading and quality of the UGM used. This study is reported in much greater detail in §4.3.2.3.

2.3.2 Permanent Strain / Strain Rate

A material's susceptibility to deformation or rutting in a pavement layer needs to be assessed for a given pavement configuration which results from imposed traffic loadings. Under loading, permanent deformations can result from slippage between particles and rotation as well as from crushing and attrition of particles. The concept of Permanent Strain Rate and its moisture dependence was introduced by the Author in MTRD Report 79-1 (Mundy, September 1992). The parameter is derived by modelling a permanent strain curve, derived from a RLT preconditioning test. An example of a permanent strain curve for a 20mm crushed rock material is illustrated in Figure 2.3. The material tested had a dry density ratio (DDR) of 98% and a relative moisture content (RMC) to optimum of 80%.

Here the permanent strain varies with the number of applied cyclic loads of deviatoric stress. This curve may be derived from RLT testing at select conditions of stress state, density and moisture content. The first 100 cycles of the test are ignored in the curve modelling process. This is due to the 'erratic' nature of the strains in these early cycles, termed 'initial bedding strain errors', which may result as the end platens incrementally bed into the specimen. This effect can be reduced by carefully controlling the preparation of the specimen ends upon compaction (refer to §7.2.2.2). The curvature of a permanent strain graph, after initial bedding strains are removed from the analysis, tends to be somewhat 'characteristic' for given material and stress conditions. This fact shall be highlighted when the modelled permanent strain curves are used to derive a strain rate, which has a strong dependence upon material conditions, especially moisture content. The Author refers the reader to the results presented in Chapter 8 for a range of materials tested under varying state conditions.

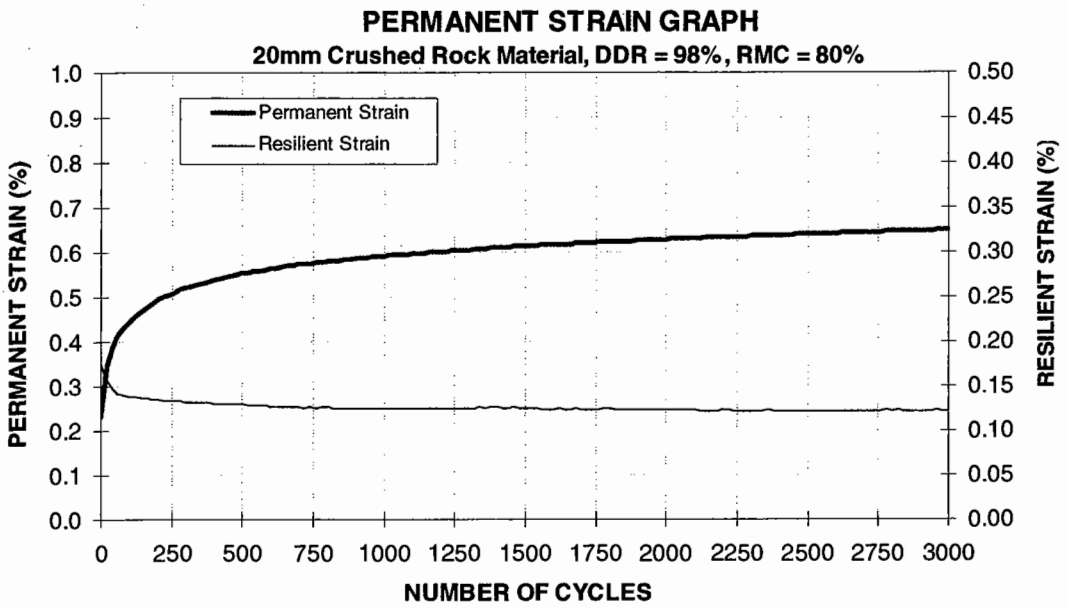

FIGURE 2.3: PERMANENT STRAIN CURVE FOR AN UGM

The permanent strain model was first used in 'VESYS' (Monismith, 1973 and Barksdale, 1972) to characterise granular materials. The model has the form:

$$\varepsilon_{1p}(N,\sigma_1,\sigma_3) = \varepsilon_{1r}\frac{\mu}{\alpha}N^{\alpha} \qquad \ldots (2.2)$$

where:

μ and α = model parameters
ε_{1p} = axial permanent strain (%)
ε_{1r} = axial resilient strain (%)
N = number of cycles

The model parameters can be derived by performing a regression analysis of $\ln \varepsilon_p$ against ln N. To illustrate the visual fit of the modelled permanent strain data with the measured permanent strains, the Author uses the constants of α and μ in Equation 2.2. An example of the matching of the permanent strains is shown in Figure 2.4.

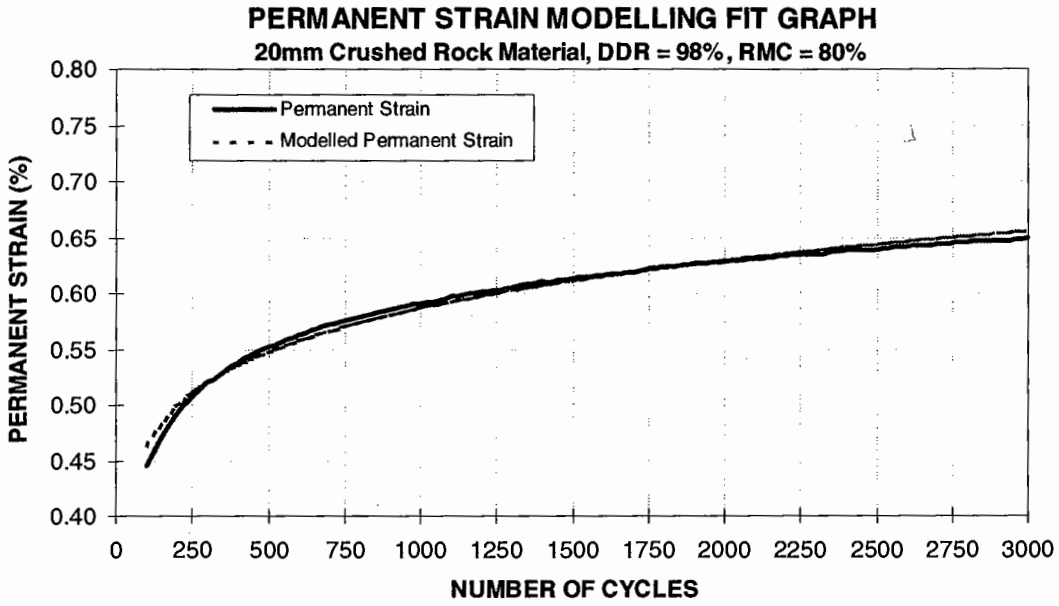

FIGURE 2.4: MODELLED PERMANENT STRAIN CURVE FOR AN UGM

Taking the derivative of the model in Equation 2.2, with respect to the number of cycles, yields the rate of permanent strain parameter at a selected cycle number (Mundy, September 1992). The permanent strain rate parameter has the general form:

$$\frac{d\varepsilon_{1p}}{dN}(N,\sigma_1,\sigma_3) = \varepsilon_{1r}\mu N^{\alpha-1} \quad \ldots (2.3)$$

where: $\frac{d\varepsilon_{1p}}{dN}$ = permanent strain rate parameter (% / cycle)

A great deal of work has been performed by the Author (Mundy, Sept. 1994 and subsequent MTRD16 Reports) in determining the permanent strain rate parameter versus RMC for a range of different materials. Some of this work is presented in Chapters 7 and 8. The parameter has been derived at the 3000th cycle of a permanent strain preconditioning RLT test and for a specific stress combination of dynamic vertical stress, $\sigma_{1\,max}$ = 300kPa / $\sigma_{1\,min}$ = 0kPa and constant static confining stress, $\sigma_{3\,max}$ = 50kPa / $\sigma_{3\,min}$ = 50kPa. This stress condition is applicable to an approximate basecourse layer stress level (at depth of approximately 110mm) beneath a thinly surfaced (35mm) asphaltic pavement (refer to Figure 5.7). Although, the test confining stress is a little higher than could be expected in order to avoid excessive shear stress developing within the material. An example of the strain rate results for

a crushed rock material, tested at a range of moisture contents relative to optimum and three different density levels, is given in Figure 2.5. The moisture levels cover those which could be expected *in-situ* over the life of the pavement, whilst the density levels reflect a range varying from a sub-base specification density of DDR = 96% to that of a highly compacted basecourse material at DDR = 100%. The results of this testing indicate that the material is much more susceptible to permanent deformation at the low density level, whilst the other two densities show similar performance.

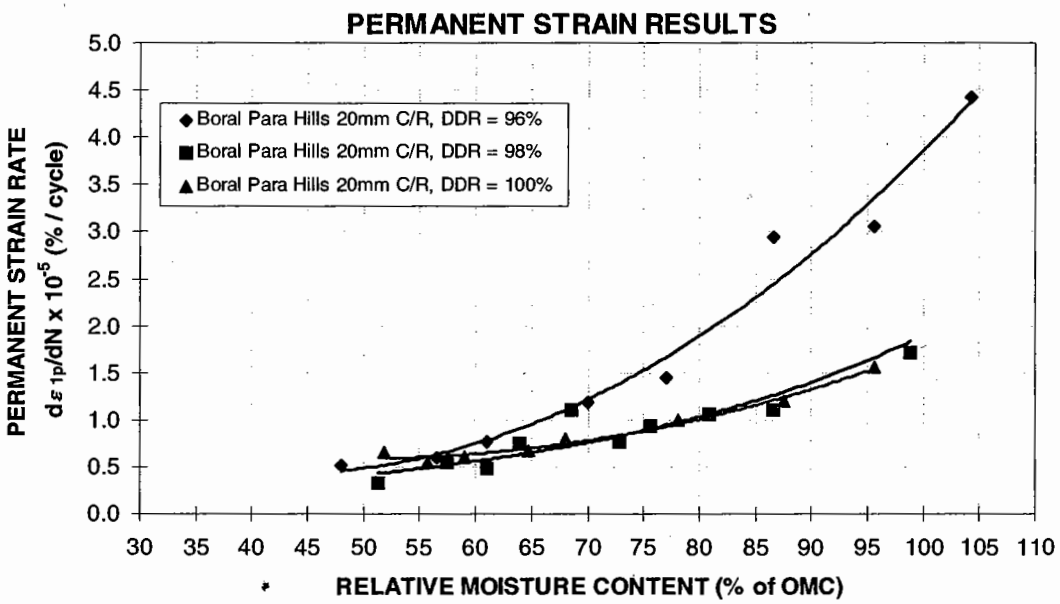

FIGURE 2.5: VARIATION OF PERMANENT STRAIN RATE PARAMETER WITH RELATIVE MOISTURE CONTENT FOR A 20MM CRUSHED ROCK AGGREGATE

On examining the same results but plotted against the Degree of Saturation (Figure 2.6), the same comments above apply, however, it can be noted that the material tested at DDR=98% now appears to be slightly more strain susceptible than the 100% DDR level. It has been found by the Author that the Degree of Saturation allows one to account for density variations which generally result in a shift of lower density (96%) materials to a higher strain susceptibility and a shift of higher density (100%) materials to a lower strain susceptibility. This result is not apparent in Figure 2.5. The importance of Degree of Saturation, in correctly interpreting material performance, is discussed in detail in a number of results presented in Chapter 8.

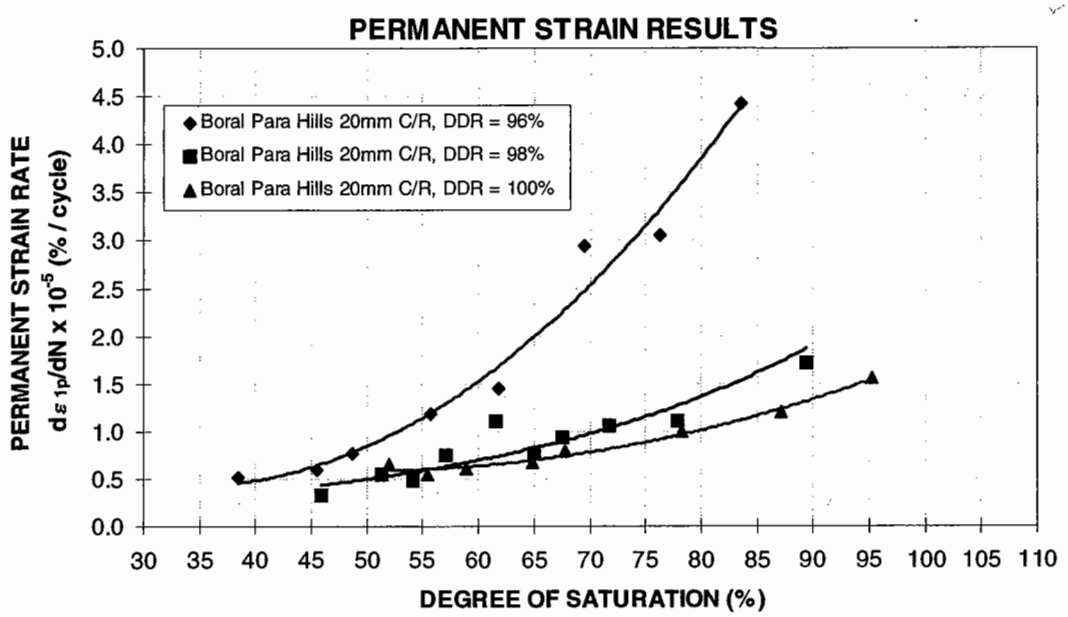

FIGURE 2.6: VARIATION OF PERMANENT STRAIN RATE PARAMETER WITH DEGREE OF SATURATION FOR A 20MM CRUSHED ROCK AGGREGATE

To further highlight the differences in the way in which material performance can be interpreted, the permanent strain test results of three materials used in the European Commission DGVII COURAGE project (European Commission, 1999), dealing with pavement construction using unbound aggregates, are examined. The strain results are graphed for three conventions commonly used to express moisture content (refer to Figure 2.7a to c). The first, which is widely used in Europe, is OMC – x%, the second is relative moisture content to optimum and the third is the degree of saturation, both of which are discussed above. From the results, it is clear that each expresses a different level of material performance ranking. The limestone material, in particular, appears to show the greatest level of strain susceptibility, relative to the other two materials, when graphed against degree of saturation, with better performance using RMC and the best using OMC – *x%*. A further, more detailed discussion shall be presented in §6.3.2 to discuss the merits of a degree of saturation approach.

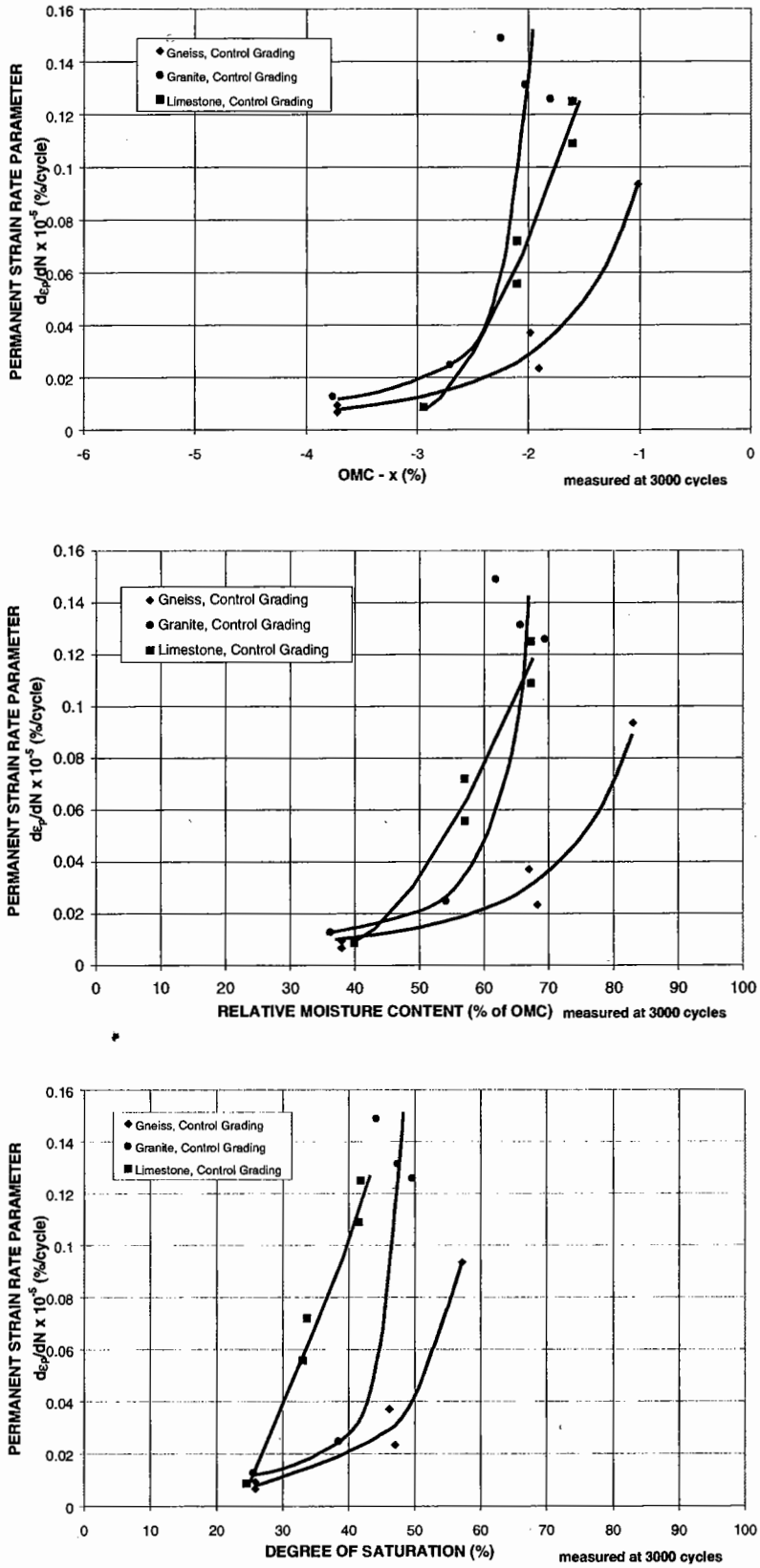

FIGURE 2.7A,B,C: VARIATION OF PERMANENT STRAIN RATE PARAMETER WITH THREE DIFFERENT MOISTURE CONTENT CONVENTIONS

The strain rate parameter, although not currently a condition specified in any design procedures, appears to provide a meaningful explanation of a material's strain susceptibility or rutting potential with RMC or DDR. Its value is considered particularly important in determining pavement layer application suitability of more marginal quality materials where the risks associated with their usage are higher than those of proven, high grade quarry products.

Another model used to model the permanent strain behaviour of an unbound granular material was that developed at LCPC (Paute, et. al, 1993). The model has the form:

$$\varepsilon_{1p} * (N, \sigma_1, \sigma_3) = A_1 \left[1 - \left(\frac{N}{100} \right)^{-B} \right] \quad \ldots (2.4)$$

where:

A_1	=	"strain rate-type" parameter
B	=	parameter
$\varepsilon_{1p}^* = \varepsilon_{1p} - \varepsilon_{1p(100)}$	=	axial permanent strain, after removal of the first 100 cycles of permanent strain (%)
N	=	number of cycles

The LCPC model, like the strain rate model, is stress dependent. In addition, this model also neglects the first 100 cycles of measured strains due to effects of bedding, etc. This model has been applied to the permanent strain test results of three materials used in the COURAGE project. All three materials were tested according to the same grading. The modelled results are presented in Figure 2.8a (European Commission, 1999).

This model has a limitation such that if the value of $A_1 > 2\varepsilon_{1p}^*$ then the value of A_1 reported uses this result. This is often found to be the case.

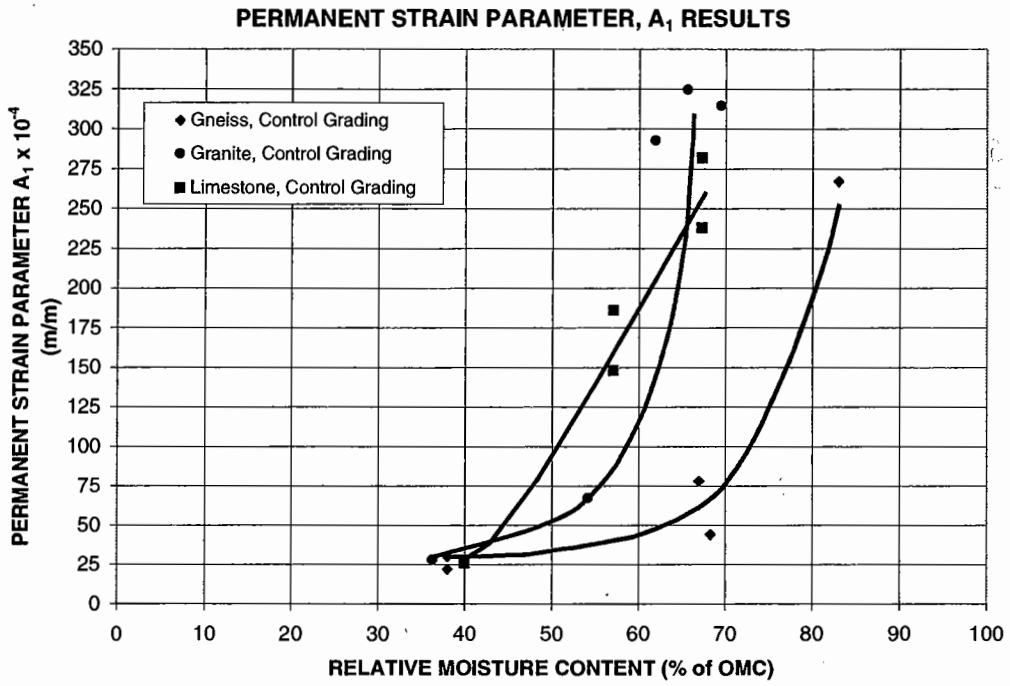

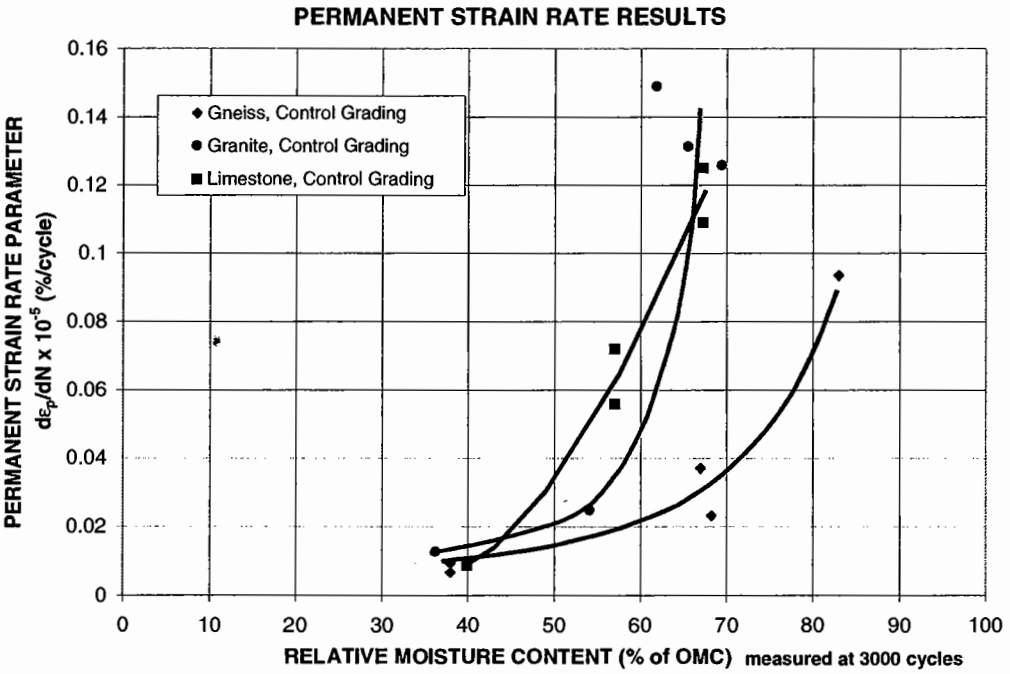

FIGURE 2.8A AND B: PERMANENT STRAIN PARAMETER A_1 AND STRAIN RATE dεp/dN FOR COURAGE MATERIALS

If the COURAGE project results are also modelled with the strain rate parameter (as illustrated in Figure 2.8A), it can be seen that the nature of the curves is very similar indeed.

This indicates that both models illustrate the same sort of strain susceptibility experienced by the different materials tested. It should be noted that these materials illustrate very high strain susceptibilities at mid-range *in-situ* pavement moisture conditions (60% of OMC). It is considered that this was due to the rather high preconditioning stresses applied to the test specimens, which aims to simulate somewhat the stress conditions at the time of compaction rather than the stress conditions expected in the sealed pavement.

It is anticipated that the laboratory permanent strain rate parameter could be linked to two field performance criteria, namely:

- deflection-based curvature function
- rut-resistance index

The relationship of permanent strain rate with curvature function will be further explored in Chapter 10, which will use some pavement case studies to relate the laboratory and field performance of the materials examined.

2.3.3 Durability

Adequate material durability is required to ensure that the material will perform according to its initially assessed properties (such as grading, permeability, strength - wet and dry, etc) during the life of the pavement.

"Durability" tests have been used world-wide to characterise the changes in material properties between those known to perform in the field (based upon long term observations of various materials placed in a variety of field conditions) compared to 'newer' unproved source materials. In addition, they are used to monitor changes in material quality within the one quarry source location.

It is reported by Bjarnason et al (1999) that these tests can be grouped into three categories, namely:

- fragmentation tests
- durability tests
- abrasion tests

Fragmentation tests cover the crushing, impact or static force types, such as the LA, ten percent fines, Bg-index. These tests can subject particles to large stress concentrations at contact points resulting in local fragmentation. Thus, the inherent strength of the aggregate and its shape largely dictates material quality. Durability tests cover the wetting/weathering types, such as Washington Degradation, Sulphate Soundness, Freeze/Thaw. Finally, abrasion tests subject samples to a wet abrading action with a low level of impact imparted, such as Texas Ball Mill, Micro-Deval and Studded tyre tests.

Unfortunately, a number of these tests do not utilise the entire product grading, only a small discrete particle size range. In addition, many do not aim to simulate local environmental conditions which one may experience in the road pavement; this can significantly bias the resulting empirical performance assessment.

Despite current 'empirical-based pavement material specifications' being developed on the basis of observed field performance, there have been many examples of constructed pavements around the world which have failed as a result of material quality assessment based solely on the results of these specifications. This will be discussed in the case studies presented in Chapter 10. The parameters adopted in these specifications were based largely on local experience, where standard products have been continually used for road construction. However, the specifications do not have the ability to predict well the *in-situ* performance of materials under different conditions. In addition, they may not predict accurately the performance of new products or alternative materials (recycled crushed concrete, asphalt planings, MSWI ash, slag waste, etc). Hence, there is a gradual move world-wide toward 'performance-based material specifications', which account more thoroughly for traffic loading and environmental conditions applied to the entire aggregate skeleton. This shall be discussed in Chapter 9.

2.3.4 Permeability

This property is closely linked to a material's compaction density during construction as well as its grading and fines content. Unbound granular materials need to allow adequate draining of the pavement structure to prevent moisture being 'locked' into

the structure, thereby reducing its stiffness and increasing its permanent strain susceptibility when under load, as will be shown in results presented in Chapter 8.

A material's grading is a balance between a dense one for high stiffness and strength and a more open-graded one for enabling good drainage and hence permeability, along with dissipation of pore pressures generated by traffic loading and for reduced frost susceptibility. The effect of grading on material stiffness is discussed in §2.4.4. Well designed pavement geometry, with adequate falls from the centre of the pavement toward the edge, coupled with side drains of sufficient depth are essential to allow water to discharge freely from the pavement layers. Conversely, the use of side-drains will act to prevent the ingress of water into the pavement due to watertable gradients. At present, typical specifications for the supply of a sub-base granular material will place requirements on the materials' grading envelope but, only *some* cases, will a minimum value of permeability be specified.

In order to allow for adequate drainage within granular materials, the coefficient of permeability, k, values have generally been specified from experience (Jones et al, 1989) as:

- 10^{-5}m/s to 5×10^{-4}m/s for capping and fill materials
- 10^{-5}m/s to 10^{-2}m/s for base and sub-base materials

A further control measure to prevent high moisture levels in the pavement is used in some European countries. Where drainage is considered a problem along sections of road, allowance has been made for very wide sealed shoulders (up to 3m in Ireland) to prevent water ingress easily into the trafficked wheel paths of the pavement (see Figure 2.9A). Conversely, where shoulders have not been sealed and do not possess adequate cross-falls to provide for satisfactory drainage, drainage channels have been found to form along the edge of the seal due to the erosion of fine materials (see Figure 2.9B). Such roads are often associated with poor performance.

FIGURE 2.9A (LEFT): TYPICAL RURAL ROAD IN IRELAND WITH A 3M WIDE SHOULDER
(Photo Supplied by NRA - Ireland)
FIGURE 2.9B (RIGHT): TYPICAL RURAL ROAD IN ICELAND WITH AN UNSEALED SHOULDER
(Photo Supplied by PRA - Iceland)

2.3.5 Cohesion

Cohesion (c) results from the mutual attraction existing between fine particles that tends to hold them together in a solid mass, unsupported, without the application of external forces. It is required to assist in providing satisfactory shear strength of layer materials, which are subjected to traffic loadings. In addition, it assists material workability during the construction phase and creates a sound, tight surface ready for the placement of subsequent bituminous layer(s). Bituminous surfacings placed on top of low level-cohesive UGMs, once cracked, tend to develop potholes partly due to a lack of cohesion and subsequent mobilisation of the fines. This can be seen on thinly surfaced roads in rural Australia.

Figure 2.10 illustrates that a material's cohesion can vary significantly with the properties of density and moisture content (Mundy, 1994). This data was determined by performing a number of multi-stage static triaxial tests on a selected material, compacted to a range of state conditions. The confining stress used for each stage of the test vary from 10 to 80kPa, to cover the range expected *in-situ*. Details concerning the testing methodology are provided in Chapter 7.

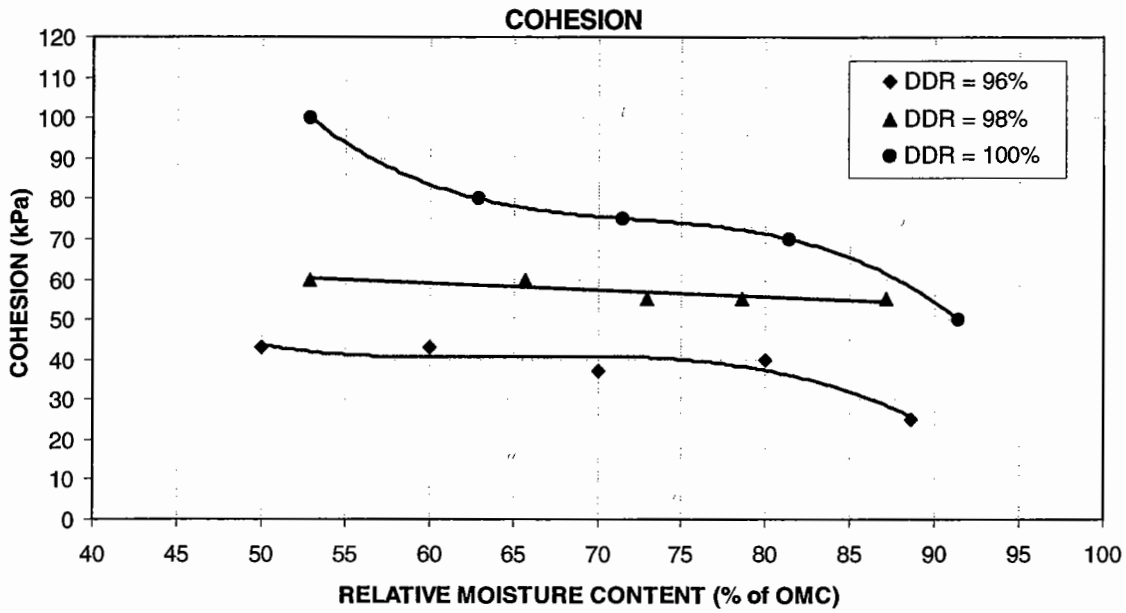

FIGURE 2.10: VARIATION OF COHESION WITH RELATIVE MOISTURE CONTENT (% OF OMC)

2.3.6 Angle of Shearing Resistance

The angle of shearing resistance or angle of internal friction (ϕ) describes the mechanical interlock within the material. The value of the angle of shearing resistance is effected primarily by the amount of surface friction between the grains, the shape of the particles (refer to §2.4.5), the degree of interlock between them and the density of the material. However, for the small changes within the density range used for compacted UGMs in the pavement (viz, DDR = 96% to 100%), the angle of shearing resistance will not be expected to undergo much change with density (see Figure 2.11). It has been found that ϕ decreases insignificantly with increasing material moisture content (see Figure 2.11). Karol (1960) also noted that "the presence of water has a minor effect on the value of the friction angle in sands and gravels".

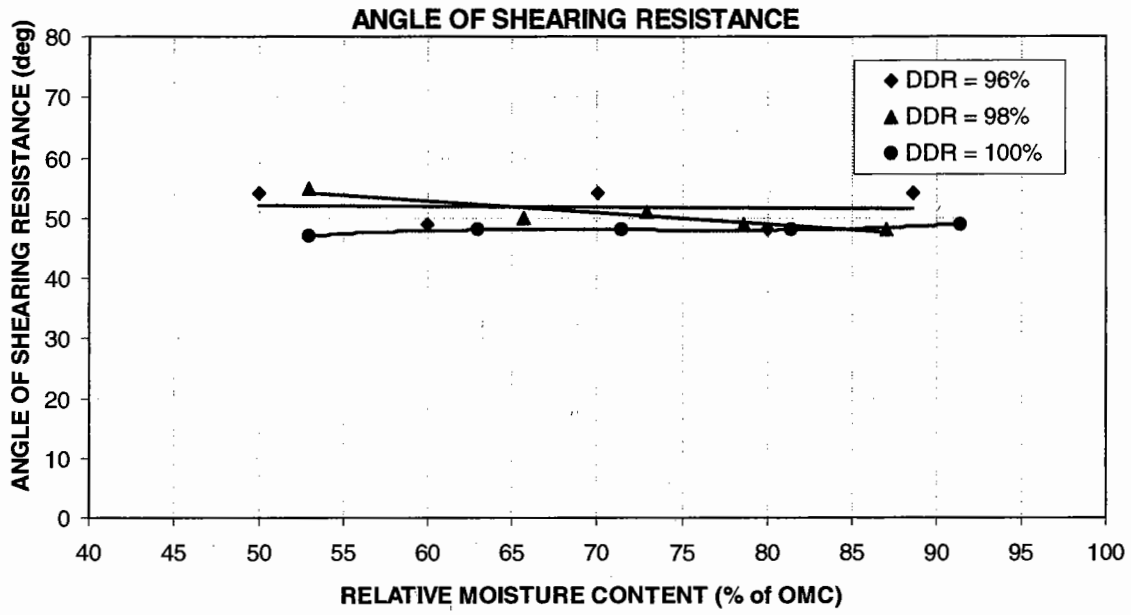

FIGURE 2.11: VARIATION OF SHEARING RESISTANCE WITH RELATIVE MOISTURE CONTENT (% OF OMC)

The angle of shearing resistance compliments cohesion (refer to §2.3.5) as together they define the shear strength of a material. Failure of a pavement material under vehicular loading will occur at any point where a critical combination of shear stress and normal stress develop, which is dependent on the shear strength parameters of c and ϕ, viz:

$$\tau_f = c + \sigma_n \tan\phi \qquad \ldots (2.5)$$

where:

τ_f = shear stress at failure or shear strength (kPa)
σ_n = total normal stress on the failure plane (kPa)
c = cohesion (kPa)
ϕ = angle of shearing resistance (degrees)

A simple classification system has been developed for technologists to rank the overall shear strength of materials in order to determine their quality, and hence, suitability for use in different pavement layers (refer to §5.6).

2.4 Influence of Material Properties & *in-situ* Conditions on Material Performance Indicators

Key factors which influence the design of road pavements include:

2.4.1 Moisture Content / Degree of Saturation

The moisture content or degree of saturation of a material has been found to significantly influence the resilient response and permanent deformation characteristics of the materials. Many researchers have found that resilient modulus decreases with increasing moisture content and that permanent deformation or strain increases. Barksdale reports that "the difference in resilient modulus for dry and wet conditions can be as large as 100% or more and must be considered in design" (Barksdale and Alba, 1997).

As materials become more saturated, pore pressures increase under repeated loading. Even with testing performed in a notionally drained condition, the ability of a material to rapidly dissipate internal pressures decreases as the material becomes more saturated. As a result, the effective stress in the material decreases with a consequent reduction in both strength and stiffness. Higher moisture levels also enhance 'slippage' of the grains and increase permanent deformation results. The ability of a material to dissipate pore pressure depends on factors such as the material's state of density and moisture, the frequency of the applied loading and its grading.

Thus, the ability to predict in-service moisture levels of pavement layers and subgrade is vital to allow:

- realistic determination of the resilient modulus of the constituent materials for input into the design modelling procedures, and
- the assessment of the suitability of the materials for use under the expected range of service conditions

Until recently, little research work has been undertaken to accurately determine the variation of moisture content with time within pavement layers. However, work conducted as part of the European RTD COURAGE project (European Commission, 1999) has provided useful information concerning the variation of moisture levels over the seasonal cycles occurring within a year. An example of the findings of this

work is illustrated in Figure 2.12, taken from a thinly surfaced granular pavement sited in Finland (Laaksonen, et al, 1999).

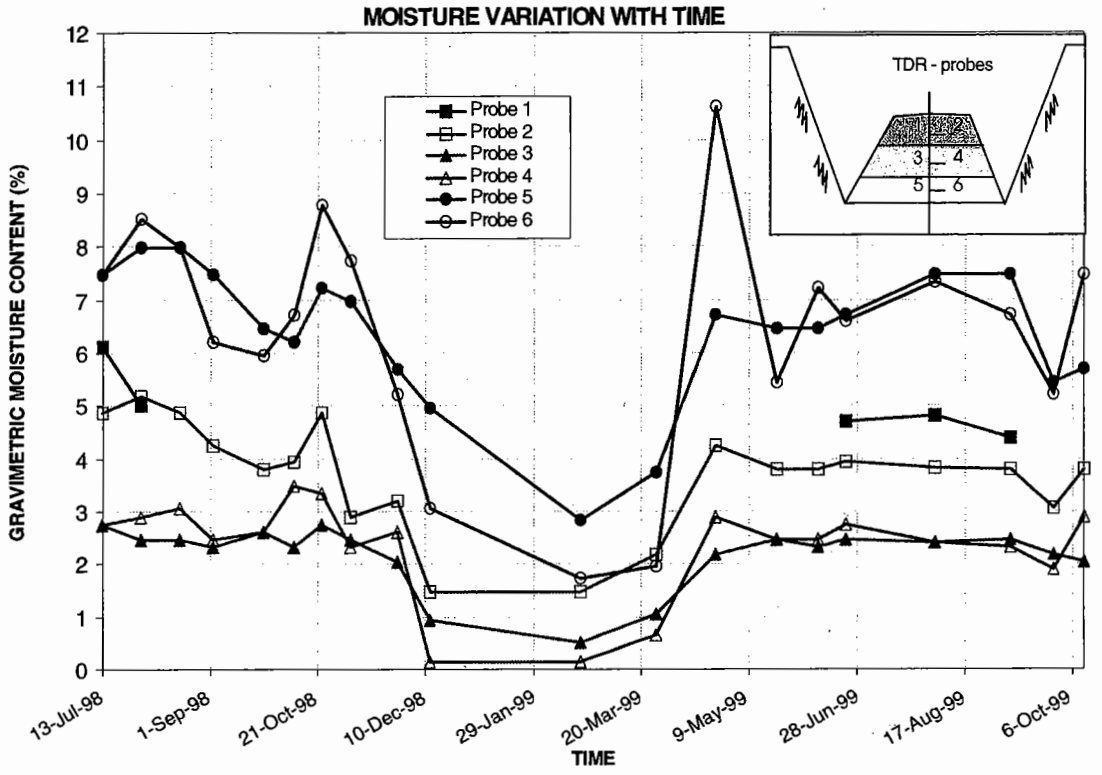

FIGURE 2.12: VARIATION OF PAVEMENT LAYER MOISTURE CONTENT WITH TIME (FINLAND)

Time Domain Reflectometry (TDR) probes were inserted in pairs at the mid-height of each of the three granular layers to monitor moisture changes. It can be seen that all layers exhibited moisture fluctuations, particularly obvious is the freezing of much of the water in the pavement layers from late November to late March of the following year. In late March thawing of the pavement released considerable volumes of water, sometimes to a level higher than before freezing. After this time, the moisture levels return to a steady state or "equilibrium" type value.

It is expected that if probes were installed in a newly constructed pavement, moisture levels would be high immediately following construction, as materials are often compacted at optimum moisture content (OMC), however, it would be dependent on whether the pavement was "dried-back" prior to surfacing (refer to §9.2). Drainage conditions (side drain provision / maintenance and road elevation) and the nature of

the seal (type, thickness and width extent) will also effect any subsequent cycles in moisture content. In Australia, it could be expected that, in many dry-climate regions, the "equilibrium" moisture content could be as low as 40% of OMC. This has been verified by a number of samples taken from test pits, dug in a range of pavement types, during the very late spring and summer periods.

The results suggest that pavements should be analysed according to their average moisture state within *each* seasonal period. This is particularly so given the high level of moisture sensitivity of permanent deformation and resilient modulus for many materials and its subsequent effect on key pavement design performance criteria (refer to the results of Chapter 8). The modelling of the environmental moisture cycle in the laboratory is very important, but is a usually neglected practical aspect of pavement design.

To illustrate this fact, a 35mm asphalt surfaced flexible pavement was analysed according to two extreme seasonal periods, namely summer and winter. The calculations are summarised in Appendix 1. The results of this study for one material product analysed (which was found from laboratory testing to be very moisture sensitive) showed that the:

- resilient modulus variation with the UGM sub-layers from winter to the summer condition was between 40 to 50%.
- vertical stress variation was up to a maximum of +6.5% at the top of the base layer for the drier pavement, which decreased to zero at 200mm depth. Below 200mm depth, the vertical stresses in the wetter pavement began to exceed those located at the same depth in the drier pavement, but only upto 5kPa in 40kPa at the bottom of the 450mm base.
- winter condition resulted in a reduction in the fatigue life of the asphalt surfacing by a factor of 9.
- winter condition resulted in an increase in the vertical compressive strain at the top of the UGM from 1420 to 1914 μstrain (by 35%).

Given the concern pertaining to the large increase in vertical compressive strain at the top of the UGM, an upper limit should be recommended upon this condition. Further discussions will be presented in §3.4.1.

2.4.2 Density

The effect of material density on the performance of granular materials is varied. Generally, researchers have found that resilient modulus changes resulting from testing materials at densities in excess of 96% of their maximum dry density is not significant (Thom and Brown, 1988). However, whilst the effect of density of the resilient response may be small in many materials, it may have a very significant effect on the permanent deformation characteristics of the material (see Figures 2.13A and 2.13B for materials tested in the COURAGE project and Figures 2.5 and 2.6 for Australian data).

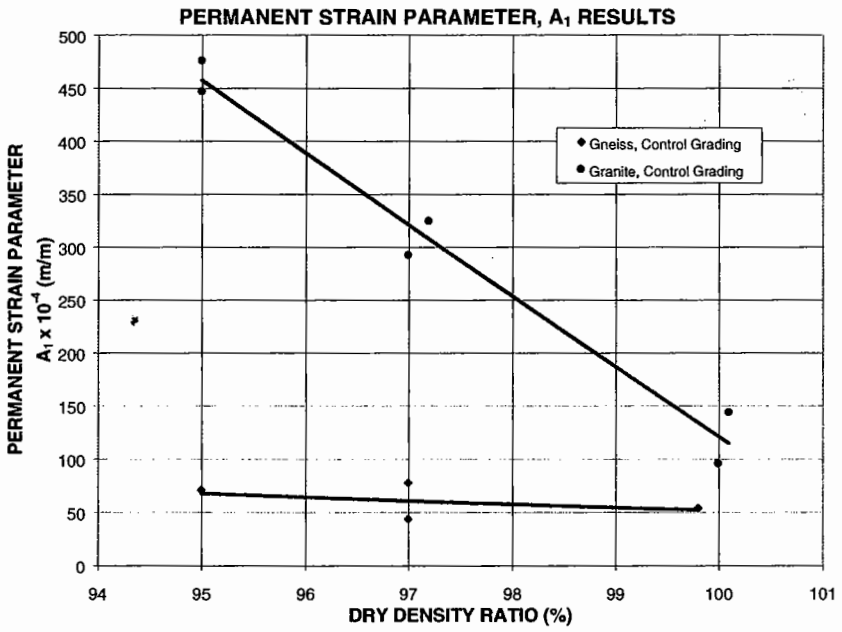

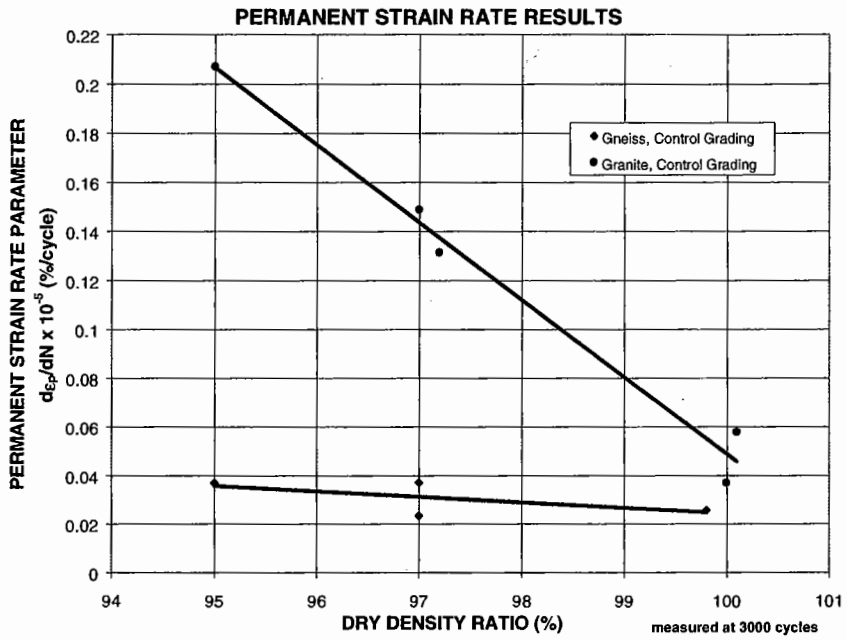

FIGURE 2.13A AND B: PERMANENT STRAIN PARAMETER A_1 AND STRAIN RATE $d\varepsilon_p/dN$ AGAINST DDR, RMC=60-65%, CONTROL GRADING

2.4.3 Soil Suction

As a compacted granular base or sub-base material air dries in either the field or laboratory (termed 'dry-back', refer to §9.2), very high resilient moduli and lower permanent strains are developed under loading. This occurs as a consequence of the increased effective stress (deceased pore pressure) due to capillary tension, frequently expressed as a soil suction value. Tensile forces are developed in the pore water menisci in unsaturated aggregate skeleton structures to generate suction forces in the pore voids. If the moisture content of a soil is reduced, the water interfaces (menisci) recede into the smaller pores, their radii of curvature decreases and the suction increases. Studies performed by Walker (1997) found that "in unsaturated conditions different suction forces initiate the movement of pore water from regions of lower to regions of higher suction. Strength of granular materials will vary with changes in moisture content". He investigated three unbound pavement materials taken from two experimental pavements. The materials of interest here were (i) quarry crushed basalt, (ii) weathered sandstone. The testing method employed was based on the filter paper method (Gardner, 1937 and also Al-Khafaf and Hanks, 1974), such that if the paper is left for a period of time in a stable environment with the soil, it will reach a dynamic equilibrium state with the suction level of the soil.

Careful measurement of the moisture absorbed by the paper can be used to compute the suction level which it achieved. Knowledge of the correlation between moisture content and suction for the filter paper is required.

Results showed that the:

(i) crushed basalt material had a total suction of 50kPa and matric suction of 5kPa at OMC. The total suction values increased to a minor (20%) degree as the moisture content reduced from OMC to 75% of OMC, but rapidly (100%) as the level decreased below 75% of OMC.

(ii) weathered sandstone had a total suction of 1200kPa and matric suction of 400kPa at OMC. The total suction values increased to a minor (25%) degree as the moisture content reduced from OMC to 87% of OMC, but rapidly (180%) as the level decreased below 87% of OMC.

It could be expected that substantial strength gains could arise at moisture contents *below* 75 to 90% of OMC, depending on material type, as a result of 'dry-back' due to rising suction forces.

2.4.4 Grading

A dense material may be obtained when its particle size distribution tends towards the theoretical distribution given by Fuller's power grading law (Fuller, 1907), whose limits have, in practice been adopted by most of the highway authorities. If fines are excessive the mixture may lack stability and retain excess moisture, conversely, if the content of the fines is low the mixture will tend to be stony and porous, and usually require additional fines to obtain good stability.

Materials produced rarely have gradings which align with the mean or target specified but, rather, tend to have gradings which lie typically within the fine or coarse limits of the specification. In addition, a material produced just outside of the specification at one or two sieve sizes is rarely rejected, and acceptance is often made with little understanding of its effect on performance.

The moisture sensitivity of granular material performance has been reported to increase with increasing fines content (Haynes and Yoder, 1963). In addition, it has been reported by Thom and Brown (1988) that permanent deformation resistance in granular materials is reduced as the amount of fines increases.

However, work conducted by the Author (Mundy et al, 1993) has shown that different materials react quite differently to grading changes. The varying response encountered is considered to vary depending on the quality of the fine and coarse fractions. In South Australia, typical production gradings generally vary between the upper and lower specification limits to the fine and coarse extremities. Sometimes, a gap-graded product called an "armchair" grading is produced (see Figure 2.14). This type of grading is quite common and tends to be very coarse on intermediate sizes (approximately 2.36mm) and very fine on the fine fractions (less than 0.425mm).

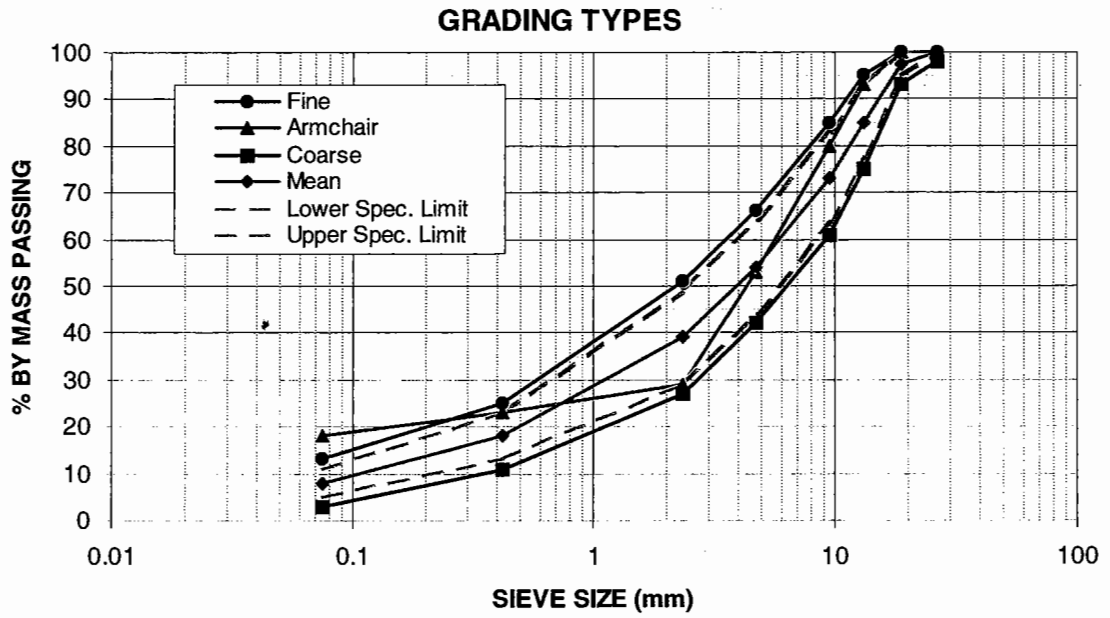

FIGURE 2.14: FOUR GRADING TYPES TESTED AT TSA

Two examples of product variability with grading change, as tested by the Author, are illustrated in Figure 2.15A/B and 2.16A/B. Key changes in the MPIs of strain rate and resilient modulus are detected with moisture variation.

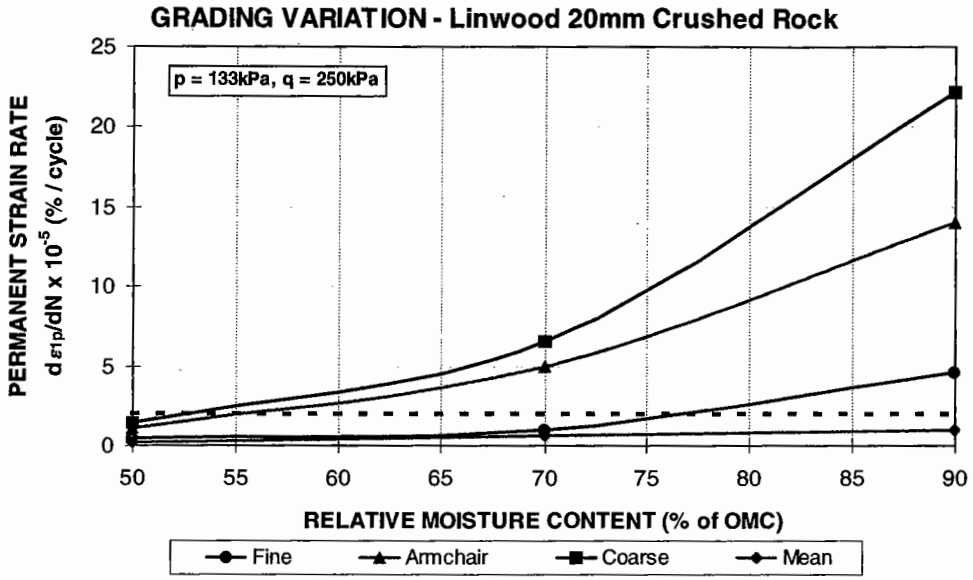

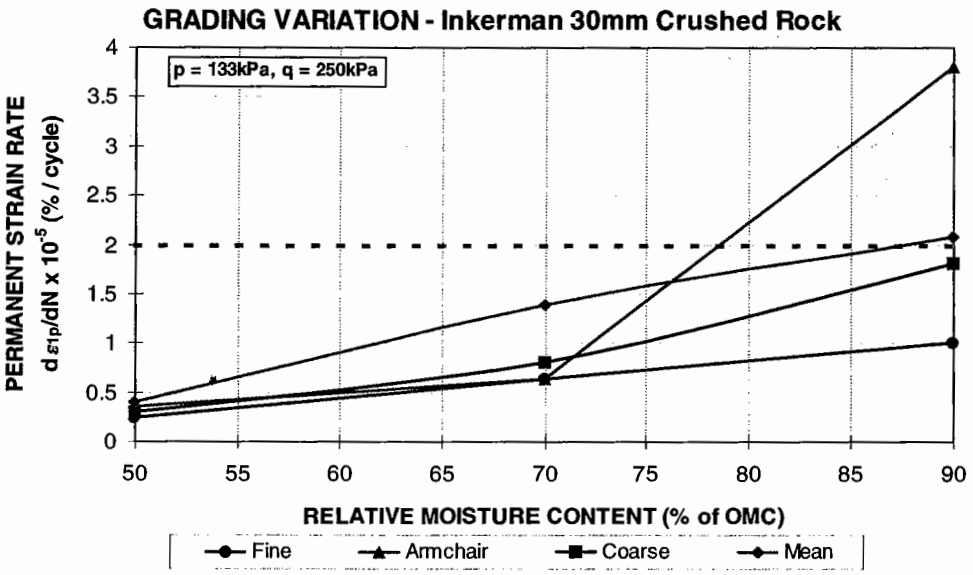

FIGURE 2.15A AND B: STRAIN RATE VARIATION WITH RMC FOR FOUR GRADING TYPES

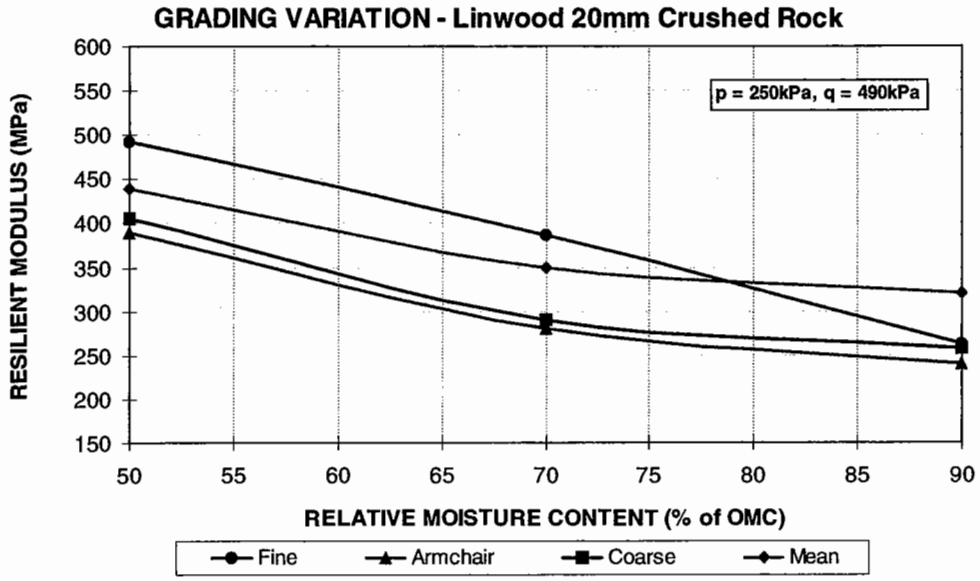

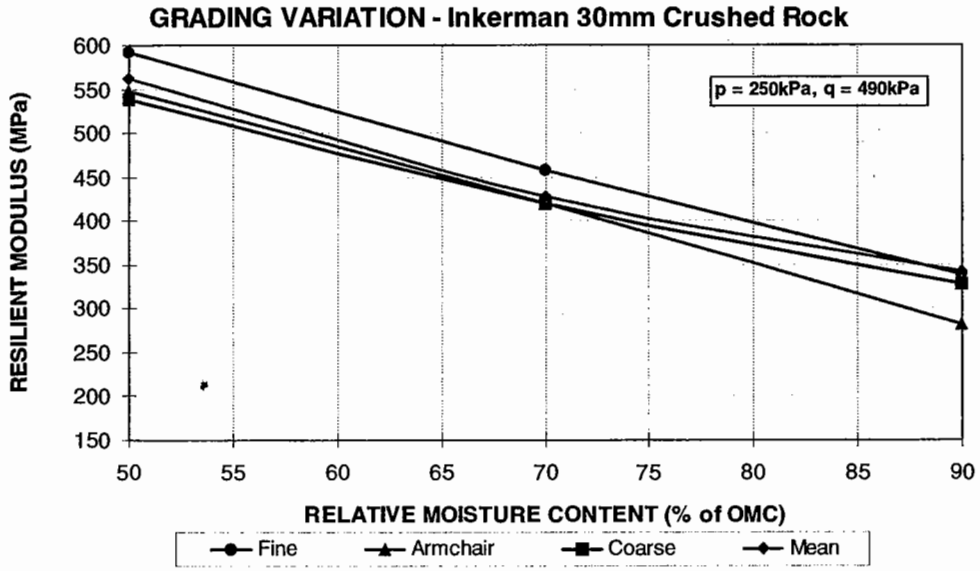

FIGURE 2.16A AND B: RESILIENT MODULUS VARIATION WITH RMC FOR FOUR GRADING TYPES

From the results of these and one other product tested for grading variation, the materials exhibited poorer performance for both coarser and armchair gradings with improved performance for finer gradings over the moisture range examined. Whilst the mean grading also performed quite well, it is noted that further performance improvement could be obtained by moving to a finer grading for *some* material products, as the results illustrate. One restriction may be in using the material at a

high moisture content, which could limit performance. As a result, the Author's viewpoint tends to agree with that concluded by Plaistow (1994) that "grading has an indirect effect on the resilient (and permanent strain) behaviour of unbound aggregates by controlling the impact of moisture and density of the system" – more accurately described by saturation control.

2.4.5 Shape

Shape is considered an important property since it provides the mechanism for particles to interlock in a material matrix, which enhances the material's shear resistance to imposed loads. Crushed rock pavement materials having angular shaped particles provide stronger interlock of the matrix to improve its shear strength and load spreading ability. This was found by Vallerga et al (1956) having conducted triaxial tests on both sub-rounded and angular sandstone aggregate at various void ratios. However, depending on the strength of the individual grains, particle fragmentation can also increase with higher angularity. In contrast, uncrushed river gravels, which contain rounded particles, often are found to have greatly reduced strength due to low levels of angle of shearing resistance (refer to §2.3.6).

A quantity of flaky particles, either randomly orientated or oriented other than parallel to the shear failure plane, increases the shear strength of the material (Selig and Roner, 1988). However, flaky particles (as defined by the ratio of thickness to width) result in problems of breakage and subsequent abrasion, larger permanent strain under repeated loading and lower resilient modulus. Selig found that the rutting from wheel tracking testing of flaky material was nearly twice that of the non-flaky material. This was attributed to particle alignment of the material.

2.4.6 Stress Conditions

As vehicles move over the pavement surface, large numbers of stress pulses, of varying magnitude, are applied to each element of material below and for some distance radially from beneath the wheel load. Practical results illustrating this fact are shown in §4.3.2.3. The duration of the stress pulses may be rapid for fast moving

vehicles and increase with decreasing traffic speed and increasing depth of a material element into the pavement.

The magnitudes of both permanent deformation and resilient modulus are very dependent on the levels of applied stress (vertical and lateral or confining) experienced by the material element (see Figure 2.17). These materials are said to be "stress-dependent".

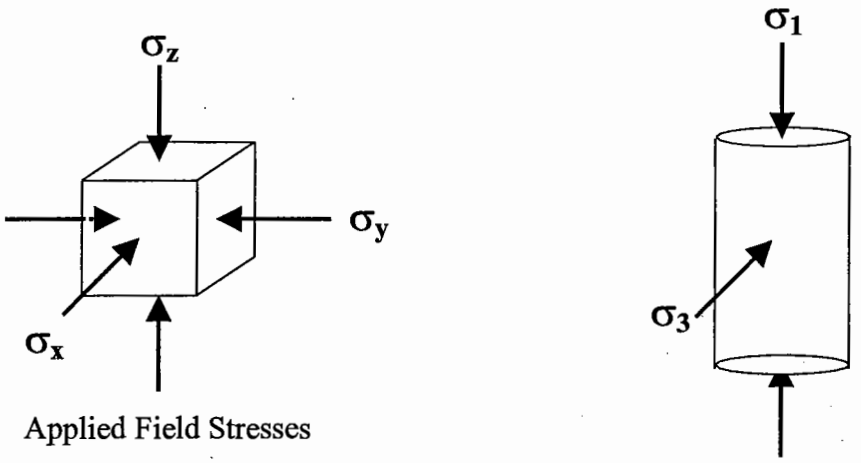

FIGURE 2.17: STRESSES APPLIED TO MATERIAL ELEMENTS IN THE FIELD AND LABORATORY

In turn, the structural performance of a layer of granular material is a function of its resilient modulus or layer stiffness. As will be seen from computations performed in Appendix 1, dealing with seasonal layer stiffness variations, layers of lower moduli do not generate the same magnitude of stress at selected points within them as opposed to stiffer layers. As a result, stress and layer stiffness are closely related.

Two parameters used to describe the stress state of a material element are the bulk or volumetric stress, p, and the deviatoric stress, q. These are defined as follows:

$$p = \frac{\sigma_x + \sigma_y + \sigma_z}{3} \text{ (field)}, \frac{\sigma_1 + \sigma_2 + \sigma_3}{3} = \frac{\sigma_1 + 2\sigma_3}{3} \text{ (laboratory)} \quad \text{(kPa)} \quad \ldots (2.6)$$

$$q = \sigma_z - \left(\frac{\sigma_x + \sigma_y}{2}\right) \text{(field)}, \sigma_1 - \left(\frac{\sigma_2 + \sigma_3}{2}\right) = \sigma_1 - \sigma_3 \text{ (laboratory)} \quad \text{(kPa)} \quad \ldots (2.7)$$

The resilient modulus increases considerably with an increase in the sum of principle stresses, p and an increase in the confining stress. Under constant p, resilient modulus may either decrease moderately with increasing deviator stress, q (see Figure 2.18) or remain virtually constant (see Figure 2.19), as can be seen from the contour lines of resilient modulus.

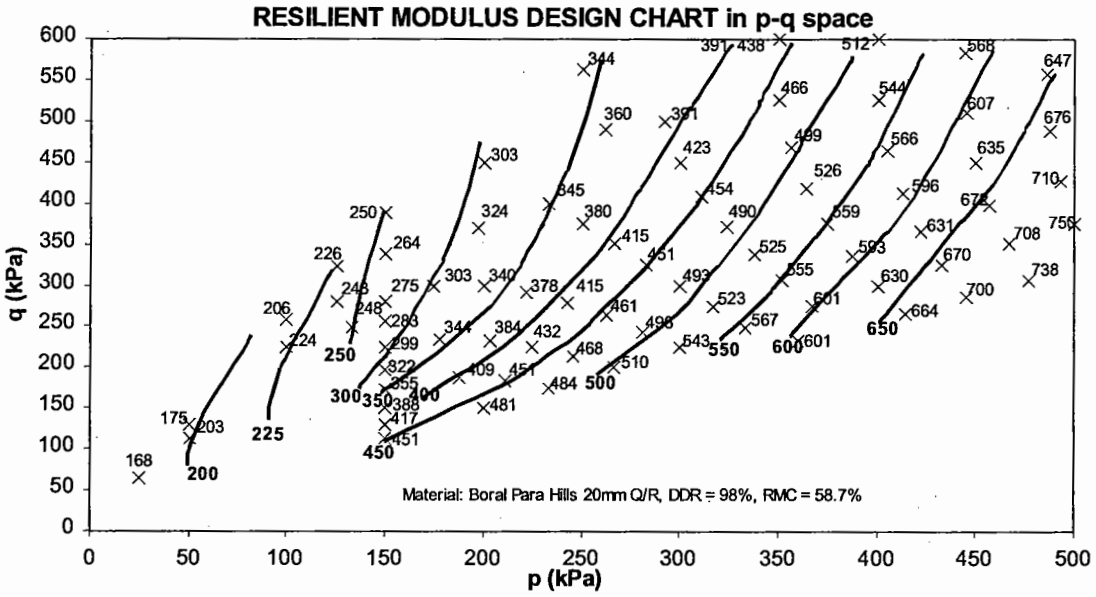

FIGURE 2.18: RESILIENT MODULUS DECREASING WITH Q, FOR CONSTANT P

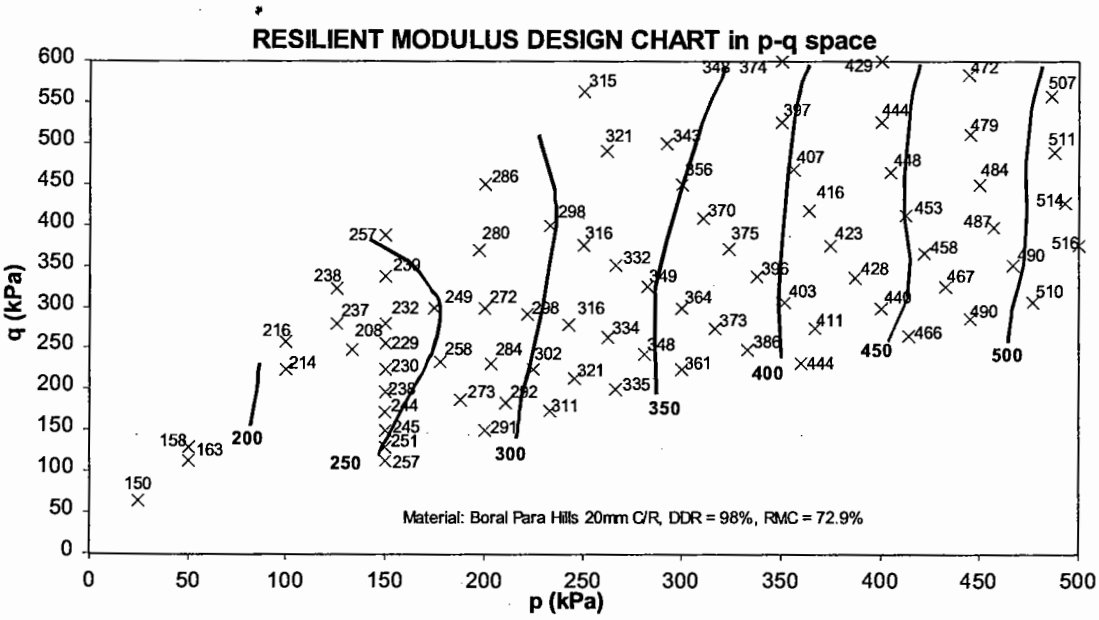

FIGURE 2.19: RESILIENT MODULUS CONSTANT WITH Q, FOR CONSTANT P

Thus, in the case of a thinly surfaced pavement structure, resilient modulus varies continuous from the top of the UGM to the bottom (refer to Figure 5.8A and 5.8B), as well as radially, and in a non-linear or stress-dependent manner. It is highest at the top of the layer, where the principal stresses resulting from an applied surface wheel load are greatest. Thus, the "modulus" of a non-linear material is not something that is 'characteristic' of a layer, but instead, pertains to a material point within that layer under a specific loading.

Permanent deformation is also strongly influenced by stress state. Higher levels of permanent deformation occur as the magnitude of applied deviator stress, q, increases in the direction of increasing stress ratio q/p, relative to confining stress, σ_3. Relating this to a pavement structure, the greatest amount of permanent deformation results in the upper 150mm of the UGM. This can be related to the dramatic change in vertical stress to confining stress which occurs over this depth (see Figures 5.8A and 5.8B). In addition, over a range of p = 175kPa / q = 450kPa to p = 127kPa / q = 320kPa, which for a thin 35mm asphaltic surfacing relates to an approximate depth of 60mm to 100mm (see Figure 5.8A), stresses within the pavement can lie very close to the shear strength failure envelope, depending on the quality of the material. Refer to §5.5 for further discussion.

To confirm this, reference can be made to wheel tracking tests performed using the Pavement Test Facility (see Figure 2.20) at the University of Oulu, undertaken as part of the COURAGE project.

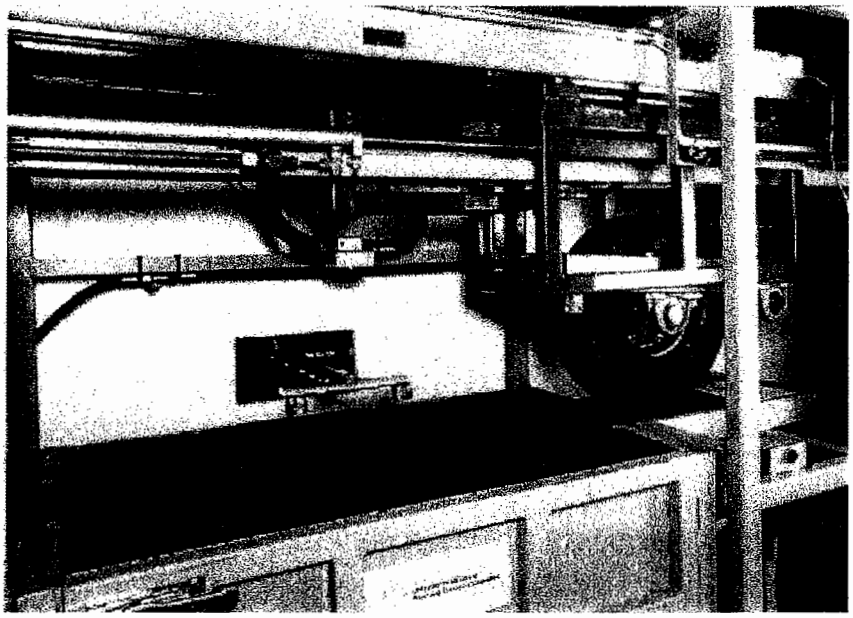

FIGURE 2.20: PAVEMENT TEST FACILITY AT THE UNIVERSITY OF OULU, FINLAND

The tests showed that for the three UGMs, tested within flexible pavements, most of the basecourse permanent deformations developed in the upper half of the layer (Lämsä, et al, 1999). The pavement configuration (refer to Figure 2.21), which consisted of 300mm base layer UGMs underlying a 30mm asphalt surfacing, was subjected to 20,000 cycles of applied loading from a 9.15kN (0.93t force) moving wheel with tyre pressure of 612kPa. On the basis of static measurements, the contact pressure at the surface of asphalt layer was found to be 670kPa. Therefore, it could be estimated that stress at the top of granular material course under wheel load was about 600kPa. It should be noted that the moving wheel load may be selected within a range of 7...25kN (0.71 ... 2.55t force) and applied in one or two directions. The wheel is a smooth truck wheel of size 6.00 – R9 with adjustable tyre pressure. The loading speed at the centre of the test box is 1.4m/s (5km/h).

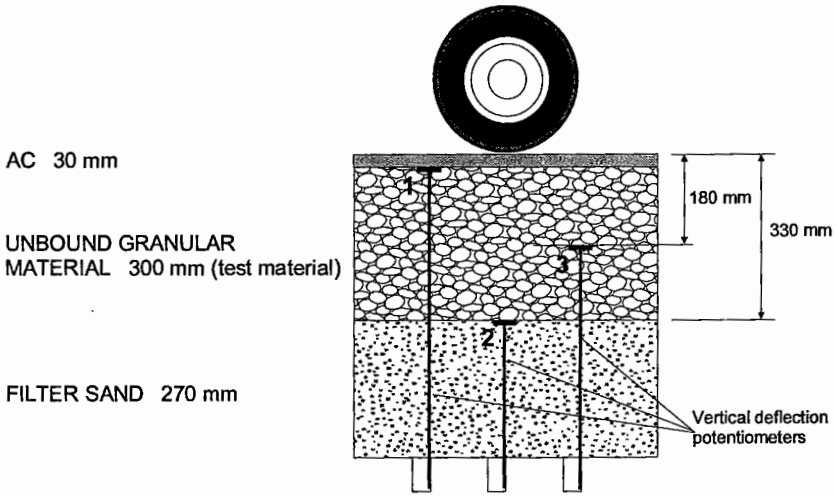

FIGURE 2.21: TEST PAVEMENT STRUCTURE

From vertical deflection potentiometers placed at the top, middle and base of the UGMs, measurements of the deformations in each layer were computed. It was found that the permanent deformations which developed in the upper half (150mm) of the layer were in the granite material (A) 97%, gneiss material (B) 73% and limestone material (C) 85% of the whole base course permanent deformations. This experimental work supports the Authors comment above that the greatest amount of permanent deformation results in the upper 150mm of the UGM.

2.5 Summary

This Chapter presented critical key material performance indicators (MPIs) which are directly linked to the performance of loaded pavement structures. The indicators deemed to most influence material and pavement behaviour are resilient modulus, permanent deformation (strain rate), durability, permeability, cohesion and angle of shearing resistance.

Material performance in the field is simulated in the laboratory using Repeated Load Triaxial (RLT) or wheel tracking tests. These tests show that performance is very strongly influenced by factors such as material type and state conditions (moisture content, grading, suction forces developed through dry-back of the materials, and sometimes density). Given some of these properties could vary dramatically within the constructed length of a road pavement, it is essential that their influence on pavement performance be established prior to design and construction. It is

recommended that this be done by monitoring the resulting changes in the key material performance indicators listed through selectively testing for material property variations under conditions within limits expected *in-situ*. In addition, the materials must be assessed at stress conditions representative of those *in-situ*, under applied design traffic loadings. This is particularly important given that resilient modulus and permanent strain rate are very sensitive to the applied stress conditions experienced by a material element (ie, stress-dependent). Figures 2.17 and 2.18 illustrate the dependence of resilient modulus on the applied stress conditions.

The *in-situ* monitoring of the UGM condition in pavements, as part of the COURAGE project, has revealed that the moisture content of the UGM layers vary considerably with the season (referring to Figure 2.11). In base layers (those immediately beneath the bound surfacing), the variation was found to be between 40 and 90% of optimum moisture content. For the lower sub-bases, an even greater variation of between 30 and >100% of optimum moisture content was measured. The structural contribution to the pavement of UGM has been investigated in the laboratory.

Laboratory-based RLT testing has shown that:

- depending on the material geological type, significant reductions in the resilient modulus and potentially large increases in permanent deformation can result as the material moisture content is increased.
- materials are sensitive to density changes over ranges commonly specified for pavement layer materials, namely, 96% to 100% of modified Proctor compaction maximum dry density, whilst other materials are not.
- materials generally exhibit poorer performance for both coarse and armchair gradings, with improved performance noted for finer gradings. One restriction, however, may be in using materials at a high moisture content, which could limit performance.

It is felt that a material's degree of saturation provides a better understanding of the moisture within the pore spaces of a compacted material than the relative moisture content. It was seen from Figures 2.5 and 2.6 that degree of saturation can better

distinguish the permanent strain dependence of a material under different density conditions. This shall be further explored by examining the results from a range of materials, which have been subjected to performance testing, presented in Chapter 8. However, it is felt that the construction Industry may struggle to comprehend the true meaning of this more geotechnical-based parameter, compared with the simple and long used parameters of moisture content and OMC.

The moisture content held within a material is closely coupled with its permeability and a pavement's drainage conditions. Layers of unbound granular materials need to adequately drainage to prevent moisture being 'locked' in, thereby reducing material resilient modulus, or layer stiffness, and increasing its permanent strain susceptibility when under load.

A study of effects of seasonal moisture variability within a thinly surfaced flexible pavement, analysed in Appendix 1, showed that:

- resilient modulus variation with the UGM sub-layers from winter to the summer condition was between 40 to 50%.
- vertical stress variation was up to a maximum of +6.5% at the top of the base layer for the drier pavement, which decreased to zero at 200mm depth. Below 200mm depth, the vertical stresses in the wetter pavement began to exceed those in the drier pavement, but only upto 5kPa in 40kPa at the bottom of the 450mm base.
- winter condition resulted in a reduction in the fatigue life of the asphalt surfacing by a factor of 9.
- winter condition resulted in an increase in the vertical compressive strain at the top of the UGM from 1420 to 1914 μstrain (by 35%).

These results confirm the necessity to model the incremental deterioration of pavement performance according to seasonal variation.

The variation of MPIs (such as resilient modulus) with a range of material properties (particularly moisture content and grading) suggests that analytical modelling procedures must incorporate the behaviour of the individual UGM sub-layers. This

is particularly important for thinly surfaced pavements given a materials' stress dependence. Chapter 3 will examine a number of currently used pavement design methods to investigate whether or not the methods adequately account for the material property variations highlighted within the modelling process.

CHAPTER 3
REVIEW OF PAVEMENT DESIGN PRACTICE

3.1 Introduction

Funds for road construction and maintenance around the world are becoming more limited due to government reforms and a wider distribution of total funds to other public assets. As a result, pavement designers must generally work within more restricted budgets and produce economic designs that consider many design variables.

Key factors which must be taken into account in the design of road pavements include:

- traffic volume and associated axle loads
- pavement foundation
- pavement materials
- environment (climatic data, drainage conditions, etc)
- quality of workmanship associated with the construction of the road
- required service life and maintenance regime

The determination of traffic volumes is quite elementary. Vehicle traffic counters are used which can easily record vehicle numbers and classify them according to vehicle classes or groupings appropriate to each vehicle's axle configuration and spacing. However, determining axle loads tends to introduce a great deal of uncertainty unless appropriate weigh-in-motion technology can be associated with the road of concern (Austroads, 2000). The accuracy of WIM systems is applied to a vehicle's individual axle mass (IAM), group axle mass (GAM) or gross vehicle mass (GVM). Whilst worldwide there is no standard method for determining accuracy, most systems report an accuracy of either 95% (or 66%) of vehicles being weighed having a GVM within 10% (or 5 to 8%) of the static GVM. Only a few high speed systems report an accuracy based upon IAM, and are generally quoted to provide an accuracy of 95% of vehicles being weighed having an IAM within 20% of the static IAM. Little information is available regarding the method used to determine

accuracy, namely, a random survey of vehicles, one vehicle passing several times, vehicle speed effects, calibration results, etc.

To simplify the design process, design methods require that real traffic data be converted into an approximated number of reference or standard axle passages. To further add to the uncertainty, traffic growth needs to be determined over the life of the pavement. This can be estimated using 'permanent traffic count meters' (which count for 24 hours a day and 365 days of the year) to measure changes in traffic composition and numbers with time across the road network. However, traffic on sections of the road can be subject to high seasonal traffic, hence loadings, during times of grain carting or harvest for example.

Pavement material properties provide an essential input into the design process. Material stiffness and allowable values of stress for UGMs, however, are seldom determined consistently in laboratory fundamental tests (such as repeated load triaxial [RLT] and static triaxial [STXL] tests) or in simulative tests (such as wheel tracking tests). The parameters used as input into analytical design procedures are often estimates based on empirical tests, for example, the Californian Bearing Ratio [CBR] test. Alternatively, values may be determined from experience or "look-up-tables", which often are non-specific to material geology, density, moisture, grading and expected *in-situ* stress conditions.

A number of countries still rely on empirical pavement design methods, thinking that analytical approaches generally need to be supported by overly complex testing systems to determine material behaviour.

Despite the complexities of material performance in real pavements, which exhibit combined resilient and plastic behaviour resulting from initial compaction and subsequent traffic loading, the procedures documented world-wide for the design of pavement structures are still highly simplistic. In fact, if one excludes field investigations, materials testing, road design (geometric considerations) and the like and focuses solely on the design, a pavement could be designed in merely one day or less! This is often the case, despite the fact that the cost of the pavement itself could

be of the order of millions of dollars. As a comparison, a substantial bridge structure along the same road could be of the same order of magnitude from a construction cost point of view, yet its elastic design alone (with no plastic design considerations) could take up to a minimum of 3 months!

Mechanistic analysis has become more widely used in flexible pavement design due to its ability to predict fatigue and rutting distress. However, many methods still use very simplistic response models, consisting of one layer for each of the principal material constituents. In addition, despite the immense amount of research data available worldwide concerning material non-linearity, the non-linear behaviour of granular base and sub-base layers, as well as the subgrade, is often over-looked in the design methodology.

This Chapter looks at pavement design practice associated with axle loads, pavement configurations and predicted design life and performance prediction criteria in Australia, America and Europe. In addition, shortcomings identified with pavement design practice, associated with the pavement materials themselves, are discussed.

3.2 Axle Loadings

As road systems have been improved over the last few decades, road hauliers have taken advantage of the technical advances in motor vehicle design by carrying larger and heavier loads. However, many roads were not designed to carry these larger loads and quickly deteriorated. Subsequently, it was necessary to limit the mass of vehicles and/or the individual axle loads in different countries in order to preserve the road network.

In Australia, pavements are designed according to the AUSTROADS Pavement Design Guide using a single, dual wheeled, Equivalent Standard Axle (ESA) loading of 80.4kN (8.2 tonnes force). In some States of Australia the statutory (legal) ESA loading has been increased. For example, in South Australia the statutory ESA loading was increased in July 1994 to 88.3kN (9.0 tonnes force), such that it is greater than the current design load. However, from January 1999, buses with a single drive rear axle may operate under the higher mass limits scheme (Transport

SA, 1999) with a 1t axle load increase above the statutory limit to provide a load limit of 98.1kN (10 tonnes force). Although, no modification to the current design process has accounted for this.

The same standard axle load is used in the United Kingdom as Australia, although the maximum axle load permitted is 115kN (11.72 tonnes force). In France, however, pavements are designed for heavy lorry traffic, the loading of which was set in 1945. The reference axle is a dual-wheeled isolated axle, weighing 130kN (13.25 tonnes force) (refer to §4.3.1, page 37, Corté et al, 1997).

The table below (Table 3.1) relates the vehicular standard or reference axle loading in a range of countries to the surface loading used for design and subsequent analysis of pavement structures.

Reference Axle Type	Total Design Axle Loading	Loading Model for Pavement Structural Analysis	Wheel Contact Pressure
Australia: isolated single axle, dual wheel	80.4kN (8.2t force)	40.2kN half axle: represented as two 20.1kN dual wheel footprints (radius 96mm) with 330mm centre-to-centre separation	700kPa (1)
France: isolated single axle, dual wheel	130kN (13.25t force)	65kN half axle: represented as two 32.5kN dual wheel footprints (radius 125mm each) with 375mm centre-to-centre separation	662kPa
Sweden: isolated single axle, dual wheel	100kN (10.19t force)	50kN half axle: represented as two 25kN dual wheel footprints (radius 100mm) with 300mm centre-to-centre separation	800kPa (2)
UK: isolated single axle, dual wheel	80kN (8.15t force)	40kN half axle: represented as two 20kN dual wheel footprints (radius 113mm) with 376mm centre-to-centre separation	500kPa
USA: isolated single axle, dual wheel	80kN (8.15t force)	40kN half axle: represented as two 20kN dual wheel footprints (radius 115mm) with 345mm centre-to-centre separation	483kPa

TABLE 3.1: STANDARD LOADING USED BY DIFFERENT COUNTRIES FOR PAVEMENT STRUCTURAL ANALYSIS

(1) a 750kPa contact pressure and wheel footprint of 92.1mm is given in the draft Asutroads Pavement Design Guide. However, the total design axle loading is unchanged. (Austroads, 2001)

(2) a 700kPa inflation pressure in a cold tyre is considered. However, during driving the pressure increases by about 10% to nearly 800kPa. (Djärf et al, 1996)

In comparing typical pavement structures from country to country, which use different axle and wheel configurations, current practice in the mechanistic process has been to consider the fatigue damage imparted to the pavement by using an

'equivalent' axle loading system. This system allows for the composite effects of different axle types, which carry different magnitudes of loading, to be converted to an 'equivalent number of standard axles' (abbreviated to ESAs or ESALs) for a given pavement type. This equivalence is based on equating the pavement damage from one system to another. The damage law is taken to be:

$$EF = \left(\frac{P}{P_o}\right)^{\alpha} \quad \ldots (3.1)$$

where:

EF = the Equivalence Factor

P = axle load considered

P_o = reference isolated axle load (if distance to next axle is greater than 2m)

α = damage power (for flexible and bituminous pavements this is taken to be α = 4 in Australia and UK). It should be noted that the damage power law, which is generally applied in many countries, utilises different power factors in some countries. The destructive effect of the axle load depends upon pavement type, layer thicknesses and stiffnesses, subgrade response to loading, its condition and the deterioration mode being analysed. The damage power has been derived from full scale accelerated load testing on a range of pavements founded on different subgrades and the consideration that different constituent materials possess differing levels of sensitivity to damage development. Lower powers (eg. 2) are usually associated with the initiation and progression of surface cracks; a power of 4 is used for rutting for flexible or bituminous pavements, whilst higher powers (eg. 6 and above) are reserved for semi rigid or concrete pavements

The relationship above was first derived from the AASHO Road Test in the USA between 1959 and 1961 (Liddle, 1962). Here, a number of pavements were tested to destruction by running various vehicles over the test track. From research, the damage effect was observed due to different vehicle loadings on the fatigue behaviour of the pavement materials, which is related to the type of structural damage and on the type of pavement.

If one considers the damage effect on Australian roads only due to the recently permitted increase in legal axle loading above the design axle loading, from 8.2t to 9.0t, the equivalence factor for the commonly used value of α is calculated to be:

$$EF = \left(\frac{9}{8.2}\right)^4 = 1.45 \quad \ldots (3.2)$$

Thus, the life of the pavement, according to this theory, is reduced by 31% by this increase of 19% in axle load magnitude. One would expect this to have a direct impact on the maintenance cost cycle of many pavements, particularly those designed with little residual strength beyond their original design life. It should be mentioned that the number of design ESAs, using a given lane, in Australia may be determined from one of three methods for flexible pavement design. Two methods consider road functional class within the Australian State of design, with one using the average annual number of total commercial vehicles and average ESA factor whilst the other considers the average ESA contribution due to each commercial vehicle's axle group type. The third method is the most comprehensive by using axle type and the load applied to each axle group.

A slightly modified form has been adopted in France (Corté et al, 1997), where the damage law is referred to as the "Aggressiveness of an Axle", is taken to be:

$$A = K\left(\frac{P}{P_o}\right)^{\alpha} \quad \ldots (3.3)$$

where:

A = Aggressiveness of an Axle

K = accounts for the axle type (for a single axle, K = 1)

P = axle load considered

P_o = reference isolated (if distance to next axle is greater than 2m) axle load

α = damage power (for French flexible and bituminous pavements, $\alpha = 5$)

The French method of ESAL determination is somewhat similar to the Australian approach. Where possible, the French convert real traffic (composed of variable combinations of vehicles with different axle loads and configurations) into cumulative numbers of reference axle passages NE. However, generally data on average daily heavy lorry vehicle count is generally sufficient, without needing to detail the exact composition. Interestingly, for narrow 2-lane roads (less than 6m wide), the French allow for the overlap of rolling wheels by probable proportioning. The method also considers a coefficient of aggressiveness (CAM) based on traffic class and pavement type. Having determined ESAL numbers, the French Guide uses risk factors, associated with probability of pavement failure, for various traffic classes. These values are used to determine coefficients to be applied to working limit strains at the base of bituminous and bound layers only for all designs but those of flexible pavements.

For the above reference **design** loadings, using the French modified law, the ***damage due to the Australian ESA relative to the French ESAL*** would be:

$$A = \left(\frac{8.2}{13.0}\right)^5 = 0.091 \text{ or } 9.1\% \text{ of the damage caused by the standard French loading} \quad \ldots (3.4)$$

As a result of this large difference in design loadings, and hence in damage differential, pavements designed in Australia tend to comprise much thinner bituminous surfacing layers due to the lower levels of load applied to them (as compared with their European counterparts) for the same relative life. Alternatively, the Australian pavements tend to have a longer relative life (by a factor of ten times) than the European pavements, for the same surfacing type. This shall be evident in §3.3

The following discussion of pavement structures will centre on those consisting of an unbound granular layer (ie, flexible or inverted pavements). Other pavement types such as full depth asphalt pavements (or thick bituminous pavements as they are referred to in Europe), fully bound or composite (bituminous and cement-treated

layered) pavements and cement concrete pavements will be omitted from discussions.

3.3 Pavement Configurations and Design Life

3.3.1 Bituminous Surface Treatment (BST) Pavements

In Australia, bituminous chip seal surfacings (otherwise known as 'surface dressings') are generally used on many rural roads to link towns separated by long distances. These pavements require sound underlying unbound granular basecourse and sub-base layers. The design life traffic loading of these type of pavements in Australia is approximately 1-2 × 10^6 ESAs (0.9-1.8 × 10^5 NEs), whilst in Europe, it is approximately 1 × 10^5 NEs (Corté et al, 1997, p.160). This is keeping with the Aust-French equivalency factor determined above, see Equation 3.4.

3.3.2 Thin Asphalt Surfaced Flexible Pavements

In the outer metropolitan areas of Australian cities, asphalt surfacings for unbound pavements may be as thin as 35mm, with around 450mm of unbound granular material (see Figure 1.3), in order to satisfy a design life traffic loading of approximately 2-3 × 10^6 ESAs (1.8-2.7 × 10^5 NEs). As a comparison in Europe, the minimum wearing course thickness is a 40mm bituminous concrete layer, which overlays a 200mm to 500mm unbound granular sub-base material (see Figure 1.5). The design life traffic loading required is approximately 1.3 × 10^5 NEs, which again is in keeping with the Aust-French equivalency factor determined. With reference to Figure 3.1 (Figure III,2,1 French Design Manual for Pavement Structures), this thickness varies linearly up to 120mm required for a design life traffic loading of approximately 1 × 10^6 NEs (Corté et al, 1997).

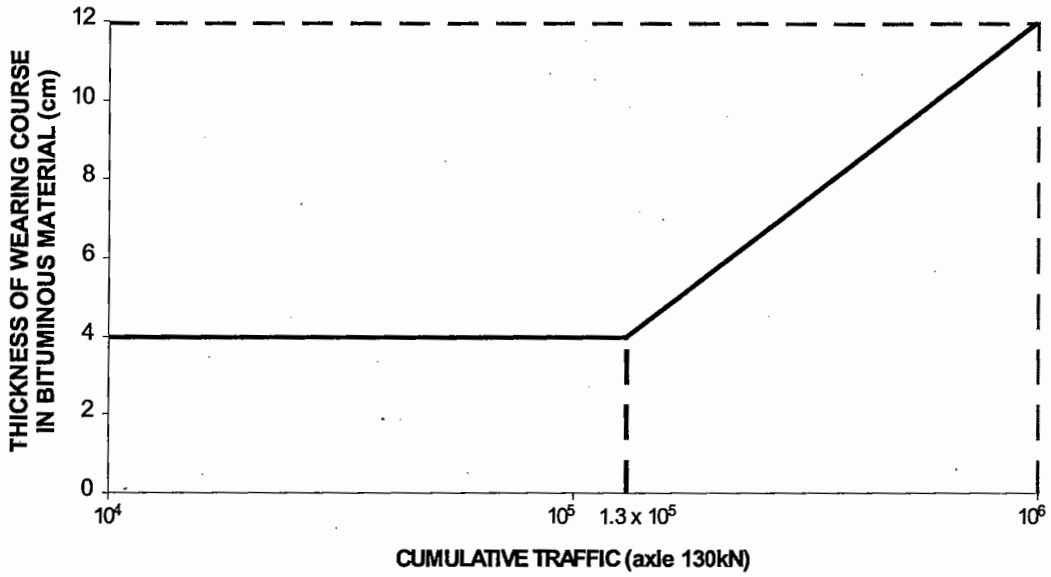

FIGURE 3.1: MINIMUM REQUIRED THICKNESS OF WEARING COURSE IN BITUMINOUS MATERIAL FOR LOW TRAFFIC PAVEMENTS WITH A GRANULAR BASE

Reference: Figure III.2.1 of the French Design Manual for Pavement Structures (Corté et al, 1997)

This figure incorporates experience derived from observations of pavement performance. A minimum thickness is specified between 10^4 and 1.3×10^5 NEs in order to prevent the wearing course from debonding. Greater surfacing thicknesses are required beyond this to service larger equivalent cumulative traffic volumes.

3.3.3 Inverted Pavements

In addition, the use of "upside-down" pavements has become more common in South Australia in the late 1980s and 1990s. These pavements generally comprise a 35mm asphalt surfacing overlying an unbound granular base material of between 125mm to 175mm in thickness, with a 300mm cement treated quarry rubble sub-base (see Figure 1.4). The expected design life for such pavements in Australia is typically up to 3×10^6 ESAs (2.7×10^5 NEs). The inverted pavements in Europe also comprise an asphaltic surfacing layer, a base layer of between 100mm to 150mm of bituminous material overlying an unbound granular material of approximately 120mm, with a hydraulically bound sub-base or capping layer between 300mm to 500mm in thickness (see Figure 1.6). The design life traffic loading required is typically 2 to 10×10^6 NEs (Corté et al, 1997).

So throughout Europe, the use of a surfacing or base layer of bituminous material, generally up to 150mm, provides a distinct difference to many Australian road pavements for the same number of standard axle loadings. This is principally due to the much higher axle loadings allowed on European roads, with secondary consideration given to environmental conditions. Depending on the bitumen content of the material, the stiffnesses of a bituminous material (depending on factors such as thickness, temperature, load frequency, etc) will be of the order of ten to twenty times that of the unbound material it replaces, when tested under the same stress conditions. As a result, the bituminous layer (depending on its thickness) tends to act as a stress spreading and reducing agent to the underlying unbound granular materials, thereby greatly reducing their stress dependence (as discussed in §2.4.5).

For inverted pavements, the thin unbound granular layer is confined or "sandwiched" between the rigid underlying bound layer and the upper bituminous surfacing layers. For these types of pavements, the stresses experienced by the unbound layer can be very high (depending on the thickness of the upper bituminous layers). As a result, the use of high quality base materials which with provide high stiffness and low permanent strain characteristics are necessary to ensure that adequate support is provided to the bituminous surfacing layer. Lesser quality materials either don't have the required stiffness and resistance to permanent deformation or undergo particle damage and thus cannot sustain a high level of performance during the service life of the pavement. This leads to rapid fatigue of the surfacing layer due to the high tensile strains, which develop at the bottom of that layer. The UGM must exhibit sound performance over the range of *in-situ* moisture conditions. The influence of construction placement conditions tends to be even more important for these types of pavements than for other flexible pavements. Moisture is confined or "locked-in" into the unbound material in-between the upper and lower bound layers, with no vertical paths to migrate through, given that the lower cement-treated layer is somewhat impermeable.

3.4 Performance Prediction Criterion

Performance prediction or failure criteria are used to predict the pavement's condition at the end of its design life, having been trafficked with a number of design

standard axles. Current analytical design methods use some or all of the following summarised criteria (see Figure 3.2 for critical strains).

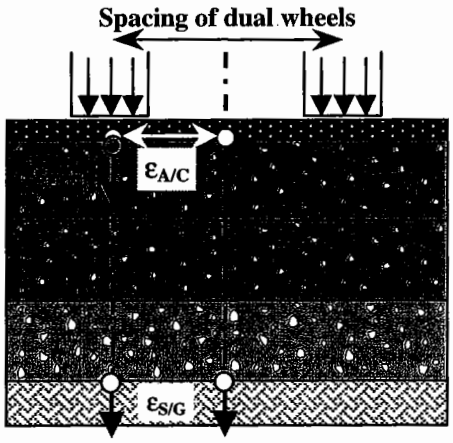

FIGURE 3.2: CRITICAL STRAIN LOCATIONS WITHIN A FLEXIBLE PAVEMENT

3.4.1 Vertical Compressive Strain – UGM

Much of the deterioration of a pavement is attributed to the stresses or strains developed in the individual pavement layers. As a result, these parameters are important to consider in developing limiting design criteria. The French design practice for flexible pavements requires that the vertical strain at the surface of the unbound granular layers (as well as the subgrade) be determined to see that it is less than a limit value. This check is undertaken to limit rutting occurring in unbound granular material layers due to high levels of imposed surface stress resulting from wheel loads (refer to §3.6.5). In Australia and other European countries, current design practice neglects the importance of some sort of check, which should be undertaken, to ensure that the strains in the unbound layer are not excessive, particularly an issue where more marginal quality materials are used in construction.

The importance of a check on the maximum permissible vertical compressive elastic strain in the UGM was highlighted in a study performed by the Author. Two identical pavement response models for a given flexible pavement configuration were assessed (both with the same applied 8.2t ESA load and material sub-layering approach) using a non-linear, elastic analysis (further details are given in Mundy, September 1992). The pavement analysed consisted of three 150mm thick granular layers compacted in three lifts, viz, a top basecouse 1 layer, a second basecouse 2

layer of the same material quality, and a third layer, a sub-base, of lower quality material. The pavement, which has a 35mm asphalt surfacing, is typical of those constructed in Australia for lower levels of traffic.

One analysis was performed using basecourse layers 1 and 2 with a low moisture content material (60% of OMC) and the other analysis was the same, however, the basecourse 2 layer material was considered at a high moisture state (90% of OMC). The material modelled in this example (from RLT test data) was an actual basecourse grade quarry product. This study aimed to simulate the effect on pavement performance when high moisture levels are 'locked-in' to a pavement. This could result from:

- insufficient 'dry-back' of the basecourse 2 layer during the staged construction cycle. In Australia it is required under the construction specification that each pavement layer is dried-back to a maximum of 70% of OMC, preferably 60% of OMC.
- the layer being exposed to a period of rainfall, thereby increasing its moisture content, and then being overlaid a short time later with the basecourse 1 layer.
- inadequate drainage allowing moisture entry into the pavement

A direct difference in the effect of sub-layer resilient modulus was found, with the high moisture state basecourse 2 layer material having a lower level of performance with much higher levels of vertical compressive strain throughout its thickness under the action of a ESA loading (see Figure 3.3). The vertical compressive strain profiles were depicted throughout the depth of the UGM layers. The pavement with the basecourse 2 layer of high moisture content produced a 61% to 100% increase in vertical strain (depending on the depth) in the pavement layer when compared to the strain levels measured at the same depths in the pavement containing the drier material. The tensile strain calculated at the bottom of the asphalt surfacing only increased by 5.6% as the basecourse 2 layer moisture content increased. This is understandable given that the upper basecourse 1 layer, which directly supports the surfacing, would play a far more critical supporting role.

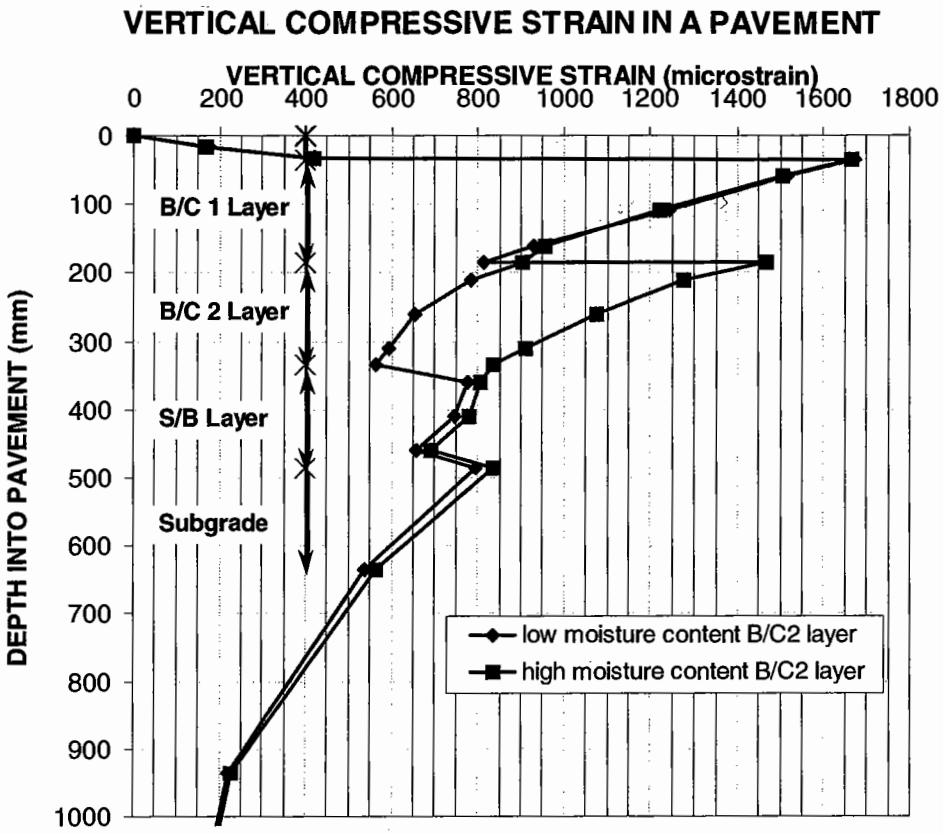

FIGURE 3.3: COMPARISON OF THE VERTICAL COMPRESSIVE STRAINS IN THE UGMS PREDICTED IN THE TWO PAVEMENTS ANALYSED

Reference: Mundy, September 1992

For the analysis undertaken, each of the granular material base and sub-base layers were sub-divided into three sub-layers each with a thickness of 50mm in order to account for the non-linearity of the materials, particularly in the top two base layers. In addition, the subgrade was also sub-layered to account for its non-linearity, although it was not that pronounced. Following a number of iterations of material sub-layer moduli with stress for the UGMs, the final response models used for the two UGM moisture cases were as presented in Figure 3.4.

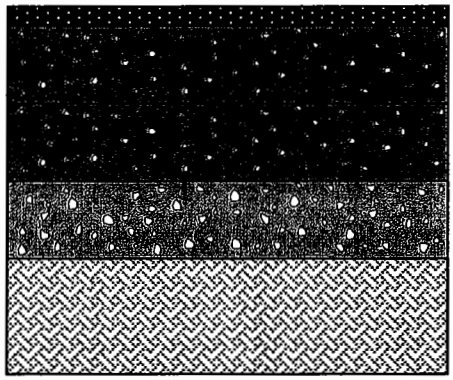

Values of Resilient Modulus for sub-layers
Case 1, 60% OMC: Case 2, 90% OMC

A/C	35mm	2000MPa	2000MPa
		310	310
B/C1	150mm	264	264
		240	240
		190	100
B/C2	150mm	170	90
		150	85
		80	80
S/B	150mm	70	70
		60	60
	300mm	50	50
S/G	300mm	70	70
	300mm	80	80

FIGURE 3.4: RESPONSE MODELS USED FOR COMPARISON OF BASECOURSE LAYER 2 UGM OF DIFFERENT MOISTURE CONTENTS

At present, very little knowledge exists concerning what levels of compressive or resilient strain in unbound granular material layers are acceptable before rutting is considered a failure mechanism. Needless to say, that UGM layers of lower stiffness will be more prone to developing higher levels of permanent deformation than stiffer layers.

In South Africa, a design criterion has been adopted from a study (Thompson and Visser, 1998) for limiting the vertical compressive strain in layers below the wearing course in the mechanistic pavement design procedure for ultra-heavy mine trucks. The trucks have axle loads up to 430kN or 43.8tonnes force, with surface pressures of the order of 600kPa. *At present, this is specific for the mechanistic pavement design procedure for heavy haul vehicle roads only.* It was found in this study that sites where pavements exhibited poor field performance with excessive deformation/maximum deflection were found to be associated with large vertical compressive resilient strain values in one or more layers from linear elastic analysis (Thompson and Visser, 1998). Analysis of the data indicated that an upper limit of 2000 microstrain should be placed upon layer vertical resilient strain values for the load repetitions found on the mine roads. This level of strain is obviously associated with the high levels of load applied to these pavements.

From the analysis performed by the Author, as discussed previously, the maximum level of resilient strain was 1670 microstrain, located at the top of the higher quality, dry basecourse 1 layer. However, the strain at the top of the basecourse 2 layer was 907 microstrain for the layer in a dry state, which increased greatly to 1467 microstrain in a high moisture state. This level of strain may well be beyond the ability of this lower grade material (due to its high moisture state) to tolerate.

Further, from the example given in Appendix 1, Table A1.1, the strain levels at the top of the two basecourse layers were:

basecourse 1 layer - 1420 (1420*) and 1914 (1914*)
basecourse 2 layer - 586 (558*) and 891 (783*)

for the summer, 50% of OMC and winter, 85% of OMC, conditions, respectively.

* or the values in brackets if the strains are determined by using the corrected lateral stress conditions which shall be discussed in Chapter 5)

Again it is evident, that lower levels of layer stiffness, caused by increased seasonal moisture conditions will impact very significantly upon strain levels in both of the basecourse layers. It shall be noted from the results above that much higher levels of strain occur in the basecourse 2 layer when this layer only is of high moisture content, compared to the top base layer. Thus, an immediate need exists to control the upper limit of strain tolerable in both layers in order to maintain sound performance throughout the wetter months of the year. Failure to do so will see a good deal of deterioration during these periods.

It is recommended that an upper limit on the vertical compressive strain of 1600 microstrain, at the top of the base layer under a thin surfacing, be used in design practice until further research can refine this value. In addition, a value of 900 microstrain could be used at the top of the second base layer. These values, in affect, tend to act to control both the material quality and, indirectly, the moisture state

tolerable in the basecourse 1 and 2 layers to ensure acceptable pavement performance where a 35mm asphalt surfacing is used.

3.4.2 Vertical Compressive Strain – Subgrade

The development of vertical deformation or rutting in the subgrade can be related to the level of vertical resilient compressive stress, or subsequent strain developed, as a result of the applied surface load (in both magnitude and number of passes). By considering a standard axle loading, a direct relationship between the number of axle passes and the magnitude of the known level of vertical resilient strain at the top of the subgrade is widely used, viz:

$$N_{ESA} = \left(\frac{A}{\mu\varepsilon_v} \right)^B \quad \ldots (3.5)$$

where:

N_{ESA} = number of ESAs to ultimate condition

A, B = coefficients

$\mu\varepsilon_v$ = vertical resilient compressive strain at the top of the subgrade (microstrain)

Note that strain values are given in μstrain as the value of the coefficient 'A' is factored by 10^6 to account for this.

Some countries use a more general form:

$$N_{ESA} = \left(\frac{A}{\varepsilon_v} \right)^B \times 10^6 \quad \ldots (3.5a)$$

where:

N_{ESA} , A, B are as above

ε_v = vertical resilient compressive strain at the top of the subgrade (strain)

The coefficients used in the design procedures vary largely from country to country as a function of the probability of survival adopted, viz:

Australia (Equation 3.5) use approx. 50% probability of survival with A = 8511, B = 7.14 (20mm rut condition).

UK (Equation 3.5a) use 85% probability of survival with A = 453, B = 3.95 (10mm rut condition).

Thus, for $N_{ESA} = 10^6$ for example, $\mu\varepsilon_v = 1229$ (Aust.) and $\mu\varepsilon_v = 453$ (UK). Thus, the Australian method permits strains, resulting from the model, that are about 2.7 times those allowed in the UK. This is due to the often very conservative subgrade moduli applied to pavements designed in Australia, which is often in stark contrast to dry climate experienced in many parts of the country.

3.4.3 Horizontal Tensile Strain – Bituminous and Cementitious Materials

Fatigue failure, in the form of accumulative cracking, results from tensile strain development during continual repeated loading. Tensile strains are a maximum either directly under the centreline of a single wheel load or may be in-between the dual wheels. A typical fatigue failure criterion equation used is:

$$N_{ESA} = \left(\frac{C}{\mu\varepsilon_h}\right)^D \qquad \ldots (3.6)$$

where:

C, D = coefficients

$\mu\varepsilon_h$ = horizontal tensile strain at the bottom of the bound layer (microstrain)

3.5 Review of Pavement Design Methods

Analytical pavement design requires three key components for its use to be implemented, namely:

- a response model for analysing the pavement. This allows the designer to compute stresses and strains throughout the pavement, knowing the applied loading. It must incorporate:
  - structure
  - material parameters
  - layer thicknesses

- applied loadings
- software and calculation process

- material performance models, which model well the relationship between stress and strain of the pavement's constituent materials. These material models allow pavement modelling software to arrive at resilient moduli, which are harmonised with the computed stresses throughout the depth of the structure. By following iterative procedures. This same result could be achieved without the use of material models if the designer is prepared to 'manually' adjust the 'seed' resilient modulus values, as designated in the response model, following each stress computation. The material performance models need to be:
  - stress dependent
  - climate dependent (state variables)
- performance prediction models so as to be able to determine the allowable strains or stresses for each of the pavement materials. This will include:
  - selection of failure criterion and values for materials/layers
  - selection of failure law to obtain the number of load repetitions for the failure criterion

A recent study by COST 333 (European Commission, 1999) showed that of the 20 countries participating in that study:

- 60% used analytical procedures
- 35% used empirical procedures
- 5% unspecified

to design a pavement to a terminal condition (maintenance after 20 years). Also, it was found that most participants who used analytical methods did so using multi-layer linear elastic pavement modeling.

In addition, COST 333 found that the source of information used to calibrate the design criteria for pavement deterioration was derived from the following sources:

- 25% road network
- 30% AASHO road test data
- 10% road network / accelerated pavement trafficking data (test pavements)
- 5% accelerated trafficking (test track) load trials (France and Germany only)

- 15% road network / AASHO road test data
- 15% unspecified

Thus, it can be seen that more research needs to be put into the formulation and validation of pavement design methodologies, accompanied by sound non-empirical material performance information.

3.5.1 Empirical Methods

Early pavement design methods were empirically-based, following methods such as the CBR Design Method. This method only applied to spray seal or very thin asphaltic surfaced full depth granular pavements. It considered only two factors, those were subgrade (CBR test) strength and design traffic, with the only failure mode acknowledged being rutting. The CBR test has been, and still is, internationally used to determine pavement layer thickness despite only providing qualitative information about the bearing capacity, which is the value of the loading intensity on the soil required to produce shear failure. Since the boundary and stress conditions in the CBR test are not comparable with those in a real pavement, the results should be applied with caution. In addition, a great deal of variability in test results has been found as the maximum particle size increases from sandy clay to crushed rocks (TSA repeatability report). This fact, along with geological variability has meant that no clear relationships between CBR and resilient modulus can be established as the scatter of data points is too great (Sweere, 1989). Although a value of 10 is used to equate the two parameters in Australia, $E_r = 10 \times CBR$ (Austroads, 1992)

Briefly, the CBR Method takes a "bottom-up" approach such that when designing a particular layer, all lower layers are considered to act as a subgrade with the CBR equal to the test CBR of the layer immediately below the layer being designed. The thickness of the layer is determined from empirical design charts, where the curves are based on equations of the general form:

$$\text{thickness} = \frac{c_3}{\sqrt{CBR}}\left(1 + c_4 \log N_{ESA}\right) \quad \ldots (3.7)$$

as determined by the U.S. Army Corps of Engineers and reported in Road Technology (Lay, 1998). Curves are derived in a number of countries with minimum thickness levels based on local practice. This method was used in Australia before the introduction of the NAASRA Pavement Design Guide (NAASRA, 1987).

Early empirical methods, which were common in the USA and in the UK, under Road Note 31, were the layer equivalency methods for the design of multi-layered pavements where the layers are of different materials. Asphalt was generally considered the standard material with an equivalency factor, E_qF of 1.0. Other materials had a lower factor (eg, granular material = 0.3 to 0.5), such that the thickness of alternative material when multiplied by E_qF would ideally perform the same as the calculated thickness of asphaltic material.

$$T_S = E_qF \times T_N \qquad \ldots (3.8)$$

where:

T_S = thickness of standard (asphalt) material

T_N = thickness of alternative material

A slightly modified form of equivalence method, still in use in the AAHSTO guide in 1986 (AASHTO, 1986), was the design structural number, SN developed from pavement performance data obtained during the AASHO Road Test. It is assumed that different materials with the same SN will behave identically. SN can be obtained from a table with subgrade CBR and design traffic as the inputs. A combination of surfacings, base and sub-base is selected according to:

$$SN = \sum_{i=1} a_i D_i \quad \ldots (3.9)$$

where:

a_i = structural layer coefficient of layer i, which is a measure of the relative ability of the material to function as a structural component of the pavement, where:

$a_2 = 0.249(\log_{10}E_{BS}) - 0.977$, base coefficient

$a_3 = 0.227(\log_{10}E_{SB}) - 0.839$, sub-base coefficient

D_i = thickness of layer i

For granular base and sub-base layers, a_i is multiplied by a 'drainage factor m_i', which depends on the drainage ability of the material or quality of drainage and on local climatic conditions or time taken to remove the water (eg, m_i = 1.4 in well-drained materials in areas of low rainfall and m_i = 0.4 for the opposite case). This factor effectively increases or decreases the structural contribution of a granular layer.

Equivalent thicknesses were also calculated from an elastic stress analysis by picking some criterion value (eg, vertical subgrade stress beneath the load) and maintaining it constant for various combinations of stiffness, E and layer thicknesses.

$$T_N = \Sigma T_i \left[\frac{E_N}{E_S} . \frac{1-\nu_S^2}{1-\nu_N^2} \right]^{\frac{1}{3}} \quad \ldots (3.10)$$

where:

E_s = modulus of the subgrade

ν_s = Poisson's ratio of the subgrade

Some of these methods are still used today in various Design Guides around the world.

3.5.2 Analytical Methods

Analytical pavement design methods first appeared in 1970s, although they were far from purely analytical, with still a clear reliance on empirically-based information.

Methods in use assume resilient behaviour of the pavement materials occurring in the loaded pavement, particularly after compaction and early wheel loadings have removed a large proportion of the permanent deformation. Thus, methods of analysis only consider a layered elastic assessment of the pavement structure which utilises elastic parameters of resilient modulus and Poisson's ratio to equate the applied stresses to their commensurate strains.

Elastic multi-layered theory was developed by Burmister in 1943 for two layered systems and in 1945 for three layered systems giving stresses, strains and displacements.

Assumptions for the systems include:

- all layers are infinite in the horizontal direction
- all layers are homogeneous, isotropic and linear elastic
- all layers have a finite thickness except the subgrade which is infinite
- full layer bonding occurs
- the applied surface loading is uniformly distributed

A fourth order differential equation is satisfied for each layer by using a stress function with four constants, viz:

$$\nabla^2\nabla^2\phi = 0 \quad \text{where stress function, } \phi = \frac{p}{2\pi}\left(r^2 + z^2\right)^{0.5} \qquad \ldots (3.11)$$

where:

p = uniform pressure

r = radius of applied surface load

z = depth in pavement layer

with principal strains determined according to the generalised Hooke's Law:

$$\varepsilon_1 = \frac{1}{E}[\sigma_1 - \nu(\sigma_2 + \sigma_3)] \qquad \varepsilon_2 = \frac{1}{E}[\sigma_2 - \nu(\sigma_1 + \sigma_3)] \qquad \varepsilon_3 = \frac{1}{E}[\sigma_3 - \nu(\sigma_1 + \sigma_2)]$$

... (3.12 to 3.14)

where:

E = elastic modulus

ν = Poisson's ratio

1, 2, 3 = indication of principal stress and strain directions

The modulus material properties assigned to each layer produce a major effect on pavement response. Burmister's theory was used to develop the Shell computer program 'Bisar' (BItumen Stress Analysis in Roads) (Shell, 1995).

3.6 Approaches of Current Pavement Design Methods

A select number of pavement design methods worldwide are to be considered in this study, namely:

- Austroads Method - Australia
- Shell Method - United Kingdom/Netherlands
- Asphalt Institute Method and AASHTO Method - USA
- Highways Agency - United Kingdom
- French Method – France
- Swedish Method - Sweden

It is intended that the methods will be reviewed in turn with a *summarised* discussion to highlight their merits and potential areas of concern, surrounding the modelling of the UGMs, as performed by pavement design engineers.

3.6.1 Australian Design

In Australia, the Austroads Pavement Design Guide (Austroads, 1992) is used to design road pavements. It considers pavements to be load-bearing structures which can be analysed in terms of stresses and strains and empirically based performance models.

In particular, the design of flexible pavements, incorporating unbound granular materials, requires the designer to follow the procedure presented in Chapter 8 of this Guide and is supported by design considerations for the pavement materials presented in Chapter 6.

The procedure allows for the subgrade to be treated as though it is a uniform, continuous material, with no rules presented for sub-layering. The unbound granular layers are considered to be uniform in quality with presumably the same material geologically and compacted to the same state conditions. The design modulus is estimated for conditions which "approximate those expected in service". Depending on the climatic region and moisture sensitivity of the materials, these conditions can vary considerable and are very dependent on temperature and rainfall (generally seasonally-based), material permeability and drainage conditions. Thus, it may be

necessary to consider not just the "equilibrium moisture content", but also other periods of marked climatic variation.

A procedure for assigning moduli to sub-layers is presented in the Austroads Pavement Design Guide (Austroads, 1992). Here, the number of sub-layers, *n*, used in the analytical model to account for non-linearity is derived from Table 8.2 in the Guide. It relies on knowledge of the stiffness at the top of the base and subgrade layers and the overall thickness of the UGM. After selecting *n*, the moduli of each sub-layer is calculated using the modular ratio relationship, viz:

$$R = \left(\frac{E_{\text{top of base}}}{E_{\text{subgrade}}} \right)^{\frac{1}{n}} \quad \ldots (3.15)$$

where:

R = modular ratio, being the ratio of the vertical moduli between adjoining sub-layers

$E_{\text{top of base}}$ = modulus at the stress level determined at the top of the unbound base layer

E_{subgrade} = modulus at the stress level determined at the top of the subgrade

n = number of sub-layers in which the total thickness of UGM is divided into

Given that the modular ratio (a number) may be calculated from the above relationship, the modulus of each sub-layer may subsequently be calculated by multiplying 'R' by the known modulus of the adjacent underlying layer, starting with the subgrade.

The new draft Pavement Design Guide (Austroads, 2001) follows this same approach, however, to ensure that an 'adequate' number of equi-thick sub-layers are used, the value of n is set to 5. For a granular pavement containing a 450mm total granular layer thickness. This equates to sub-layers of 90mm each. This is considered too great to provide for significant non-linearity which occurs particularly in the top 200 to 250mm of a thinly surfaced pavement, where stress gradients are

the greatest (refer to §5.4.1). In addition, under a 35mm asphaltic surfacing, the vertical modulus of the top sub-layer is given as either 425MPa for a high standard granular material or 300MPa for a normal standard granular material, or as a value determined mathematically from the subgrade modulus and total granular layer thickness. This is considered a backward step which does not provide a modulus profile which (i) reflects the stress level at which the material operates in a sub-layer, (ii) incorporates material variations for layer to layer caused by either product variation or in-service conditions.

It is reported by Uzan (Witczak and Uzan, 1988) from analytical studies that the "subgrade modulus has a negligible effect on the base modulus. This is due to the fact that changes in the subgrade modulus has a minor effect on the stress distribution in the base layer" (as has also been determined by the Author in §5.2). Uzan also reports that "sub-base modulus (and also base modulus) are only slightly dependent on subgrade modulus assuming that the sub-base material throughout the depth of the layer is the same". However, it is reported by Witczak and Uzan that "studies have shown that the compaction of the granular sub-layers (sub-base) can produce sub-layers of different properties, depending upon the specific subgrade support encountered. This could well make the UGM a little more sensitive to subgrade stiffness".

With consideration given to *in-situ* stress levels and moduli determined from material performance-based laboratory testing, it is often apparent that the modulus of low-lying sub-base sub-layers will be substantially greater than that at the top of the subgrade. Thus, the modular ratio will under-estimate the stiffness of these lower sub-layers.

To further compound the problem, a table of presumptive modulus values for granular materials is provided in the Design Guide (Table 6.4a) when no other source of material performance indicators is available. These presumptive values have no relationship to material geology, state conditions or the stress conditions at which they are recommended for use. From the extensive testing of UGMs undertaken in Australia over the years to determine their resilient properties, it appears that the

suggested 'typical' numbers are most often too high in magnitude. A value of 500MPa is suggested for a high quality crushed rock overlying a granular material or stiff cement material. A significant number of pavement failures have resulted throughout Australia by applying 'high' figures in a pavement design response model without substantiation from performance-based laboratory testing. A contributing factor to this was that most State Road Authorities (SRAs) considered their commercial crushed rock materials to be of high quality, hence the high moduli adopted for design. As a result, the work undertaken by the Author (Chapters 8 and 10) may be used in conjunction with that of other SRAs, to modify this table of values in the new revision of the Guide.

The revised draft 2001 Austroads Pavement Design Guise (Austroads, 2001) recognises the importance of permanent deformation as a "primary distress mode" and it is considered in §6.2.4 that a "number of models are available which can be used to estimate rutting potential (eg, VESYS) for material ranking (comparative) purposes". This is in line with the views of the Author, although it is considered that the Guide could have presented some data for a range of materials and should have provided some guiding limiting values in order to advise the designer of an acceptable ranking scale. Without this information, the designer has little to apply to a material assessment.

3.6.2 Shell Method

The Shell Pavement Design Manual (SPDM) documented one of the first analytical pavement design procedures (Shell, 1978). It is stated that "care must be taken that any unbound layers used in the road pavement are capable of developing an adequate modulus and resistance to shear *in-situ*". However, the method does little to ensure these factors are accounted for. To limit the number of design charts documented within the Manual, the moduli of the unbound layers are not considered as independent parameters, but relate to the subgrade modulus and thickness of the granular base layer (see Equation 3.16). This is somewhat similar to the modular ratio approach adopted within the Australian procedure.

$$E_2 = k \times E_3 \, , k = 0.2 \times h_2^{0.45} \, , 2 < k < 4 \qquad \ldots (3.16)$$

where:

E_2 = modulus of the unbound layer

E_3 = modulus of the subgrade

h_2 = thickness of the unbound layer (mm)

When the SPDM was formulated, only limited field measurement information was available concerning this modulus relationship, given the scatter of the variable 'k' which was found to exist. As a result, "the eventual design may contain some degree of uncertainty related to the properties of the unbound base layer(s)" (Gerritsen and Koole, 1986). Further work conducted by Gerritsen and Koole, having assessed some 250 pavement data sets using the Falling Weight Deflectometer (FWD), found that the value of 'k' varied considerably. This was attributed to the type of unbound material used which suggests that the modulus of the unbound layer(s) is better determined from laboratory performance testing than by using a subjective ratio. The approach of fixing E_2 as a function of E_3 renders the SPDM insensitive to the quality of the material used as the granular base. As mentioned in the paper by Sweere (1989), the "Addendum to the Shell Pavement Design Manual" (Shell, 1985) recognises the shortcomings of fixing E_2 as a function of E_3 so correction formula are given that allow for stiffnesses of the granular base E_2 to be used as entry to the design. However, this is still not the same as using results obtained from direct measurement.

3.6.3 Asphalt Institute Method and AASHTO Method

These methods are based on a mechanistic design methodology. The Asphalt Institute method (Shook et al, 1982) has produced a series of charts to hasten the design of a pavement. The process used to derive the charts has considered the untreated aggregates bases to have stress-dependent modulus properties by adopting the $k_1\theta^{k2}$ model in the analytical modelling process. From the analysis of RLT testing undertaken by a range of investigators, material modulus model parameters have been subsequently reviewed and a range then adopted for this method. The method recognises the importance of environmental effects on UGM modulus by providing a tabulation of the parameter 'k_1', which can be seen to vary in magnitude according to the month of the year. This variation is to account for freezing and

thawing effects and variable moisture conditions expected within the granular base material throughout a yearly analysis period. The method encourages the use of direct measurements to account for the properties of the unbound materials and subgrade where possible to conduct such performance tests.

The AASHTO Guide for Design of Pavement Structures (AASHTO, 1993) was based on the results of the AASHO Road Test, supplemented by existing design procedures. This method, which was first published in 1972, goes further than the Asphalt Institute method. Pavement layer materials are principally characterised in terms of resilient moduli, which should be determined using cyclic loading triaxial tests. However, if the designer has a great deal of experience with 'layer coefficients' (see §3.5.1), then moduli characterisation is not essential, and the structural number approach can be followed. The Guide provides relationships between resilient moduli and structural layer coefficients, given in Equation 3.9.

Interesting, §3.3.3 of the Guide states that "the strength of the material is important in addition to stiffness, and future mechanistic-based procedures may reflect strength as well as stiffness in the materials characterisation procedures". The Author will discuss the importance of this fact in §5.6 and presents a classification model that identifies the quality class of material, as linked to pavement layer usage.

The AASHTO Guide identifies seasonal moisture to "quantify the relative damage a pavement is subjected to during each season of the year and treats it as part of the overall design". The moduli of granular materials are given values based on either laboratory testing or according to the $k_1\theta^{k2}$ model mentioned above; with $k_1 = 3000$ (wet) to 8000 (dry) and $k_2 = 0.5$ to 0.7. For the subgrade, an effective resilient modulus is established which is equivalent to the combined effect of all the seasonal modulus values. The seasonal moisture conditions for which the roadbed soil samples are tested will yield "significantly different moduli". "For example, in a climate which is not subjected to extended sub-freezing temperatures, it would be important to test for differences between wet (rainy) and dry seasons". The year is separated into various component time intervals (of not less than ½-month) during which the different moduli are effective (up to 24, ½-months). For flexible pavement

design, the weighted value of effective modulus is that which gives the equivalent annual damage obtained by treating each seasonal separately and summing the damage.

Given the concern over lower material modulus due to high moisture levels, a number of Agencies in the USA are now considering or constructing pavements with a drainage course or layer, where either:

(i) the base is used as the drainage layer

(ii) the drainage layer is part of, or below, the sub-base

The Guide tables information for estimating the permeability of various material types and materials must meet vertical drainage permeability criteria. Specification for both the design and construction of drainage courses are "currently under development". Target permeability values for drainage layers of 1000 to 3000ft/day (3.5×10^{-3} to 1.1×10^{-2}m/s) combined with grading limits are specified in the Guide. These values compare favourably with those given in §2.3.4 for a base material.

3.6.4 Highways Agency, UK Method

The UK pavement design procedure is empirically based, having been established through monitoring service levels and maintenance cycles of pavements. The procedure utilises charts for determining sub-base and capping thickness, based upon a known subgrade CBR. Roadbase materials used in flexible pavements are bound with bituminous binder and are, therefore, not a focal point for discussions. Interestingly, analytical pavement design is not generally used in the UK. Where it is to be used, "the Overseeing Department must be consulted before such methods are used to produce designs other than those given in the appropriate Chapters" (Highways Agency, 1994).

A key aspect of this procedure is the importance of drainage, which is of little surprise given the rainfall in this geographic region. Drainage is considered "of vital importance to keep water out of the sub-base, capping .... both during construction and during the service life of the pavement". To support this statement, the Manual states that a downslope route from the sub-base to the drain should always be

present. Further, the method considers it "useful to check the speed at which water can drain out of a granular sub-base as a result of ingress". A procedure for calculating this, using a method proposed by Jones and Jones (1989), is referred to.

The method also states that "drainage of the sub-base may only be omitted if the underlying materials (capping and subgrade) are more permeable than the sub-base *and* the water table never approaches the formation closer than 300mm."

3.6.5 French Method

The French method is covered by the French Design Manual for Pavement Structures (Corté et al, 1997). It combines "useful aspects of rational mechanics plus lessons gained from experimentation". Some key aspects of this design method involving UGMs are discussed below.

The use of untreated graded aggregates in flexible structures is limited to low and medium traffic pavements, depending on the stiffness of the foundation. The materials may be used as a road base layer for low traffic roads, with an annual daily mean volume in both directions of less than 150 heavy lorries (French traffic class T3). Alternatively, they may be used for sub-base layer applications on (low or) medium traffic roads, with an annual daily mean volume in both directions of up to 750 heavy lorries (French traffic class T1) for a pavement foundation of at least 50MPa stiffness.

Knowledge derived from observation of the behaviour of real pavements, such as those experiments conducted on the road structure test track at Laboratoire Central des Ponts et Chaussées (LCPC), have been used to specify criteria to check the permanent strains of the subgrade ***and*** unbound layers. In the case of low traffic pavements ($< 2.5 \times 10^5$ NEs) composed of a thin wearing course over a based of untreated granular materials, no criterion is introduced. With reference to Figure 3.1, this type of granular pavement could be expected to have a wearing course thickness of approximately 40 to 50mm. It is considered that through the choice of characteristics for the materials that, empirically, an acceptable rutting strength of the untreated graded aggregates will exist. However, for medium traffic pavement types

(bituminous pavement with a granular sub-base, inverted structure, etc), the rutting strength is verified at the top of the UGM layer as per the criteria of the same type as that chosen for the subgrade. Generally, given that UGMs are of higher quality than subgrade materials and their thickness can be thinner in nature (particularly for inverted structures), the limiting strain is allowed to be 20% higher than that chosen for the subgrade, namely:

$$\varepsilon_{z,ad}\,(\mathrm{GRH}) = 1.2 \times 0.012(\mathrm{NE})^{-0.222} \quad \text{for medium traffic} \qquad \ldots (3.17)$$

where:

$\varepsilon_{z,ad}$ (GRH) = working vertical compressive strain for graded aggregate

In the French method, the material modulus values used for the design of the UGM pavement layers are dependent on the pavement type, amount of traffic and characteristics of the aggregates, as reported in Table V.3.2 (Corté et al, 1997). The method will allow moduli to be used directly from repeated load triaxial testing in keeping with calculated structural stresses, determined under the most unfavourable hydraulic conditions the pavement layer is expected to encounter. However, the guide states that "in the absence of results from triaxial tests, and while waiting for a unified procedure ..." a table of values is used in practice". RLT testing (at stress conditions of p_{max} = 250kPa and Δq = 500kPa) has been used to *characterise* the material for suitability in terms of characteristic modulus of elasticity, E_c, and a value of permanent axial deformation, A_{1c}, obtained during the conditioning phase of the test (as discussed in §2.3.2).

Table V.3.2 in the French Manual generally states:

- for low traffic pavements
  - the road base may be assigned a modulus of either, E_c = 600, 400 or 200MPa, depending on the traffic category (ranging from a limit of T3, being 150 heavy vehicles per lane per day to T5, being 25 heavy vehicles per lane per day).

  - the sub-base is divided into sub-layers 250mm thick, and a modular ratio is applied such that $E_i = k\ E_{i-1}$, starting with E_{i-1} being that of the pavement foundation and with k varying (from 2 to 3) depending on the traffic category
- for medium traffic pavements
  - the sub-base is divided into sub-layers 250mm thick, and a modular ratio is applied such that $E_i = 3\ E_{i-1}$, starting with E_{i-1} being that of the pavement foundation and with E limited to 360MPa
- for inverted structures, E = 480MPa

Critical to the success of pavements designed with these modulus values is the link between proven field performance of the local UGMs (having been tested in structures constructed within the experimental accelerated loading test track) with laboratory RLT testing results, which characterise the materials at a stress condition appropriate to the pavement configuration and axle loadings.

3.6.6 Swedish Method

The Swedish method is a mechanistic / empirical design system for local conditions (Djärf et al, 1996). This method recognises a number of contributing causes, which create soil stiffness variations within and between pavement sites. It is required that pavements be designed to consider two seasonal periods for subgrade soil moduli namely, spring (thaw) and summer/autumn. A "freezing index" is used to classify the road into one of six climate zones, which in turn controls the length of the two design seasonal periods. The method presents tabular values for a range of subgrade soil types and also considers that higher formation moduli may exist where materials are located on an embankment > 1m in height, where drainage conditions are improved beyond pavements constructed within cuttings. In addition, the groundwater level beneath the formation level is considered to effect the soil moduli.

For unbound materials, fixed moduli have been introduced into the design system, unlike for the subgrade soil mentioned above. In fact, the same values are quoted (p.39, Djärf et al, 1996) for *both* of the seasonal periods. This is contrary to "good practice" considering the strain rate and resilient modulus data presented in Figures 2.15A and 2.15B and those in Chapter 8 from testing a wide range of materials,

where moduli decreased with increasing moisture content. The Swedish method considers that during the initial stages of thawing, when a good deal of moisture has been released from the solid form, possibly leading to saturation, that the "roadbase modulus is assumed not to decrease". The method also has not allowed for sub-layering of the UGMs to account for non-linear variations of moduli with stresses.

3.7 Other Studies Indicating Potential Modifications to Current Methods

3.7.1 "Finite Thickness" of Flexible Pavement

The South African study of Thompson and Visser, discussed in §3.4.1, of unpaved granular roads used by ultra-heavy mining trucks included the measurement of four individual pavement layer deflections using multi-depth deflectometers. Four different load applications were measured, ie front and rear axle loads each being either empty or full. Here it was found that no load induced deflections were recorded below approximately 3.2m depth, assuming no deflection of the 5 to 9m deep reference points of the instruments. This fact indicates that an "equivalent stiff layer" could be included in the multi-layer elastic response model of a pavement below this depth. The depth could be taken as 3m for modelling ultra-heavy mining trucks on unsealed granular pavements.

To determine an 'appropriate' depth to specify for pavements loaded in the range of an equivalent standard axle, reference is made to the work of Goode (1993). Here five different flexible granular pavements (referenced to as Sites 1, 2, 6, 7 and 8), each with a bituminous surfacing of thickness 65mm or less, were tested with a FWD to measure deflection bowls. Dynamic drop loads of 40 and 60kN were applied to a 300mm diameter plate (equivalent to a surface stress of 565 and 850kPa). The aim being to model the pavement using a back-analysis program to best match the computed deflection bowl to that measured. Critical to minimising the error between the two bowls is the application of sound modelling principals, such as the one described above. The study found that best overall agreement between the two deflection bowls (computed and measured) occurred when a very stiff layer was modelled at a depth of 2m below the pavement surface. Only for one pavement, 3m

provided the best matching solution. In addition, the study also found this method provided the best agreement between the back-calculated stiffness values and the resilient modulus values determined by laboratory RLT testing.

This analytical approach is very important to implement when calculating surface deflections of the pavement structure under a wheel load. If one is modelling a granular pavement placed upon soft clay subgrade of 'infinite depth', as is commonly done by pavement designers, a linear elastic procedure will compute all the contributions to the surface deflection from the granular sub-layers and subgrade. Often a 'constant value' subgrade resilient modulus is used in the pavement response model. However, it is well known from laboratory testing that material elements located deeper into the subgrade are subjected to lower deviator stresses (often 15 to 20kPa or less), upon which subgrade modulus is often highly dependent. This testing has shown that resilient modulus can increase greatly with decreasing deviatoric stress (Mundy, 1992). Thus, the subgrade becomes apparently much stiffer with depth. The placement of a very rigid layer (high resilient modulus, approximately 10GPa) at this depth ensures that deformations computed in all granular sub-layers and subgrade sub-layers, to a depth of 2 or 3m only, will contribute to the resulting surface deflection. In addition, if a very stiff layer is placed an acceptable depth, rather than using an infinite subgrade depth, this in turn allows much smaller deflections and predicted strains in the pavement layers to be calculated, which in turn results in a longer pavement design life.

This positive approach is taken in Sweden for linear-elastic modelling of flexible pavements by constructing a response model with "a rigid layer of infinite thickness placed 3m below the road surface" (Djärf et al, 1996).

3.8 Summary of Key Findings

As a result of the work undertaken in this Chapter, there is a need to highlight the important factors concerning UGMs which should be considered in the pavement design process. Improved analytical modelling, using sound principals to account for material property variations and *in-situ* conditions within the structure, is necessary

for correctly calculating the performance of flexible pavements. Some essential considerations from this study include:

Material Performance Information:

A1 assessing the shear strength of constituent UGMs (according to material failure law). Refer to §5.6 for detail.

A2 considering the influence of material functional performance, or quality of *all* pavement layer materials, particularly those higher up in the pavement (eg, basecourse 1 and 2 layers). Refer to §3.4.1 and §3.6.1 for detail.

A3 avoiding the use of presumptive values without sound basis (eg, avoid non-geologically based, non-stress level linked, those which do not account for moisture sensitivity, not linked to field performance, etc). Refer to §3.6.1 and §3.6.5 for detail.

A4 avoiding the use of empiricism to describe material properties (UGMs and subgrade). Refer to §3.5.1 for detail.

Pavement Modelling:

B1 accounting for non-linearity where the extent of sub-layering in the UGMs (and subgrade) needs to be linked to the stress change gradient within the pavement layers (eg. spray seal surfacing versus thin bituminous surfacings versus thick bituminous layers). Refer to §5.4.1 for detail (particularly Figures 5.8A, 5.8B and 5.9).

B2 dividing one year into different seasonal periods, in keeping with moisture content changes in the UGMs, each with a unique set of material properties assigned. Refer to §2.4.1 for detail. The notion for separating a year into 24-½ month intervals (see §3.6.3), and subsequently aggregating the ½-months into seasons, is considered a sound approach.

B3 assuming there are no load-induced elastic deflections below 2 to 3m with an "equivalent stiff layer" included in the multi-layer elastic response model of a pavement. Refer to §3.7.1 for detail.

B4 accounting for overburden and residual stresses (refer to Chapters 4 and 5)

Pavement Design Performance Criteria:

C1 establishing upper limits on the maximum level of vertical compressive strain tolerable in the UGMs. Refer to §3.4.1 and §3.6.5 for detail.

C2 assessing the influence and limits for the plastic behaviour of UGMs. Refer to Chapter 8 for detail.

Having assessed a number of different pavement design procedures in §3.6, a table of limitations, summarising the points above, has been prepared (Table 3.2).

It can be seen from the results of Table 3.2, that hydrological conditions in pavement design methods (Item B2) are considered to a very limited fashion. However, this effect is acknowledged as being an important issue affecting the pavement's performance, being clearly illustrated in Chapter 2.

Item	Pavement Design Method					
	Australia	Shell	AASHTO/AIM	HA - UK	France	Sweden
A1	×	×	× (1)	×	×	×
A2	✓ partial	×	✓	×	✓ partial	×
A3	×	×	✓ partial	×	✓ partial	×
A4	✓ partial	×	✓	×	✓	✓ partial
B1	✓ partial	×	×	×	✓ partial	×
B2	×	×	✓	×	×	×
B3	×	×	×	×	×	✓
B4	×	×	×	×	×	×
C1	×	×	×	×	✓ partial (2)	×
C2	×	×	×	×	✓	×

TABLE 3.2: PAVEMENT DESIGN METHOD LIMITATIONS

Note: (1) Strength classification assessment is currently being considered for the AASHTO procedure.

(2) In the case of low traffic pavements ($< 2.5 \times 10^5$ NEs) composed of a thin wearing course over a base of untreated granular materials, no criterion is introduced. It is considered that through the choice of characteristics for the materials that, empirically, an acceptable rutting strength of the untreated graded aggregates should exist.

The use of an incremental pavement design procedure that can take into account material changes due to climatic effects and time effects was also recommended by COST 333 (European Commission, 2000). Computations were performed in Appendix 1, by considering a thinly surfaced flexible pavement, to demonstrate the importance of using a methodology that allows for estimating the modulus of *all*

subgrade and unbound layers for different seasons. The variability of the modulus of the subgrade soil and other unbound materials will depend on the materials themselves, their position in the pavement, and on the annual variability of the hydrological and pavement drainage conditions. The use of layer moduli for different seasons or transient conditions allows the designer to determine more accurately the damage induced by traffic loads in each season. This effect was seen in the markedly different vertical compressive strain profiles resulting from the examination of two identical pavements, subjected to standard axle loading, where one had a higher moisture content locked into the basecourse 2 layer.

Earlier design methods tended to rely on a somewhat crude assessment of material parameters for input into the design model, upon which design calculations are based. However, on examining a number of design methods it was found that many Authorities are now beginning to specify the RLT test as a 'preferred method' for determining material properties relevant to the design modelling process – which is essentially resilient modulus. It was noted though that many methods still allow for a good deal of empiricalism, especially for the determination of subgrade properties. Despite the complexities of material performance in real pavements, which exhibit combined resilient and plastic behaviour (as illustrated in Chapter 2), the latter is very seldom specified in any design methods. The French are the only country (for the methods examined) which act to limit the damage which could result from the plastic behaviour within the UGMs; however, they only apply the performance criteria for medium traffic (and not low traffic) roads. An upper limit on the vertical compressive strain of 1600 microstrain, at the top of the base layer under a thin surfacing, should be used in design practice until further research can refine this value. In addition, a value of 900 microstrain could be used at the top of the second base layer.

Inconsistencies or shortcomings have been highlighted in a number of the pavement design procedures examined. These methods enable pavement designers to undertake detailed computational analysis of the modelled structural response, but rely on empirical parameters or relationships to provide resilient modulus of the

materials (see limitation Items A3 and A4 above). The Shell Pavement Design method is one such example of this.

In summary it is considered that some of the pavement design methods and practice examined above are severely limited by:

- adequate procedures to correctly model the pavement structure by using sufficient sub-layering to account for the stress-dependence of the materials. Thus, the non-linear behaviour of the pavement materials and subgrade should be modelled well in the design process. This was supported by the findings of the "Science project" (summarised by de Boissoudy, 1996). Here it was proposed that "an iterative procedure for taking account of the non-linear behaviour of granular materials in classical multi-layer linear elastic analysis, by dividing the granular layer into several elastic layers, with different elastic moduli" be adopted. This shall be highlighted in Chapter 5 by mechanistically analysing pavements with surfacings of different thicknesses.
- calculations performed to 'accurately' determine the range of expected stress conditions in the pavement due to compaction processes, overburden, material failure criteria and traffic loading. This shall be examined further in Chapter 4.
- inappropriate (or sometimes absent) material performance information in the modelling process, taking into account calculated stress conditions and local climatic conditions.
- performance criteria, not extending to material shear strength assessment and vertical compressive strain (or stress) limitations placed upon the UGMs to reduce the risk of permanent deformation or rutting occurring within the material.
- lack of usage of iterative techniques to derive a final solution to the designed pavement – not ensuring final agreement is achieved between stress and moduli in the output.

As stated by Sweere (1989), "the future in pavement design clearly lies with the mechanistic methods. They are more versatile in dealing with new conditions and materials than the empirical methods based solely on experience". In addition, they will allow engineers to consider the different axle loadings, which have been adopted for design from country to country.

Finally, it is considered that for the pavements currently in-service that limited pavement capacity is available in reserve to accommodate the heavier and longer vehicle combinations now using the road network. This statement is supported by the fact that statutory axle mass limits have increased dramatically over the last 15 to 20 years and now, in many countries, exceed the design axle loading. In Australia, a 10t limit is allowed for certain buses (representing a 22% overloading beyond the design value of 8.2t), whilst in the United Kingdom a 11.72t maximum loading is permitted for certain vehicles (representing a 44% overloading beyond the design value of 8.15t). This situation should be addressed immediately to achieve better compatibility between operating conditions and design.

CHAPTER 4
PRACTICAL DETERMINATION OF INSITU STRESSES

4.1 Introduction

To fully describe pavement response, one needs to accurately measure stresses, strains and deflections and apply sensible analytical models which model well all of these conditions. The level of accuracy obtained in the measurement of a stress field in a soil medium requires an understanding of the interaction between the pressure cell and the surrounding material and correct installation of the instrumentation. Even so, the soil stress measurement task still may possess considerable uncertainty. This Chapter investigates research studies undertaken worldwide to practically measure stresses within the pavement. The stresses measured as part of the studies are to be compared with theoretical stress determinations. For vertical stress experiments, measured values are compared with results from linear elastic layered theory or Boussinesqu theory. Whilst for lateral residual stresses, resulting from compaction loading, measured values are compared with results from theory presented by key researchers and the Author.

4.2 Measurement Techniques

Stress determinations within unbound materials are arguably the most difficult condition to measure. The manner in which the cell interacts with the soil medium can severely effect the performance of the cell. Pressure cells used for this task are either of the diaphragm type or are hydraulic cells. Diaphragm cells contain a thin circular diaphragm attached to an outer annulus (see Figure 4.1). The deflection response of the active diaphragm face to external pressures is measured through internally bonded resistive or vibrating wire strain gauges.

Hydraulic cells, however, consist of two plates welded together around their periphery. The chamber in between the plates is filled with a fluid (oil, glycol, water), with a pressure transducer used to measure the internal pressure of the fluid.

A detailed discussion on the cells types and their advantages or disadvantages is provided by Dunnicliff (1988) and Hovorslev (1976). In both cases the plane of the cell is orientated normal to the direction in which the pressure is to be determined.

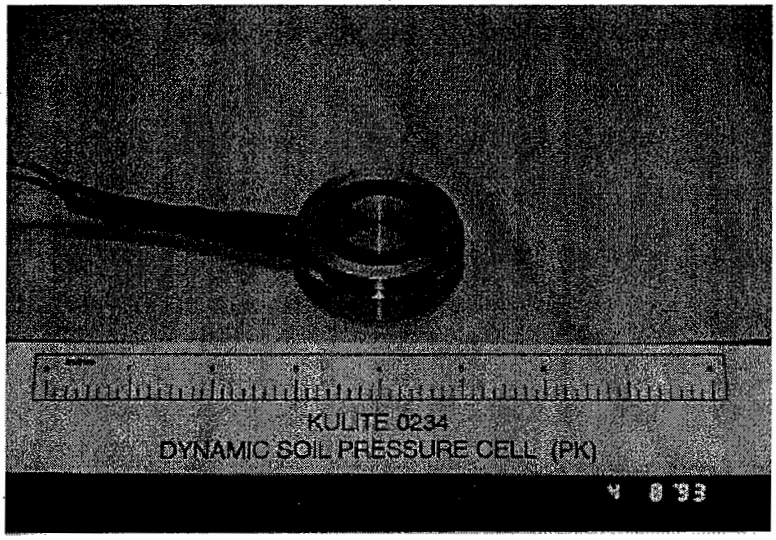

FIGURE 4.1: DIAPHRAGM PRESSURE CELL FOR MEASURING *IN-SITU* STRESSES

The pressure registered by the cell can be greatly influenced by many factors. These include the stiffness of the cell to that of the surrounding material, the geometry of the cell (defined by the aspect ratio of thickness to diameter), the packing of the grains on the diaphragm face, installation techniques/placement conditions (hole cut for cell, cell orientation, disturbance of soil around the cell, etc) and the nature of the surface loading (rigid or otherwise). The effect of cell stiffness is particularly important as the presence of the cell distorts the free-field stress in the soil. If a cell is soft compared with the surrounding soil medium, the cell will under-register the soil stress measured. Conversely, a very stiff cell will over-register. For any given combination of soil and cell, the larger the inward displacement, the larger is the stress distribution in its vicinity, and therefore, the larger is the measurement error.

Askegaard (1978) has shown that the signal from a diaphragm-type stress cell would particularly consider two of the factors above, of aspect ratio and stiffness ratio, and have the form of:

$$q = C \times \sigma_z + D \times (\sigma_x + \sigma_y) \quad \ldots (4.1)$$

where

q = pressure in cell liquid (kPa)

σ_z = stress within soil acting normal to the plane of the active cell face (kPa)

σ_x , σ_y = stress within soil acting parallel to the plane of the cell (kPa)

C = aspect ratio dependent constant

$$= \frac{B}{D} \quad \ldots (4.2)$$

where B = cell thickness (mm)

D = cell diameter (mm)

D = stiffness ratio or flexibility factor (cell to soil) dependent constant

$$= \quad \ldots (4.3)$$

where E_s = Young's modulus of the soil (MPa)

E_c = Young's modulus of the cell (MPa)

d = diameter of the cell diaphragm (mm)

t = thickness of the cell diaphragm (mm)

One method of comparing the stress measurement results is to compute the registration ratio, Cr, for each cell (see Equation 4.4)

$$Cr = \frac{\text{normal stress measured by the cell}}{\text{free field normal stress that would exist if the cell were not present}} \quad \ldots (4.4)$$

A positive value of Cr means over-registration because the gauge is giving too high a reading. Conversely, a negative value of Cr means under-registration.

It was found by Collins et al (Collins, 1972) that the registration ratio is highly dependent on the aspect ratio of the cell used and the stiffness ratio of the soil medium. By minimising the aspect ratio, the registration ratio may in turn be minimised. In addition, Selig (1989) states that "the best situation is to have a high gauge to soil stiffness ratio to minimise the change in error as soil stiffness changes" (with depth into the UGM). In addition, registration ratio is effected by deflection characteristics of the sensing element, ratio of the soil stress transverse to the gauge

to the stress normal to the gauge (Selig, 1989). As stated by Van Deusen (1991) in a field and laboratory study of soil-stress cells, "a sound knowledge of soil-cell interaction is very important if cell stress measurements are to be clearly interpreted".

A design procedure for pressure cells with free diaphragms is presented by Brown (Brown, 1977) which allows the cell registration to be correctly determined by designing for a range of factors including aspect and stiffness ratios, cell material, maximum aggregate size, minimum stress measured and stress resolution.

Information on the accuracy and precision of stress measurements in soil is insufficient to draw conclusions concerning their benefits, due to the lack of procedures directed at the 'best practice of selection and usage'. Selig (1989) observed that the coefficient of variation for cell stress measurement is as "high as 60% in field tests, although more likely values are ±25%. The contribution of this variability due to placement has been reported to be ±6 to ±15%". Values of –40% to +80% of the mean (under and over-registration, respectively) are reported as clearly possible and inaccuracies of 20% should be expected. Brown (1977) also stated that "because of the many difficulties involved, accuracies better than about 20% cannot be expected".

4.3 Vertical Stresses

4.3.1 Background

The measurement of vertical stresses in pavements is just as difficult to achieve as for determining lateral stresses. The success of the measurements in unbound granular materials can be largely attributed to the nature and quality of the cells and the methodical care applied to the cell placement preparation in the compacted materials.

The magnitude of vertical stress at a point due to a load at the pavement surface will depend on the applied pressure as well as the magnitude of the load, as represented by Equation 4.5.

$$p = \frac{P}{\pi r^2} \qquad \ldots (4.5)$$

where p = tyre pressure (kPa)

P = total wheel load (kN)

r = radius of the approximate tyre patch at the tyre / pavement surface interface (m)

Figure 4.2 represents the Boussinesq calculated vertical stress in an "ideal soil mass" (one of constant modulus and homogeneity) due to two combinations of tyre pressure and total wheel load. The wheel of 2.05t represents one-quarter of the 8.2t ESA loading commonly used in a number of countries (see Table 3.1). The higher loading of 3.25t is one-quarter of the 13t French ESAL.

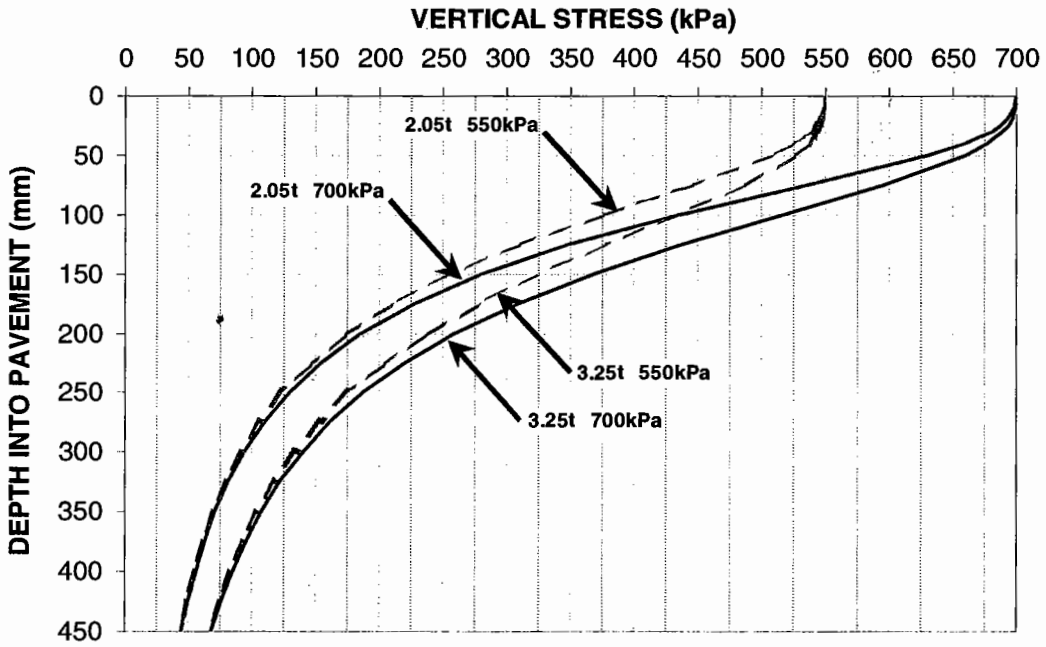

FIGURE 4.2: VARIATION OF VERTICAL STRESS WITH DEPTH, USING BOUSSINESQ

It can be seen that the effect of the high tyre pressure is pronounced in the upper layers of the pavement to a depth of about 200 to 250mm, depending on the magnitude of the applied load. As a result, higher tyre pressures will dictate the use of higher quality materials in the upper pavement layer regions to accommodate the

greater stresses to be carried. On the other hand, for a constant tyre pressure, an increase in total load increases the vertical stress for all depths.

Other factors will also effect the vertical stress measured at a point such as the variation in the resilient modulus within the UGM and the ability of the material itself to spread the load radially in a pyramidal manner. Both factors will depend on the quality and geological nature of the material (eg, sand, gravel, crushed rock). This will be seen in load transmission experiments performed at the CAA Technical Development and Evaluation Center at Indianapolis (§4.3.2.3).

A number of separate studies are examined below to determine the "fit" of the measured pressures to those computed from elastic theory (either layered systems, Burmister, or single layer, Boussinesq).

4.3.2 Measurement Studies

4.3.2.1 Plate Loading on Pavement, Centre d'Experimentations Routières, France

A recent study to measure *in-situ* vertical stresses within a flexible pavement was undertaken at the Centre d'Experimentations Routières (CER) in Rouen, France. Two lower traffic flexible pavements were built with two different granular materials, one a crushed granite and the other a crushed limestone. A 60mm bituminous wearing course provided the surfacing. The cyclic load applied to the pavement was through a ϕ400mm rigid steel plate with a 10mm thick neoprene interfacing plate. The applied load varied up to a maximum of 65kN.

It should be noted that the modulus of the asphalt and subgrade were found to be 2084MPa and 212MPa, respectively. In addition, the 0/20mm granular materials were compacted at OMC in a single layer of 350mm, which was to yield a DDR of only 95.5% of modified Proctor.

Two vertical KIOWA pressure cell transducers were placed very near the top (pA1 and pA2), at a depth of 50mm, and two near the bottom (pA3 and pA4) of the granular layer. All transducers were placed at a radius of 100mm from the centre of the plate. The upper transducers were compacted in a manually excavated hole,

which was filled by 5mm of fine sand, then granular material followed by compaction.

The vertical pressures measured in the granite material from the experiment are compared with those computed by the Author, having performed a non-linear elastic analysis using modulus values calculated from the Boyce model parameters (Boyce, 1980) reported in the paper by Hornych (Hornych et al, 2000). Overburden stresses were added to the stresses calculated from the imposed plate loading of 65kN.

Briefly, the pavement was modelled using non-linear elastic theory by sub-layering the UGM layer into five sub-layers, as represented in Figure 4.3. The final values of resilient modulus obtained for each sub-layer are shown in the Figure, having used the isotropic Boyce parameters for the Granitic material as reported by Hornych of K_a = 41.4, G_a = 74.6 and n = 0.309. Moduli were determined initially by using 'seed' values in the response model, then determining the stresses at the midheight of the sub-layers having performed a calculation using the computer program NONCIRL. The 'new stress' derived from the program were then used to calculate new moduli according to the Boyce equations given in §6.3.6. These values were then input to NONCIRL and an iteration, based on stress, was again performed. The procedure was repeated until convergence of stress and moduli occurred. The theoretical stress levels, determined at each cell positions, could then be computed.

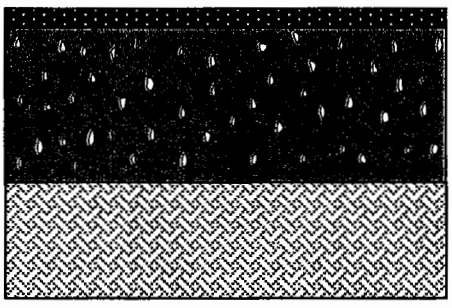

FIGURE 4.3: PAVEMENT RESPONSE MODEL USED FOR ROUEN EXPERIMENT

The large discrepancy between the measured and theoretically determined results can be seen in Table 4.1. The registration ratios calculated for the four cells are all

approximately equal to 2, except for cell pA1 which may have under-registered based on the results of the other three cells.

The study found difficulties with the pressure measurements as the cells, which are known to work quite well in fine-grained soils, did not perform well in the UGMs. Hornych reported that "the measured pressures appeared to be very high; when compared with pressures calculated using linear elastic or non linear models, they were about twice as high *(this is in agreement with the findings of the Author)*. In addition, pressure transducers pA1 and pA2, placed at symmetrical positions of 100mm radially from the central loading axis, gave quite different results (40% difference for the 65kN load)". The results were also well scattered. In addition, Boussinesq calculated stresses have been determined, and reported in Table 4.1, which also show that the pressure cells were over-registering.

Vertical Pressure Determination	Cell Id.			
	pA1	pA2	pA3	pA4
Measured Stress (kPa)	**550**	**760**	**290**	**295**
Theoretical Stress – Burmister (kPa)	**388**	**388**	**141**	**141**
Registration Ratio	**1.42**	**1.96**	**2.06**	**2.09**
Theoretical Stress – Boussinesq (kPa)	**462**	**462**	**168**	**168**
Registration Ratio	**1.19**	**1.65**	**1.73**	**1.76**
Cell Depth (mm)	110	110	390	390

TABLE 4.1: PRESSURE DETERMINATIONS (KPA) FROM LCPC, ROUEN EXPERIMENT COMPARED WITH THOSE CALCULATED BY THEORY

The Experimenters concluded that "the pressure measurements were not reliable, probably due to the discontinuous nature and coarse grading of the granular materials". However, it should be remembered that consideration should have been given to correction of the results for aspect and stiffness ratios, which in turn effect the registration ratio. Another consideration is that the surface loading pressure distribution used for the analysis is assumed to be constant whereas the reality is more likely to be a parabolic distribution for granular materials, due to a rigid plate used for applying the load. As a result, higher stress levels could be expected to be measured under the *centre* of the loading. To allow for this fact in the Rouen experiment, the pressure cells were placed 100mm radially from the centre of the

plate where more of an 'average' pressure could be experienced. However, at this distance, the applied surface pressure would still be above the 'average' pressure if the loading was found to follow a parabolic distribution, typically given by:

$$\sigma_o(r) = 2 \times \sigma_o \times \frac{a^2 - r^2}{a^2} = 2 \times \sigma_o \times \frac{200^2 - 100^2}{200^2} = 1.5\sigma_o > 1.0\sigma_o \quad \ldots (4.6)$$

where σ_o = mean stress level under the loading plate (= 600kPa here)

a = radius of plate = 200mm

r = radial distance from the centre of the plate = 100mm

Note: that the factor of 2 in the Equation 4.6 could vary depending on the shape of the stress distribution

If a parabolic stress distribution could be applied to the pavement response model, instead of a uniform stress distribution, it would be expected that the difference between the measurement stresses and the theoretical stresses would be reduced as the theoretical values would be higher in magnitude.

Vertical pressure measures were also performed at LCPC, Nantes, France as part of the COURAGE project. The same pressure cells were used and similar conclusions were drawn from the results as the Rouen experiment.

4.3.2.2 FWD Loading on Sand, Technical University of Denmark

Two double diaphragm and one electro-hydraulic stress cells were used in a simple experiment in sand that was loaded with a falling weight deflectometer (FWD) (Ullidtz, 1996). The diaphragm cell had a diameter of 68mm and thickness not specified, whilst the hydraulic cell had a diameter of 150mm and thickness of only 4mm.

The three gauges were placed in a line at a depth of 280mm within the sand. The FWD loading applied an average contact stress of 300kPa over a plate of radius 150mm. The FWD was placed at 25 positions with different distances from the

gauges, but in the line of each gauge in turn. The measured and theoretical stresses are shown in Figure 4.4 as a function of distance from the centre of the FWD.

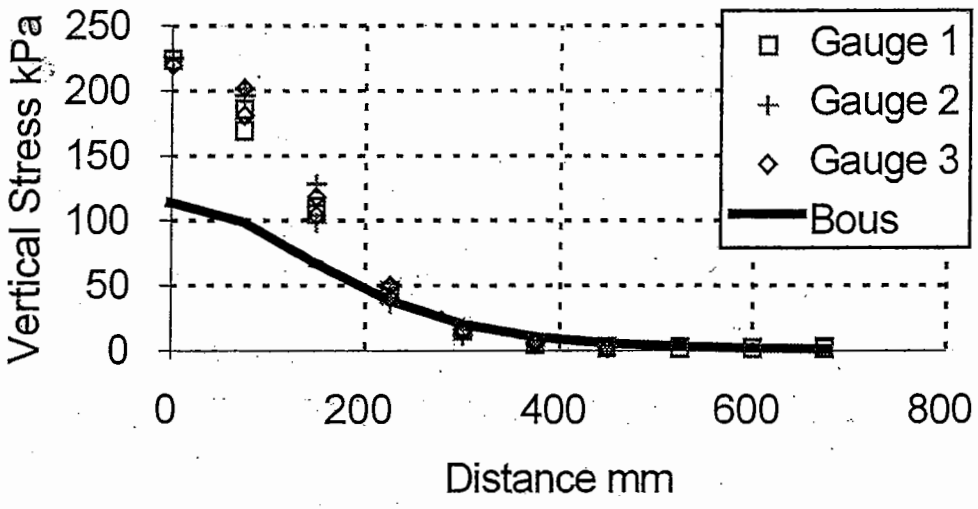

FIGURE 4.4: MEASURED AND THEORETICAL STRESSES IN THE SAND

It was found that the results of the three cells were in good agreement, however, these results were quite different to the theoretical stresses determined by Boussinesq's equation and assuming the stress under the FWD plate followed a parabolic distribution. Ulliditz suggests that if a uniform stress distribution had been used for Boussinesq calculations, then the variation in results would have been even greater. The stress calculated at the centre of the rigid plate according to Boussinesq's equation would have been 94.5kPa, compared with 115kPa using a parabolic distribution. He also states that the "total force on the plate, at the level of the gauges, may be found by integrating the stress bulb". In performing the calculations, per Ulliditz found the total force was 10-14% larger than the FWD load or actual mean stress. It can be concluded, therefore, that the accurate modelling of the applied stress distribution is required under rigid plate apparatus (which produces a parabolic distribution of loading stress) in order to more accurately match measured and theoretically calculated stresses.

4.3.2.3 Load Transmission Project, Indianapolis, USA

In the 1950s, a load transmission project was conducted at the CAA Technical Development and Evaluation Center at Indianapolis (Herner, 1955). The project consisted of a series of static loading tests on full-scale pavement sections, conducted

under laboratory conditions. However, the natural subgrade was replaced by a flexible 10ft (3m) square platform, composed of 3600 steel plungers, placed in 60 rows of 60 each, with each plunger supported by a calibrated steel spring. Deflections of the springs were converted to values of vertical stress by means of calibration curves.

The load-distribution characteristics of a number of different basecourse material types and subgrade combinations were measured at the bottom of the base. It was found that the different materials distributed the load to the subgrade to varying extents.

Three experiments were performed using three different thicknesses of UGMs, of different material type, and loading the pavement surface with an aircraft tyre inflated to a pressure of 100psi (690kPa). In each case, a different total loading was applied, ranging from 5 to 20kips (or 22.25 to 89kN) (see Table 4.2 for a summary).

Test	Parameters		
	Thickness of UGM	Total Load	Loaded Tyre Radius
Pavement Test 1	24in (610mm)	20kips (9t)	8in (203mm)
Pavement Test 2	16in (406mm)	10kips (4.5t)	5.64in (143mm)
Pavement Test 3	8in (203mm)	5kips (2.25t)	4in (102mm)

TABLE 4.2: PAVEMENT THICKNESS AND LOAD COMBINATIONS USED FOR TESTS

Figures 4.5 to 4.7 show the results of the test, comparing the longitudinal load distribution patterns for various basecourse materials at depths corresponding to the thickness of the UGM. In addition, the Boussinesq distribution is plotted for comparative purposes.

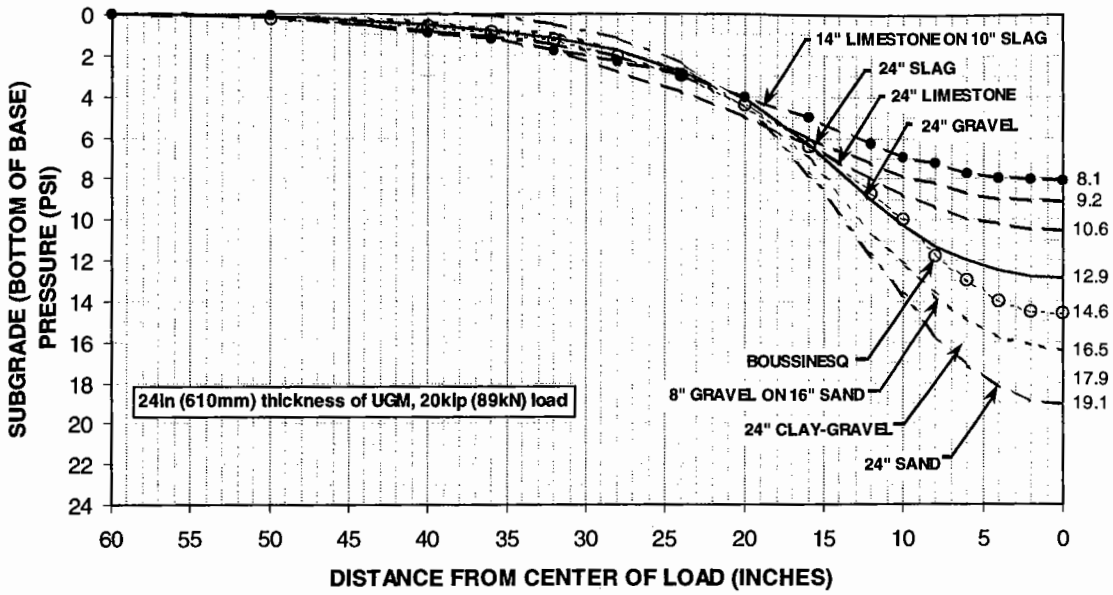

FIGURE 4.5: LONGITUDINAL LOAD DISTRIBUTION PATTERNS FOR VARIOUS BASECOURSE MATERIALS AT A DEPTH OF 610MM, 89KN LOAD

Reproduced figure from the paper by Herner (1955), Boussinesq distribution added

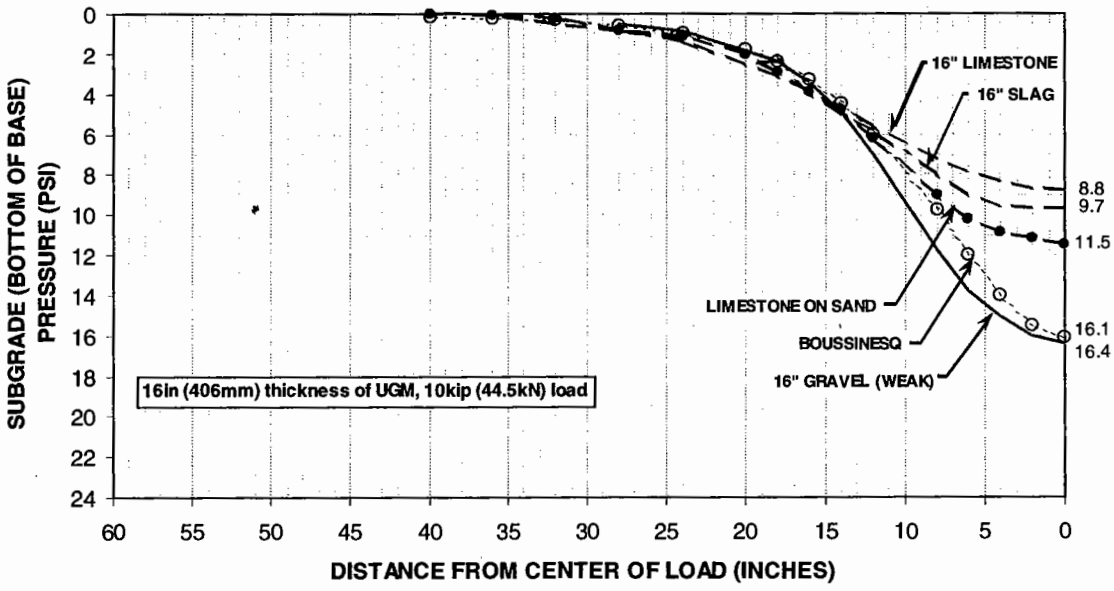

FIGURE 4.6: LONGITUDINAL LOAD DISTRIBUTION PATTERNS FOR VARIOUS BASECOURSE MATERIALS AT A DEPTH OF 406MM, 44.5KN LOAD

Reproduced figure from the paper by Herner (1955), Boussinesq distribution added

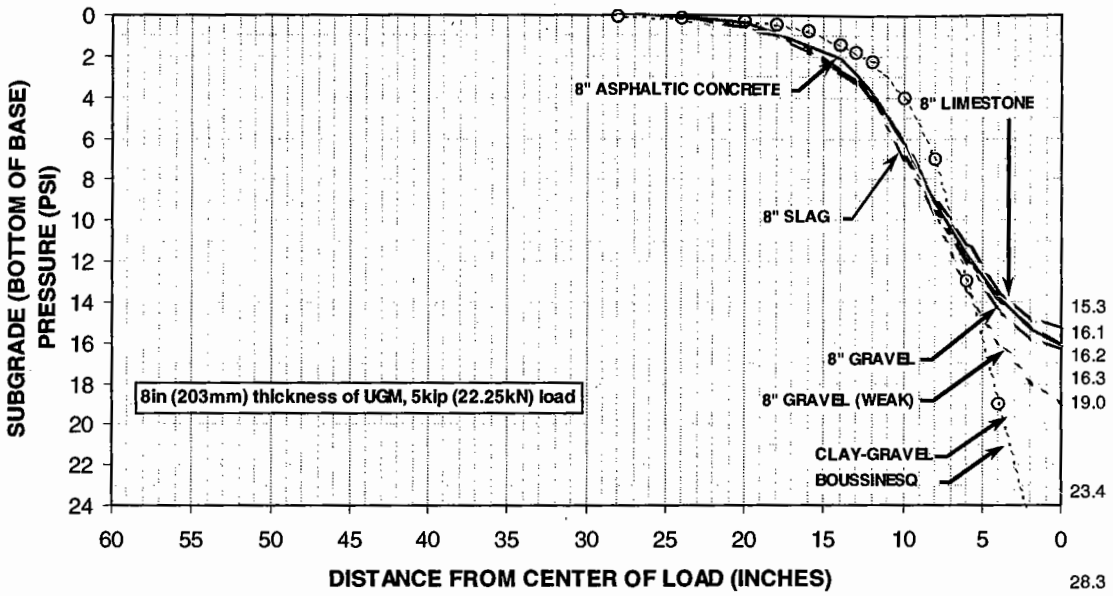

FIGURE 4.7: LONGITUDINAL LOAD DISTRIBUTION PATTERNS FOR VARIOUS BASECOURSE MATERIALS AT A DEPTH OF 203MM, 22.25KN LOAD

Reproduced figure from the paper by Herner (1955), Boussinesq distribution added

The results of the load transmission tests clearly highlighted a number of factors, with the principal ones being that:

- subgrade stress distributions caused by the application of static loads to a pavement structure is affected to an important degree by the physical characteristics of the base and sub-base materials.
- The higher quality materials were able to limit the transfer of stress to the subgrade more effectively than others. Limestone, slag and gravel materials performed this load-spreading function much better than weaker materials such as clay-gravel and sand. As a result, the former well-graded materials would be expected to 'carry' greater stresses within their particle framework than the finer grained materials. Thus, the stress regimes within UGMs can vary *very* significantly depending on the quality of the layer materials. From load transmission tests it was found that the measured stresses recorded centrally under the load at the bottom of a base material were reduced by up to 53% by the high quality crushed limestone compared with the low quality clay-gravel. This was for the result of an applied wheel load of 2.27t (22.25kN), which is in keeping in magnitude with a single wheel load within an 8.2t single axle, dual

wheel, ESA group. The stress reductions were found to be greater for higher applied wheel loads (Figure 4.5 and 4.6). These findings were supported by research performed by McMahon and Yoder in the 1960s, who conducted field pressure cell measurements on a two-layer system of base on subgrade, loaded at the surface by a rigid plate. They found in all test cases that the base acts as "a load spreading medium, with a definite reduction in the stress in the zone directly beneath the base-soil interface". Also, they stated that "the stress distribution in the two layer system depended to a large extent upon the strength and thickness of the upper (base) layer".

- the Boussinesq relationship for the longitudinal load distribution, at a given depth of measurement, fitted the measured stress distribution best for the lower quality finer grained materials. Thus, higher up in the granular layer, the Boussinesq result could be expected to over-estimate the stress in the well-graded angular aggregate products, in keeping with the first point. This could not be confirmed by this series of tests due to the fact that all measurements were made only at the bottom of the base layer. Ideally, vertical stress measurements would be required for the same load and loaded area, but for a number of different base thicknesses. Hence, a Boussinesq distribution with depth could be established.
- The material performance ranking derived from load transmission tests coincided well with laboratory static triaxial tests performed on the same materials which measured principal stresses at failure (not reported further here), that is, materials could be 'ranked' by this laboratory test.

4.3.2.4 MnRoad Project, USA

An experiment currently running in the State of Minnesota, United States, is the MnRoad project, which has seen the use of many pressure cells placed in both granular base/sub-base layers as well as cohesive subgrades. These cells are being used to measure the vertical stress distribution within the granular layers. They were located at interfaces of the A/C / base, concrete / base, base / sub-base and base / subgrade layers, with some additionally installed within the layers. The experiment consists of forty 500ft (152.4m) pavement test sections, with 23 loaded with freeway traffic since August 1994 and the remainder with loaded calibrated trucks. The purpose of this facility is "to verify and improve existing pavement design models,

learn more about the factors that affect pavement response and performance, and develop new pavement models that will allow more economical roadways to be built and maintained" (Baker, et al, 1994).

In general the experiences gathered to date at MnRoad with the sub-surface pressure measurements has not been good, especially measurements in the base / sub-base layers. No sensors failed as a result of the paving operations, instead the problems were reportedly "mainly due to the design of the pressure cell that was used". These cells were Geokon 3500W/Ashcroft transducers, large-diameter (9in.) hydraulic "pancakes" with a pressure transducer mounted to the side. Comments by Dave Van Deusen (Research Operations Engineer, Mn/DOT Materials and Road Research) suggest that "due to either air in the cell fluid or the structural make-up of the cells (there are theories to support both) they exhibited a high frequency, undamped oscillation when loaded. The manufacturers were to have addressed the problem before the cells were installed on a large scale at Mn/ROAD. As it turned out, approximately half of these sensors installed at the Mn/ROAD site had the oscillation. Most of these cells were installed beneath rigid pavement test sections." However, the MnRoads experience with the Kulite 0234 smaller diameter (2in) liquid-filled hollow diaphragm cells installed in subgrade layers has been better. Staff are currently collecting data from these cells installed in new test sections constructed last year. It has been reported that the cells were installed just below the base using "hopefully an improved installation method".

4.4 Tensile Capacity of Unbound Granular Materials

Linear elastic computer models of flexible pavements, comprising UGMs, predict positive confining pressures for very thinly surfaced pavements which diminish rapidly to zero at shallow depths (approximately 75 to 90mm). Below this depth, tensile lateral stresses are calculated by the modelling process with a peak magnitude of approximately 32kPa (for 35mm asphalt surfaced pavements) and 50kPa (for BST sealed pavements) in the longitudinal direction of vehicle travel.

Despite these findings, there has been little work performed in determining the tensile strength of unbound road bases. It has been assumed that such materials

possess negligible tensile strength. Work has been undertaken by Wallace (1998) to investigate this condition by conducting a series of carefully controlled laboratory experiments. Tests have been performed on 100mm thick, high quality, fine, 20mm crushed rock base materials compacted to only DDR = 93% MDD using *standard* compaction. This low level of compaction is well below that of constructed pavements, which is generally in the density range of DDR = 96 to 100% MDD using *modified* Proctor compaction.

The 100mm thick pavement was compacted in a 300mm wide by 600mm long plywood box, split in the middle, with the split being clamped shut during the construction stage. The box was mounted on a rigid steel 'subgrade' supported in turn on a set of low friction rollers. The left-hand side of the box and the subgrade were fixed against movement, whilst the right hand side was able to move at a constant rate of displacement (0.3mm/min) by two longitudinal threaded shafts driven by a motor. Displacement and strain gauge force transducers were mounted at the bottom of the box.

The results showed:

- an apparent peak stress of 2.8kPa when the layer was tested at its compaction moisture content, OMC standard
- an apparent peak stress of 14kPa (with a repeatability of CV = 5%) when the layer was dried back to 50% of OMC standard. This was to simulate dry base conditions during the summer period
- the strength of the bituminous spray seal had no effect on the tensile strength.

In addition, it could be expected that higher compaction densities would tend to be associated with higher tensile strengths, greater than 14kPa.

Thus, given that most pavements world-wide do undergo some sort of dry back following construction, they could be expected to have only a modest capacity to withstand the predicted tensile stresses calculated from linear elastic theory. Another form of stress condition may need to be present to overcome these sometimes large tensile stresses, particularly for unsealed roads.

4.5 Residual Lateral Stresses

4.5.1 Background

As discussed in §4.4, unbound granular materials cannot withstand significant levels of tensile lateral stress within them. Elastic solutions of modelled flexible pavement systems often predict tension toward the bottom of base or sub-base layers. As elastic modelling often gives a reasonable analysis of behaviour, it is necessary to explain this mis-match. Researchers such as Selig (1987) and others have proposed that these predicted tensile stresses in the lower portions of the UGMs are offset by larger compressive "residual stresses" which become locked in to the materials following the passage of heavy compaction loadings.

In its unloaded state, a pavement already has lateral stresses due to overburden and possible pore pressures (which may be positive or negative depending on whether the material is fully or partially saturated, refer to §2.4.3). Traditionally, lateral stresses due to overburden have been determined by assuming a value for the coefficient of earth pressure at rest, K_o, which is the ratio of horizontal to vertical stress under conditions of zero lateral strain. When horizontal stress states in a loaded pavement condition are combined with these overburden lateral stresses, the resulting horizontal stresses are usually still tensile and thus a failure condition is predicted. However, this approach will not account for additional stresses induced by compaction of the pavement layers resulting from repeated passes of heavy plant equipment (such as vibratory rollers, multi-tyred rollers and the like) and subsequent traffic loading.

The heavy compaction loadings applied to UGMs provide increased strength and stiffness of the layer as the individual particles undergo re-arrangement and densification within the material matrix to act as a positive resistance to the applied loads. During this loading process, the stress path is along the material's failure law envelope (as a loading condition cannot cross the failure envelope) and is expected to be accompanied by dilation (volumetric expansion) of the material. Upon unloading, some compressive residual stresses may remain "locked in" to the material due to confinement and particle interlock. It is expected that compaction quality could improve with each layer "lift" due to a stronger foundation developing on compacted

layers immediately below. As a result, it could be expected that residual stress states may increase in magnitude within each subsequent compacted granular layer. That is, residual stresses, following compaction, would decrease in magnitude with increasing depth into the UGM.

Residual lateral stress is considered one very important factor in determining the total confining pressure at which to evaluate the resilient modulus of a material element in the pavement structure. It is reported by Barksdale and Alba (1997), that "an additional confining pressure of 3psi (21kPa) can cause an increase in resilient modulus in a base in the order of 10 to 15% or more compared to neglecting this effect". This is considered to be a reasonable, average value, however, it should be remembered that this is very dependent on the material's stress level and the magnitude of its stress-modulus variation.

It is reported by Uzan (1985) that "residual compressive stresses induced by compaction during construction of a pavement or during repeated traffic loadings, or both, may be the cause of the compatibility between common engineering values (field measured) and the results of analyses of the sophisticated models". Also, compaction produces a stable layer that will not deform under further rolling of the compaction equipment. This suggests that the finished material is confined.

4.5.2 Measurement Studies

Measured stresses from a number of laboratory and full-scale field studies indicate that the process of load application and removal can result in marked increases of the lateral pressures, which greatly exceed the theoretical at rest values. If these residual stresses are of significant magnitude, the elastic stiffness of the constituent unbound materials would increase significantly, thereby altering the distribution of stresses throughout the pavement structure. In addition, the presence of residual stresses in the horizontal direction reduces surface and subgrade deflections by reducing the vertical compressive strains in the pavement (Garg, et al, 1998). This is also clearly shown in Figure A5.3 in Appendix 1. Thus, to correctly model pavement response, the contribution of lateral stresses due to overburden and construction traffic must be evaluated to determine the stress states of UGMs.

However, residual lateral stresses are very difficult to measure, due to their nature and small magnitude. Some researchers have tried to measure residual stresses in the pavement. Sweere placed two soil pressure cells in the granular layer of a test pavement, but measurements failed to indicate the existence of residual stresses (Sweere et al, 1987). This was the first "test" in a series of experimental pavements and it is recognised that measurement procedures need to be developed in these early trials through experience.

Studies, mentioned by Garg et al (1998), have indicated that these stresses can range from 10kPa to 35kPa. According to the research of Uzan (1985) and Stewart et al (1985), the horizontal residual stresses were found to be as high as 14 to 28kPa in cohesionless granular materials.

4.5.2.1 Triaxial Compressometer Experiment

Zeilmaker and Henny (1989) used a triaxial compressometer, with a series of 16 circular steel rings which tightly enveloped the specimen of ϕ400mm × 800mm height, to measure horizontal strains. The "Kettle" formula ($\sigma_{rr} = \sigma_{\theta\theta}/R$) was used to calculate the residual stresses. Specimens were only compacted to DDR = 95% MDD. The time-dependence of the residual stresses was measured, after three axial load levels were applied, by making determinations at 0min, 10min and 300min intervals immediately after unloading (see Table 4.3). The results, *averaged* over the two active recording rings, were

Time (min)	Vertical Stress (kPa)		
	1185	1046	490
0	**29.5**	**19**	**11.5**
10	**17**	**13**	**11**
300	**15**	**N/A**	**N/A**

TABLE 4.3: RESIDUAL STRESS (KPA) VARIATION WITH TIME AND APPLIED STRESS

The measurements showed that residual stresses are time-dependent and dependent on the applied vertical stress. It is expected that:

- the magnitude of the residual stresses would be greater for higher compaction density states,

- laboratory tests do not allow for the natural confinement provided by the surrounding aggregate material – interlock could increase and the residual stresses rise as a result,
- residual stresses decrease with time when no load applications are applied.

4.5.2.2 Lateral Stress in Track Foundations

Norman and Selig (1983 and 1985) constructed a ballast box with instrumented side and end panels to measure horizontal stresses due to repetitive wheel loads. The box had a flexible bottom to simulate the effect of subgrade conditions.

With reference to Figure 4.8, Norman and Selig found that as the ballast was cyclically loaded through a tie (sleeper) segment, that horizontal stresses increased from 0.2psi (1.4kPa) to 8.6psi (59kPa) (loaded state) and returned to 2.6 psi (18kPa) (unloaded state) after 1 cycle. With subsequent load cycles, the residual stresses (in the unloaded state) increased gradually from 2.6psi (18kPa) to 3.6psi (25kPa) after 10,000 cycles. However, it was found that the horizontal stress in the loaded state gradually diminished from 8.6psi (59kPa) to 4.3psi (30kPa) after 10,000 cycles. These measurements were made at a depth of approximately 2in (50mm at location 5) within a 12in (300mm) total thickness of ballast layer.

It should be noted that a slightly higher magnitude of lateral stress was measured at a depth of 6in (150mm at location 6) or midheight of the ballast layer. After 10,000 cycles, the residual stresses (in the unloaded state) had increased gradually from its initial value of 3.4psi (23kPa) to 4.7psi (32kPa). It is expected that the magnitude of residual stresses may decrease further toward the surface as the material in the upper regions of the base is less confined. At a depth of 10in (250mm at location 8) the residual stress after 10,000 cycles was only 1.1psi (8kPa).

A negative incremental horizontal stress did not occur, that is, the loaded stress always remained greater than the unloaded stress. It was observed that $K_{o\ max} = K_p$ determined as a ratio of σ_{1f}/σ_{3f}, was found to be as high as 11 in the box. No further measurements were reportedly made to see if the measured residual stresses subsequently decreased with time whilst the material remained in the unloaded state.

Selig (1985) later reported that "analytical (pavement) models for layered system behaviour will not predict the development of residual stress because their soil constitutive relationships did not represent inelastic behaviour associated with the progress changes in the early stages of cycling. Such models are most appropriate for predicting resilient layer response after many load cycles. To avoid predicting failure at the bottom of the upper stiff layer, and to model layer response properly, residual stresses must be incorporated by superposition." (Author's underlining)

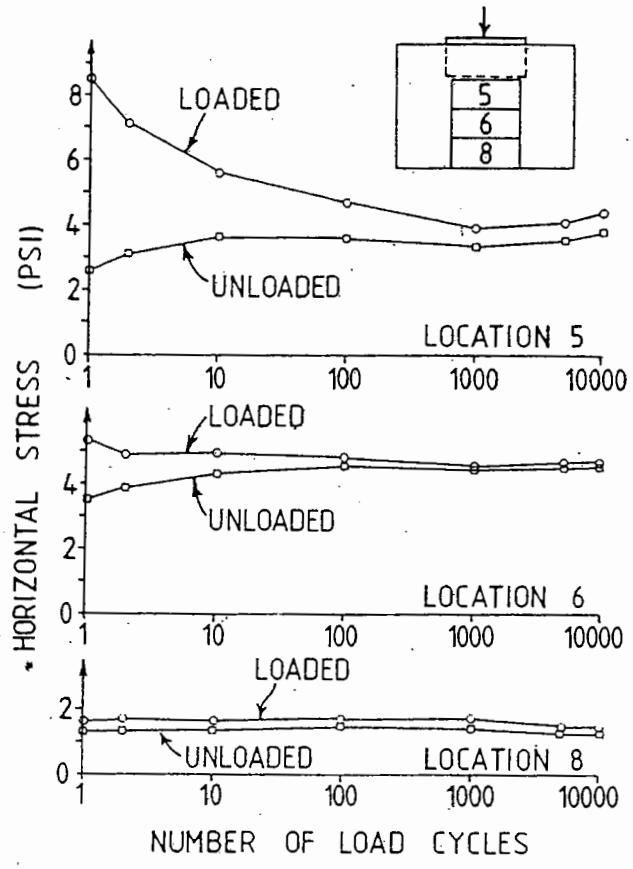

FIGURE 4.8: HORIZONTAL STRESS ON SIDE PANELS (REF: NORMAN AND SELIG, 1985)

4.5.2.3 Residual Stress Experiment Field Study

Barksdale and Alba (1997) conducted a full-scale field study to evaluate residual stresses in a 1.5in (38mm) maximum size crushed granite base 12in (305mm) thick. The base was placed in two 6in (152mm) lifts and compacted with a 10 ton smooth drum, vibratory roller. Lateral compaction and residual stresses were measured using a free field pressure gauge consisting of an aluminium cube approximately 2.5in (64mm) on each side. The shape was chosen to be as rigid as practical to simulate aggregate. The active diaphragm of the gauge was placed in one face of the

gauge with fluid (water and anti-freeze) between it and a low displacement, miniature pressure cell located on the opposite face of the gauge. The active diaphragm was orientated horizontally and recorded measurements near the bottom of a 6in (152mm) base and near the bottom of the upper and lower 6 inches of a 12in (305mm) base compacted in two lifts. In the 12in (305mm) thick aggregate base, compacted in two 6in lifts, a residual stresses of 3psi (21kPa) was measured near the bottom of the upper 6in layer (at a depth of approximately 5in or 127mm). In addition, near the bottom of the lower 6in of the 12in base (at a depth of approximately 11in or 279mm) and near the bottom of a single 6in base layer (at a depth of approximately 5in or 127mm), a residual stresses of only 0.5psi (3.5kPa) was measured. However, the corresponding surface pressure due to the impact of the vibrating roller (which is a function of its embedment into the base being compacted) was not specified in the report. However, on subsequent consultation with Barksdale, the results were reported for the case where the width of the roller contact area at the completion of rolling was about 3in. This corresponds to a depth of embedment of 0.05in (1.27mm).

From this study, it is apparent that the magnitude of the residual stresses is dependent upon:

- the strength and stiffness of the underlying foundation – a stronger working platform immediately under the lift being compacted results in higher residual stresses (as found by Barksdale and Alba),
- the number of granular layer lifts involved in the compaction process which relates to the first point,
- the depth beneath the load at which the stresses are measured (as found by Norman and Selig),
- the magnitude of the dynamic mass (vibratory roller) used for compaction of the layer (as found by Zeilmaker and Henny),

Other factors which influence the development and magnitude of residual stresses, but not covered here, are:

- the number of passes (related to the target final compaction density) used in compacting the material which is a function of the total energy imparted to the material
- material properties

4.5.3 Proposed Theory

Stewart (1985) states that "methods have been used to limit horizontal stress states to allowable values by incorporating either special conditions for the failed zones within the layer(s) or by employing specific failure criteria for the UGMs".

One such method is that proposed by Raad and Figueroa (1980) who set numerical limits on the major and minor principal stresses that can be developed at depths within the granular layer. "The limiting stresses are based upon principal stress ratios for active and passive failure, using the calculated values of (vertical stress) σ_v in each soil element as one of the principal stresses. A computed minor principal stress, σ_3 within a soil element is compared with these limiting values and adjustments are made to the element stresses so that the modified stresses result in a Mohr circle, tangent to the failure envelope but having principal stresses between the $(\sigma_1)_{max}$ and $(\sigma_3)_{min}$ limits". These modified stresses, which are non-tensile, are used to determine the stress-dependent resilient moduli for each layer.

Classical earth stress theory has been proposed by Zeilmaker and Henny (1989) to limit the lateral stresses which can be developed due to compaction loading and unloading conditions of cohesionless materials.

According to Zeilmaker and Henny, under loading conditions, the vertical stress increases and the horizontal stress is assumed to be unchanged until limit equilibrium is reached (see Point 2 in Figure 4.9). Then both the vertical and horizontal stresses increase according to the active case with horizontal compression developing (see Point 3 in Figure 4.9), viz:

$$\sigma_h = K_a \sigma_v \quad \ldots (4.7)$$

where K_a = active coefficient of earth pressure = $\frac{1-\sin\phi}{1+\sin\phi}$ ... (4.8)

Under unloading conditions, the vertical stress decreases and the horizontal stress is unchanged until limit equilibrium is reached. [The Author considers that as the vertical stress decreases the lateral stress decreases incrementally along an unloading line (see Point 4 in Figure 4.9)]. Then both the vertical and horizontal stresses decrease according to the passive case with horizontal compression developing, viz:

$$\sigma_h = K_p \sigma_v \quad \ldots (4.9)$$

where K_p = passive coefficient of earth pressure = $\frac{1+\sin\phi}{1-\sin\phi}$ ... (4.10)

The final total horizontal or lateral stress state is reached when the vertical stress returns to the overburden stress, σ_{vo} (see Point 5 in Figure 4.9). It is considered that the total unloaded lateral stress is composed of the residual stress (due to the compaction loadings), σ_{hr}, plus the at-rest lateral stress, σ_{ho}, viz:

$$\sigma_{h\,total} = \sigma_{hr} + \sigma_{ho} \quad \ldots (4.11)$$

To test this theory, the research work performed by Barksdale and Alba (discussed in §4.5.2.3) is now used. The pressure gauge is positioned at a 5in depth within the top 6in lift of a 12in thickness of compacted granular base, that is, at a depth of 127mm. A cohesionless material of friction angle = 50° with unit weight of 18kN/m^3 is considered. According to the theory, a residual lateral stress (see Figure 4.9) is predicted of:

$$\begin{aligned}\sigma_{hr} &= K_p \sigma_{vo} - K_{ho} \sigma_{vo} \\ &= 7.55 \times 0.127 \times 18 - 0.5 \times 0.127 \times 18 = 16.1\text{kPa}\end{aligned}$$

However, a residual stress of 3psi (20.7kPa) was measured.

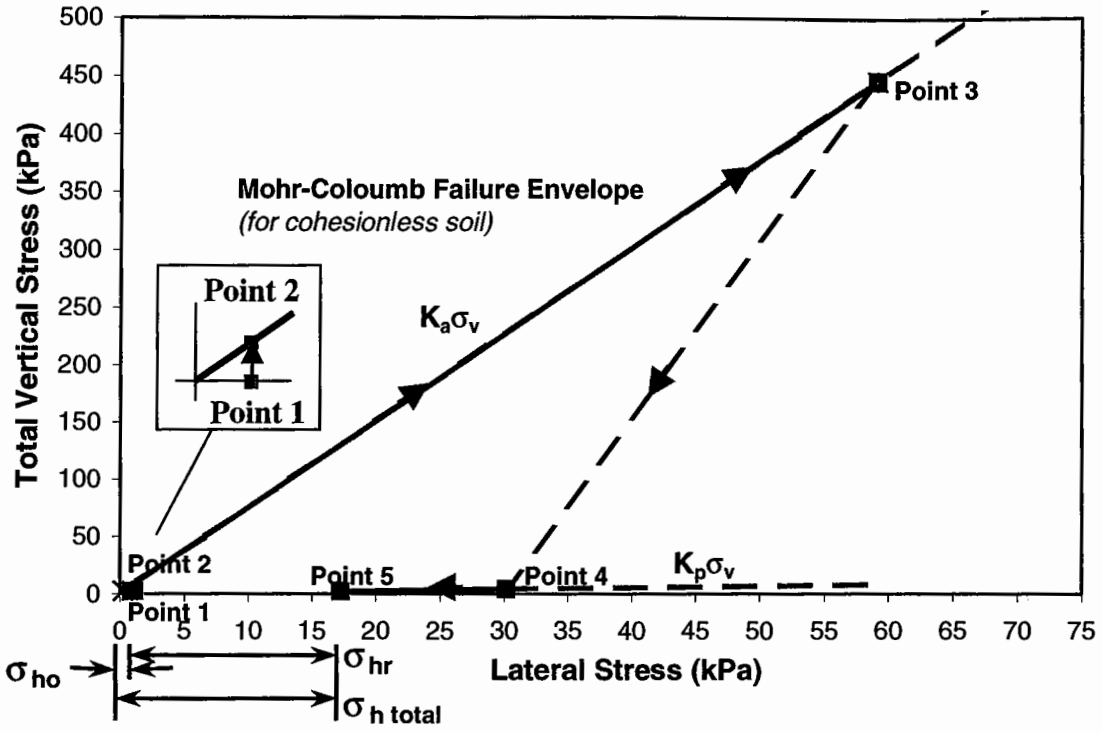

FIGURE 4.9: INTERPRETATION OF STRESS PATH DURING COMPACTION

Selig (1987) stated that the residual horizontal stress σ_{hr} is relatively large and can be expressed as a function of the vertical overburden stress:

$$\sigma_{hr} = K_{or}\sigma_{vo} \quad \ldots (4.12)$$

where:

σ_{vo} = vertical overburden or geostatic stress (in the unloaded state)

K_{or} = coefficient of lateral earth pressure considering residual stress

> 1,

< passive coefficient of earth pressure, K_p which may vary between 5.8 and 10.1 for typical crushed rock materials where ϕ varies between 45 to 55 degrees

This represents the difference in horizontal stress between that from the unloaded stress state to that of the overburden stress state. In the Barksdale and Alba experiment, the measured horizontal residual stress was 20.7kPa. The vertical overburden stress was 2.29kPa. Thus, K_{or} is calculated as

$$K_{or} = \frac{20.7}{2.29} = 9.04 \text{, which is} > 7.55 = K_p \text{ for a friction angle of } 50^o$$

Note, that Selig also observed $K_{o\,max}$ values to be as high as 11 in his experiments (as reported in §4.5.2.2). By this theory, Selig would calculate an angle of internal friction equal to 56.4°. Thus, it would appear that this theory is somewhat questionable.

4.5.4 Proposed Approach

The general principals discussed by Selig relating to the mechanisms for the rise and fall of the confining stress under load seem sensible, however, this theory tells us that the confining stress returns to a value governed in magnitude by K_p and the vertical overburden stress. However, the magnitude of K_p merely relies on the material's resistance of internal friction. It is considered that the magnitude of the applied load is also an important consideration currently overlooked. This is supported by the fact that greater pavement material densities, and hence increased particle interlock, are achieved in the field by using higher force compaction equipment. It can be seen from the results obtained by Zeilmaker and Henny, reported in Table 4.3, that greater residual stresses were measured for higher levels of applied vertical stress.

The work of Barksdale and Alba has been analysed, with calculations presented in Appendix 2, to investigate if a better approach can be adopted to calculate residual stresses in unbound granular materials within pavements. It is aimed to establish a basic relationship to calculate residual stresses based upon the applied compaction loading and the depth at which the stresses are to be determined.

With reference to the experimental details of Barksdale and Alba, the 10ton vibratory roller of diameter 60in (1.52m) applied a maximum dynamic force of 199.2kN over a length of 2.13m (93.4kN/m). Rectangular surface pressures of 35psi (241kPa) and 53psi (366kPa) were reported by Barksdale to be generated when the 10 ton vibratory roller presses 0.1in (2.5mm) and 0.05in (1.27mm) into the pavement surface, respectively. The later case of higher pressure and lower embedment represents the final stages of the compaction process.

For Barksdale and Alba's data, vertical stresses at depth z have been calculated by superposition using Fadum charts (Craig, 1987) to determine the values under the centre of the roller drum where the residual stresses were measured, ie, 5in (127mm) and 11in (279mm) depth. The results calculated by the Author are presented in Appendix 2. The report by Barksdale does not clearly state the surface pressure (which is a function of roller embedment) at which the residual stresses were measured. Although, subsequent correspondence with Barksdale suggests measurements were taken for an embedment depth of 0.05in to which he equated the estimated width of roller contact area as being approximately "2 to 3 in at the completion of rolling" [in recent e-mail correspondence] (the value determined by the Author being 3.5in). On this basis, surface stresses of 750kPa and 1062kPa have been deduced for a 0.1in and 0.05in embedment, respectively. Here, the same values of residual stress will be used for both the 0.05in *and* 0.1in embedment determinations, given that it was not reported by Barksdale what the magnitude of these stresses were for the 0.1in embedment.

The stress ratio of vertical stress at depth, z, (due to the compaction loading) to the measured total unloaded lateral stress (lateral residual stress *and* overburden), has been calculated. Table 4.4 summarises these findings:

Stress Determination	0.05in embedment		0.1in embedment [1]	
	z = 127mm	z = 279mm	z = 127mm	z = 279mm
Calculated $\sigma_{v\ (at\ depth\ z)}$ (kPa)	**446**	**212**	**409**	**207**
Measured residual stress $\sigma_{hr\ (at\ depth\ z)}$ (kPa)	**20.7 (3psi)**	**3.45 (0.5psi)**	**20.7 (3psi)**	**3.45 (0.5psi)**
Calculated $\sigma_{ho\ (at\ depth\ z)}$ (kPa)	**1.14**	**2.51**	**1.14**	**2.51**
Calculated $\sigma_{h\ total\ (at\ depth\ z)}$ (kPa)	**21.84**	**5.96**	**21.84**	**5.96**
Stress ratio, $\sigma_v / \sigma_{h\ total}$	**20.4**	**35.5**	**18.7**	**34.6**
Selig Stress ratio, $K_{or} = \sigma_{hr} / \sigma_{vo}$	**9.1**	**0.7**	**9.1**	**0.7**

TABLE 4.4: STRESS DETERMINATIONS (KPA) AT DEPTH Z UNDER THE VIBRATORY ROLLER

Note (1): The same values of residual stress are used for both the 0.05in *and* 0.1in embedment determinations, given that it was not reported by Barksdale what the magnitude of these stresses were for the 0.1in embedment.

These results are graphed in Figure 4.10 below. The results of the two compaction stages show the points connected by straight lines (which are not intended to represent the true relationship, but purely depict the inter-connection of the data points). Due to the influence of the vertical stress variation with depth, the relationship is expected to vary somewhat parabolically (as depicted in Figure 4.10 by the illustrative solid line for the 0.05in roller embedment). It is *anticipated*, in the absence of much experimental data but noting the findings of the work by Norman and Selig §4.5.2.2, that the magnitude of residual stresses may remain steady or slightly decrease further toward the pavement surface, where the material in the upper regions of the base is less confined. In contrast, the vertical stress at depth, z, (due to the compaction loading) would increase rapidly toward the surface of the pavement. Thus, the rate of increase of vertical stress relative to the residual stresses would see the stress ratio increase (as illustrated by the fine dotted line in Figure 4.10), but to an unknown extent? At the surface of the UGM layer during compaction, the vertical stress would be equal to the roller pressure applied, whilst the total lateral stress would be zero as the material is unconfined. Thus, the ratio of the two parameters would be infinity.

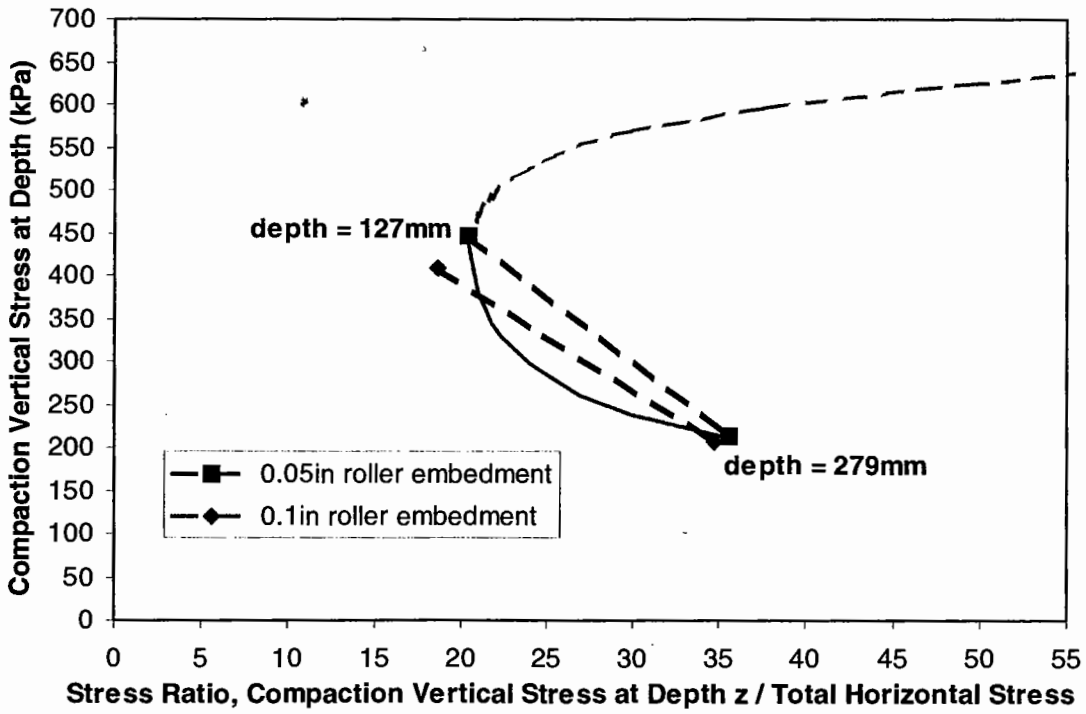

FIGURE 4.10: SUMMARY OF WORK OF BARKSDALE AND ALBA (1997)

Also reported in Table 4.3 is Selig's stress ratio, K_{or}, according to Equation 4.12. It can be seen that the range of this ratio is less than one at a point 279mm into the granular layer (the value is 0.7) and greater than $K_p = 7.55$ for ϕ of 50° (the value is 9.1 at 127mm). This is in contrast to the range quoted by Selig (of >1 and $<K_p$).

From the Uzan paper of 1985, the vertical stress determined under a vibrating roller load of 100kN/m, at a depth of 152mm, was determined to be $\sigma_v = 420$kPa. For material properties of $\gamma = 20$kN/m^3, $\phi = 45°$ and c = 5kPa, the vertical overburden pressure was calculated as 3kPa and the at-rest lateral pressure was 1.5kPa. The predicted residual lateral stress was 16.2kPa (Uzan stated that "a maximum horizontal stress of about 40kPa is *expected* to be induced"). Thus, a stress ratio of

$$\frac{\sigma_v}{\sigma_{h\ total}} = \frac{420}{17.7} = 23.7$$

is predicted, which is very similar to the data presented in Figure 4.10. From the work of others examined, it is considered that the magnitude of residual stresses depends primarily upon the material properties and the stress imparted at depth z, as a result of the compactive rectangular loading pressure (vibratory roller) operating at the pavement surface. In addition, researchers agree that continual heavy traffic loadings also impact upon residual stresses.

As Uzan (1985) states, "the analysis evaluating the induced lateral pressures can be only approximate because large deformations are involved and the stress path in each material element is quite complex".

Thus, having analysed the work of Barksdale and Alba (1997) together with Uzan (1985) and in the absence of further field trials to collect more detailed data, the use of a minimum stress ratio accounting for unloaded state lateral stress contributions from residual stresses and overburden stresses only, is now proposed:

for depths down to approx. 190mm (σ_v>300kPa): $\sigma_{h\ total} = \sigma_{v\ compaction\ (at\ depth\ z)} / 20$

for depths approx. 191 to 270mm (300>σ_v>225kPa): $\sigma_{h\ total} = \sigma_{v\ compaction\ (at\ depth\ z)} / 25$

for depths approx. 270+mm (σ_v<225kPa): $\sigma_{h\ total} = \sigma_{v\ compaction\ (at\ depth\ z)} / 30$

These ratios are appropriate for a 10ton vibratory roller, typically used in construction. This view is supported by Barksdale following discussions, indicating that "use of a depth ratio would be appropriate".

It should be remembered from the work of Zeilmaker and Henny that residual stresses are time-dependent, showing a reduction with time. They found the reduction to be greater when very high vertical stress loadings were applied (in the order of those expected at the finished surface from compaction loading). However, greater relaxation could be expected through their UGM-steel ring interaction than UGM-UGM interaction.

4.6 Summary

Instrumented pavement experiments used to measure *in-situ* stresses should not be undertaken lightly given the high level of cost associated with the instrumentation and labour involved. These costs may not be well rewarded with high benefits resulting from the recorded measurement, particularly given the number of potential sources of error which may be present in the process. Satisfactory results require suitable hardware, proper calibration to determine registration ratios and careful installation procedures, given the presence of the gauge alters the soil stresses that would exist if the gauge was not present. Given the time, expense and difficulty of stress measurements, the procedures are unattractive to most engineers. As a result, the number, particularly of recent years, and accuracy of measurements is not high.

Nevertheless, the stress measurement studies reported on by the Author have shown considerable benefits which can assist in the development of improved pavement design procedures. Some very significant findings from the worldwide research are summarised as:

- the vertical stress regimes within UGMs can vary *very* significantly depending on the quality of the layer materials. From load transmission tests it was found that the measured stress recorded centrally under the load, at the bottom of an 8in (203mm) base material, was reduced by up to 53% by a high quality crushed

limestone compared with a low quality clay-gravel. This was for the result of an applied wheel load of 2.27t (22.25kN), which is in keeping in magnitude with a single wheel load within an 8.2t single axle, dual wheel, ESA group. The stress reductions were found to be greater for higher applied wheel loads. Thus, higher quality materials would be expected to 'carry' greater stresses within their particle framework than lower quality materials and spread them over a greater area (by the action of vertical and lateral particle interlock). The granular base tends to act as a load-spreading medium and is most effective for higher quality materials (see Figure 2.2).

- apparent tensile stress of 14kPa was found by Wallace (1998) for granular material of low compaction level (93% MDD standard compaction) having dried the material out of 50% of OMC. It could be expected that higher stresses could be obtained when testing materials at higher compaction densities more in line with constructed pavements.
- residual lateral stresses were found to exist from a number of studies conducted and varied from 3kPa to approximately 21kPa higher up in the UGM pavement layer. Measurements by Zeilmaker and Henny (1989) showed that the magnitude of residual stresses was greater the higher the applied vertical stress states. For a given level of applied vertical stress, Norman and Selig (1985) found that the residual lateral stress was a maximum at a depth of approximately 150mm into the granular material, and decreased in magnitude significantly with depth. A slight decrease was noted to occur at shallower depths (50mm). The Author presented theory for estimating the residual lateral stresses. It makes use of a minimum stress ratio to account for unloaded state lateral stress contributions from residual stresses *and* overburden stresses only. It requires knowledge of the vertical stress imparted at depth z in the layer resulting from compaction apparatus working at the final passage of the roller. This theory is used in Chapter 5, concerned with theoretically predicting stress conditions, to allow for 'correct' RLT testing stresses to be determined, therefore, allowing 'correct' resilient modulus values to be assigned to UGM sub-layers within the analytical pavement modelling process.

Care must be taken not only in the placement and calibration of pressure cells, but also in interpretation and hence calculation of the modelled or theoretical stress distribution. Beneath a dual tyre load, the loading conditions are relatively uniform across the diameter of the load area (see Figure 4.11A). For plate loading tests, consideration must be given to the loading conditions immediately under the plate. For the rigid plate experiment reported in §4.3.2.2, a parabolic distribution provided a closer fit between measured and calculated values at the load centre-line, compared with a uniform one (see Figures 4.11B and C). The assumption of a uniform pressure is more readily met for pavements having a stiffness comparable to the material used in the construction of the loading plate.

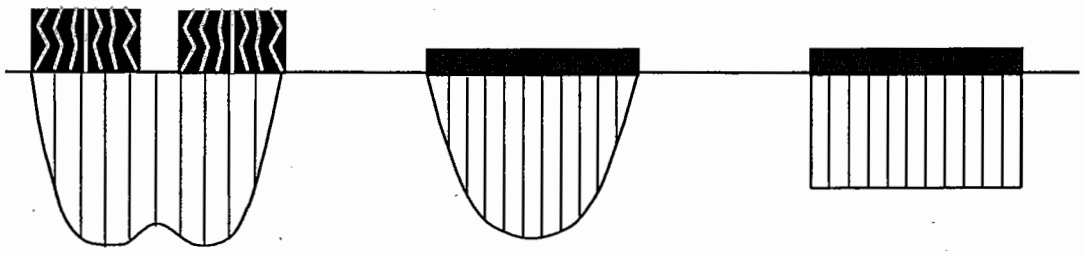

Dual Wheel Distribution | Rigid Plate Parabolic Distribution | Flexible Plate Uniform Distribution

FIGURE 4.11A B & C: LOADING CONDITIONS DIRECTLY UNDER A TYRE OR PLATE

CHAPTER 5
THEORETICAL PAVEMENT STRESS CONDITIONS

5.1 Introduction

A theoretical study has been conducted to determine stress regimes experienced by UGMs in a wide range of different flexible pavement types, subjected to two design standard axle traffic loadings, namely the Australian and the French.

As a result of the discussion presented in §1.1 and §3.1, it is logical that different flexible pavement configurations and applied axle loadings will produce different stress distributions throughout the unbound granular layers. This is principally due to the magnitude of the loading, the thickness of upper bituminous layers and the stiffness of the unbound and subgrade materials themselves.

It is important for pavement design practice that the values of modulus, assigned to the sub-layers or layers of the pavement structure, are determined by testing all constituent materials at a range of expected *in-situ* stress, density and moisture content conditions. Thus, the testing of UGMs requires the initial determination of stress levels that will be experienced by "material elements" *in-situ* within the pavement. Once a pavement designer has a trial pavement configuration determined, with surfacing type, thickness and granular layer thicknesses approximated, the key MPIs need to be determined and input into the design response model. To ease the process of determining the stress conditions which should be applied to test specimens, a series of design charts have been created by the Author (Mundy, September 1992), and these are now described.

5.2 Vertical Stress Determination

The calculated vertical stress has been determined from the non-linear elastic analysis computations described below in §5.4.1 and includes overburden stresses. An example of the "Vertical Stress Variation with Depth Charts" for a spray seal and

one thickness of asphalt surfaced pavement (35mm), as determined from this procedure, are shown in Figure 5.1A and 5.1B.

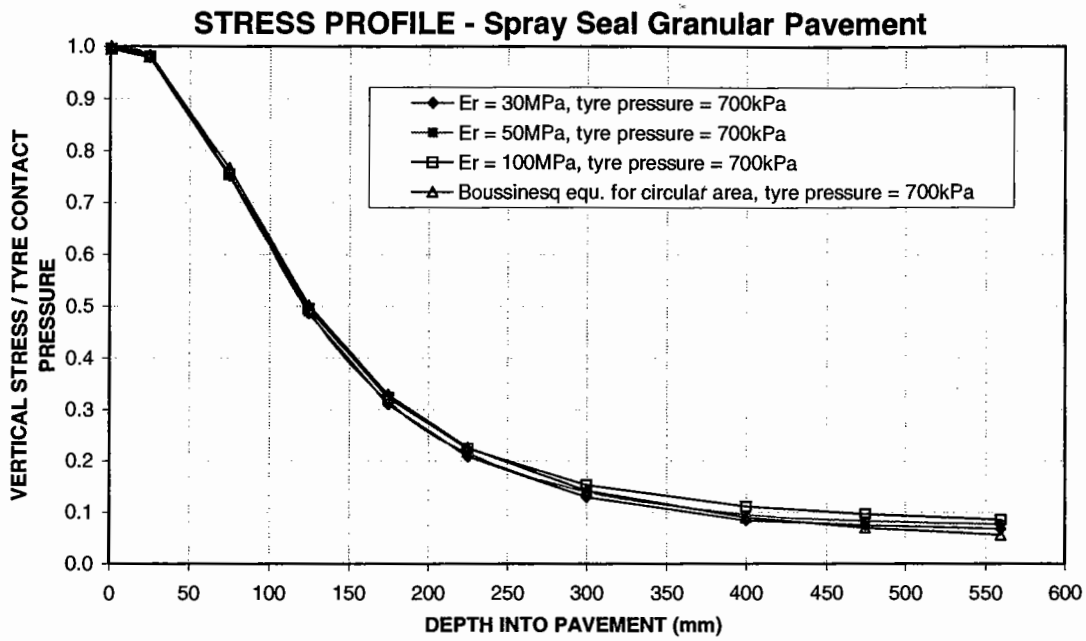

FIGURE 5.1A: VERTICAL STRESS VARIATION WITH DEPTH FOR A SPRAY SEALED PAVEMENT

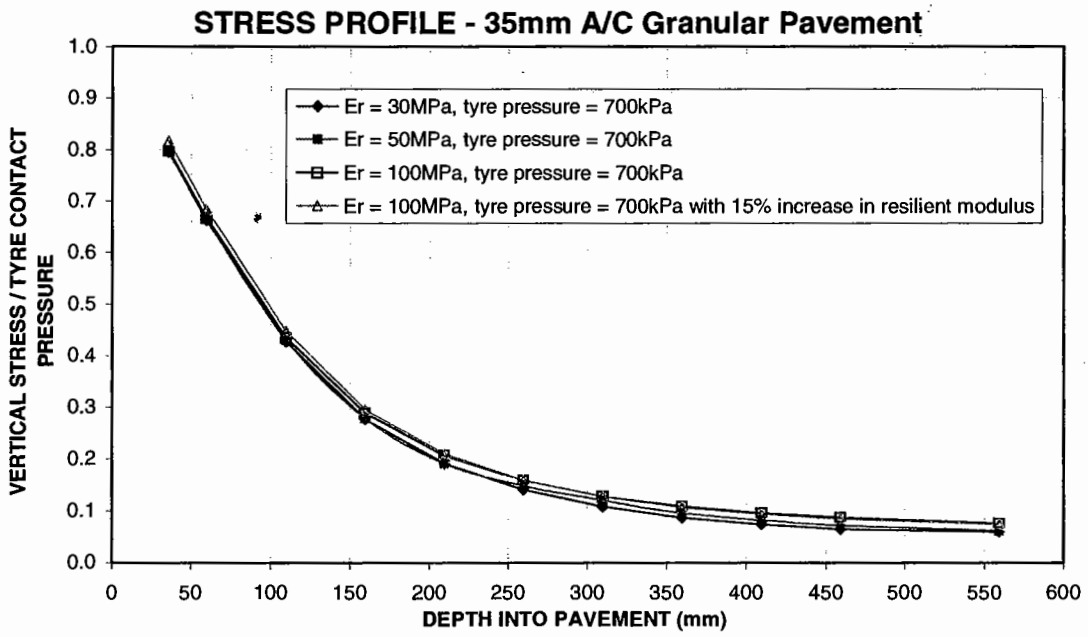

FIGURE 5.1B: VERTICAL STRESS VARIATION WITH DEPTH FOR A 35MM ASPHALT-SEALED PAVEMENT

Two other stress profile charts were illustrated in MT79-1 Report (Mundy, September 1992) for different asphalt thicknesses (50mm and 75mm). It can be seen from the vertical stress charts that the magnitude of stress is not greatly effected by

variations in subgrade resilient modulus over the range considered (namely, 30, 50 and 100MPa). This conclusion is supported by the findings of Plaistow (1996), who analysed a granular pavement with a 50mm asphalt surfacing. The results showed that the stress condition at the top of the granular layer, expressed as a stress ratio, changed by only 2% for a subgrade modulus change between 90MPa and 40MPa.

In addition, Figure 5.1B also illustrates the shift in the stress profile, for one subgrade condition (Er = 100MPa) if the resilient modulus values for all of the UGM sublayers are increased by 15% in the pavement response model and the model is then re-analysed. It is evident that only a very slight increase in the values of the stress profile results (a maximum increased shift of only 2.4%).

If one considers the calculated vertical stress in Figure 5.1A above, as determined from the non-linear elastic analysis computations, including overburden stresses, and compares it with the Boussinesq equation for a distributed load (Equation 5.1), the results are virtually the same as for the case of the spray seal pavement (Figure 5.1A). However, this is only determined for an unsurfaced pavement with a total granular layer thickness of 450mm under a standard axle loading. Many further computations should be conducted to verify these findings for a range of other structural thicknesses and loading cases, particular in light of the findings from measured vertical stress determination as presented in §4.3.2.

$$\sigma_1 = \sigma_o \left\{ 1 - \frac{1}{\left(1 + \left(\frac{a}{z}\right)^2\right)^{1.5}} \right\} + \gamma z \qquad \ldots (5.1)$$

where:

σ_o = uniform normal contract stress/pressure

a = radius of the loaded area = $\sqrt{\frac{P}{p\pi}}$, ... (5.2)

where P = total load, p = surface (tyre) pressure

z = depth below the surface

γ = unit weight of granular material

It should be remembered that the granular medium in the Boussinesq analysis is considered to be a homogeneous, isotropic, linear elastic semi-infinite space. However, in reality, these conditions can be quite different since compacted granular materials tend not to be homogeneous due to there being more than one material type layer within the system with variations occurring due to density, moisture content and composition over the length of any constructed road. The variations are somewhat controlled by quality control procedures. In addition, granular materials are generally anisotropic, having greater stiffness and strength in the vertical direction compared to the horizontal resulting from the vertically applied compaction forces. The materials also display non-linear behaviour with increasing stress, as will be illustrated in §5.4.1, in particular figure 5.9

5.3 Lateral Stress Determination

As discussed in Chapter 4, it is noted that many computer-based pavement design modelling programs, particularly linear-elastic ones, predict very low confining or radial stresses (either approaching zero or tensile stresses) acting on unbound granular materials as the depth within the pavement structure increases away from the surface load. This is particularly the case where a bituminous material, which is stiffer than an UGM, is used as the surface treatment. These programs (such as the French ALIZE, the UK/Dutch BISAR and the Australian CIRCLY) are considered to be underestimating the confining stress experienced by the materials *in-situ* by neglecting to incorporate compressive lateral stress contributions resulting from the following effects, deemed most critical (Mundy, September 1992):

(a) overburden stresses (due to the self-weight of overlying pavement materials),

$$\sigma_3 = K_o\sigma_1 \qquad \text{with } K_o = 0.5 \quad \ldots (5.3)$$

(b) Mohr-Coulomb shear failure theory stresses (of the constituent materials),

$$\sigma_3 = \frac{\sigma_1 - 2c.\tan\left(45 + \frac{\phi}{2}\right)}{\tan^2\left(45 + \frac{\phi}{2}\right)} \quad \ldots (5.4)$$

The vertical and lateral stress combinations experienced by elements of material in the pavement must never transgress the Mohr-Coulomb shear stress failure line. To elaborate on the significance of the failure relationship the following example is presented (Example 5.1).

EXAMPLE 5.1:

Illustrated in Figure 5.2, in a graph of total vertical stress, σ_1 against the lateral stress, σ_3 are typical failure envelopes corresponding to two material conditions, one of low and one of high moisture content relative to optimum. Figure 5.2 also illustrates a stress combination within the top granular sub-layer of a 35mm A/C, unbound granular pavement (of nine 50mm sublayers) subjected to a 700kPa surface tyre loading. Initially, under no load conditions, and ignoring residual stresses for the moment the stress point considered in the top sub-layer appears as Point 1 purely due to overburden stresses. This point resides well below the failure envelope. If a form of surface loading (ESA) causes the total vertical stress to increase, with some incremental increase in confining stress, then the stress point will move along a loading line illustrated until the stress state is reached on the failure envelope (Point 2). By the failure theory, any additional increase in total vertical stress in each granular sub-layer (above that of Point 2), must be supported by a consequential increase in the lateral stress. That is, the stress point moves along the failure envelope (to Point 3). For a 700kPa surface load, the total vertical stress at the midheight of the top 50mm granular sub-layer is 490kPa. However, this vertical stress can only be supported if the lateral stress increases. For the low moisture content material the lateral stress will increase to 13.5kPa, whilst for the high moisture material it will increase to 30kPa due to its much lower shear strength. As discussed in §4.5.3, upon unloading, the lateral stress decreases incrementally as the vertical stress decreases along an unloading line. Then both the vertical and horizontal stresses decrease according to the passive case with horizontal compression developing.

The final total lateral stress state is reached when the vertical stress returns to the overburden stress. It is considered that the total unloaded lateral stress is composed of the residual stress (due to the compaction loadings), σ_{hr} plus the at-rest lateral stress, σ_{ho} as illustrated in Figure 4.9.

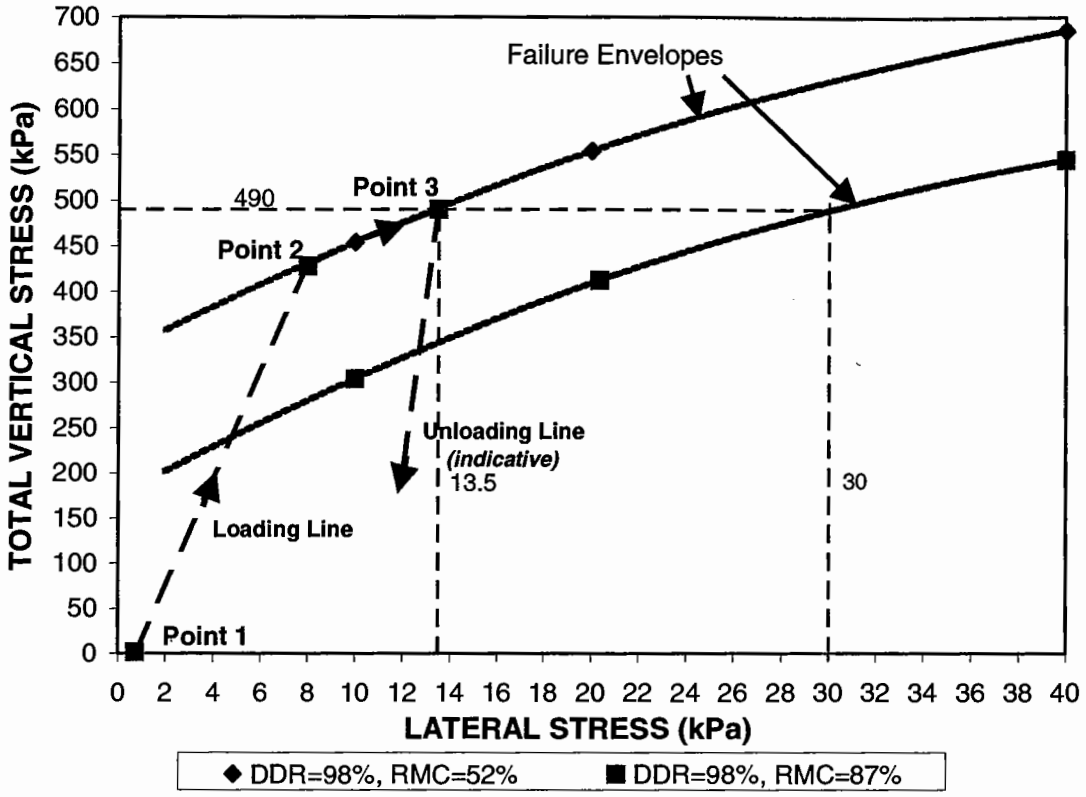

FIGURE 5.2: TOTAL VERTICAL STRESS AGAINST LATERAL STRESS FOR AN UNBOUND GRANULAR PAVEMENT MATERIAL

The example illustrates that the confining stresses reacting on the loaded granular materials are higher than the values currently predicted in computer modelling. If a vertical load is to be supported which exceeds failure conditions, a much more significant increase in the confining stress, greater than the incremental increase along the loading line, must occur. Figure 5.2 illustrates that the increase in lateral stress required, to support a given level of vertical stress, will be greater when the shear strength of the material is lower. The existence of higher lateral stresses will act to increase the resilient modulus of the granular material (due to its strong dependence on mean normal stress as seen in figure 2.19). This results in a reduction in surface deflections (and consequently a reduction in the asphalt tensile strain) and the gap between measured and predicted deflections, stresses and strains.

At present, the use of elastic response models to predict pavement performance is limited to the stress space within the bound of the failure envelope. Outside of

this region, considerable plastic deformation occurs and an elastic/plastic analysis is required. Attention to material plastic strain susceptibility may also be required inside the bounded stress space if the materials are prone to significant permanent strain there, but have not undergone complete shear failure.

Mohr-Coulomb failure theory can be used to provide a very reasonable estimate of the lateral stress for a given level of vertical stress experienced in the granular material. The curvature of a failure line will only contribute a minor error in the determination of the lateral stress (approximately 1 to 2kPa maximum based on the example in Figure 5.2) in the working vertical stress range of 350 to 600kPa.

(c) residual stresses (induced by initial compaction during construction and/or by compaction due to vehicular traffic loading post construction - through mechanical interlock), are very difficult to account for by the use of a modelling equation given that:

- very little research has been conducted into measuring this effect, although the work which has been undertaken *does* confirm their existence
- they are dependent of the many varying factors discussed in §4.3.2 (compaction pressure, compaction density, depth of measurement, time following compaction, etc)

As a result, residual stresses were accounted for by considering that their magnitude *primarily* depends upon the stress imparted at depth z, as a result of the compactive rectangular loading pressure (vibratory roller) operating at the pavement surface.

Having analysed the work of Barksdale and Alba (1997) and Uzan (1985), as described in §4.5.4, and in the absence of further field trials to collect more detailed data, the use of a minimum stress ratio accounting for unloaded state lateral stress contributions from residual stresses and overburden stresses only, was proposed in §4.5.4:

for depths down to approx. 190mm (σ_v>300kPa): $\sigma_{h\ total} = \sigma_{v\ compaction\ (at\ depth\ z)} / 20$

for depths approx. 191 to 270mm (300>σ_v>225kPa): $\sigma_{h\ total} = \sigma_{v\ compaction\ (at\ depth\ z)} / 25$

for depths approx. 270+mm (σ_v<225kPa): $\sigma_{h\ total} = \sigma_{v\ compaction\ (at\ depth\ z)} / 30$

... (5.5a to c)

As a result, the theoretical lateral stress values determined by the Author (Mundy, September 1992) have taken these factors into account when determining their magnitude at the mid-height of the sub-layer, directly under the load centre. The lateral stress at the mid-height of each sub-layer was considered by the Author to be the *maximum* lateral stress from the following Conditions, namely:

- **CONDITION 1** - Mohr-Coulomb effect + K_o × overburden stress, *or*
- **CONDITION 2 or 3** - the lateral stress determined from non-linear elastic analysis + K_o × overburden stress (for either spray seal or bituminous surfaced pavements, respectively), *or*
- **CONDITION 4** - residual stress effect (simplification using a minimum stress ratio) + K_o × overburden stress

As an example, if at depth z, negligible lateral stress existed as a reaction to the applied wheel load and insufficient residual stress was present, the vertical stress would need to be supported by a lateral stress increase according to the Mohr-Coulomb theory.

A spreadsheet has been established to determine the maximum lateral stress conditions expected to prevail for spray sealed and asphalt-surfaced pavements. The calculated lateral stress is a function of the properties of the UGM (c and ϕ, with cohesion being strongly dependent on DDR and RMC as discussed in §2.3.5) and σ_1 as determined from the non-linear elastic analysis computations described below in §5.4.1. An example of the "Lateral Stress Correction Charts" for a spray sealed pavement and an asphalt-surfaced pavement, as determined from this procedure, are shown in Figure 5.3A and 5.3B.

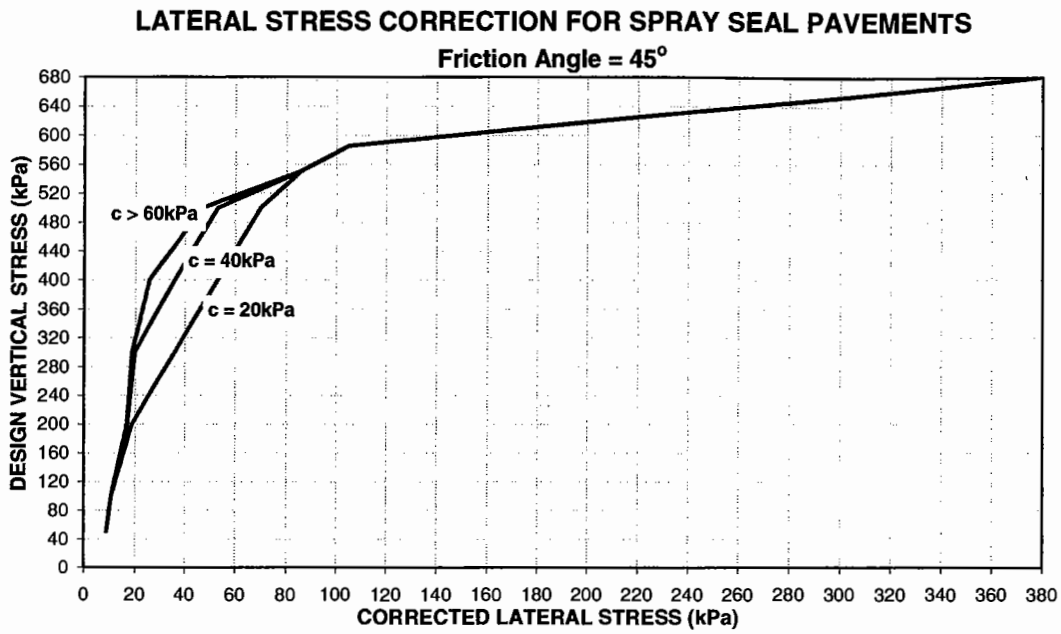

FIGURE 5.3A: LATERAL STRESS CORRECTION FOR A SPRAY SEALED PAVEMENT ($\phi = 45^{\circ}$)

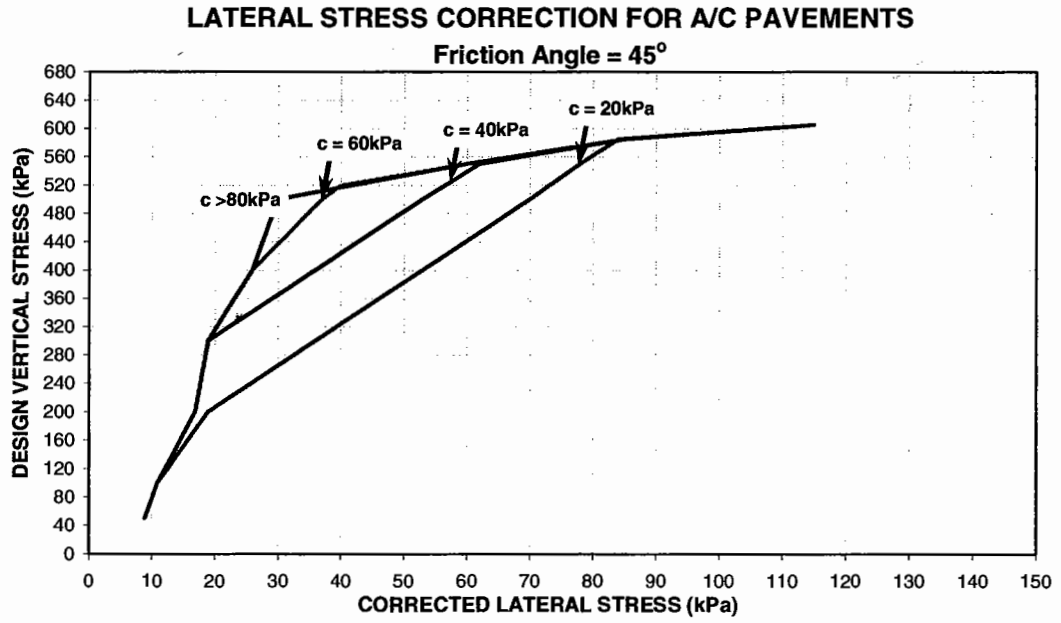

FIGURE 5.3B: LATERAL STRESS CORRECTION FOR ASPHALT SEALED PAVEMENTS ($\phi = 45^{\circ}$)

The charts illustrated above are further refined on those reported in MT79-1 (Mundy, September 1992) which reflect 5° changes in friction angle, with a range from 30° to 55° considered. This range covers a large selection of materials used in pavement construction. Linear interpolation is recommended for friction angles of materials between the 5° intervals.

5.4 Stress Regime and Stress Paths - Australia and Europe

5.4.1 Studies Performed

A separate study has been performed in Australia by Mundy (1994) and in France by Balay et al (1998) to determine the stress regime or stress locus applicable for the testing of unbound granular materials. Both parties independently examined a range of typical pavement configurations, typical of those which have been constructed in their respective countries. In addition, each analysis performed has drawn upon the use of constituent material properties (for asphalt, unbound granular and bound layer materials) applicable to the materials of each country.

The pavement types analysed in the studies to determine the stresses, and subsequent stress loci boundaries, obtained in the unbound granular material layers were:

(i) Australian study

- fully flexible pavements and inverted pavements
- bituminous surfacing thicknesses varying from 0mm (spray seal) to 100mm
- UGM - using some different materials which were high and marginal in quality
- non-linear elastic modelling of material modulus with stress
- E_v/E_h used varied between 1.0 and 2.0
- pavement foundation - a range of subgrade stiffness conditions for the analysis, namely 30MPa, 50MPa and 100MPa

(ii) French study

- fully flexible pavements
- bituminous surfacing thicknesses varying from 40 or 60mm to 120mm
- UGM - using high quality local materials
- non-linear elastic modelling of material modulus with stress
- E_v/E_h used for the analysis was unknown
- pavement foundation - subgrade stiffness condition for the analysis was 50MPa.

Different approaches were used to model the pavement structures. The Author used a non-linear elastic iterative analysis to arrive at a solution for each pavement analysed using the computer program NONCIRL. NONCIRL has the ability to use the k-θ modulus model parameters, applicable to the constituent unbound granular materials, as input parameters to arrive at a solution by iteration of modulus with stress. This non-linear model is similar to the Hicks and Monismith (1970) model and has the form:

$$E_r = E_1 \left(\frac{\sigma_m}{\sigma_{ref}} \right)^n \qquad \ldots (5.6)$$

where E_r = resilient modulus of the granular material (MPa)

E_1 = material constant (MPa)

σ_m = mean normal stress (kPa)

σ_{ref} = reference stress = 100kPa

n = material non-linearity constant

Model parameters of E_1 and n were derived from the MT16 series of reports (Mundy et al, 1990-1994). Briefly, a regression analysis was performed between the measured laboratory resilient modulus and mean normal stress data for each individual stress path (and hence stress ratio) tested. The parameter values used for each sub-layer in the NONCIRL analysis were selected using the regression results for the stress ratio in each sub-layer. This allowed a new stress ratio to be computed from NONCIRL output stresses following an iteration. An iterative approach produced a harmonised stress/modulus combination after 3 or 4 iterations (see worked Example 5.2).

It should be stated that after convergence, the modulus values obtained from the k-θ model analysis for the given stress conditions were checked against the values obtained directly from testing measurements (plotted on "Resilient Modulus Design Charts", refer to §5.7). The modulus values determined from the Charts, unlike those derived from the k-θ model called upon NONCIRL, used 'corrected' lateral stresses

appropriate to each sub-layer vertical stress. The lateral stresses were determined by the procedure outline in §5.3. This was necessary to ensure that the correct modulus values for each sub-layer were arrived at for each given stress condition in the sub-layer. If necessary, an additional computer run was performed using the new resilient modulus values, as read from the Design Charts, as the input parameters. It was found from modelling many pavements that the difference in the modulus determined by accounting properly for the lateral stress and not doing so could be up to 10%. This occurs at depths within the UGM sub-layers where positive confining pressures, resulting from the influence of the surface loading, are not calculated by elastic theory. Barksdale (1997, p.6) reports that "an additional confining pressure of 3psi (21kPa) can cause an increase in resilient modulus in a base of the order of 10 to 15% or more compared to neglecting this effect", confirming the Author's findings. Once the stresses and moduli were harmonised, the strain values could be computed according to equations 3.12 to 3.14. The effect of not correcting the strain values is most pronounced where lateral stress correction produces stresses that are markedly different from that which result from a non-linear elastic stress computation. The Author found that vertical compressive strains can decrease by up 35%, typically being a maximum at the bottom of the sub-base layer (refer to example in Appendix 1).

EXAMPLE 5.2:

Consider the seasonal pavement presented in Appendix 1. A 35mm asphaltic surfacing overlaying a 450mm granular layer upon a uniform subgrade. The lateral stress at the midheight of the top 50mm sub-layer, under an ESA loading, is well predicted by the linear elastic computer program NONCIRL. For all sub-layers below this one, the lateral stress is always calculated as a tensile stress. It is for these layers that the lateral stresses are required to be corrected according to the information in §5.3.

At the midheight of the second sub-layer, a depth from the pavement surface of 110mm (=35+50+25mm), The corrected lateral stress is determined to be 18kPa (determined from a chart similar to Figure 5.3B, but for $\phi = 50^o$ and c = 80kPa), corresponding to a vertical stress of 322kPa. From the measurement of resilient modulus derived from testing this material at the conditions used for analysis, the stress conditions would be:

No lateral stress correction:

$p = (321+2 \times 0)/3 = 107kPa$, $q = 321kPa$, thus, $E_r = 280MPa$

With lateral stress correction:

$p = (322+2 \times 18)/3 = 119kPa$, $q = 304kPa$, thus, $E_r = 307MPa$

Thus, the % variation $= \left(\frac{307-280}{280}\right) \times 100\% = 9.6\%$ *which is within the 10% stated.*

As mentioned in §5.2, the magnitude of the vertical stress levels, determined throughout the depth of the UGMs, were not significantly effected by the different levels of subgrade resilient modulus.

The results of the analysis, by the Author, for a select range of pavements commonly constructed in Australia are presented in Figure 5.4.

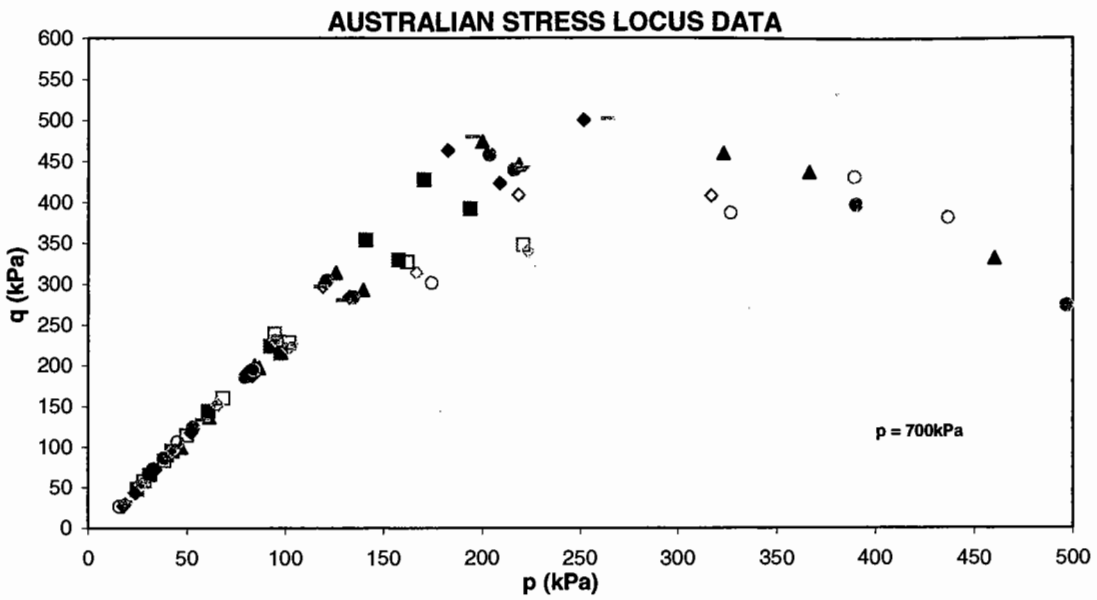

FIGURE 5.4: STRESS LEVEL DATA FOR THE AUSTRALIAN ANALYSED PAVEMENTS

Balay, on the other hand, used the finite element calculation code, CESAR LCPC to determine the French results. This program calls upon Boyce model parameters (Boyce, 1980) for the unbound granular materials. The modelling used by LCPC did not take any of the lateral stress factors mentioned in §5.3 into account. Lateral stresses were only determined from a non-linear elastic analysis, which used the Boyce model as the basis for determining granular material layer stiffnesses (refer to equation 6.8).

In both cases, the layer moduli were calculated along the line of the load axis and the appropriate standard axle loadings were applied, depending on the country in question.

Taking the results of the Australian study, the Author as placed a boundary locus around the stress level data points for the range of pavements analysed. Similarly, Balay applied a boundary locus to the French data. The resulting loci for the Australian and French studies are presented in Figure 5.5.

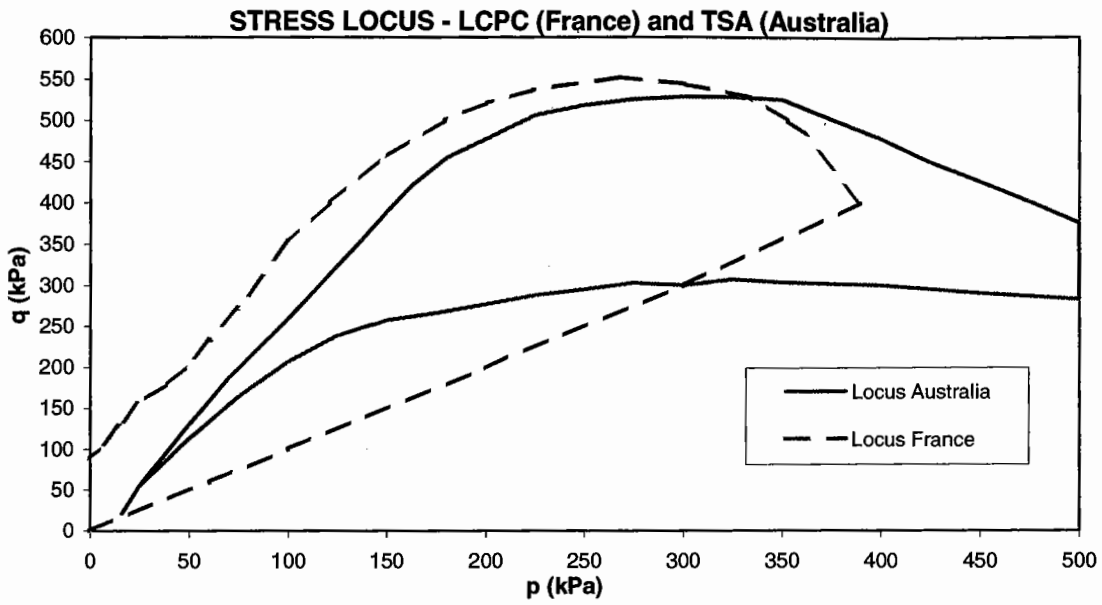

FIGURE 5.5: STRESS LEVEL BOUNDARIES FOR AUSTRALIA AND LCPC ANALYSED PAVEMENTS

From this analysis it can be stated that the stress levels for an unbound granular material, within a given pavement configuration, will be found to lie within the locus boundaries shown in Figure 5.5. Hence, testing stress paths should be concentrated within the stress boundaries defined.

In addition, for a range of pavements analysed (including BST granular, thin 35mm asphalt surfaced granular and inverted pavements) the stress levels relevant to the base layer, sub-base layer and fill layer are plotted in Figure 5.6. From this data, the highest stress levels of p and q identified allow upper limits of stress to be determined for the sub-base and fill layers.

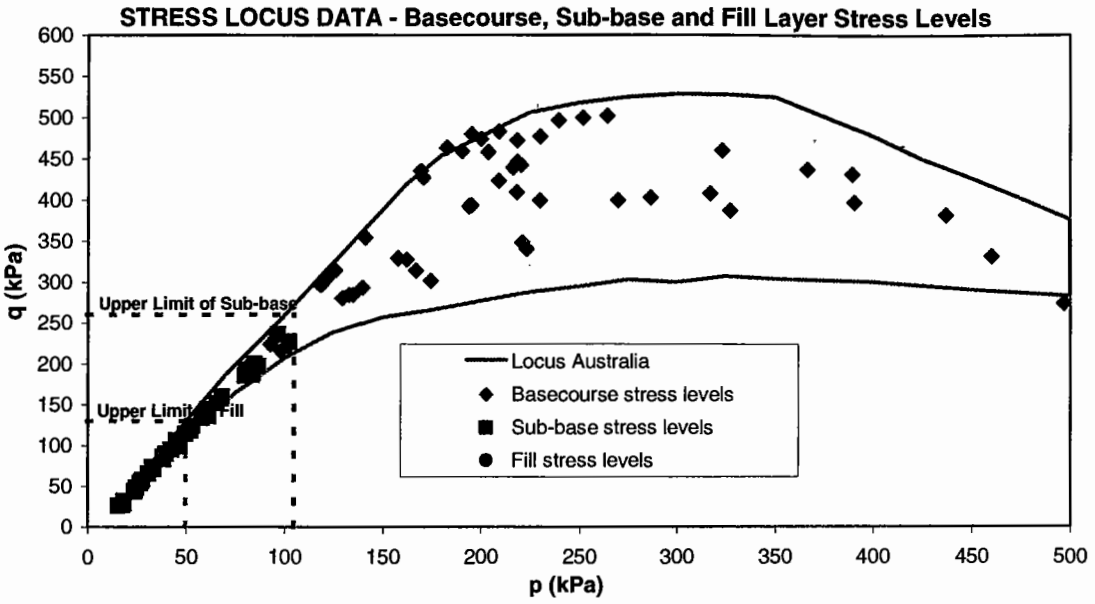

FIGURE 5.6: STRESS LEVELS WITHIN THE LOCUS WHICH ARE LOCATED IN THE BASE, SUB-BASE AND FILL LAYERS OF A RANGE OF PAVEMENTS

There are some distinct differences between the shapes and shift of the two envelopes, which should be clarified:

- The LCPC locus boundary for low q values increasing with p is a straight line commencing at p = 0kPa, q = 0kPa. The researchers responsible for the derivation of this locus (Balay et al, July 1998) stated that the lower boundary is merely a pictorial limit rather that a defined and calculated one. Obviously, no point would exist in a granular material directly under an applied wheel load that would be p = 0kPa, q = 0kPa. The vertical stress reduces in the pavement as the point of stress determination moves deeper beneath the wheel load, however, the overburden stresses become greater. The lateral stress also would be highest near the underside of the wheel load, and then decrease with depth until the affect of overburden causes it to increase again. In addition, given the non-linearity of typical pavement type stress distributions, one would not expect to see a linear stress path in p-q space. The straight-line portion represents a constant stress ratio of q/p = 1.0.
- The Australian locus extends to higher levels of p due to the very thin bituminous spray seal pavements analysed.

- The French locus extends to higher levels of q, for a given level of p, than the Australian locus. One factor causing this result is that no correction for lateral stress was undertaken in the French study, hence, q values are higher and p values are slightly lower.
- It should be remembered that the standard French axle carries a much higher load than its Australian counterpart, 130kN as compared to 80.4kN. In addition, the wearing course tends to be thicker.

As an example of pavement p and q stress combinations, four pavements (two Australian and two French) have been analysed with program NONCIRL using a multi-layered non-linear elastic iterative approach, to illustrate where the approximate *in-situ* stress paths lay within the loci. The granular layers of the pavement have been divided into a number of sub-layers to account for the non-linear variation of stress, and hence stiffness, with depth. The lateral stresses determined from the computer analysis have been corrected according to the process mentioned in §5.3. The pavement examples analysed and assumptions applied were:

(i) *Australian pavement*

- 35mm asphaltic surfacing (isotropic, Temp. = approx. 25°C, E = 2800MPa, $\nu = 0.25$)
- 450mm of unbound Australian Quartzite/Siltstone granular material – DDR = 98%, RMC = 60% (analysed in three 50mm and four 75mm sub-layers, E_v = 290MPa top sublayer to 150MPa bottom sublayer, $E_v/E_h = 2.0$, $\nu = 0.35$)
- subgrade (E_v = 50MPa, $E_v/E_h = 2.0$, $\nu = 0.35$) to depth of 3m.
- surface loading Australian ESA = 80.4kN (8.2t force loading, see Table 3.1)

(ii) *Australian pavement*

- bituminous surfacing treatment (BST) - spray seal (not modelled as no structural ability)
- 450mm of unbound Australian Quartzite/Siltstone granular material – DDR = 98%, RMC = 60% (analysed in three 50mm and four 75mm sub-layers, E_v = 530MPa top sub-layer to 150MPa bottom sub-layer, $E_v/E_h = 2.0$, $\nu = 0.35$)

- subgrade (E_v = 50MPa, E_v/E_h = 2.0, ν = 0.35) to depth of 3m
- surface loading Australian ESA = 80.4kN (8.2t force loading, see Table 3.1)

The resulting stress combination line plots for each Australian pavement are shown in Figure 5.7 below. It should be noted that depending on expected pavement design, climate, traffic and material conditions, approximate upper limits of sub-base and fill layers are indicated in Figures 5.6 and 5.7. These points indicate the maximum stress combinations that could be expected to occur in these layers under standard design loadings. The upper limits of the sub-base and fill layers are based upon and analysis by the Author of very thin BST flexible pavements, of the type commonly constructed in arid rural areas of South Australia. They consist of a BST, 150mm base layer, and 100 to 150mm sub-base layer. The stress combinations, which will be found to be a maximum at the top of the layers, provide a conservative upper limit for stresses appropriate to these layers given the very thin nature of these pavements. The significance of the combinations will be discussed in §5.5.

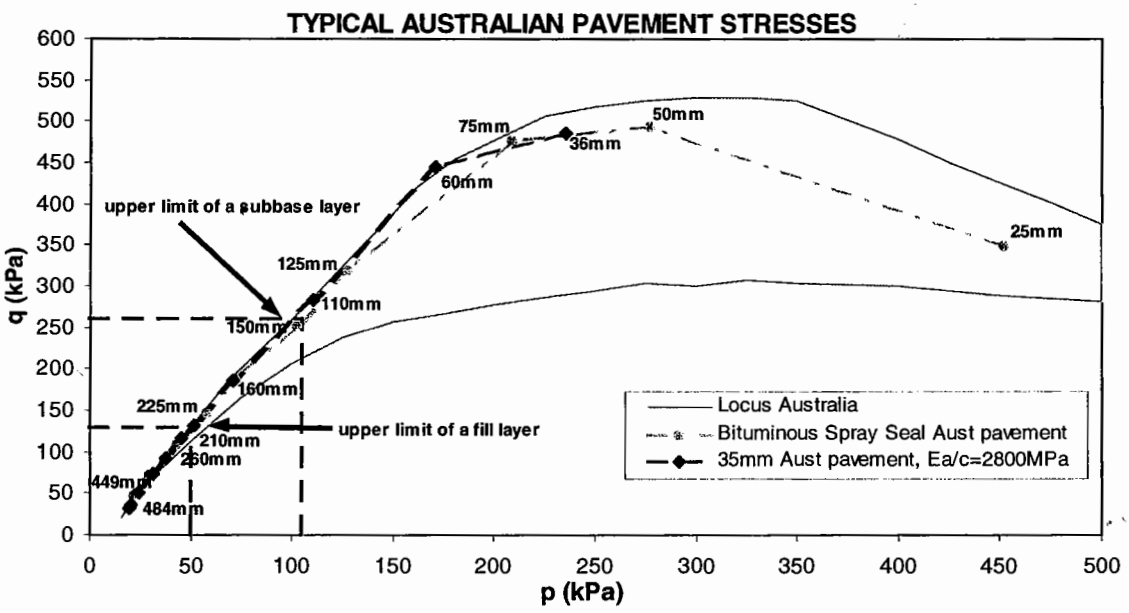

FIGURE 5.7: STRESS COMBINATION LINE PLOTS FOR AUSTRALIAN ANALYSED PAVEMENTS

It should be noted that the two stress profile examples shown in Figure 5.7, determined for E_v/E_h = 2.0, follow closely the upper boundary of the locus. For E_v/E_h = 1.0, the stress profiles will be found to more approach the lower boundary

because for this ratio, the calculated confining stress is higher, hence, p is higher and q is lower at the same point of determination within the pavement. The individual stress distributions (σ_1 and σ_3) in the two Australian pavements analysed above are shown in Figure 5.8A and 5.8B below. In addition, the pavement material resilient modulus profile is also shown.

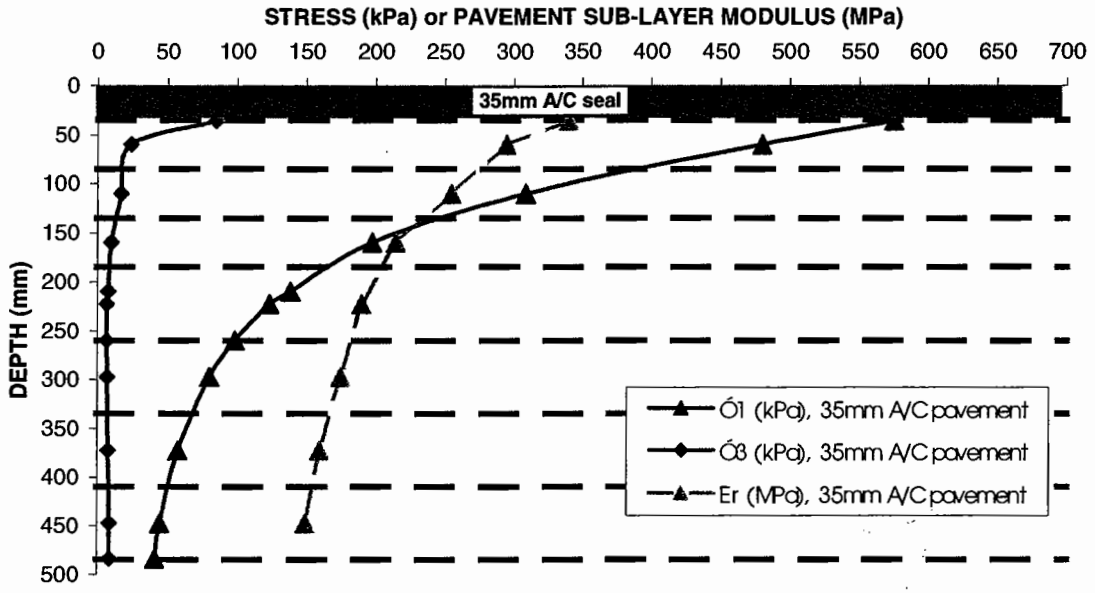

FIGURE 5.8A: STRESS COMBINATION LINE PLOTS FOR 35MM A/C AUSTRALIAN PAVEMENT

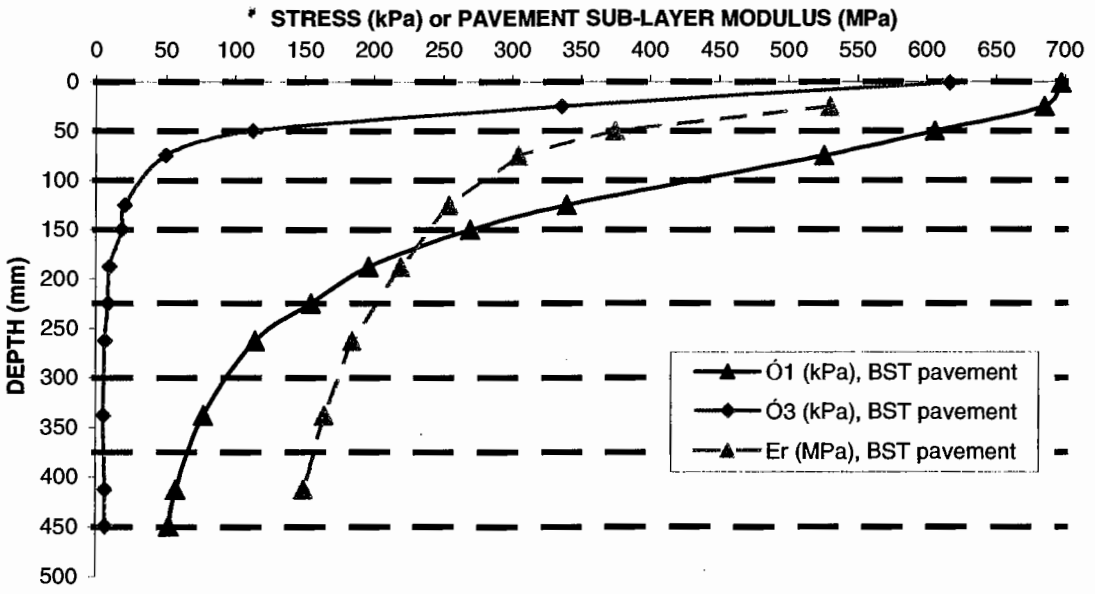

FIGURE 5.8B: STRESS COMBINATION LINE PLOTS FOR BST AUSTRALIAN PAVEMENT

Stress levels, and hence resilient modulus, can be seen from Figures 5.8A and 5.8B to vary significantly within the upper constructed UGM base layer (generally 150mm in thickness) of a thinly surfaced pavement. The non-linear behaviour of the material, with increasing stress conditions, can clearly be seen. In the analysis, the upper base layer of 150mm thickness was divided into 50mm sub-layers to allow resilient modulus to vary non-linearly with pavement depth, where the gradients of vertical and horizontal stress are the greatest. These Figures illustrate that adequate sub-layering needs to be introduced into the design response model to accommodate this fact, for without it, linear elastic theory will not cope with the stress-dependent nature of unbound materials. Below this depth, thicker sub-layers could be used (75mm proposed) for the next two granular pavement layers, which show much reduced stress dependence, particularly for layers at a depth greater than 300mm into the pavement. Each sub-layer is assigned a resilient modulus consistent with the stress levels (both vertical and horizontal) within them.

To highlight further the non-linearity of resilient modulus, within the UGMs, Figure 5.9 illustrates the variation of this parameter with depth into the pavement, for three different thicknesses of surfacing, namely (BST and 35mm – as above – and 80mm). The 80mm asphalt surfaced pavement was analysed in the same manner as the other two pavement types. It can be seen that the more thinly surfaced pavements exhibit much greater non-linearity than the thicker surfaced pavements allow. As mentioned, this is due to the much higher vertical stresses imparted to the UGMs within thinly surfaced pavements.

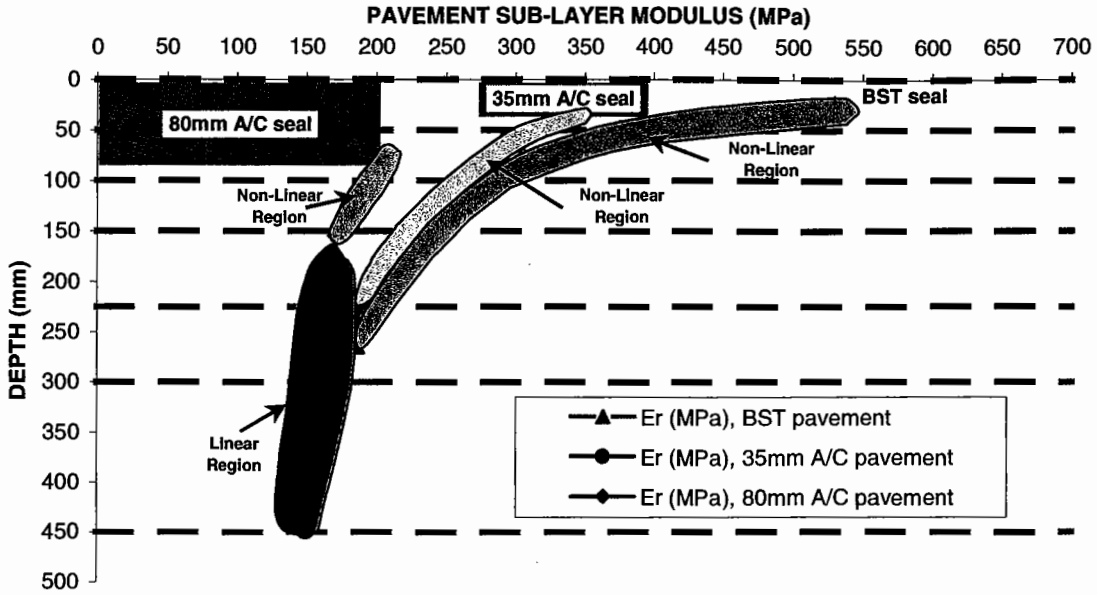

FIGURE 5.9: PROFILES OF RESILIENT MODULUS VARIATION WITHIN THREE AUSTRALIAN ANALYSED PAVEMENTS

Figure 5.9 illustrates the two response zones (linear or non-linear) which exist for each of the three pavements. For the 80mm asphalt-surfaced pavement, a linear elastic analysis of the structure is nearly possible. However, for the more thinly surfaced pavements, adequately sub-layering of the UGMs is critical to the analytical pavement modelling process to allow for accurate resilient modulus and stress harmonisation, as was discussed in §3.8 Item B1. Table 5.1 illustrates the depth to which the non-linear region penetrates into the pavement. In order to model the non-linearity provided by the UGMs, the Author recommends the number and thicknesses of the sub-layers that should be adopted for analytical modelling purposes. Reference should be made to §3.6.1 for discussion of the newly proposed Austroads (Austroads, 2001) approach.

Surfacing Thickness (mm)	Extent of Non-linear Region Below Pavement Surface (mm)	No. of sub-layers	
		50mm sub-layer	75mm sub-layer
0	260	3	2
35	215	3	1
80	160	2	1

TABLE 5.1: DEPTH TO WHICH THE NON-LINEAR REGION EXTENDS INTO THE PAVEMENT

(iii) *French pavement*

- 40mm asphaltic surfacing (isotropic, Temp. = approx. 22°C, E = 3500MPa, $\nu = 0.25$)
- 450mm of unbound French Granite granular material – DDR = 97%, RMC = 68% (analysed in three 50mm and four 75mm sub-layers, E_v = 270MPa top sub-layer to 110MPa bottom sub-layer, $E_v/E_h = 2.0$, $\nu = 0.35$)
- subgrade (E_v = 50MPa, $E_v/E_h = 2.0$, $\nu = 0.35$) to depth of 3m
- surface loading French ESA = 130kN (13.25tonnes force loading as per Table 3.1)

(iv) *French pavement*

- 40mm asphaltic surfacing (isotropic, Temp. = approx. 12°C, E = 9870MPa, $\nu = 0.25$)
- 450mm of unbound French Granite granular material – DDR = 97%, RMC = 68% (analysed in three 50mm and four 75mm sub-layers, E_v = 250MPa top sub-layer to 100MPa bottom sub-layer, $E_v/E_h = 2.0$, $\nu = 0.35$)
- subgrade (E_v = 50MPa, $E_v/E_h = 2.0$, $\nu = 0.35$) to depth of 3m
- surface loading French ESA = 130kN (13.25tonnes force loading as per Table 3.1)

The resulting stress combination line plots for each French pavement are shown in Figure 5.10 below. It can be seen that the magnitude of asphalt resilient modulus significantly effects the stress levels generated in the UGMs, due to the structural load carrying capacity of the asphalt layer. Given that the resilient modulus of UGMs is stress dependent, higher moduli are generated for higher levels of stress transferred through softer (lower modulus) asphalt. At a depth of approximately 200mm into the UGM, the differences in the asphalt moduli have little effect. These findings are supported by the work of many researchers such as Plaistow (1996) and Dawson (1999).

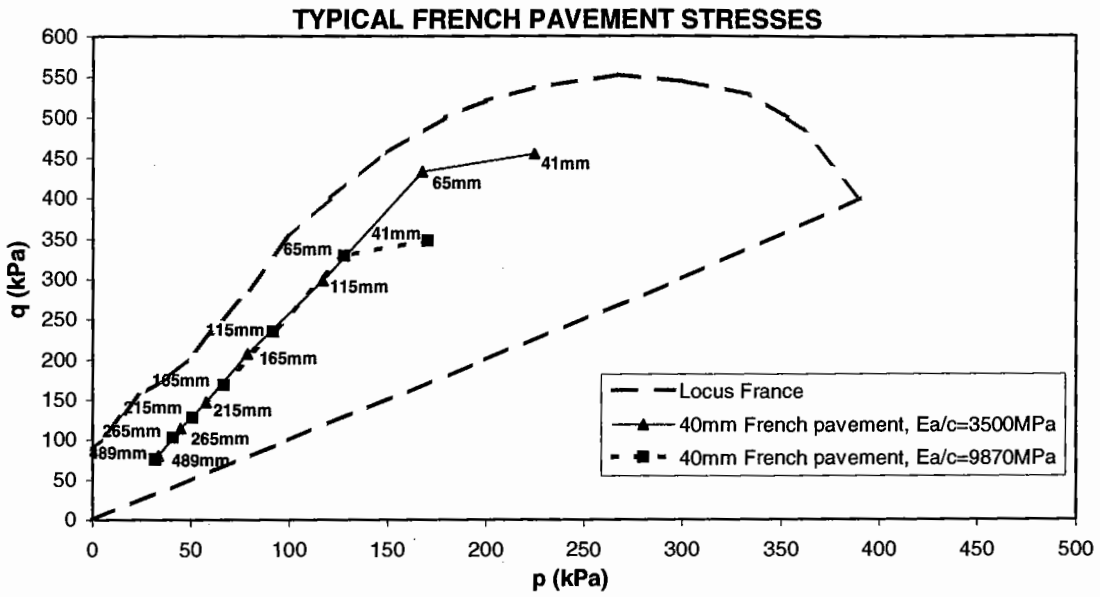

FIGURE 5.10: STRESS COMBINATION LINE PLOTS FOR FRENCH PAVEMENTS

The difference between the Author's stress line plots for the pavements analysed and the actual French stress locus could be due to factors such as:

- lateral stress correction was applied by the Author which would tend to shift the line plot to a region of lower q and higher p,
- the level of anisotropy applied to determining the French locus is unknown. A level of E_v/E_h greater than 2 will result in the locus being positions at higher q and lower p,
- a difference between the French FE-determined stresses and those resulting from a non-linear elastic analysis.

In addition, the stresses tend to merge toward a constant q/p stress ratio (with reference to Figure 5.10) which will be the case for materials of high cohesion (>60kPa), according to the lateral stress correction charts for asphalt surfaced pavements (see Figure 5.3B). From this chart it can be seen that below a vertical stress of 400kPa, constant σ_1/σ_3 stress ratio is followed, thus a constant q/p stress ratio will also be followed. This is largely due to the dominant condition of residual stress (which is related to σ_1) within these lower stress regions of the pavement layer.

As a result of this study, the stress levels and stress paths used for testing unbound granular materials by American, European and Australian Authorities should be expected to be located within the loci determined. This would imply that laboratory stress levels adopted for testing should relate closely to those determined in the field from pavement structural analysis. A comparison of current RLT testing stress levels employed for the European CEN and the Australian Standard test procedures should be made with the loci graphed in Figure 5.5. The testing stress levels graphed below are those defined in the test procedures used by the authorities of America (SHRP and AASHTO 1992), Europe (CEN, September 1997) or Australia (DRT, January 1991 and Standards Australia, 1995) as at March 1999:

- SHRP, Protocol P46, AASHTO Designation: T 294-92 I (refer to Figure 5.11)
- CEN, prEN13286-7, Method A using variable confining pressure (refer to Figure 5.12)
- CEN, prEN13286-7, Method B using constant confining pressure (refer to Figure 5.12)
- DRT, Method 107.14 (refer to Figure 5.13)
- Australian Standard, AS1289.6.8.1 (refer to Figure 5.14)

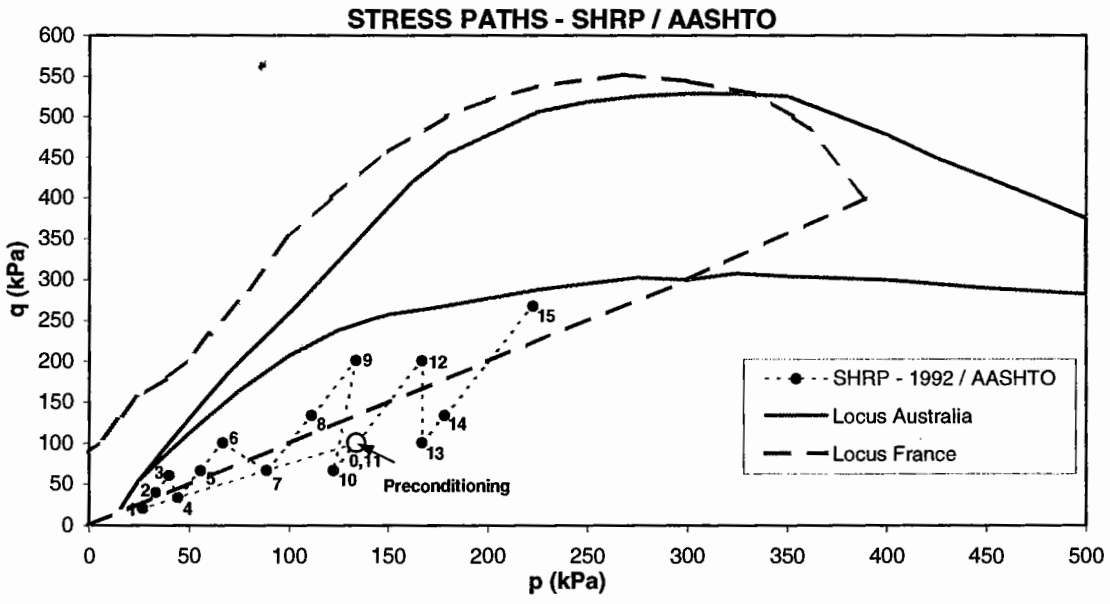

FIGURE 5.11: STRESSES USED FOR RLT TESTING OF UNBOUND GRANULAR MATERIALS - SHRP / AASHTO METHOD

From Figure 5.11, it can be seen that the American stress paths followed border near the French Stress Locus, with a number of stress levels outside of it. A number of points fall well outside of the Australian derived boundaries as well.

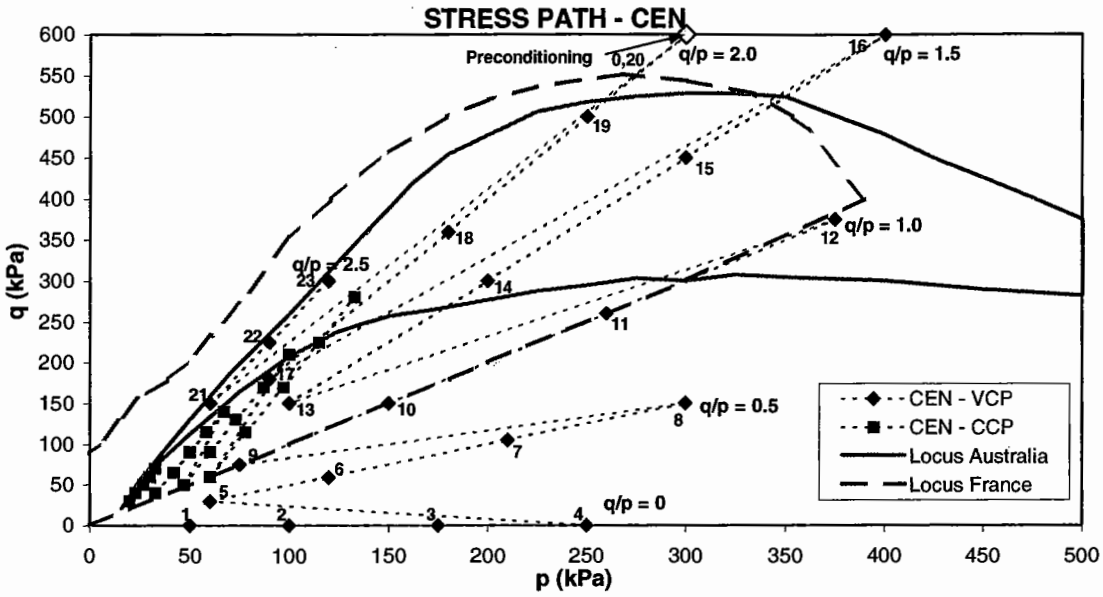

FIGURE 5.12: STRESSES USED FOR RLT TESTING OF UNBOUND GRANULAR MATERIALS - CEN METHODS A AND B

From Figure 5.12, it can be seen that for the variable confining pressure test (CEN-VCP, Method A) the stress paths for q/p=0, 0.5 and 1.0 fall outside of the French Stress Locus, given that the lower boundary is not fully defined (see earlier comments associated with Figure 5.5). Thus, one could argue that only the stress paths for q/p=1.5, 2.0 and 2.5, which fall within the stress loci, should be used for modelling purposes. It could be expected that the regression fit of a material behaviour model based on all stress paths would be significantly affected. This hypothesis will be checked in §6.3.6 using some RLT test data obtained for the COURAGE Project.

In addition, many of the stress levels used for the constant confining pressure test (CEN-CCP, Method B) fall outside of the Australian derived stress space, but many may still lie within the French locus. However, they lie in the region of uncertainty for this locus, which was discussed above.

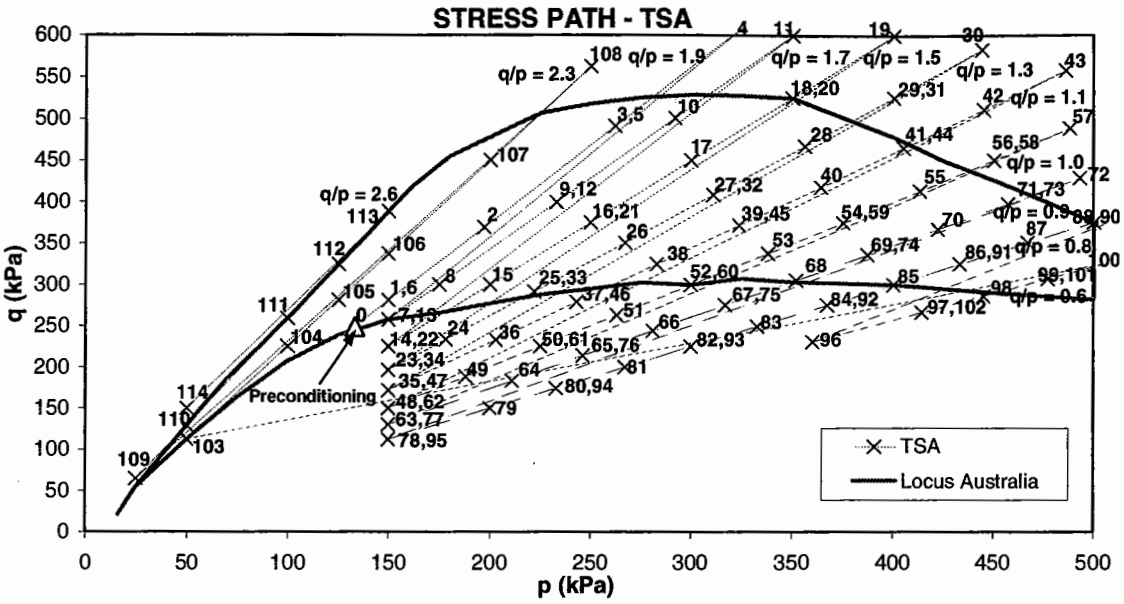

FIGURE 5.13: STRESS USED FOR RLT TESTING OF UNBOUND GRANULAR MATERIALS - TSA

From Figure 5.13, it can be seen that the TSA stress paths tightly covers the area of the Australian Stress Locus, with some levels extending beyond and below the stress locus. Although some of these could be removed from the testing procedure. The stress paths adopted by TSA have small 'step sizes', which provides minimal disturbance to the material specimen from one stress increment to the next, thereby minimising induced permanent deformations and the onset of possible specimen failure. It should be mentioned that the TSA procedure required a considerable number of stress levels to be tested in order to have sufficient data available, at close stress intervals, to allow for the spatial contouring of the resultant modulus values obtained. The result was a pavement designer's "Resilient Modulus Design Chart" (further discussion is presented in §5.7).

The Repeated Load Triaxial test first became an Australian Standard test procedure in 1995. This procedure was formulated from the TSA procedure (Mundy, 1991) by the APRG working group (APRG, 1993) established to investigate the development of a RLT System Specification and an associated Test Procedure. The Australian Standard procedure rationalised the number of stress levels from 82 different stress combinations (or 115 if duplicate stress levels are included) to 61 (refer to Figure 5.14), with the principal aim being to reduce testing time.

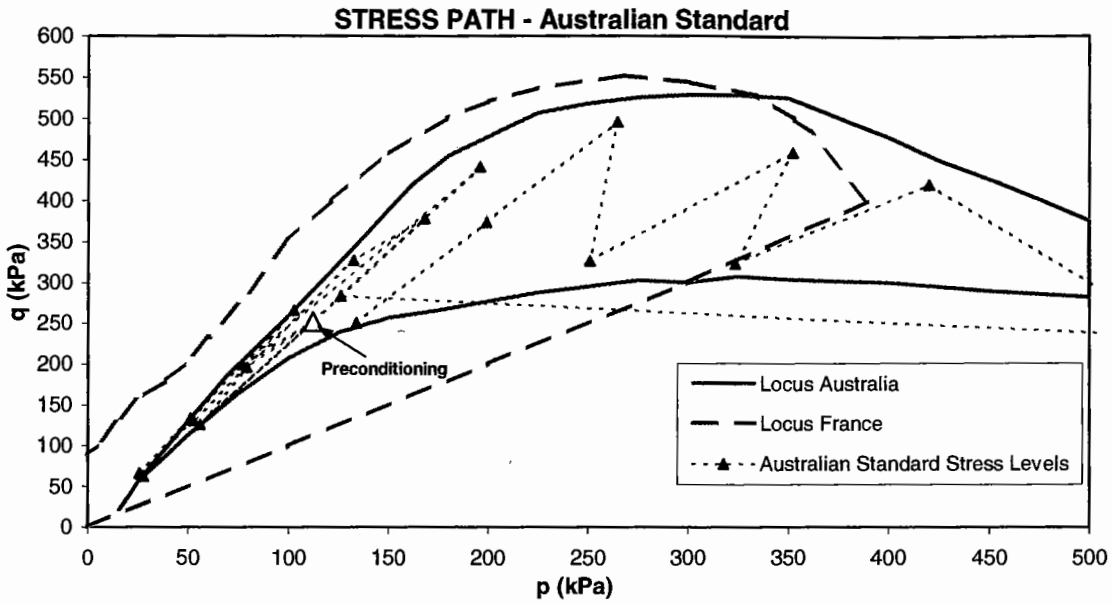

FIGURE 5.14: STRESS USED FOR RLT TESTING OF UNBOUND GRANULAR MATERIALS - AUSTRALIAN STANDARD

The next phase of work was completed over three years (1997-1999) by the APRG Working Committee, investigating the Repeated Load Testing equipment and test procedures. The group, called AWGRU, conducted some precision studies into the existing repeated load triaxial system used for the testing of unbound granular materials. The results of this work have been reported in a paper prepared for the Lisbon Workshop on Modelling and Advanced Testing for Unbound Granular Materials (Vuong, 1999). Here it is recommended that due to the fact that a "large variation in resilient modulus between (Australian) laboratories (involved in the precision studies) occurred at high confining stresses (σ_3) and low stress ratios (σ_1/σ_3), it was decided to exclude some stress stages of high confining stresses and low stress ratios". Thus, the new stress paths are limited to "a maximum confining pressure value of 150kPa and stress ratios σ_1/σ_3 in the range of 3 to 20". These restrictions are drawn in Figure 5.15 as limit lines and are labelled as "Condition Boundaries" in the legend. As a result, a new set of 60 stress levels was proposed by the AWGRU for stress stage RLT testing which are illustrated in Figure 5.15 and tabled in Appendix 3, Table A3.1 (Vuong, 1999).

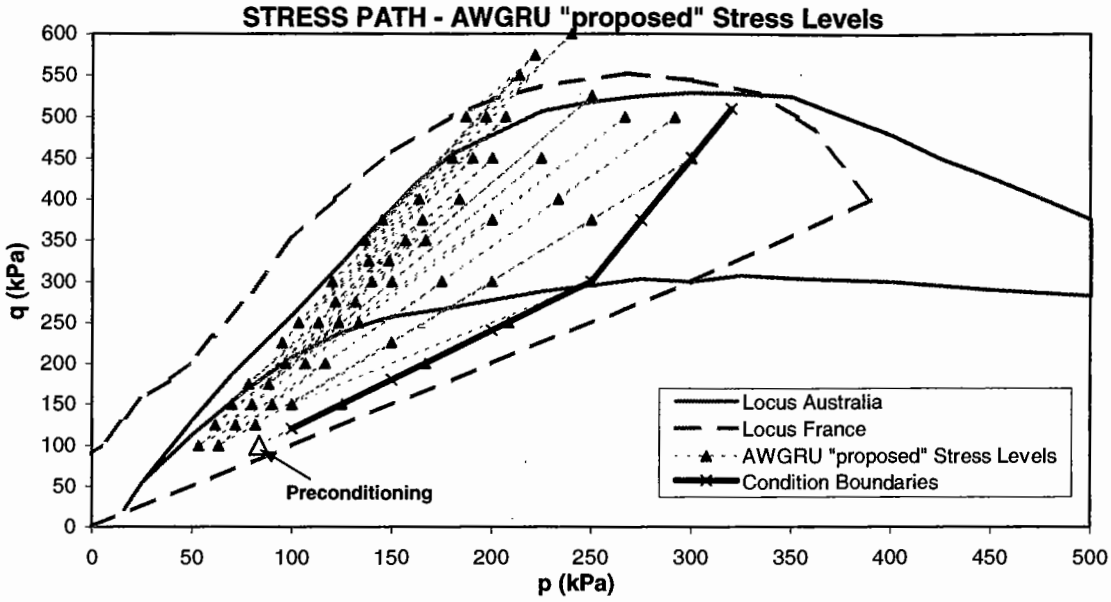

FIGURE 5.15: AWGRU PROPOSED SET OF STRESS LEVELS FOR RLT TESTING OF UNBOUND GRANULAR MATERIALS

It can be seen from Figure 5.15, that a number of stress levels still exist well beyond the upper limits of the Australian and French loci. With reference to Figure 5.15A, which is an enlargement of Figure 5.15, the stress increments (in Δp and Δq) between stress stages are very large in many cases with the Δp being often greater than 75kPa; the highest separation is 104kPa, between points 49 and 50. It is felt that the number of stress levels could be further reduced as the separation between stress paths beyond stress stage 25 is only a $\Delta(q/p)$ of 0.1. A preferred set of stress levels and test sequence will be presented in §6.3.5.

From Figure 5.15A, it can be seen that the sequence defined is somewhat 'haphazard' in nature, particularly after cycle 11. After testing at cycle 34, the stress path moves to cycle 35 at a stress combination where shear failure could well occur unless the material is one applicable to a high quality base layer. This will become more apparent to the reader after noting the discussions presented in §5.5 and §5.6. If a significant degree of shear strain occurs in this stress region, it will most severely effect the quality of the data to be modelled using available material behaviour models. Data obtained from subsequent stress paths may, in effect, relate to a different material condition following the shear induced.

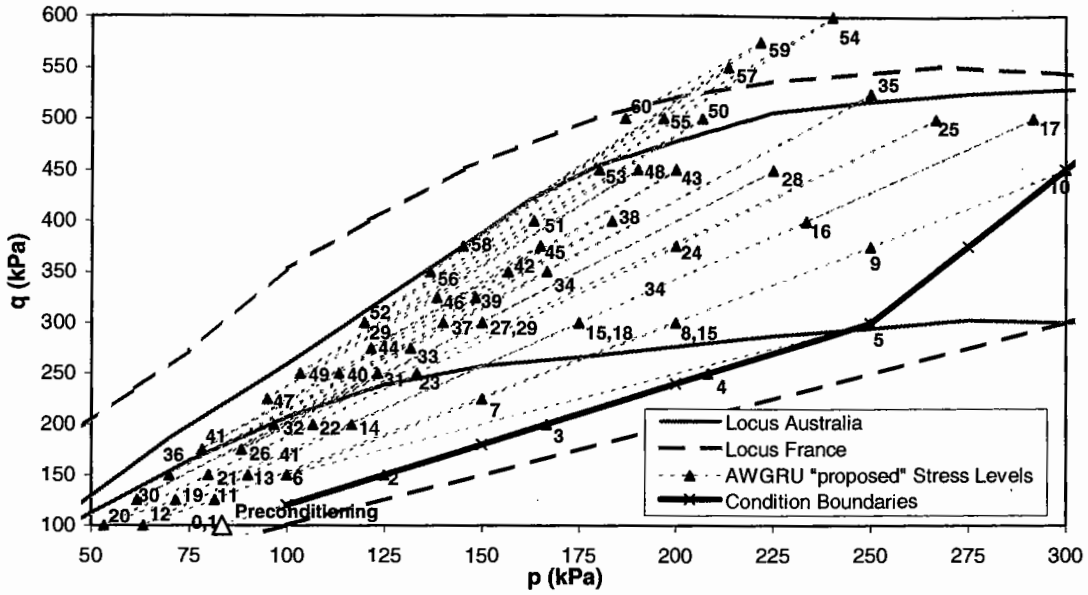

FIGURE 5.15A: ENLARGEMENT OF AWGRU PROPOSED SET OF STRESS LEVELS

5.5 Shear Strength Classification

A need exists to establish whether a classification system could be developed to identify the potential shear failure of a material, depending on the stress levels it encounters within the pavement structure, which in turn depends on the layer position. To do this, a number of Mohr-Coulomb failure envelopes were plotted in p-q space, along with existing loci, for a wide quality range of different materials (with a select few shown in Table 5.2). The failure envelopes were derived from monotonic, drained, static triaxial tests (Mundy, Sept. 1994).

Material	DDR (%)	RMC (%)
A - South Australian coarse grained quartzite material, with a blend of fine siltstone material at -4.75mm sieve	98	52
B - South Australian coarse grained quartzite material, with a blend of fine siltstone material at -4.75mm sieve	98	87
C - French gneiss	97	80
D - Dolomitic limestone (recovered from a failed, 2 month old, inverted Australian pavement, reported in §10.4)	98	85

TABLE 5.2: MATERIALS USED IN FIGURE 5.16 DEPICTING FAILURE ENVELOPES

The static triaxial tests performed were 4 stage tests, with the each stage having a static confining pressure of either, σ_3 = 10, 20, 40 or 80kPa applied in sequence.

These lateral pressures were selected to represent a typical range which could exist in the UGMs under thin asphaltic surfacings. The maximum vertical stress values, appropriate to each confining stress level, were determined in the conventional manner for this type of test. A loading rate of 0.5mm/min was used to allow sufficient time for dissipation of internal pore pressures to occur. The material densities and moisture contents are relative to the maximum values obtained in a modified Proctor compaction test.

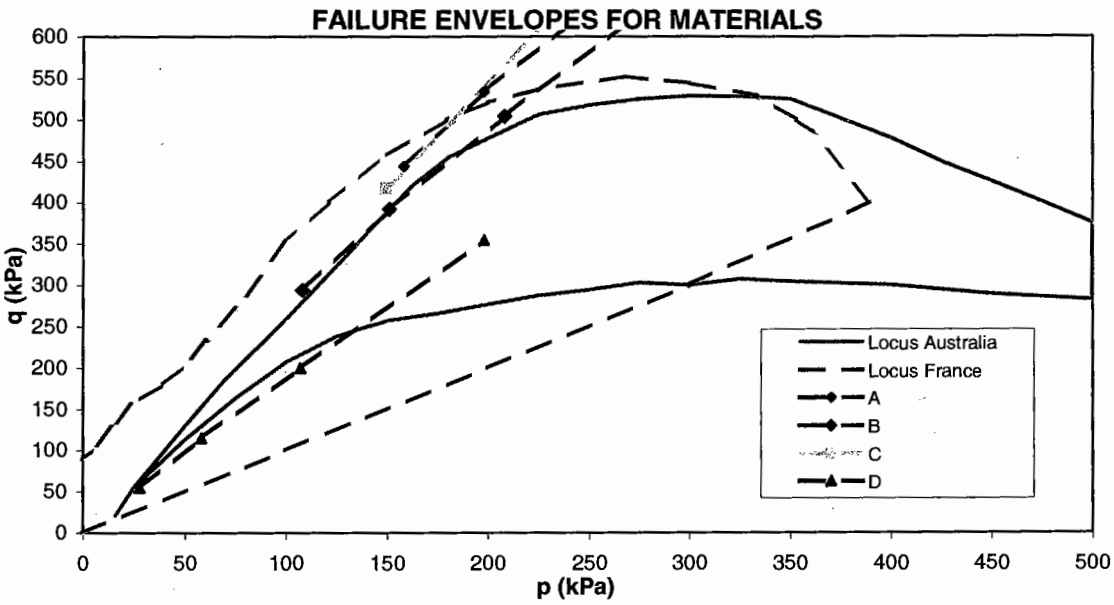

FIGURE 5.16: STRESS LEVEL BOUNDARIES FOR TSA AND LCPC ANALYSED PAVEMENTS ALONG WITH SOME SELECT MATERIAL FAILURE ENVELOPES

These results, when plotted in p-q space in Figure 5.16, illustrate the position of the failure envelope relative to that of the stress loci.

The crushed rock quarry product tested at a low moisture content (material "A") was found to be satisfactory, with the shear failure envelope not intercepting the Australian Stress Level Boundaries. At a high moisture content the material borders the same stress locus (material "B"). As a result, shear failure of this material would not be expected in a pavement layer under Australian standard axle loading conditions. However, the other poor quality material, which was at a high moisture state and retrieved from a failed pavement (material "D"), appears to be most

unsuitable for basecourse or sub-base application unless it was modified as its failure envelope encroaches significantly upon the stress level boundaries. The failure envelope for the French material (material "C") also indicates adequate shear strength relative to the French or Australian Stress Loci.

It should be noted that when stress applications are applied to a material at a p-q combination below the failure envelope, then the closer the stress point is to the failure envelope for that material condition, the greater the magnitude of shear and hence permanent strain expected to be induced in the material. This is supported by work of other researchers. Thom (1988) has suggested that the permanent shear strain is related to a shear ratio $(q_{failure} - q_{max})/q_{max}$. From this approach, the closer the stress point is to the failure envelope, the lower is this shear ratio. Paute et al (1993) defined a limit value, A, for permanent strain which varies according to shear ratio $q/(p + p^*)$ and the slope of the static shear failure line.

Generally, it has been found from extensive testing as part of the MT16 program (Mundy, 1991-1994) that the position of the static triaxial test failure envelope correlates well with dynamic repeated load stress combinations which result in material failure. Remote from the failure envelope, resilient moduli obtained by following the stress path from point to point (according to Figure 5.13) were found to show continuity when plotted graphically (see plots such as Figure 2.18 and 2.19). However, for weaker materials of low shear strength, values of resilient modulus were found to be non-sensical in continuity and very high (due to large loading deformation and low unloading rebound, hence high modulus) at stress levels of 103 or greater (see Figure 5.13). Thus, the failure line provides a good indication of the stress levels at which shear failure may be expected to occur in a material subjected to dynamic loading.

Depending on the geology of a material and factors such as those mentioned in §2.3, it can be expected that the material shear strength, as given by the position of the failure envelopes in p-q space, will generally fall within the upper limit defined by materials "A" and "C" and a lower limit defined by material "D". This has been found to be the case for more marginal alternative pavement materials, which may be

sourced through a recycling process. One such material tested at the University of Nottingham, as part of the COURAGE project, was a low grade recycled crushed concrete and asphalt plannings material. When tested in the triaxial apparatus, the failure envelopes for a range of material conditions tested (appearing in Table 5.3), lay between that of a high quality material of high moisture content (denoted by "B") and that of the failed pavement material (denoted by "D") illustrated below (see Figure 5.17).

Material	DDR (%)	RMC (%)
E - Recycled crushed concrete and asphalt plannings material, with a small % blend of brick	95	88
F - Recycled crushed concrete and asphalt plannings material, with a small % blend of brick	96.7	48
G - Recycled crushed concrete and asphalt plannings material, with a small % blend of brick	98.6	82

TABLE 5.3: MATERIALS USED IN FIGURE 5.17 DEPICTING FAILURE ENVELOPES

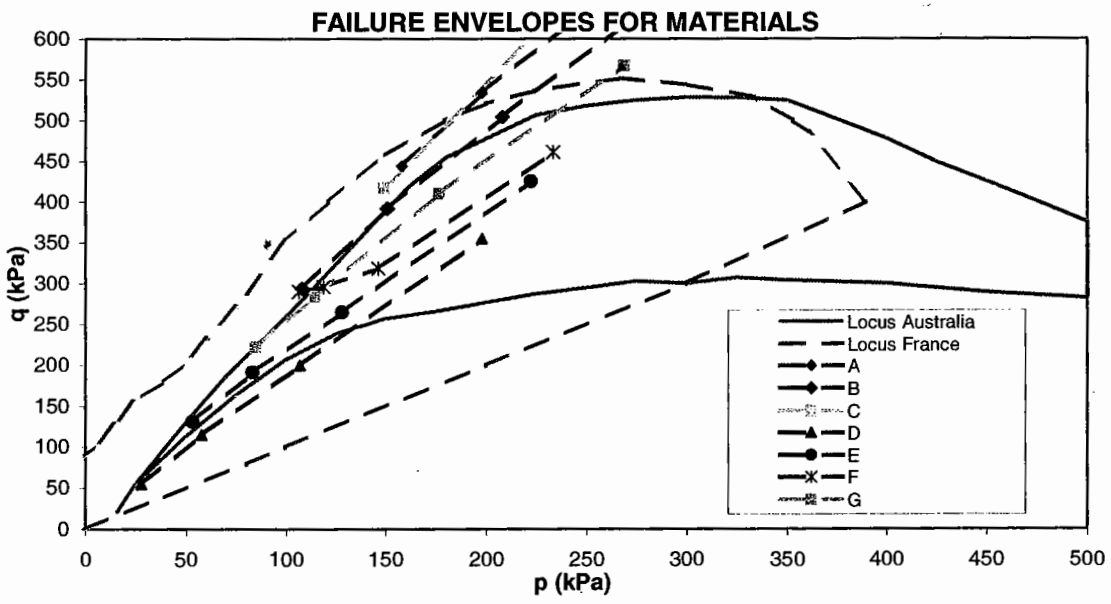

FIGURE 5.17: STRESS LEVEL BOUNDARIES FOR TSA AND LCPC ANALYSED PAVEMENTS ALONG WITH A RANGE OF MATERIAL FAILURE ENVELOPES

5.6 A New Shear Strength Classification

A new classification system could be derived for materials considering their suitability for different classes, and hence pavement layers, based upon a material's

shear strength, as determined from its failure envelope in p-q space. It is considered that this system is the *first* means of assessment for "how a material could be used in the pavement" before one even begins to think of testing for suitability in terms of permanent strain, resilient modulus or other such parameters.

5.6.1 Deriving the Shear Zones for the Model

To derive shear zones in p-q space that reflect a material's quality, the Author has analysed a range of loaded pavements, including BST surfaced granular, thin 35mm asphalt surfaced granular and inverted pavements. Consideration to material quality and state conditions has been given in the analysis. Figures 5.18A to 5.18C below show the range of stress levels within the pavement layers computed using non-linear elastic modelling with program NONCIRL and correcting for lateral stress as discussed in §5.3. The stresses have been separated into those combinations associated with fill, sub-base and base pavement layers, with upper limit boundary lines shown for the fill and sub-base layers. The stress combinations all lie within the stress locus illustrated in Figure 5.5. To ensure that shear failure does not occur within these layers, stress zones have been created (depicted in Figures 5.18A to 5.18C) in which a material's failure stresses must reside. These stress zones are based at a higher p-q stress state than those experienced by the material within the loaded pavement, as computed. The stress zones represent materials classed as either poor, marginal or high quality, which for thinly surfaced pavements, could be classed as fill, sub-base and base pavement layers. The stress limit lines for the fill and sub-base layers correspond to the maximum levels of stress that could be encountered within these layers beneath BST-surfaced granular pavements. The depths are approximately 150mm beneath the surface of the pavement for the sub-base layer and 250mm for the fill layer. The base layer thickness of 150mm and sub-base layer of 100mm are typical minimum thicknesses used in the construction of the arterial road network and corresponds to a design traffic of 2-3 $\times$ 10^5 ESAs and a subgrade stiffness condition of 100MPa or greater. A good deal of the rural road pavements in South and Western Australia are founded on dry sandy subgrades with high strength and stiffness. Many such pavements have been simply designed using basic charts (such as Figure 8.4, Austroads 2001) depicting a minimum thickness of granular

material for a given design traffic and foundation material strength (refer to Austroads, 1992, Chapter 8).

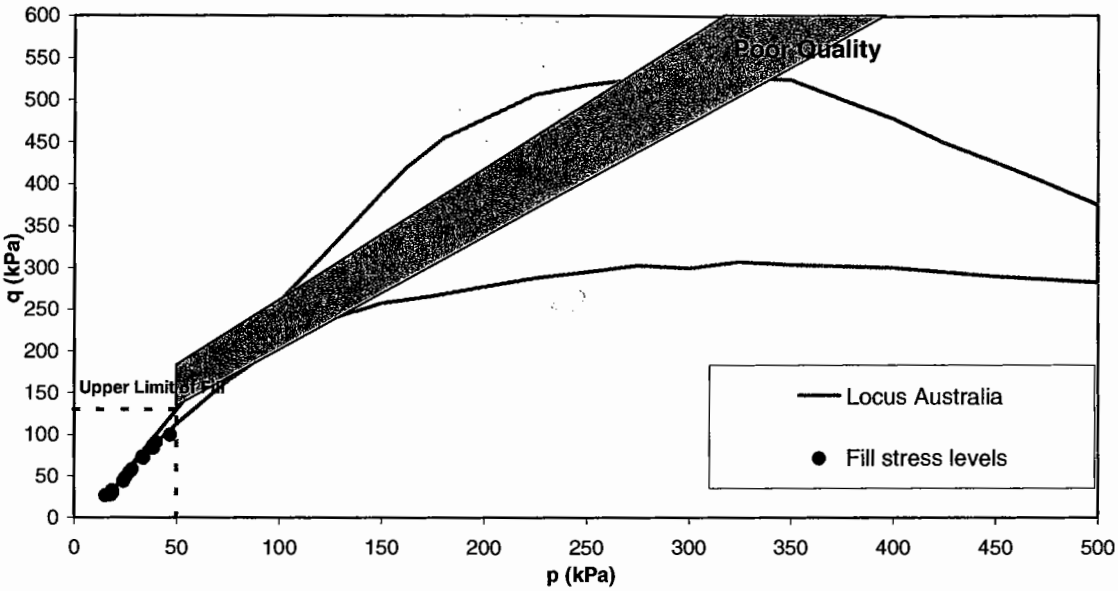

FIGURE 5.18A: STRESS LEVEL ENCOUNTERED IN FILL LAYERS – POOR QUALITY ZONE

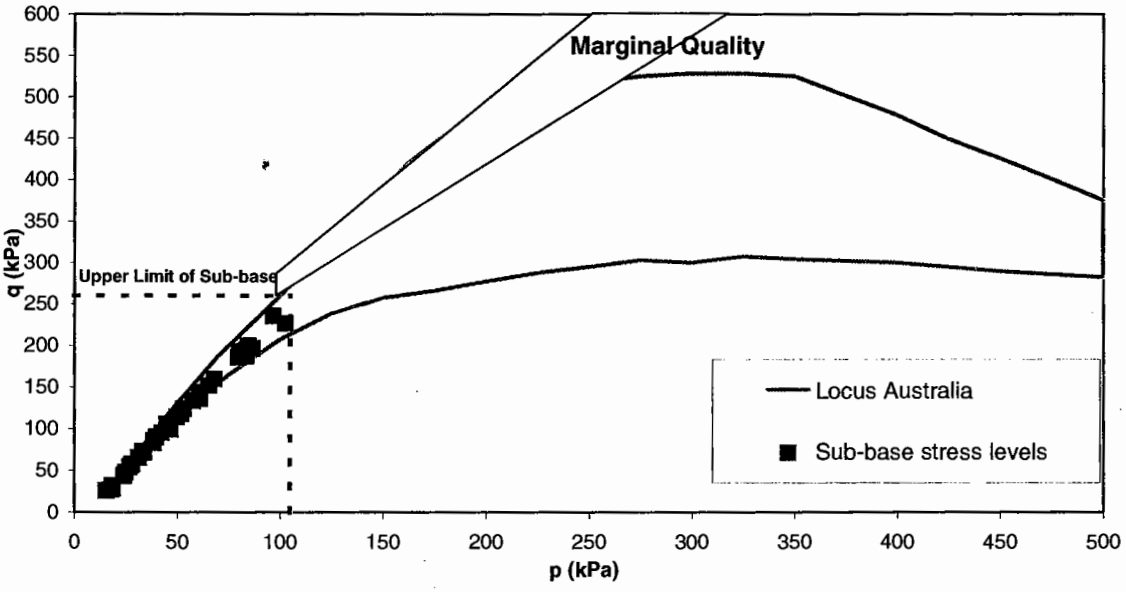

FIGURE 5.18B: STRESS LEVEL ENCOUNTERED IN SUB-BASE LAYERS – MARGINAL QUALITY ZONE

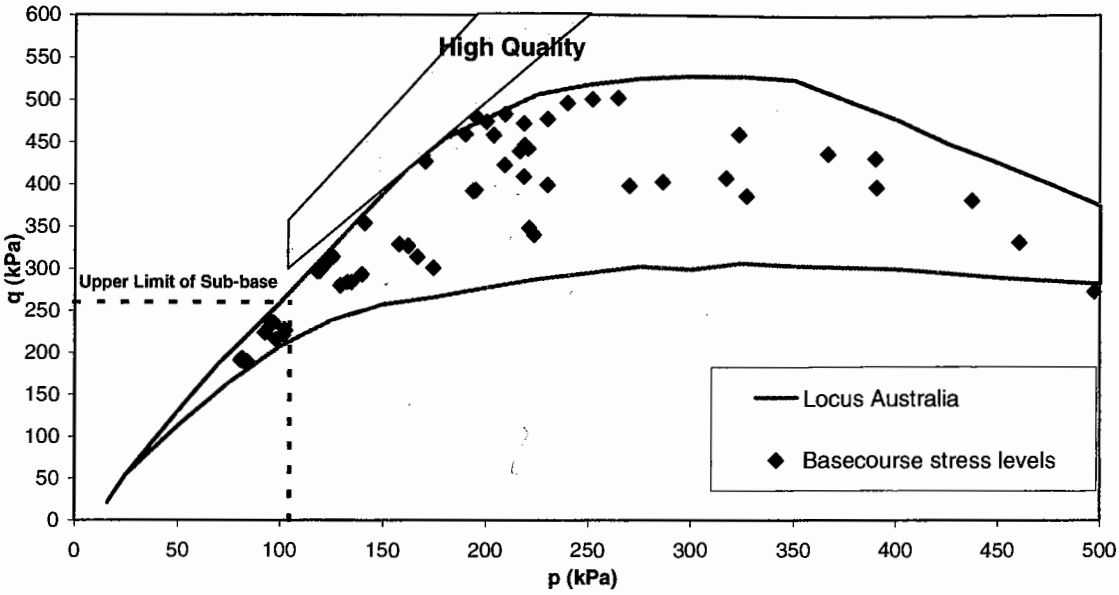

FIGURE 5.18C: STRESS LEVEL ENCOUNTERED IN BASE LAYERS – HIGH QUALITY ZONE

By combining all shear zones, as shown in Figure 5.19, the new shear strength classification system can be seen to evolve.

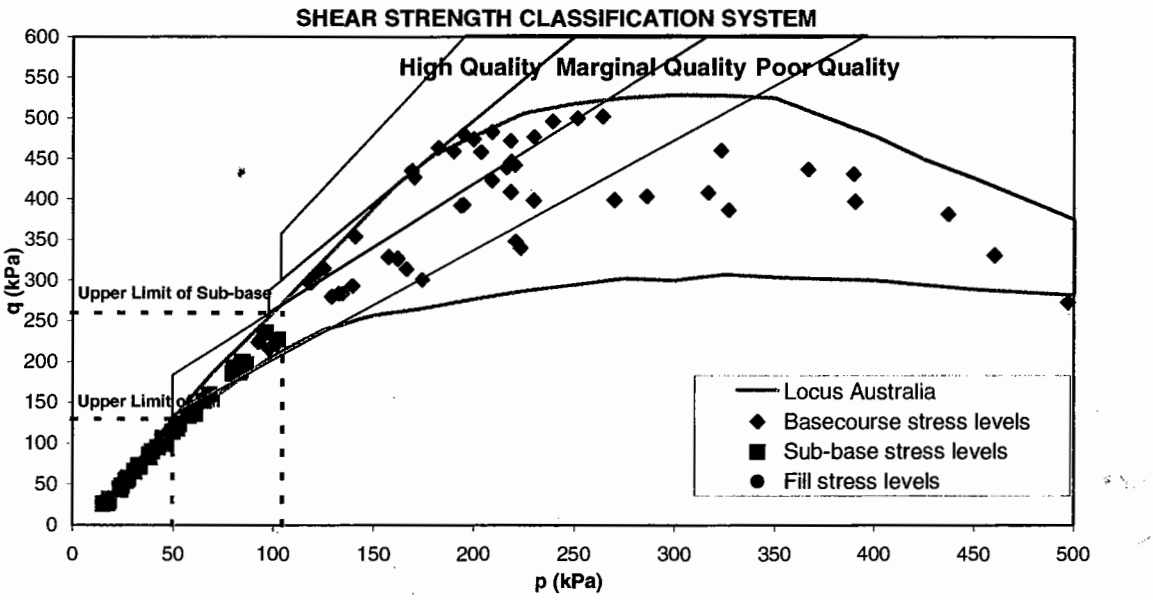

FIGURE 5.19: ALL STRESS LEVEL ENCOUNTERED IN PAVEMENT LAYERS – ALL QUALITY ZONES

This system depicts the quality zones that exist in order to separate the many different compacted pavement materials according to their shear susceptibility.

5.6.2 Model For Thin Surfacings (less than 40mm asphalt)

The boundaries considered for high, marginal and poor quality materials are presented in Figure 5.20 below ***for the Australian design case only. In addition, the material quality zones designated also describe the appropriate layer usage considering that the materials are to be used for thin surfacing applications only (ranging from a BST seal to approximately a 40mm asphaltic concrete surfacing).*** Before material boundaries can be derived for the French locus, further clarification concerning the boundaries reported by Balay et al (1998) is required. As mentioned in §5.4.1, uncertainties exist concerning the French locus derived, especially considering that the Author's analysis of French pavements under French loading show the stress combinations to lie within the Australian locus.

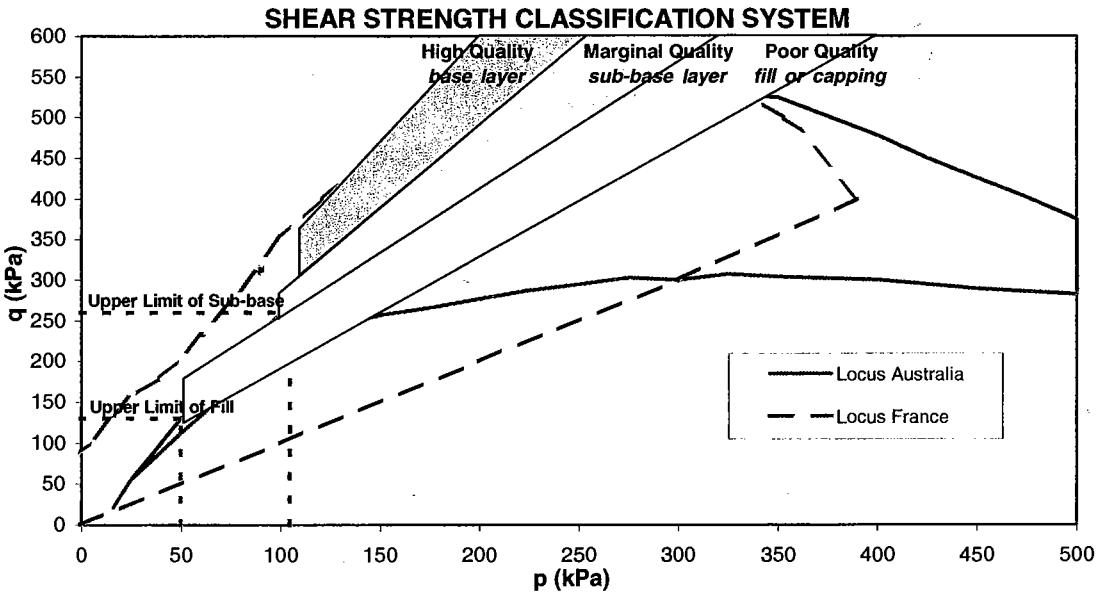

FIGURE 5.20: NEW SHEAR STRENGTH CLASSIFICATION SYSTEM

The 'rules' for the derivation of the three boundaries are as follows:

- define "High Quality" material as being suitable for basecourse layer applications; "Marginal Quality" material as being suitable for sub-base layer

applications; "Poor Quality" material as being suitable for fill or capping layer applications,

- a shear failure envelope for a basecourse material, for example, must lie predominately within the "High Quality" material boundary class such that only a minor proportion may lay outside of its boundaries,
- the material boundary classes cater for the orientation of the shear strength failure envelopes (ie, q increases proportionally with increases in p),
- each of the boundary classes has been positioned such that they remain outside (at a higher q and lower p) of the stress locus region considering the layer application of concern. For example, the "High Quality" material boundaries do not lie within any portion of the stress locus that is relevant to the expected basecourse material stress levels – see Figure 5.18C. Also, the "Marginal Quality" material boundaries do not lie within any portion of the stress locus which is relevant to the expected sub-base material stress levels (as defined by the upper stress limits of the sub-base, relevant to BST pavements with a thin basecourse layer) – see Figure 5.18B,
- the final positioning of the boundary classes should also take full account of knowledge of material performance *in-situ*. This aspect is assessed (for the boundary classes) in Chapter 8.

By superimposing Figures 5.17 and 5.20, it is shown that different type pavement materials that were tested fit into this shear strength classification system (see Figure 5.21).

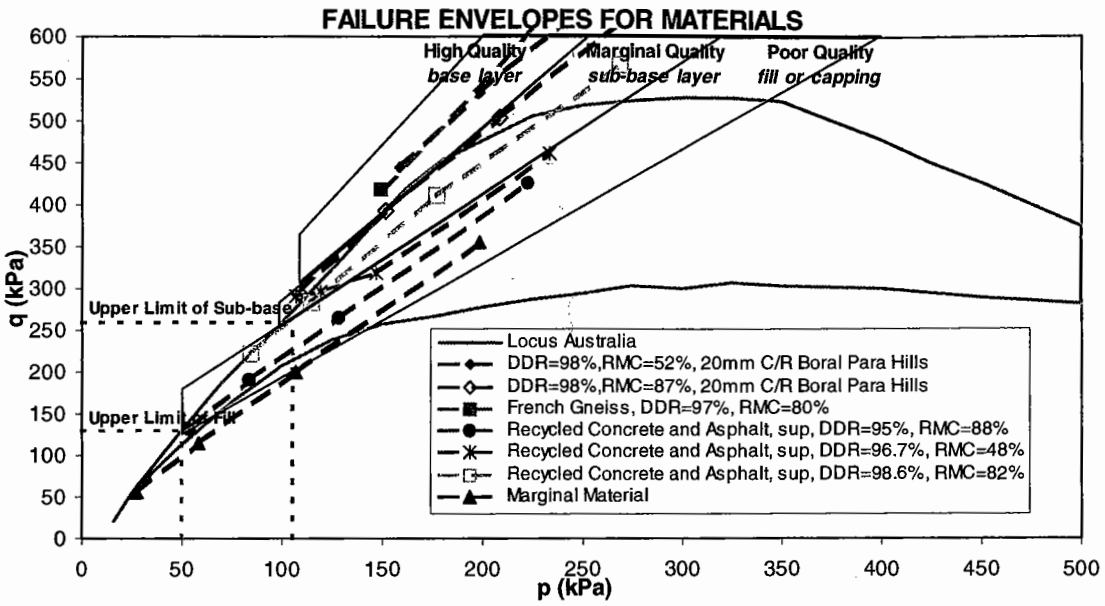

FIGURE 5.21: THE CLASSIFICATION BOUNDARIES FOR PAVEMENT MATERIAL FAILURE ENVELOPES WITH SOME TYPICAL MATERIALS

Illustrated in Figure 5.22 are the VCP and CCP CEN Stress Paths used for the RLT test. It can be seen that the "High Quality" material would not be expected to fail when tested along either of these stress paths, making it suitable for basecourse layer applications. The "Marginal Quality" material may fail at a range of stress combinations which exist in a basecourse layer, but these materials possess a shear strength above that of typical sub-base stress levels (generally stresses below an upper limit of p = 105kPa and q = 260kPa). Meanwhile, the "Poor Quality" material may fail at a range of stress combinations which exist in a sub-base layer, but these materials posses a shear strength above that of typical fill or capping material stress levels (generally stresses below an upper limit of p = 50kPa and q = 130kPa).

It can be seen from Figure 5.22 that the current CEN RLT test procedure does not address material quality in determining the appropriate stress levels, which should be used to assess the materials' performance properties. It is considered that the CEN stress levels are applicable only to high quality UGMs. With reference to Figure 5.22, a marginal quality (sub-base type) material could fail at CEN Method A, VCP stress combinations of:

p = 250kPa, q = 500kPa

p = 300kPa, q = 600kPa (including the preconditioning stress level)

p = 125kPa, q = 300kPa

Whilst a poor quality (fill or capping type) material could fail at CEN Method A, VCP stress combinations of:

all q/p = 2.0 (including the preconditioning stress level)

all q/p = 2.5

and also at some CEN Method B stress combinations

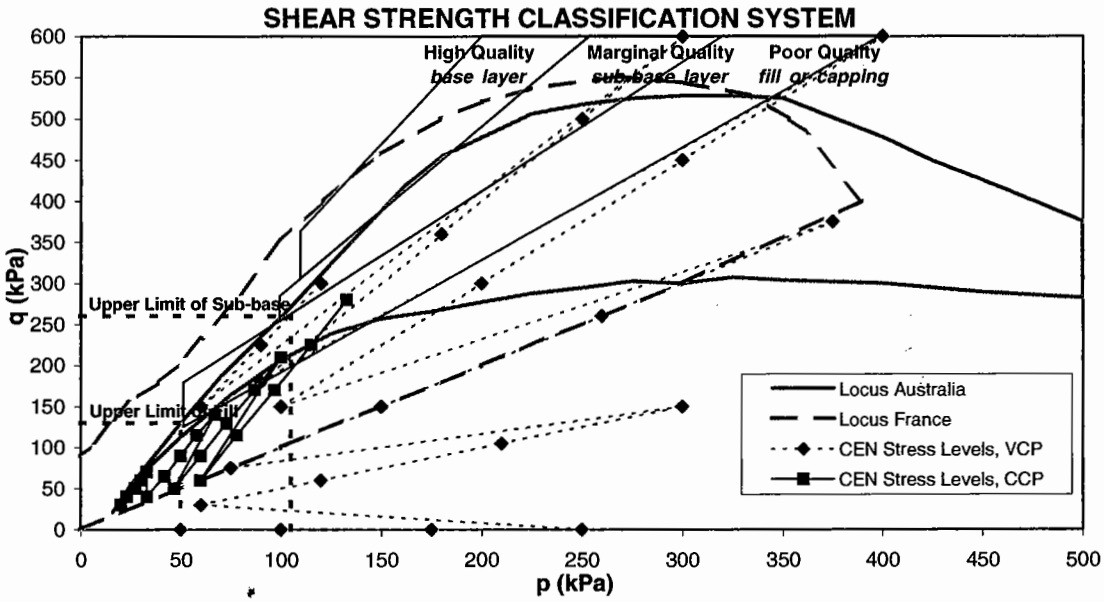

FIGURE 5.22: STRESS LEVEL BOUNDARIES FOR TSA AND LCPC ANALYSED PAVEMENTS ALONG WITH THE CLASSIFICATION BOUNDARIES FOR PAVEMENT MATERIAL FAILURE ENVELOPES

It is recommended that the current CEN RLT test procedure be re-designed according to material usage in the pavement, which is closely aligned with its inherent quality and the imposed stresses it will be required to resist. After all, the primary requirement of an unbound granular mixture in a pavement structure is that it should be able to withstand the stresses imposed upon it from vehicular wheel loadings. As a rationalisation of the stress levels used to date, stress levels are proposed appropriate to either high quality base materials or marginal quality sub-

base materials (see Appendix 2, Tables A2.1 and A2.2, along with the discussion presented in §6.3.5).

5.6.3 Model For Thick Surfacings (greater than 80mm asphalt)

It should be noted that if materials were to be used for granular layers under thicker surfacings, the layer application assigned to the quality zones should be re-interpreted from further analysis, however, the general quality class category, is of course, unchanged. This is so, because as the thickness of the surfacing increases, the levels of stress carried within the granular material, throughout the depth of the layer, will greatly decrease. This is due to the greater load carrying capacity of the asphalt - to a level perhaps now below the shear strength of the material. From analysis, the stresses beneath a ESA loaded 80mm asphalt layer have been calculated to be approximately σ_1 = 235kPa and σ_3 = 16kPa (p = 89kPa and q = 219kPa). These stresses fall within those of a sub-base layer material according to Figure 5.20. Thus, a shear failure envelope for a material used under a thick surfacings must lie predominantly within the "Marginal Quality" (or better) material boundary class such that only a minor proportion may lie outside of its boundaries.

5.7 'Resilient Modulus Design Charts' for Granular Materials

'Resilient Modulus Design Charts' have been prepared for all the unbound granular materials tested at TSA under the MT16 Project which deals with the Resilient Modulus Characterisation of Granular Materials (Mundy, 1991-1994 and Andrews, April 1997). The resilient modulus values determined at each stress condition shown in Figure 5.13 can be used to provide a contour plot of the lines of constant modulus (see Figure 5.23). The Design Charts have been plotted in p-INV space, where INV stands for inverse stress ratio or (σ_3/σ_1). This parameter was adopted as a means of defining the shear stress state of a material. The other parameter used to define the volumetric stress was the mean normal stress. The inverse stress ratio, which is the "inverse" of the commonly known "stress ratio" used in soil mechanics, provides a finite and continuous range (between 0 and 0.6) in which to plot resilient modulus test data. This discrete range allows the measured modulus values, corresponding to individual stress states tested, to be plotted and contoured. This form of data analysis

and presentation was first proposed by the Author (Mundy, 1991) and is unique in the materials testing world. The charts allow materials technologists to visualise the spatial relationship between volumetric and shear stress parameters with resilient modulus. A typical example is provided below (Figure 5.23) for the South Australian quarry product, Boral Para Hills 20mm crushed rock material, having been tested at state conditions of DDR = 98% and RMC = 50% (Mundy, September 1994).

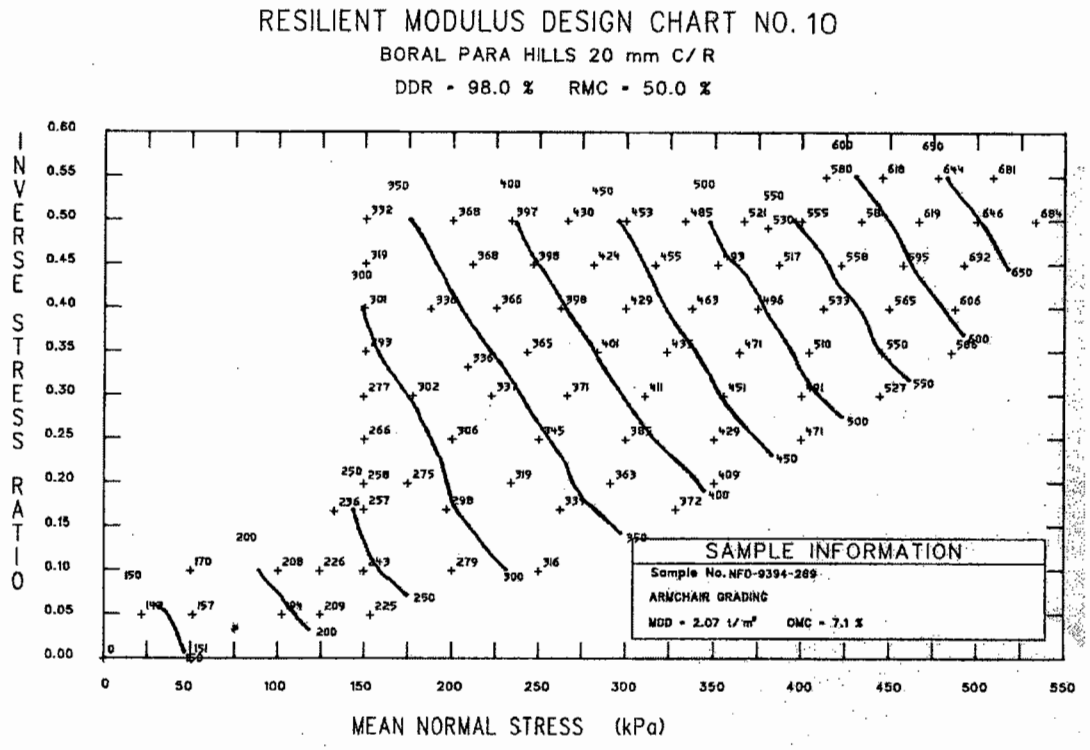

FIGURE 5.23: TYPICAL 'RESILIENT MODULUS DESIGN CHART' USED BY TSA (P-INV SPACE)

These charts can be used by pavement engineers to determine modulus values for assignment to individual unbound granular material pavement (sub-) layers in a mechanistic design process. It requires knowledge of the analytically determined *in-situ* stresses (vertical and lateral) resulting from the imposed surface wheel load and, thus, relies on using an iterative design process until a convergent solution is obtained (Mundy, September 1992). A different example of the Design Chart, but reworked in a different stress space (p-q), is shown in Figure 5.24.

The stress path sequence used previously by Transport SA in the repeated load triaxial system follows incremental changes in mean normal stress along a given inverse stress ratio. Once the path along a particular inverse stress ratio is covered, testing along the next highest inverse stress ratio path is covered. This has the same affect as testing along constant q/p ratio stress paths, as shown in Figure 5.13, except the sequence is somewhat different.

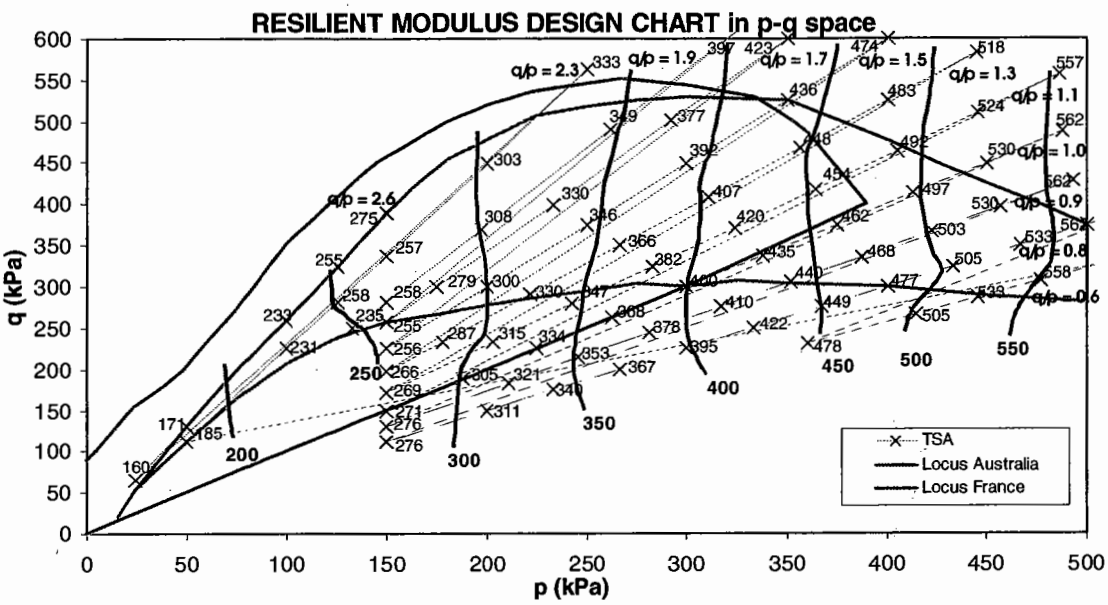

FIGURE 5.24: TYPICAL 'RESILIENT MODULUS DESIGN CHART' USED BY TSA (P-Q SPACE)

5.8 Summary

Stress levels, and hence resilient modulus, can vary significantly within the upper constructed UGM base layer (generally 150 to 200mm+ in thickness) of a thinly surfaced pavement. This can be seen from Figures 5.8A and 5.8B where the upper base layer of 150mm thickness was divided into 50mm sub-layers to allow resilient modulus to vary non-linearly with pavement depth. As a result, adequate sub-layering needs to be introduced into the design response model to accommodate this fact, for without it, linear elastic theory will not cope with the stress-dependent nature of unbound materials. Below this depth, thicker sub-layers could be used (75mm proposed) for the next two granular pavement layers, which show much reduced stress dependence, particularly for layers at a depth greater than 300mm into

the pavement. Each sub-layer is assigned a unique resilient modulus value consistent with the stress levels (both vertical and horizontal) within them.

The importance of correcting the horizontal stress to allow for conditions of overburden stress, material failure criterion and residual stresses has been discussed in detail. It was found from modelling many pavements that the different in the resilient modulus determined by accounting properly for the lateral stress and not doing so could be up to 10%. Barksdale (1997, p.6) reports that "an additional confining pressure of 3psi (21kPa) can cause an increase in resilient modulus in a base of the order of 10 to 15% or more compared to neglecting this effect". This chapter presented a framework for correcting for lateral stress by using 'Lateral Stress Correction Charts'. The lateral stress determined from the charts is reliant upon knowledge of the vertical stress at the point of determination in the pavement as well as knowing the material shear strength properties of the angle of shearing resistance and cohesion.

It was found that the magnitude of vertical stress was relatively insensitive to variations in the subgrade modulus (referring to Figures 5.1A and 5.1B). In addition, vertical stresses within UGMs are not greatly affected by changes in sub-layer resilient modulus, particularly at stress levels below about 150kPa (at a depth of approximately 200mm into the pavement). This was found by mechanistically analysing a thinly surfaced pavement of different seasonal conditions, where levels of resilient modulus were substantially greater in the summer condition than those of winter (40 to 50% increase from winter to summer). Here, the maximum variation in vertical stress was 6.5%, which occurred at the top of the upper base layer (refer to Appendix 1). Another analysis reported separately in Chapter 5 noted that for a resilient modulus variation of 15%, the variation in vertical stress was only 2.4%.

The various stress level combinations used for RLT testing in a range of procedures used worldwide have been discussed. These combination will be rationalised in §6.3.5 in order to develop a new standardised stress coverage applicable to *all* countries, which will cover all possible stress combinations expected within the

UGMs of any loaded pavement configuration – in keeping with the stress locus developed (Figure 5.5).

The static triaxial test provides a good indication of a material's shear strength, a knowledge of which is required to determine the capacity of the material in the pavement to support the applied traffic induced stresses. This in turn affects the position in which the material may be placed in the pavement structure. A simple new classification system has been proposed which will allow designers to assess a range of materials' to be used for road construction, according to their intended layer position in the pavement. Needless to say, that more highly stressed materials *in-situ* will need to be of a higher quality class than materials used lower down in the pavement, where stress conditions are much more favourable. This assessment should be made before further testing for other key MPIs is undertaken.

CHAPTER 6
TRIAXIAL ASSESSMENT DEVELOPMENT

6.1 Introduction

The repeated load triaxial test now plays a major role in characterising pavement material behaviour. The dynamic loading used in the test aims to closely resemble that experienced by an element of material within a base or sub-base layer under traffic loading.

The work performed to date concerning pavement stress conditions illustrates that the stress levels and sequences currently used in various repeated load testing procedures, to assess UGMs for their design performance properties, are in serious need of revision (see Chapter 5). This revision is considered necessary to cater for a diverse range of varying quality pavement materials (such as those currently used in construction and new alternative materials) and different pavement types. A separate procedure is proposed, depicting stress conditions and sequences, for testing high-quality basecourse-type materials and another for testing lower quality sub-base and fill type materials.

The contribution of the Author in developing RLT equipment for potential Industry use and testing procedures developed into Australian Standards, is described in detail along with recommendations for existing procedural modifications.

6.2 Background of Development of Pavement Materials Testing Systems and Procedures

To adopt mechanistic pavement analysis requires the elastic material properties of resilient modulus and Poisson's ratio of pavement materials to be determined. However, affordable equipment for use at the practitioner level was unavailable commercially in the mid to late 1980s, with the lowest priced apparatus costing in the order of A$250,000. This system, which was electro-hydraulic (eg, Instron or MTS) with associated controlling equipment, required a large floor space to house it.

By the late 1980s, a number of road authorities and research centres had purchased expensive electro-hydraulic testing systems to carry out characterisation testing of UGMs, but there was little uniformity in the testing procedures or application of results.

6.2.1 Australian Pavement Materials Testing System

One of the earliest triaxial loading facilities in Australia was based at ARRB, being designed and manufactured by CSIRO in 1970. It was modified and improved by ARRB in 1984. However, the equipment was not applicable for the 'routine' assessment of pavement materials due to its cost, complexity and test-time. To bridge this gap, TSA initially produced a pneumatically operated testing system based upon manual control and collection of data by continuous observation of a dial gauge to measure sample deformation, and a proving ring to measure applied loads. This manual system was very labour intensive and subject to human inaccuracy due to the requirement of constant vigilance over a six-hour period.

A project (MT 8) was established to greatly refine the 'simple' repeated load triaxial equipment used to test ϕ100 × 200mm specimens. To achieve this objective, and provide the most economical solutions to meet Departmental needs, it was required that a new system be designed, manufactured and commissioned utilising an automated electronic data acquisition system to replace manual data collection and test parameter calculations. This was essentially performed in two stages.

The *first stage* was to produce a basic system, which required that the pressure gauges, to independently control vertical and lateral pressures, be manually adjusted by a laboratory technician. In addition, vertical deformation values for the load/unload cycle were recorded from a 1μm resolution dial gauge. Once this was achieved, a *second stage* of the project was entered into to develop an electronic data acquisition system and customised software to automatically log data and provide the necessary manipulation to produce the desired elastic and plastic material parameters. The commercial data acquisition software product `ASYST', which is also capable of equipment control, was purchased upon which to develop the applications software. To obviate the need to develop expert `ASYST' programming

skills and expedite the development, the University of South Australia, School of Applied Physics were engaged to write the software, according to a TSA Departmental Equipment Specification (Mundy, May 1991), applicable to the testing of unbound materials.

The specification established the following requirements for the RLT testing equipment, with some of the key points listed briefly below:

- a flow chart of the test procedure established the modules for control and operation of the system (including input parameters, calibration, test setup, real-time display of instrumentation outputs and results, test control),
- design layout and details of all screens to ensure a user-friendly system,
- range and sensitivities of the load system and all instrumentation to ensure satisfactory load control and accuracy in strain measurement,
- stress sequence could be defined by the user, through establishing a simple ASCII input file, which was interpreted by the system. A requirement was stipulated that for any increasing stress level change, the constant cell pressure must be adjusted to the higher level before the total vertical stress is increased, to avoid damage to the specimen by overstressing. On decreasing the stress level, the total vertical stress is decreased before the cell pressure.
- measurement conditions which affect when results are logged (condition 1: last 6 modulus values vary by $\pm$ x MPa, condition 2: after x cycles last 6 modulus values vary by x %, condition 3: after cycle x. (These conditions allowed the user to control the data logged according to a variation in modulus, usually 2MPa or a percentage variation),
- ASCII output file formats which may be easily read for spreadsheet analysis,
- real-time display of material response (applied load waveform, accumulation of permanent strain with the number of cycles), with the capability of auto re-scaling as the test develops with time. This was necessary to allow significant changes in parameters calculated to be detected by the operator viewing the screen during operation. As a result, action could be taken by the operator if necessary.

The 'ASYST' software for the RLT test performed the following tasks:

- controlled data acquisition from the load cell and transducers
- provided a sampling rate of the waveforms in-keeping with the test frequency
- collected the test data
- selectively determined the peak and trough on the load and deformation waveforms, by curve smoothing, to remove transients (noise)
- performed calculations for stress, strain and resilient modulus
- plotted load / unload and deformation / recovery waveforms in real time on the PC monitor

Further details can be found in MTRD Report 8-1 (Mundy, January 1992). A prototype electronic signal conditioner control unit was designed and manufactured by Applied Measurement Pty Ltd (Melbourne) to the Departmental specification mentioned above.

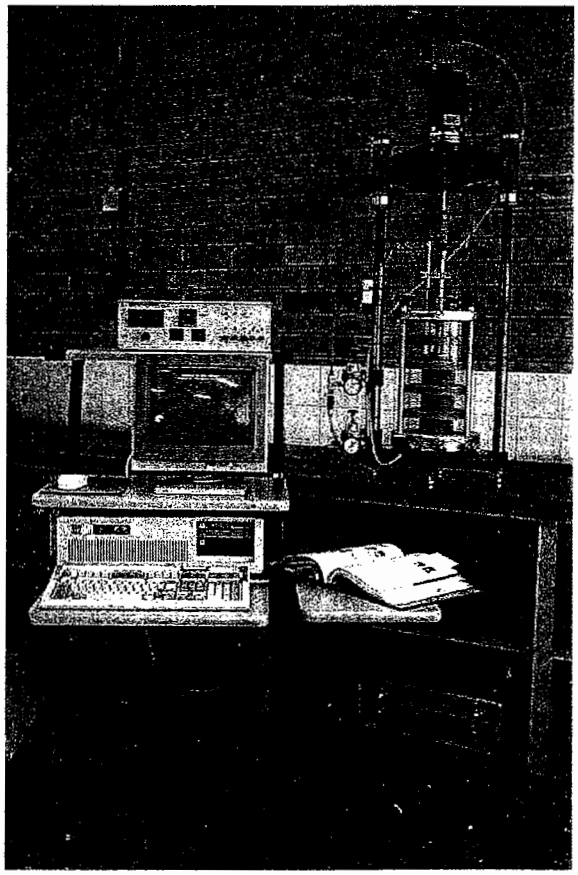

FIGURE 6.1: 'TSA' SEMI-AUTOMATED SYSTEM FOR TESTING UGMS

A semi-automated system (without automatic system pressure control) was developed (by the Author and a technical officer) which still required the manual adjustment of pressure gauges (see Figure 6.1).

The development of the semi-automated system allowed testing units to be built at a very economical price (A$20,000 compared to the expensive system mentioned previously) to meet the testing requirements of TSA. The semi-automated system reduced the cost of a single test from A$1,000 to A$450 to meet routine applications economically. Equally important, semi-automation consequently permitted technicians to concentrate on analysis of data rather than its acquisition.

A *third stage* was subsequently undertaken (by the Author and a technical officer) to purchase additional hardware and enhance the customised software to automatically control the stress sequence test to replace the manual adjustment of pressure gauges. This system was an open-loop one, with no feedback applied to regulate the control of applied pressures through E-P converters.

Stage 1 was reported in MTRD Report No. 16-1 (Mundy, January 1991). MTRD Report No. 8-1 details all developments that were proposed for Stage 2 (Mundy, January 1992), whilst Stage 3 was reported in MTRD Report No. 8-2 (unpublished).

Once the automated system was operational, the TSA Departmental Equipment Specification was further refined and a "detailed equipment and software specification was produced in close cooperation with IPC" (Tritt, 1991). This draft specification was produced by Mundy and deVos (1991). Later, a more generalised specification, which met the requirements of all Australian SRAs and deemed suitable for tender, was then developed. This latter specification, produced by the APRG Working Group on Unbound Materials formed in July 1991, was published by APRG (APRG, 1993). It was made available in the form of a tender document to manufacturers wishing to produce a system for resale on a commercial basis to TSA and other Road Authorities, Educational Institutions or Private practitioners. Industrial Process Controls Pty Ltd in Victoria, Australia worked very closely with TSA, and the Author in particular, to produce the first commercial system for testing

unbound pavement and subgrade materials, referred to as the UMATTA (Unbound MATerials Testing Appartus).

This system (see Figure 6.2), which was developed from the specification, was subsequently purchased by the CSIRO and a number of Australian State Road Authorities for evaluation and materials testing.

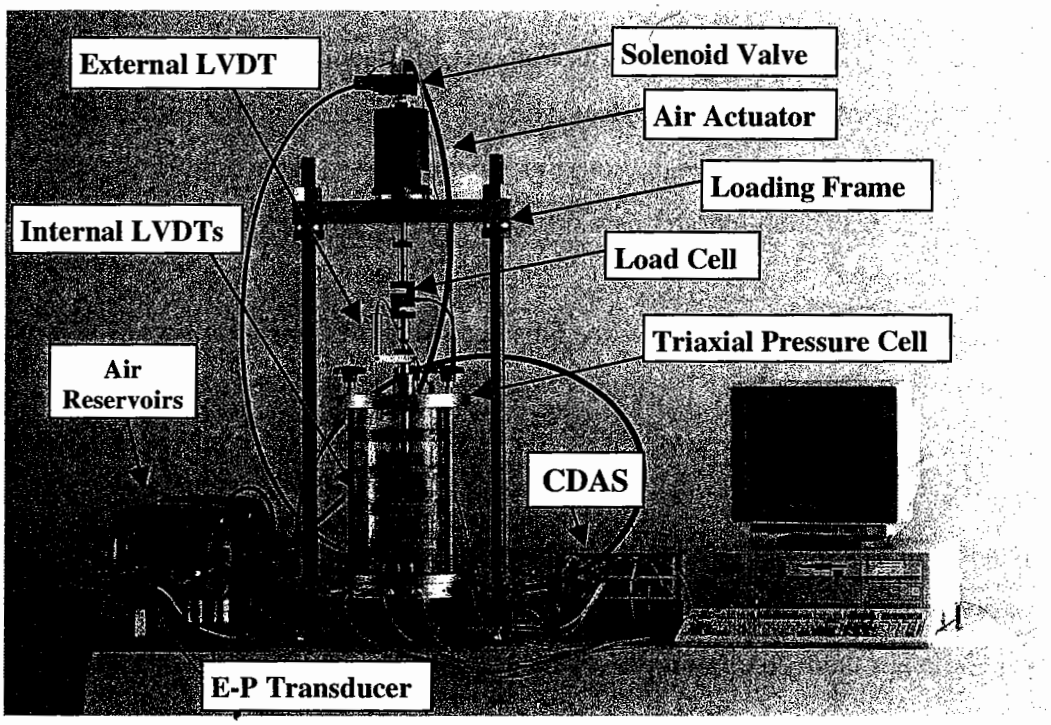

FIGURE 6.2: EARLY 'UMATTA' SYSTEM FOR TESTING UNBOUND GRANULAR MATERIALS

With reference to Figure 6.2, this servo-pneumatic system operates on the basis of an 800kPa filtered air supply feeding two voltage to pressure (E-P) conversion transducers. One controls the vertical force by supplying pressurised air to a 12 square inch bellofram diaphragm-type actuator, with the force monitored by means of a calibrated load cell, whilst the other controls the cell pressure. The solenoid value, connected to the actuator, allows switching of the air supply thereby enabling the vertical force to be pulsed. The supplied air pressure is regulated for fluctuations through two air reservoirs prior to the air passing into the triaxial pressure cell, which provides the confining pressure on the specimen. The control and data acquisition system (CDAS) has provision for measuring eight analogue channels, namely:

- two internal vertical linear variable displacement transducers (LVDTs)

- one external (to cell) vertical linear variable displacement transducer (LVDT)
- one volume change transducer (not used for air confining medium)
- one vertical force load cell strain gauge
- one confining stress cell pressure strain gauge
- one pore pressure transducer (not used)
- one elastometer radial transducer (which consisted of a fine single coiled wire capacitor inside a polymer to measure circumferential expansion of the specimen. This linear device measures to approximately 0.65μm for a frequency output readable to 1 Hertz, using a 250mm unstretched length and has a 10mm range). The device is reported further by the Author (Mundy, 1991) and encouraging results were obtained, but not published at the time.

The CDAS unit is computer controlled using software developed by deVos according to the Author's original specification (Mundy, 1991) and the subsequent specification (Mundy and deVos, 1991).

This initial UMATTA system development played a major part in making available a commercial testing system for the road authorities and materials industry / research organisations. Since the production of the first unbound pavement materials testing system in 1992, the UMATTA system has undergone a number of further refinements to improve system performance. Improvements in pneumatic actuators, which control the loads, have allowed the development of a closed-loop control system. In addition, improvements in measurement technology from capture and conditioning through to control, as well as to end-user graphical interfaces has occurred in recent years.

6.2.2 European Materials Testing System

One of the first systems to be developed in Europe was by Boyce (Boyce, 1976) for the University of Nottingham, used for testing ϕ150 × 300mm specimens. The hydraulic test system, which underwent a number of modifications, has the ability to cycle the vertical and confining pressures applied to the specimen. The pressures are applied by hydraulic actuators, which are controlled by servo-valves in a closed-loop system. The applied axial load and confining pressures are continuously monitored

by the internally mounted load and pressure cells. 'On-sample' instrumentation in the form of two diametrically opposed vertical LVDTs attached through embedded studs and two epoxy hoops for measuring radial deformations are utilised. All control and data capture is performed by a servo-valve amplifier and transducer signal conditioner unit, respectively, using the ATS software.

A French-developed system (see Figure 6.3A & B), which has also recently been purchased by IST, Portugal and ZAG, Slovenia, is a servo-pneumatic loading system, and tests UGM specimens of $\phi 160 \times 320$mm size (Paute et al, 1993).

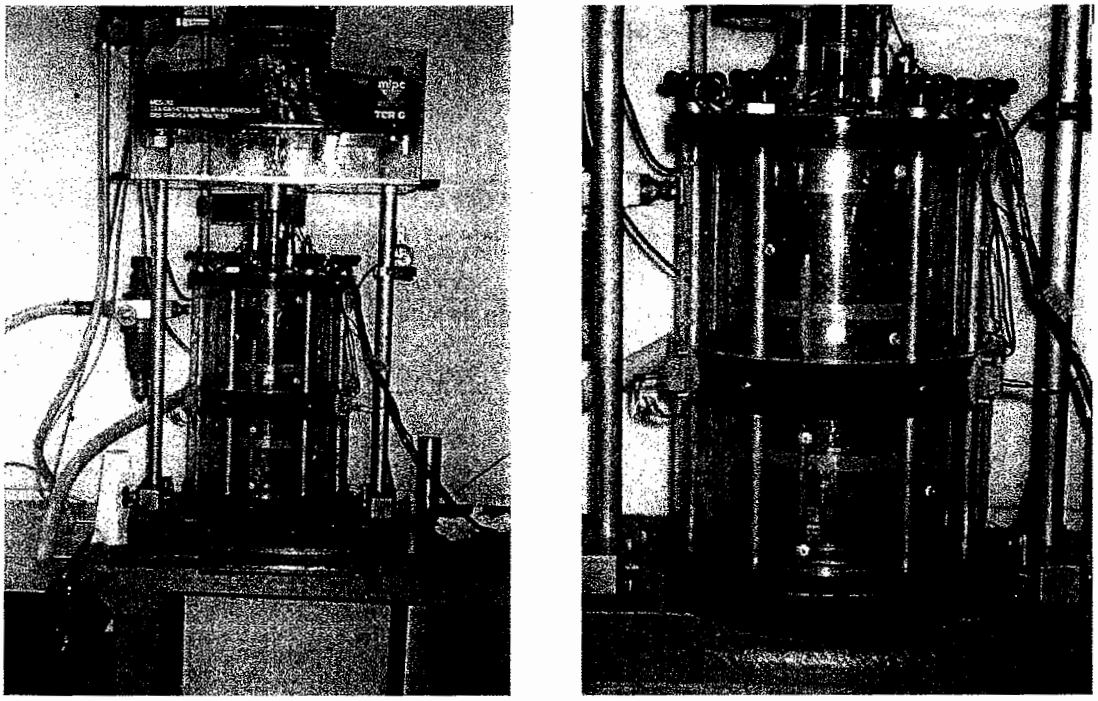

FIGURE 6.3A & B: EUROPEAN SYSTEM FOR TESTING UNBOUND GRANULAR MATERIALS

Given the vertical and confining pressures are controlled by air, this system is similar in principle to the UMATTA one. The only marked difference being the ability of the French system to pulse independently or simultaneously (in phase) the air confining pressure through a second pneumatic servo-valve controlled actuator.

The pressures are applied by air actuators, which are controlled by servo-valves in a closed-loop system. The applied axial load and confining pressures are continuous monitored by the internally mounted load and pressure cells.

Instrument capability is similar although the French have opted for three vertical and three radial LVDTs, placed at 120° from each other, in order to provide a more reliable average of the results and to allow the operator to more reliably detect if one LVDT is not responding consistently in comparison to the other two. The vertical devices are mounted to a rigid 2-ring instrumentation frame, which is mounted in turn to the specimen. Following careful positioning, the operator uncouples the rings to allow them to move independently as the specimen deforms under load and then recovers. The three radial LVDTs are connected through the cell wall to target points mounted on a rubber strip around the central region of the specimen.

A tabulation of the main characteristics of all the systems described are presented in Table 6.1.

System Specification	Australian	Uni. Nottingham	French
Vertical Actuator Type	Air Solenoid	Hydraulic	Air Solenoid
Vertical Actuator Capacity (kN)	10kN	20kN	20kN
Lateral Actuator Type	Static air pressure	Hydraulic or Static air pressure	Air Solenoid
Lateral Actuator Capacity (kN)	800kPa	400kPa	500kPa
Triaxial Cell			
Max. Specimen Size	ø100mm × 200mm	ø150mm × 300mm	ø160mm × 320mm
Cell Fluid	Air or Water	Silicon fluid or Air	Air
Vertical Stress Measurement	Automatic control	Automatic control	Automatic control
Load cell Int. / Ext. to cell	External	Internal	Internal
Lateral Stress Measurement	Automatic control	Automatic control Manual control (air)	Automatic control
Vertical Strain Measurement			
LVDT Int. / Ext. to cell	External	Internal	Internal
number – angle of placement	1 – N/A	2 – 180°	3 – 120°
Range (mm)	10mm	10mm	10mm
Lateral Strain Measurement			
LVDT Int. / Ext. to cell	Internal	Internal	Internal
number – separation	2-¼ points on spec.	2-¼ points on spec.	3-½ point on spec.
Range (mm)	5mm	5mm	5mm
Waveform Shape	Ramped Square	Haversine	Ramped Square
Frequency of waveform	0.5Hz	1Hz	1Hz
Duration of loading pulse	1s	0.5s	0.5s

TABLE 6.1: KEY COMPONENTS OF THE AUSTRALIAN AND EUROPEAN SYSTEMS

6.2.3 Australian Testing Procedure

A systematic procedure for the testing of 20mm nominal size unbound granular materials, using the pneumatic apparatus described, was first developed by the

Author as a result of Project MT16 (Mundy, January 1991). This procedure consisted of two stages of testing. The first stage was deemed the "Preconditioning test", in order to condition the specimen (prior to measuring resilient modulus), using a single stress level of $\sigma_{1\ max}$ = 300kPa / $\sigma_{1\ min}$ = 0kPa and $\sigma_{3\ max}$ = 50kPa / $\sigma_{3\ min}$ = 50kPa (p_{max} = 133kPa and q_{max} = 250kPa, q/p_{max} = 1.88). This corresponds to the approximate level of stress expected in the granular material, under a 35mm asphaltic surfacing, at a depth of 100 to 110mm (see Figure 5.7). The single stress condition was chosen to adequately 'condition' the specimen for the second stage of the test. The second stage of the test was termed the "Stress Stage" test, where resilient strains were measured for a range of 99 stress levels (70 different stress combinations, with 29 duplicate or repeat points) within the stress locus described in Figure 5.5. This wide stress range covers all expected *in-situ* stress conditions such that values could be interpolated for use in pavement design response models. Note that the duplicate (or repeat) points were tested upon unloading from a maximum mean normal stress, to a lower level, along each given stress path. This allowed a repeatability check in order to ascertain the variation in material resilience *at selective stress combinations* throughout the "Stress Stage" test. The "Stress Stage" test was slightly modified in 1992 to account for even higher stress ratios (σ_1/σ_3), gradually approaching the failure condition. The test then measured 115 stress levels (82 different stress combinations, with 33 duplicate or repeat points). The repeatability of the test is discussed in Chapter 7.

The Author's (TSA) test procedure, became the starting point for discussion of the special APRG Working Group on Unbound Materials, with the first draft method delivered to the Group in July 1991. It should be noted that the Author was the Secretary of that Group from its inception. The Group's aim was to take the TSA test procedure as a starting point and broaden it to principally accommodate different sample preparation techniques and different drainage conditions, which were reflected in the practices adopted by the various SRAs. This followed the same principle of development as the equipment or system specification reported in §6.2.1. The resulting "APRG test procedure" was then refined with the view to developing an Australian Standard test procedure. The modified TSA test procedure was first reported by the APRG Working Group (APRG, 1993) prior to it being drafted into an

Australian Standard. The Australian Standard procedure was approved by the Council of Standards Australia in November 1994 and was first published in March 1995 as a draft for comment (Standards Australia, 1995).

Soon after the release of the draft Australian Standard, there were concerns that the modifications made to the original TSA procedure (which generally provided good repeatability, with reference to the work performed by the Author summarised in §7.2.1.2, §7.2.3.1 and §7.2.3.2), particularly in the different sample preparation techniques, may effect the repeatability and reproduceability of the RLT results. In response, a RLT Users Working Group (AWGRU), made up of representatives from State Road Authorities, research institutes and industry, was formed in August 1995. This group conducted a national inter-laboratory precision study of resilient modulus and permanent strain testing of unbound materials to validate the procedure (including the effects of different sample compaction methods) and check the equipment and software.

Following this work, as reported by Vuong (Vuong, January 1999), the test procedure is expected to be further refined in the near future. The findings indicated that loading friction at the shaft/cell interface must be minimised. Regardless of the interface system adopted for testing, it is considered that good maintenance practices must be applied to the shaft and to the cell's shaft housing to minimise errors. Errors should fall to within a coefficient of variation of less than 10 to 15% for all stress combinations tested (which is considered acceptable). It is expected that feedback of key scientific factors identified in this thesis will impact on future revisions of triaxial testing Standards.

6.2.4 European Testing Procedure

The European Committee for Standardisation or CEN has developed a testing procedure (CEN, 2000), which is the result of European research from a number of principal contributing research organisations, namely:

- LCPC, Nantes, France
- University of Nottingham, United Kingdom
- Delft University of Technology, The Netherlands

- Laboratório Nacional de Engenharia Civil, Portugal

This research took place through joint participation in the "Science" project (Galjaard et al, 1996). Also, later, the work of:

- LCPC, Nantes, France
- University of Nottingham, United Kingdom
- Instituto Superior Téchnico, Portugal
- ZAG, Slovenia

through participation in the COURAGE project (EC, 2000), will provide further input into the CEN procedure. The CEN Procedure, prEN13286-7 (October 2000), is presently a draft European Standard specifying a method for determining the resilient and permanent behaviour of unbound granular materials. The drafting work for this standard started in October 1990 in CEN/TC 227/WG 4 "Cement bound, unbound granular, waste and marginal materials". At the time of writing, this procedure is at public comment stage prior to final approval, which is expected to occur in 2003.

6.3 Critique of the Repeated Load Triaxial Test

The following commentary concerns the draft CEN Procedure, the Australian test procedure and may also have applicability to other methods used for determining the resilient and permanent behaviour of unbound granular materials.

6.3.1 Simple Test versus Complex Test

The European CEN procedure currently employs a 'complex' VCP RLT test to determine resilient modulus values for unbound granular base materials. The use of VCP aims to offer wider possibilities and better simulate field loading conditions. However, this procedure requires additional hardware (confining pressure actuator, servo-value, etc) as well as instrumentation and software, capable of providing adequate gain control whilst cycling both vertical and confining pressures in phase. In addition, for hydraulic fluid control systems, such as the one located at the University of Nottingham, this test requires a liquid medium to be used in the cell. The fluid selected is usually silicon oil when conventional instrumentation is used; the oil is expensive and "messy" to use. For some systems, water can be used which requires that the instrumentation be electrically inert. In both cases the tests are time-consuming to set-up due to the array of on-sample instrumentation (for measuring

vertical and lateral strains), filling/emptying procedures involving bleeding the air from the system prior to running a test.

In Australia and the USA, RLT tests have been simplified from the 'complex' VCP ones to utilising a CCP, in which air can be adopted as the confining medium. This allows quick 'routine' assessment of unbound granular materials, which is particularly important if the goal is "performance-based" specifications for these materials. Certainly, if the quarry industries themselves were to undertake such testing to ensure that supply products comply with the limits of a "performance-based" specification, then the testing would need to be quick and relatively simple to perform. As a result, in Australia (as in Sweden), a single transducer placed external to the cell has replaced all of the on-sample instrumentation, in order to further simplify the test. This document does not aim to dictate and define an approach to be adopted for strain instrumentation. The advantages and disadvantages of internal and external to cell mounted devices present a considerable research study in itself. Many researchers have studied the effects including Barksdale and Alba (1997), and the Author in unpublished research. Barksdale found that, generally, an external device can under-estimate the measured resilient modulus for stiff specimens (approximately 340MPa) with a difference between clamp mounted devices being approximately –6%. In addition, permanent deformation could be expected to be over-estimated. However, it should be realised that the errors can be increased for the external device by a range of factors including the quality of specimen end preparation, use of end caps that restrain the specimen and whether porous stone filters are used. Even internal LVDT clamps are not always found to be satisfactory. Problems including slippage and/or rotation of the clamp, sometimes movement of the LVDT targets if insufficient compaction is applied around the embedded targets and higher coefficients of variation in the measured strains due to the smaller values captured.

6.3.2 Material Preparation State Conditions

It has been illustrated in §2.3 and §2.4 the strong dependence of material performance indicators on the moisture content of a given material relative to its optimum moisture content, or more importantly, its degree of saturation. The CEN

procedure, however, suggests preparation moisture states which are less than the optimum value by 1%, 2% and 4%. Thus, depending on the OMC of the material, the RMC or S_r could either cover a complete or incomplete range of moisture contents which the material may experience *in-situ* in a pavement. It has been found in Europe that quite a number of quarry crushed aggregates exhibit an OMC of around 6%. As a result, the relative moisture scale of these materials would be similar and the CEN procedure would give comparable results. However, some "new" recycled materials, such as crushed concrete and masonry mixed with asphalt plannings can also contain some proportion of natural soil/clay through the reclaiming process. Such materials can yield optimum moisture contents of at least 12%. Table 6.2 below illustrates some different materials, their optimum moisture content and their relative moisture states by applying the CEN specimen preparation procedure.

Material Type (% fines passing 75μm sieve)	Mod. Proctor OMC (%)	Mod. Proctor MDD (kg/m^3)	G_s (g/cm^3)	RMC to OMC (%)			S_r (%) ρ_d = 97% MDD		
				OMC %			OMC %		
				-1	-2	-4	-1	-2	-4
Slovenian Limestone (3%)	4.1	2205	2.71	76	51	2	31	21	1
Portuguese Granite (5%)	5.9	2311	2.75	83	66	32	59	47	23
French Gneiss (7.4%)	6.0	2200	2.62	83	67	33	58	46	23
UK Recycled Crushed Concrete & Asphalt (2.7%)	12.0	1944	2.52	92	83	67	83	75	60
South Australian Dolomitic Limestone (12%)	6.5	2310	2.76	85	69	38	65	54	30
South Australian Quartzite/Siltstone blend (11%)	7.0	2140	2.45	86	71	43	82	68	41

TABLE 6.2: MATERIAL STATE CONDITIONS FOR RLT TESTING, PREPARED ACCORDING TO CEN, FOR A RANGE OF DIFFERENT MATERIALS

This illustrates that a direct comparison of resilient modulus and permanent strain properties of different material products (for ranking purposes) can obviously not be made unless the same relative moisture content (or more importantly degree of saturation) is used from one material to the next. With reference to §2.4.1 and Figure 2.12, it was found that the moisture content of UGMs will fluctuate about an equilibrium value depending of the season, level of rainfall, drainage ability of the structure and other factors. It is important, therefore, to assess materials over a range

of moisture levels for design and performance evaluation purposes in keeping with those expected to be encountered *in-situ*. Thus, CEN should nominate specimens to be tested at a RMC to optimum or, better still, to S_r so that direct material comparisons are possible.

In addition, as stated above, the CEN procedure should recommend that materials be tested to the moisture/density state which resembles the range of *in-situ* conditions expected in the pavement. Thus, the resilient moduli obtained can be directly related to stiffness levels in the pavement so that performance may be modelled. In the examples given in Table 6.2, clearly OMC-4% is well below the equilibrium moisture content which may be expected in the pavement itself. In fact, for specimens at moisture contents in this range, suction affects would significantly effect the stiffness and permanent strain characteristics of the material. It was discussed in §2.8 that in base layers, the moisture levels could vary between 40% and 90% of OMC.

The method of preparation (CEN, Clause 6.4.2) also requires moulding all specimens to OMC and then allowing 'dry-back' to the required test moisture state. The time lag between moulding and testing is obviously greater for target low-moisture specimens. This will have a very significant affect on permanent strains and resilient modulus determinations for time-dependent cementitious materials, such as limestones and recycled crushed concrete products. The latter materials will often contain some proportion of unhydrated cement, which will undergo a binding reaction with time. Thus, material comparisons by moisture content will be greatly distorted by the additional affect of cementation.

If materials are properly mixed and cured prior to specimen compaction, the moisture within the specimen should be well dispersed for most materials. It is recommended that all materials be moulded to the desired RMC so that the influence of material moisture can be directly determined. Also, for materials with expected cementitious properties, additional time-dependent tests should be conducted to isolate the influence of this effect.

6.3.3 Sample Compaction

It was considered by Vuong (1999, page 70), reporting on an Australian RLT precision studies project dealing with different compaction methods, that "the differences between laboratory results and field performance (from trials) is used as the main criterion for the selection of a laboratory compaction method, ie. the preparation method selected should consistently produce the smallest differences in modulus and permanent strain, compared with the field results". It should be remembered, however, the this statement assumes that one:

- accurately models the stress regime within the pavement (both vertical *and* lateral, accounting for the findings of Chapters 4 and 5) in order to derive laboratory moduli and permanent deformations which relate to the *in-situ* conditions,
- applies a sensible pavement response model, adequately sub-layered (as discussed in §5.4.1), to allow moduli to be determined from back-analysis with some degree of accuracy. Often moduli determined through a back-analysis process do not realistically relate to laboratory modelled values due to a 'crude' modelling procedure not accounting particularly for material non-linearity by including many (sub-)layers,
- selects a method which has a satisfactory level of repeatability when compared to the other compaction methods, ie. it is of little benefit if the method selected produces values close to those determined from examination of the pavement but specimens compacted in the laboratory yield values of poor repeatability and hence reliability.

In the absence of field moduli and permanent strain data, the AWGRU agreed to use the dynamic compaction method as the standard method. It was reported by Vuong (1999, page 75) that "some problems in the preparation of the crushed rock samples using the dynamic compaction method were experienced by different laboratories, viz. variation in compaction equipment and variation in compactive effort". This relates closely to the concern mentioned in the third point above and is in keeping with the Author's experience as discussed in §7.2.2.2.

The Australian studies found that the static compaction method, to be described in §7.2.2.2, produced the lowest resilient modulus and the highest permanent strain, whilst vibratory compaction produced the highest resilient modulus and the lowest permanent strains. They found that the difference in modulus could be as high as 100% (over the TSA stress range reported in Figure 5.13), whilst the differences in permanent strain could be up to 600% (for $\sigma_{1\,max}$ = 300kPa / $\sigma_{1\,min}$ = 0kPa and $\sigma_{3\,max}$ / σ_{3min} = 50kPa). Dynamic compaction produced a difference in modulus of up to 45%, whilst the differences in permanent strain were up to 400%. The results of resilient modulus testing obtained from specimens prepared using static compaction clearly had the lowest scatter of results than the other two methods.

Science project studies (Galjaard et al, 1996) recommended that a method of compaction, in which vibration is supplemented with a small axial compression in one layer, be used. This method was found to yield homogeneous density over the central part of the specimen.

6.3.4 Preconditioning

Preconditioning is undertaken to stabilise the permanent strains induced in a material when it undergoes continual axial deformations due to the applied repetitive stress. It is aimed to bring the specimen to a stable state of full resilient behaviour.

In the first phase of the TSA repeated load triaxial test, each specimen was preconditioned for 3000 cycles using an applied maximum vertical stress of 300kPa (and a minimum of 0kPa) and a static confining stress of 50kPa (thus σ_1/σ_3 = 6). This stress combination is in keeping with the testing of thinly surfaced granular pavements. Barksdale (1997), in Table 47 of this report, recommends that a pavement of light structural strength with an equivalent full depth asphalt thickness less than 8in (203mm) is conditioned for permanent deformation using a stress state of σ_1/σ_3 = 6 and a confining stress of 42kPa. This equivalent asphalt pavement equates to flexible pavement with a 35 to 40mm asphalt surfacing, a 300mm basecourse and a 150mm lower quality sub-base (with reference to §3.5.1, EF = 1.0 for the asphalt, 0.4 for the base and 0.3 for the sub-base). The stress combination applied by the Author to the TSA testing program is closely related to that proposed

by Barksdale. The purpose of this preconditioning is to properly bed the end caps to the specimen ends, where irregular particle contacts may occur, and to relieve localised stresses/strains induced during the compaction and extrusion processes. Preconditioning consequently supports the repeatability of resilient modulus determined within the stress stage test which is to follow.

The preconditioning stresses and the number of applied loading cycles, used by the countries those tests procedures have been examined, are presented in Table 6.3.

Test Procedure	p_{max} (kPa)	q_{max} (kPa)	q/p_{max}	$\sigma_{1\,max}$ (kPa)	$\sigma_{3\,max}$ (kPa)	$\sigma_{1\,max}/\sigma_{3\,max}$	No Cycles
TSA Australia (1991)	133	250	1.7	300	50	6.0	3,000
Australian Standard (1995)	133	250	1.7	300	50	6.0	3,000
AWGRU (1999)	83	100	1.2	150	50	3.0	1,000
CEN (Method A) (2000)	300	600	2.0	700	100	7.0	20,000
CEN (Method B) (2000)	133	280	2.1	320	40	8.0	20,000
AASHTO (1992)	134	100	0.8	200	100	2.0	1,000

TABLE 6.3: PRECONDITIONING STRESS LEVELS FOR RLT TESTING BY SELECTED COUNTRIES

The stress level adopted by the CEN procedure is p_{max} = 300kPa and Δq = 600kPa (or $\sigma_{1\,max}$ = 700kPa and $\sigma_{3\,max}$ = 100kPa). This corresponds to the maximum stress level applied during the test, namely the largest applied 'q' for the second to highest 'q/p' ratio. This stress level is considered very high and, if compared with the Australian and French 'in-service' pavement stress loci illustrated in Figure 5.12, it can be seen to fall outside of this regime for thinly surfaced pavement structures. The stress combination used by CEN aims to simulate the stresses dynamically imparted to the materials during the final compaction stage of the pavement layers by construction traffic (although very little research has been conducted to quantify the magnitude of these stresses).

However, the number of stress pulses performed during preconditioning is 20,000 compared with only six to ten passes of a heavy vibrating roller at this high compaction stress regime. Such a large number of load pulses are required at this stress level in order to stabilise the resilient volumetric and shear strains. However,

often the material can suffer some shear failure and exhibit very excessive rates of permanent deformation at only moderate moisture contents, as seen by high A_1 or strain rate values due to the magnitude of the applied loading (see Figure 6.4 for COURAGE project materials tested).

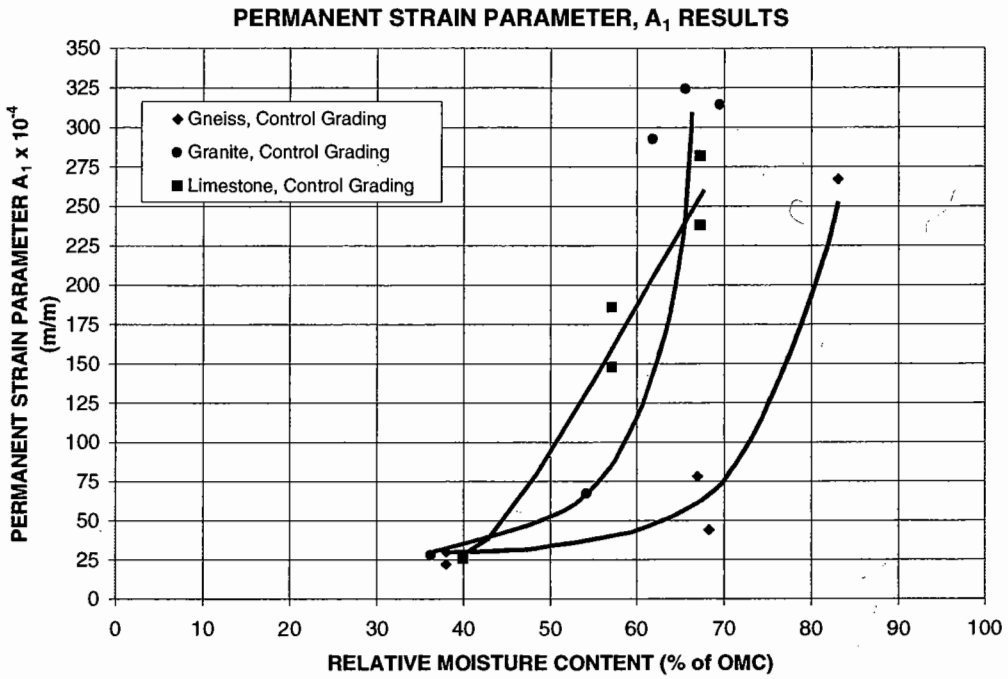

FIGURE 6.4: PERMANENT STRAIN RATE PARAMETER A_1 FOR COURAGE MATERIALS

As a result, the strains developed at this high compaction stress state could not be used to "characterise" the material behaviour once it is functioning in a finished surfaced pavement structure, which operates in a totally different stress regime. In fact, trying to do so could lead to a very harsh assessment of material behaviour. Using the COURAGE data as an example (EC, 2000, §6.4.2), the materials may perform quite satisfactorily from a permanent strain point-of-view, at a higher moisture condition, just by testing at a lower stress state. In addition, the CEN Method A preconditioning stress could be expected to significantly alter the designed density state condition of the test material.

The question remains, however, as to why we precondition? The Author considers that we should *"preconditioning at a 'mean' stress combination to stabilise the permanent strains to enable repeatable resilient strains to be measured in the stress*

stage test. This in turn will provide resilient modulus and Poisson's ratio values to be used in pavement design or in the back-analysis process to assess an existing pavement".

If, during preconditioning, the test specimen fails or exhibits "excessively large deformation" (with no value or level of deformation being defined by CEN), then the CEN procedure recommends performing a new test with a new specimen at p_{max} = 310kPa and Δq = 600kPa (or $\sigma_{1\ max}$ = 700kPa and $\sigma_{3\ max}$ = 110kPa), minimum values are 0kPa. With reference to the initial stress levels for preconditioning and Figure 5.12 it can be seen that the "new preconditioning stress condition" is only a very small stress increment away from the original one. Thus, if the material did happen to fail during preconditioning and was subsequently re-tested at the "new" stress level, it is more than likely that it will fail again. The CEN procedure states that "if this specimen also fails before 20,000 cycles are completed"....."note the material as being unsuitable for road construction". From the discussion and analyses presented in Chapter 5, this material may well be quite suitable for use as a sub-base material if it possesses a satisfactory shear strength, stiffness and limited susceptibility to permanent deformation. Alternatively, the material maybe considered for use as a base layer beneath thick asphalt. In this case, the stresses in the base layer will be well below those of the CEN preconditioning assessment condition. For example beneath a 80mm asphalt layer stresses have been calculated to be approximately σ_1 = 230kPa and σ_3 = 16kPa, which are well below the $\sigma_{1\ max}$ = 700kPa and $\sigma_{3\ max}$ = 110kPa CEN preconditioning level. The material may be found to undergo little deformation at the lower stress conditions.

It is recommended that the stress level used for preconditioning the material be reassessed in line with the points of discussion raised. The high initial stresses to which the material is subjected during compaction will be largely realised during the specimen compaction process, where material breakdown and particle re-arrangement will largely occur in achieving the desired material density. As a result, the new level for preconditioning should be selected to fall within the boundaries of the stress loci examined, as expected during the life of the pavement (see Figure

5.12); although a q/p stress ratio with a maximum value of 2 is considered satisfactory and in keeping with that used in other countries.

6.3.5 Resilient Modulus

The stress levels used by the CEN procedure to assess modulus cover a greater area of the p-q space than any other methods (Australian or American) discussed in §5.4. It has been stated already the stress levels for the CEN with stress ratios of q/p = 0 and 0.5 are irrelevant to possible *in-situ* pavement stress levels which a material may experience, based on the expected stress loci presented in Figure 5.5 of Chapter 5.

In addition, the step size from one stress level to the next is considered large, $\Delta p = 75$ to 100kPa and $\Delta q = 150$kPa for q/p = 1.5 and 2.0 ratios. Thus, interpolation of resilient modulus values in a spatial sense (for given set of *in-situ* pavement stress conditions) possesses greater uncertainty compared with the TSA Design Chart approach where a greater number of stress levels are used in the stress domain of interest. Thus, one relies primarily on the modulus model, such as the Boyce model (see §6.3.6), to determined modulus values. The obvious statement then arises that the confidence in the modulus values determined (regardless of the model used) is strongly related to the strength of the regression fit of the model to the test data.

As a result, it is recommended that the CEN stress levels be reviewed in order to focus the testing stresses in a more concentrated manner within the determined pavement stress loci. Having reviewed the stress levels used in a number of countries, and their advantages and disadvantages, the Author proposes a new set of stress combinations, one to suit basecourse layer material usage and the other to suit sub-base and fill layer material applications. These combinations have been carefully selected to suit expected *in-situ* pavement stress levels, stress stages restrictions recommended by the AGWRU (§5.4.1) and to suit modelling purposes, either using iso-moduli contouring or material models (eg, Boyce, etc). The 38 basecourse quality material stress stages (including 7 additional duplicate or repeat points) and 10 sub-base quality material stress stages are presented in Appendix 4, Tables A4.1 and A4.2, respectively, and are illustrated in Figure 6.5. The new stress levels proposed here will be assessed through experimentation, with the results

presented in Chapter 7, to ensure that a repeatable set of combinations has been selected.

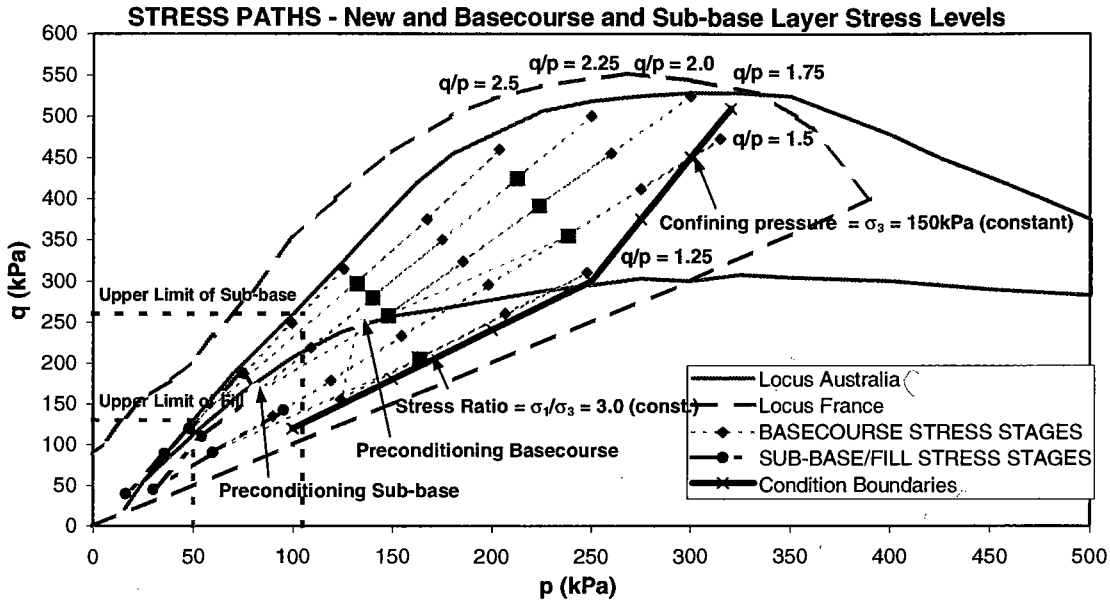

FIGURE 6.5: NEW STRESS COMBINATIONS FOR STRESS STAGE RLT TESTING

The benefits of the new stress combination proposed are considered to be that they:

- suit expected *in-situ* pavement stress levels, account for stress stages restrictions recommended by the AWGRU, and suit modelling by using either iso-moduli contouring or material models (eg, Boyce, etc)
- have smaller Δp and Δq step sizes between each subsequent stress stage than the current CEN procedure. Thus, one might expect better continuity of results and less conditioning required at each stress stage (50 cycles instead of 100 cycles).
- have sufficient stress stages in a triangularly divided plane to provide for sound iso-moduli contouring. This form of analysis and illustration provides a sound visual method for checking data quality by highlighting discontinuities.
- provide separation of testing stress stages into basecourse (high quality material) and sub-base/fill (marginal quality material) stress levels appropriate to material use in the pavement, on the assumption that the shear strength failure envelope has previously been assessed for the materials to determine which category they initially fall into.
- reduce the number of stress stages proposed by AWGRU by nearly 40%.

- remove q/p ratios of 0, 0.5 and 1.0 which have been found to diminish the quality of the modelled data due to the very small strains measured.
- propose two separate preconditioning levels, depending upon the stress stage approach applied (either basecourse or sub-base/fill). In addition, these two preconditioning levels fall within the regions of basecourse quality or sub-base quality materials as defined by Figure 5.20
- restrict the confining stress applied to a value less than 150kPa and stress ratio range of between 3 and 20 is imposed as a restriction. This is in line with the findings of the AWGRU group's precision studies work, aimed at operators being able to obtain a high level of repeatability (less than 7 to 8%), as reported §5.4.1 and by Voung (1999).

6.3.6 Modelling of Results

The model used in the CEN RLT test procedure to model test data from the variable confining stress test is the non-linear elastic Boyce model. This isotropic model, which was developed at the end of the 1970s (Boyce, 1980), has been modified to the anisotropic form (Hornych et al, 1998) given by the following stress-strain relationships:

$$\varepsilon_v{}^* = \frac{1}{K_a}\frac{p^{*n}}{p_a{}^{n-1}}\left[1+\frac{(n-1)K_a}{6G_a}\left(\frac{q^*}{p^*}\right)^2\right] \quad \text{and} \quad \varepsilon_q{}^* = \frac{1}{3G_a}\frac{p^{*n}}{p_a{}^{n-1}}\frac{q^*}{p^*}$$

... (6.1 and 6.2)

where

$$p^* = (\gamma\sigma_1 + 2\sigma_3)/3 \quad = \text{modified mean normal stress} \qquad \ldots (6.3)$$

$$q^* = (\gamma\sigma_1 - \sigma_3) \quad = \text{modified shear stress} \qquad \ldots (6.4)$$

with: $\varepsilon_v{}^* = \varepsilon_1/\gamma + 2\varepsilon_3$ = modified volumetric strain ... (6.5)

and $\varepsilon_q{}^* = \frac{2}{3}(\varepsilon_1/\gamma - \varepsilon_3)$ = modified shear strain ... (6.6)

K_a, G_a, n and γ parameters of the model; p_a constant equal to 100kPa

γ parameter of anisotropy ($\gamma < 1$ indicates a material stiffer in the vertical direction as opposed to the horizontal direction)

Note, that when $\gamma = 1$, the expressions simplify into those of the (isotropic) Boyce model.

The four parameters are determined by using a classical least-squares optimisation process to minimise the sum of the squares of two terms (for the N selected stress paths modelled of each RLT test), namely:

$$MIN = \frac{\sum_{i=1}^{N}\left(\varepsilon^{i}{}_{q\,meas} - \varepsilon^{i}{}_{q}{}^{*}{}_{calc}\right)^2}{N} + \frac{\sum_{i=1}^{N}\left(\varepsilon^{i}{}_{v\,meas} - \varepsilon^{i}{}_{v}{}^{*}{}_{calc}\right)^2}{N} \qquad \ldots (6.7)$$

where:

$\varepsilon^{i}{}_{v\,meas}$ = measured volumetric strains relevant to each test stress combination

$\varepsilon^{i}{}_{q\,meas}$ = measured shear strains relevant to each test stress combination

$\varepsilon^{i}{}_{v}{}^{*}{}_{calc}$ = Boyce calculated volumetric strains relevant to each test stress combination

$\varepsilon^{i}{}_{q}{}^{*}{}_{calc}$ = Boyce calculated shear strains relevant to each test stress combination

Using classical elastic transformation relationships, the formula for calculating the vertical modulus is given by:

$$E_v = \frac{9G_a\left(\frac{p^*}{p_a}\right)^{1-n}}{3 + \frac{G_a}{K_a}\left[1 - \beta\left(\frac{q^*}{p^*}\right)^2\right]} / \gamma^2 \qquad \ldots (6.8)$$

where:

$$\beta = \frac{(1-n)K_a}{6G_a} \qquad \ldots (6.9)$$

Both the Isotropic and Anisotropic Boyce models have been used to model measured triaxial data obtained at three different sets of stress ratios, which form all or part of the sequence adopted in the present CEN Method A procedure. The models use stress/strain data derived by testing three different materials within the COURAGE Project. The materials analysed were the French Gneiss, Portuguese Granite and Slovenian Limestone. The different stress ratio sets modelled are:

- all q/p ratios
- only the q/p = 1.0, 1.5, and 2.0 ratios
- only the q/p = 1.5, 2.0, and 2.5 ratios

The key parameters compared are:

- the measure of fit (ρ) – defined in Appendix 5,
- the calculated modulus of elasticity, E_{calc}, assuming linearity and isotropy, determined from measured stresses and computed strains, using Equations 6.1 and 6.2, the parameters of the equations having been fitted to the measured data (applying 3-D Hooke law)
- the measured modulus of elasticity, E_{meas}, assuming linearity and isotropy, determined from measured stresses and measured strains (applying 3-D Hooke law)
- the modulus of elasticity, E_v, assuming non-linearity and anisotropy, was calculated from Equation 6.8 based on the computed parameters
- the percentage variation of the modulus values obtained – defined in Appendix 5

The moduli values, reported in Appendix 5 for comparison, were derived at p = 250kPa and q = 500kPa (or σ_1 = 583kPa and σ_3 = 83kPa) which is the condition specified in Europe for determining a characteristic modulus for comparing different materials. This stress combination represents that at the top of the basecourse, directly beneath a 35mm asphalt surfacing.

It was found that for the:

Isotropic Boyce Model

- the moduli determined from strain measurement, Hooke E_{meas} , were closest in value to those calculated using the Boyce model-determined strains, Hooke E_{calc} , when only the critical stress ratios q/p of 1.5, 2.0 and 2.5 only were used to determine the model parameters.
- for the test results analysed:

➢ average isotropic Hooke moduli variation of E_{meas} to Hooke E_{calc} = 6.6%, standard deviation = 3.1%, for q/p of 1.5, 2.0 and 2.5,

➢ average isotropic Hooke moduli variation (appropriate to compare with q/p of 1.5, 2.0 and 2.5) of E_{meas} to Hooke E_{calc} = 9.9%, standard deviation = 5.1%, for all q/p.

➢ average isotropic Hooke moduli variation of E_{meas} to Hooke E_{calc} = 11.8%, standard deviation = 5.2%, for q/p of 1.0, 1.5 and 2.0,

➢ average isotropic Hooke moduli variation (appropriate to compare with q/p of 1.0, 1.5 and 2.0) of E_{meas} to Hooke E_{calc} = 13.1%, standard deviation = 6.4%, for all q/p

Thus, lower error in the resilient modulus values applied in the pavement design response model by modelling just the q/p of 1.5, 2.0 and 2.5 ratios.

- the Boyce modulus values calculated using the isotropic Boyce formula (ie Equation 6.8 with $\gamma = 1$), E_v were much lower than the Hooke E_{meas} or Hooke E_{calc} values.

Anisotropic Boyce Model

- the best fit to experimentally measured shear and volumetric strain data was obtained with the Anisotropic Boyce model modelling only the critical stress ratios q/p of 1.5, 2.0 and 2.5, as opposed to all stress ratios (q/p = 0 to 2.5).
- the Boyce modulus values calculated using the anisotropic Boyce formula (ie Equation 6.8 with $\gamma \neq 1$), E_v were much lower than the Hooke E_{meas} to E_{calc} values.

Figures 6.6A & B present a typical example of the improved fit of the Anisotropic Boyce model by only modelling the critical stress ratios q/p of 1.5, 2.0 and 2.5 to experimentally measured results obtained in a RLT test. Whilst the results shown represent those for one material, these findings are generally true for a wide range of materials. It shall be noted that two other materials, a limestone and a granite used within the COURAGE project (EC, 2000) testing program, were examined in this manner. The figures illustrate the variation in shear and volumetric strains with mean stress p obtained for each of the three load sequences. It is not intended here to compare the results with a wide variety of other model fits.

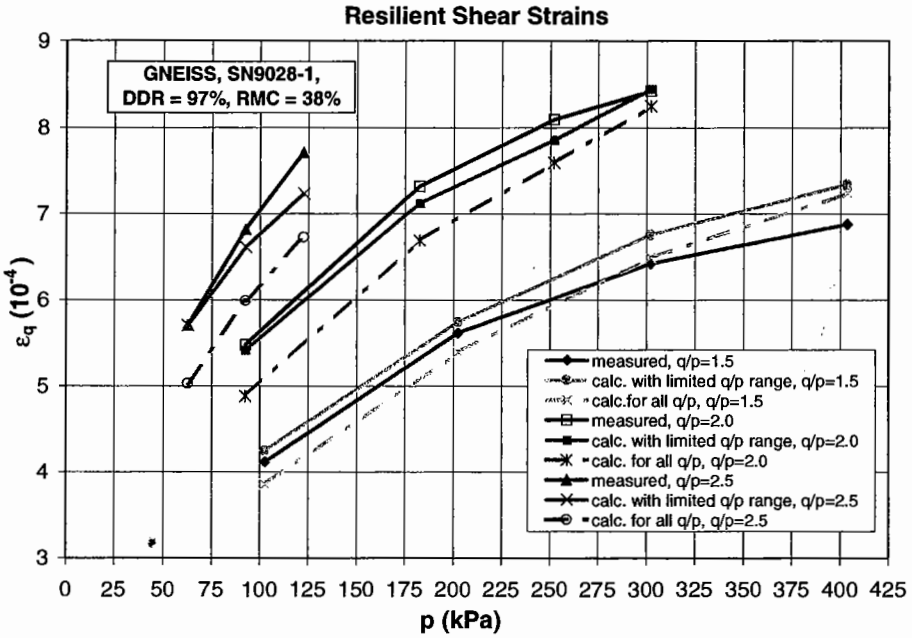

FIGURE 6.6A: EXAMPLE OF IMPROVED FIT OF ANISOTROPIC BOYCE MODEL TO SHEAR STRAIN DATA USING LIMITED Q/P STRESS RATIO DATA FOR MODELLING

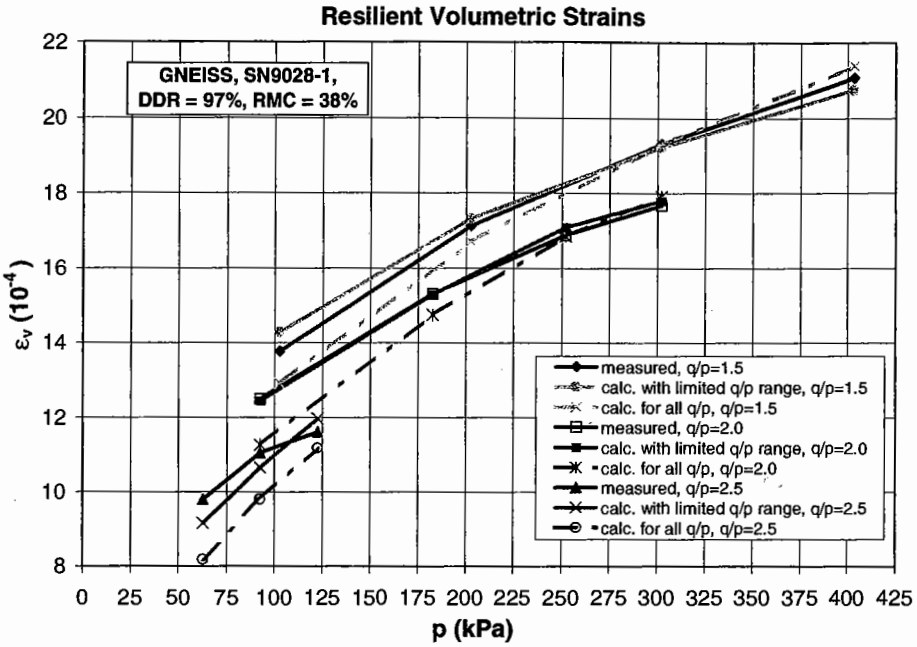

FIGURE 6.6B: EXAMPLE OF IMPROVED FIT OF ANISOTROPIC BOYCE MODEL TO VOLUMETRIC STRAIN DATA USING LIMITED Q/P STRESS RATIO DATA FOR MODELLING

As a result of this study, factors which need to be considered in the modelling analysis are:

- low q/p stress ratios (less than 1.0) should not be used in the modelling of RLT data, given the limits of the strain measuring devices (in terms of the maximum error, determined from regression analysis, over the calibrated range for the strain measuring devices). The transducers are expected to measure very small magnitudes of the strain at low q/p ratios, which may in many cases be smaller than the maximum error. This is particularly the case for measurements on dry, stiff specimens, leading to a scatter in the measurements.
- the stress ratio of q/p = 2.5 is considered acceptable for modelling purposes *provided* that the aggregate has been found to possess sufficient shear strength (as determined by static triaxial testing described in §5.5 and §5.6), otherwise significant material shear could result and adversely affect the quality of the modelling results. This has been considered in the new stress sequence presented in Figure 6.5.

6.4 Summary

The contribution of the Author in developing RLT equipment specifications and testing procedures for use by practitioners was discussed in detail. These documents were developed by the Author following an extensive materials testing program. Others were to contribute at a later stage, through a national working committee, in order to advance the development of the documents into national standards. From the Author's initial equipment specification was developed the first commercial RLT system for Australian pavement materials research. With the equipment and procedures described, a comprehensive testing program is detailed in Chapter 7.

A brief appraisal was presented in this Chapter to support the simplification of the more complex European RLT test procedure, which is more appropriately used to determine data for the material models applied to finite element analysis modelling of pavements. In addition, following on from the stress analyses within Chapter 5, stress conditions used for the RLT test have been rationalised with a new set of stress levels proposed to cater for a wide range of combinations expected within the UGMs of any loaded pavement configuration. The benefits of the new stress levels include their separation into those encountered in basecourse (high quality material) and sub-base/fill (marginal/poor quality material) layers. Small Δp and Δq steps were devised in the testing sequence to improve the continuity of modulus test results for graphical presentation or modelling purposes.

The model applied in the CEN RLT test procedure was analysed using data from the European COURAGE project. It was found that an improved precision in modelling the data could be obtained by incorporating only the critical stress ratios of $q/p = 1.5$, 2.0 and 2.5. The lower stress ratios, particularly 0 and 0.5, were found to lower the data fit, which is not surprising given the difficultly in accurately measuring strains for these ratios.

CHAPTER 7
TRIAXIAL TESTING PROGRAM & DATA ANALYSIS

7.1 Introduction

This chapter presents a testing program for the characterisation of unbound granular materials subjected to both static and repeated load triaxial testing.

The project, in its early stages, was used to develop a statistically reliable testing procedure to allow the parameters, critical to sound material performance in-service, to be determined.

Once this was accomplished, a number of existing aggregate products were characterised in order to form a databank of material parameters. This 'relational' data may then be used to 'rank' materials and establish preliminary limiting values linked to usage. In addition, the results could be incorporated into the mechanistic design process.

7.2 Test Program for Material Characterisation in Australia

Following a significant pavement failure in South Australia, as reported in §10.4, which was one of the first designed by mechanistic methods, an extensive testing program was initiated in 1989 to characterise and 'rank' a number of unbound granular materials. Mechanistic design was first introduced into Australia in 1987 (NAASRA, 1987).

The test program, which took approximately five years to complete, was to cover all major quarry source materials used by TSA for the construction of flexible pavements. Concern existed over the magnitude of resilient modulus values used in the pavement design. It was found that the presumptive values for resilient modulus tabled in the AUSTROADS Pavement Design Guide (1992), were somewhat 'high' in magnitude.

In addition, evidence existed that a number of granular materials used in the construction of pavements did not possess the stiffness required of heavily loaded thin-surfaced pavements. As a result, a testing program including a wide range of local materials was conducted to:

- determine the elastic (resilient modulus) and plastic (permanent strain) characteristics of the materials at a range of expected *in-situ* conditions,
- determine resilient modulus values for the input into mechanistic design procedures,
- determine material properties critical to their performance which would enable guidelines for selection and specification to be established.

7.2.1 Overview of the Conduct of the Test Program

It should be clearly stated that the Author undertook all of the initial testing activities to ensure that techniques were adopted that provided the level of repeatability aimed for. Without this, it was seen as little value to embark on a substantial and relatively costly characterisation program to "rank" the materials in terms of perceived quality. Once these techniques had been "perfected" using the 20mm Boral Lobethal and the Para Hills crushed rock materials, the Author took more of an operator training, data analysis and testing management role to monitor the work of the 'new' testing operators. Before the 'handover phase' of the project to these 'new' operators, the Author wrote a number of work instructions to supplement the test procedure (for example, one is detailed in Mundy, 1992, MTRD8-1, Appendix 2). These assisted in the training role also undertaken by the Author to ensure consistent quality of results amongst different operators.

7.2.1.1 Material Test Conditions

All materials were to be tested at three different density conditions, namely DDR = 96, 98 and 100%. In addition, it was deemed that a moisture range covering that expected in the field should be examined. This range was determined to be from RMC = 100% of OMC (the condition at which materials are often compacted in the field) reducing in increments of approximately 12.5% of OMC down to a minimum moisture content of 40% of OMC. Thus, six different moisture levels were aimed for which covered the range discovered in UGM pavement layers of roads within the

Adelaide metropolitan area from numerous diagnostic pavement material studies undertaken. The results highlighted the moisture and density sensitivity of the different materials in terms of MPIs.

7.2.1.2 Repeatability RLT test

It should be briefly mentioned that a detailed sensitivity study was conducted using a Monte Carlo method of simulation, with these factors in mind. The method involved determining, for a given set of mean design parameters, a large number of structural thickness designs considering the random variation in design parameters (such as resilient modulus). One output of the study (summarised by Barksdale, et al in 1997) was the effect of resilient modulus measurement error for a 6in (152mm) asphalt surfacing overlying an aggregate base of variable thickness. It was found that for the design parameters used in the study, a typical experimental error in measuring the resilient modulus of each layer (about 15%) caused about a 12 to 14% increase in the total equivalent aggregate pavement thickness. The parameters used were a mean modulus for the strong base of E_{base} = 276MPa, with $E_{A/C}$ = 2756MPa and $E_{S/G}$ varied between 15 to 70MPa. In determining the error effect caused by modulus measurement of the specific layers, the measurement of modulus for the other layers was assumed to be perfect. For a weak base of E_{base} = 138MPa; the pavement thickness error was 8 to 11%. Although these errors are modest in terms of base thickness, resilient modulus will have a significant effect on the expected life of thin surfacings (particularly those less than 80mm), as seen in Appendix 1.

In order to ensure repeatability of the test results, each moisture condition was tested using three to four different specimens. The levels of permanent strain rate and resilient modulus were statistically assessed for acceptable levels of variation. The coefficient of variation is a convenient way of expressing the variability of material properties. For an unstabilised base material, Barksdale and Alba (1997), consider that "a coefficient of variation of the resilient modulus of 15% due to testing errors (sample preparation, sample alignment and instrumentation measurement) is considered reasonable when materials are tested in a production oriented laboratory". The level of repeatability aimed for in the TSA testing program was 10% for resilient modulus determination and 30% for permanent strain rate. Given that permanent

strain measurements are very sensitive to the preparation of the specimen ends and localised material movements in this area, this level of repeatability is considered acceptable for one to aim for.

In addition, the levels of repeatability selected are important when applying laboratory determined resilient modulus values to pavement design models. Variations in modulus of the UGMs will have a direct influence upon pavement thickness and the type of asphalt surfacing selected.

7.2.2 Summary of Test Procedure and Key Techniques Adopted

7.2.2.1 Sample Preparation

Given that high repeatability was a target of the testing program, material grading was seen to be one material property which, if uncontrolled, could very significantly effect the results obtained.

In order to provide maximum control over the particle size distribution of each test specimen, the bulk material was split into five fractions for subsequent proportionate re-mixing, viz:

-19.00, + 13.20mm
-13.20, + 9.50mm
-9.50, + 4.75mm
-4.75, + 1.18mm
-1.18mm

Weighed portions of each fraction were combined to produce a single test specimen. The target PSD of the manufactured sample was the mean of the distribution associated with Departmental Specification PM32 (Department of Road Transport, 1990), see Figure 7.1 below.

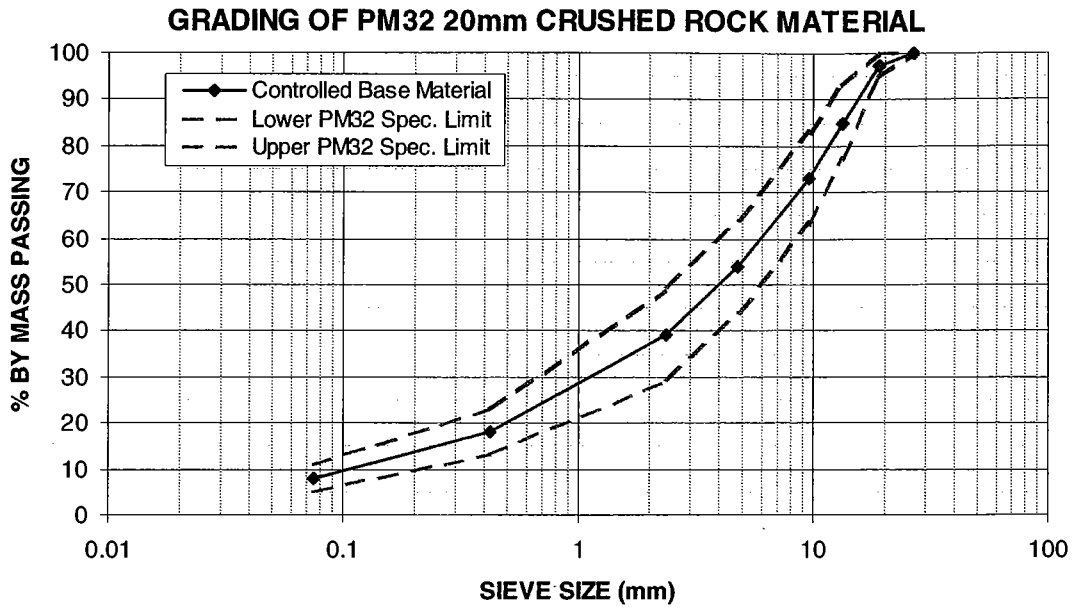

FIGURE 7.1: SPECIFICATION GRADING OF SOUTH AUSTRALIAN 20MM CRUSHED ROCK

7.2.2.2 Compaction

Test specimens were initially prepared via 5-layer dynamic compaction using a modified Proctor hammer providing 25 blows per layer. Layer formation was found to be unsatisfactory with layer interfaces clearly visible. After testing, cracking along the interfaces had developed, particularly in lower RMC specimens, and a more uniform preparation was sought. In addition, it was soon realised not long into the program that the prepared specimens did not yield the level of repeatability required. It was considered that operator skill was one key factor involved. In addition, the ends of the manufactured specimens were not deemed to be smooth and level enough, nor the aggregate to be sufficiently tightly packed to give the results required. This was considered one of the most important factors by the Author, particularly in producing quality permanent strain and resilient modulus results, with a low scatter in duplicate test results. A similar kind of operator variability was experienced by the AWGRU in tests performed during 1997-1998 aimed at assessing different compaction methods (see §6.3.3).

The Author then developed a static sample compaction technique using an open-ended solid steel mould and forming the specimens in two layers, with the surface of the first layer being well scarified prior to the compaction of the second layer (refer to Figure 7.2). Three plungers were manufactured to suit the mould. One plunger

formed the base to the mould, a second long plunger enabled the first material layer to be formed and a third plunger allowed the second layer to be compacted. The Author experimented with the loading rate applied by a concrete press machine to ensure that preferential orientation of the particles could occur. A tamping tool was used on the loose material of each layer, prior to layer compaction, to assist in particle orientation and packing. A consistent number of rodded strokes (25) was used for each layer. When a compacted specimen was examined upon dissection, it was found to consist of tightly packed aggregate grains of random orientation, largely attributed to the tamping process. After the specimen was formed, both plungers were rotated several times (whilst still in the mould) by the operator, also applying compression, to enable smooth sample ends to be formed. This could be seen once the two plungers were removed from the mould. The $\phi 100 \times 200$mm length specimens, after being hydraulically extruded from the mould, were found to be very well formed, smooth sided and considered to be 'single layered' (no layer interface was visible). At this stage, after extrusion, the membrane was placed over the specimen using a former.

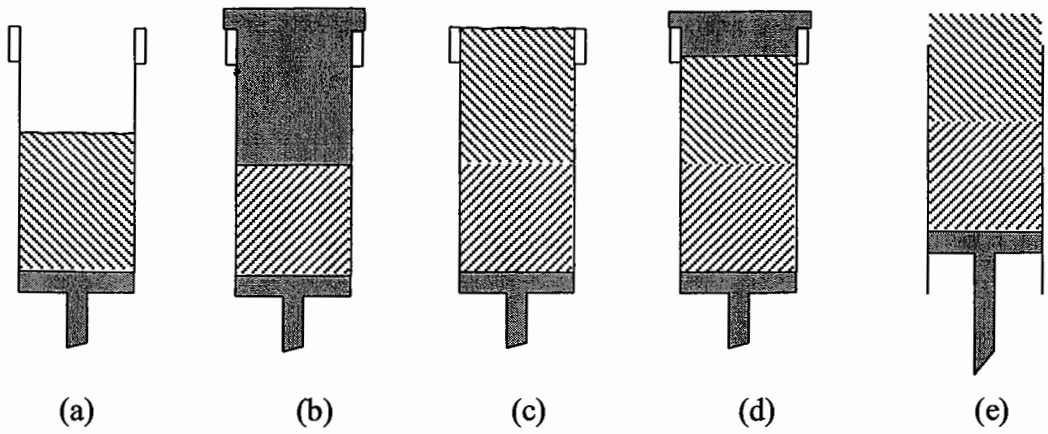

FIGURE 7.2: SPECIMEN COMPACTION PROCESS

As a result of this work, all samples were subsequently prepared using the static compaction technique, which was found to produce test results from specimens produced by this method of very good repeatability. Repeatability figures were within 30% for permanent strain rate and 10% for all resilient modulus stress stages (see §7.2.3.1 and §7.2.3.2).

7.2.2.3 Static Triaxial test

This test was performed to determine the shear strength of the material and the consequential static failure stress combinations *relative* to those applied in the RLT test. Four stages, utilising consecutively increasing confining stresses of 10, 20, 40 and 80kPa, were performed at loading rate of 0.5mm/min. Axial loading was halted during each stage when the axial stress increase was less than 5kPa (0.04kN for ø100mm specimen) for each of six consecutive 15 second recording intervals and the axial strain was limited to within approximately 2.5%.

7.2.2.4 Preconditioning RLT test

In the first phase of the repeated load triaxial test, each specimen was preconditioned for 3000 cycles using an applied maximum vertical stress of 300kPa (and a minimum of 0kPa) and a static confining stress of 50kPa (thus $\sigma_1/\sigma_3 = 6$). The point of this stress combination is shown in Figure 7.3.

7.2.2.5 Stress Stage Sequence RLT test

At the completion of the preconditioning test, the stress stage modulus test was conducted to systematically determine the stress dependence of resilient modulus. This test followed the 115-point stress sequence presented in Figure 5.13 for all but the first 'trial' product tested which had 102 points. A further 13 points were added to more rigorously map the entire Australian stress locus presented in Figure 5.5. The new points were for high shear regions in the pavement where stress conditions may approach the failure condition. The order of the stress sequence is shown in Figure 7.3.

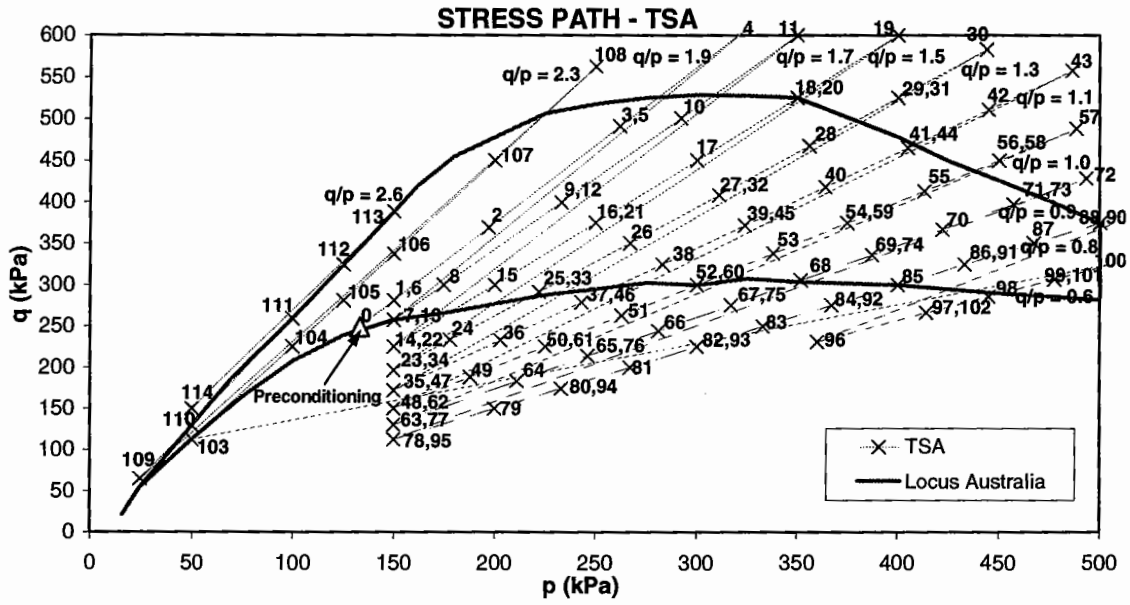

FIGURE 7.3: STRESS PATH SEQUENCE USED FOR RESILIENT MODULUS DETERMINATION

7.2.3 Findings of the Statistical Analysis of RLT Test Results

All test results were statistically analysed throughout the course of the testing program to ensure that repeatability levels were consistently being obtained with the techniques adopted within the testing procedure.

As mentioned, for any given density, generally three to four specimens were tested at a target moisture. The mean, $\bar{x}$, and standard deviation, s_x, were determined for each stress level and the Pearson's Coefficient of Variation was also calculated as:

$$\text{Coefficient of Variation, } CV = \frac{s_x}{\bar{x}} (\%)$$

Only the 95th percentile of values within the total range of values was used to determine the level of repeatability of permanent strain rate and resilient modulus. This allowed extreme values to be rejected.

7.2.3.1 Permanent Strain Rate

The Coefficient of Variation of the permanent strain rate, for each of the target moisture conditions mentioned in §7.2.1.1, was found to be a more reliable parameter than permanent strain accumulated by the end of the preconditioning test.

The comparison between these two parameters is reported in the MTRD16 series of reports (Mundy, 1992-1994). It is expected that this was largely due to the variable initial bedding of the load end caps into the specimen, which could significantly effect the total magnitude of permanent strain. It should be remembered from §2.3.2 that the permanent strain rate parameter is determined by modelling the permanent strain curve, but *excluding* the first 100 cycles of data.

For the Boral Lobethal (MT16-1 Project) and Boral Para Hills (MT16-2 Project) materials, at DDR = 98%, the Coefficient of Variation values obtained for permanent strain rate determinations, at a given target moisture content, are presented below (Table 7.1).

Average Relative Moisture Content (%)		**No. of Tests (x)**		**Coeff. of Var^n (%) Perm. Strain Rate**	
Lobethal	*Para Hills*	*Lobethal*	*Para Hills*	*Lobethal*	*Para Hills*
-	51.4	-	2	-	NA
58	57.5	3	4	13.1	32.2
61.5	61.0	2	4	29.1	16.0
-	64.0	-	4	-	27.3
68.2	68.6	3	4	5.9	29.6
73.8	72.9	3 (2)*	4	71.1 (28.6)*	21.5
76.2	-	2	-	25.8	-
-	81.0	-	3	-	3.6
85.4	86.7	2	3	NA	4.6
-	98.9	-	4	-	24.7
AVERAGE FOR ALL TESTS				*29.0 (20.5)**	*19.9*

TABLE 7.1: STATISTICAL SUMMARY OF RLT TESTING OF BORAL LOBETHAL AND PARA HILLS 20MM CRUSHED ROCK MATERIALS – PERMANENT STRAIN RATE

* Note: By excluding one outlier test result, an alternative Coefficient of Variation value is reported

Having first tested the Boral Lobethal material, variations were found to be less than approximately 30% for all but one level of relative moisture content (see Figure 7.4). One higher strain rate result at this level, which was approximately 200% higher than the average of the other two results, produced a high resultant value. By excluding this one high result, the CV based upon two test results reduced to 28.6%

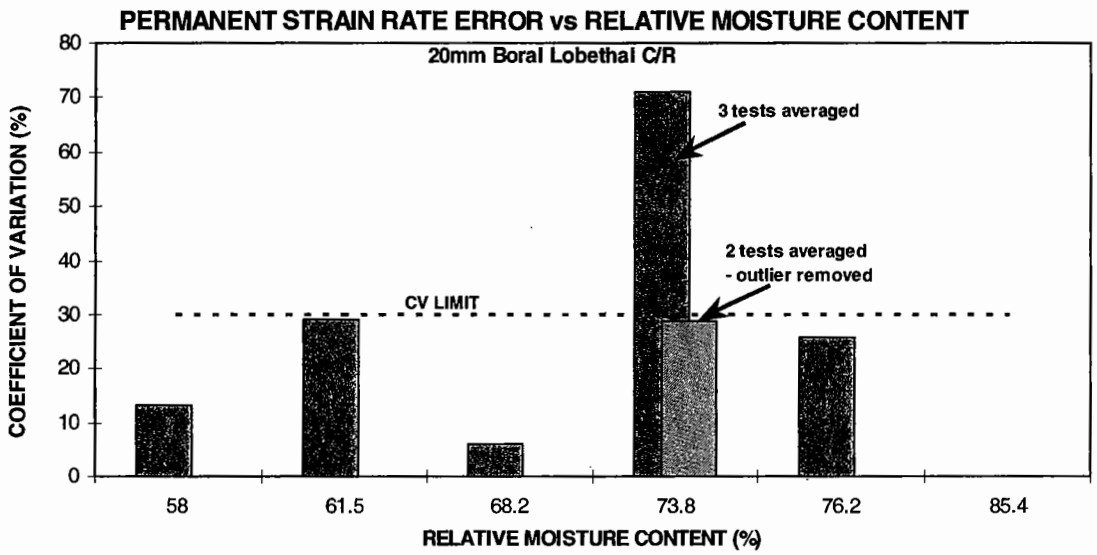

FIGURE 7.4: VARIATION IN PERMANENT STRAIN RATE (20MM BORAL LOBETHAL C/R) VS RELATIVE MOISTURE CONTENT

For the second material tested, Boral Para Hills 20mm C/R (Figure 7.5), variations were again found to be less than 30% except for one specimen moisture content where the coefficient of variation was 32.2%.

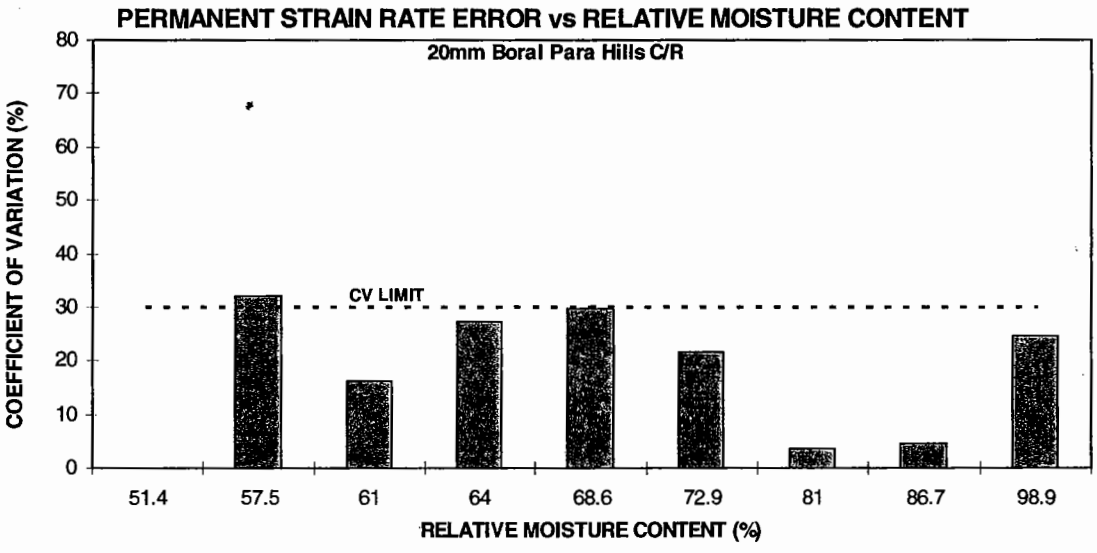

FIGURE 7.5: VARIATION IN PERMANENT STRAIN RATE (20MM BORAL PARA HILLS C/R) VS RELATIVE MOISTURE CONTENT

Overall for the two materials, the coefficient of variation was found to be in the order of 20%.

7.2.3.2 Resilient Modulus

The results for the standard deviation of the resilient modulus tests for each "moisture level" are markedly different for each stress level. This is due to the magnitude of the strain induced under the applied stresses being measured. A stress combination with a low mean normal stress and high lateral stress level provides quite small strains which are difficult to measure accurately. Hence, consistent results are more difficult to achieve at low deviator stress ratio levels and consequently, a large standard deviation results. With reference to Figure 7.6, this corresponds to stress stage combinations labelled by points 14, 22, 23, 24, 34, 35, 47, 48, 49, 62, 63, 77, 78, 79, 95. In addition, Figures 7.6 and 7.7 contain stress combinations which represent repeat or duplicate test points (denoted by 'R'), as discussed previously in §6.2.3.

Average Relative Moisture Content (%)		**No. of Tests (x)**		**Coeff. of Var^n (%) (95th Percentile) Resilient Modulus**	
Lobethal	*Para Hills*	*Lobethal*	*Para Hills*	*Lobethal*	*Para Hills*
-	51.4	-	2	-	7.7
58	57.5	3	4	6.6	12.6
61.5	61.0	2	4	11.3	7.2
-	64.0	-	4	-	9.5
68.2	68.6	3	4	12.2	7.0
73.8	72.9	3	4	10.5	12.2
76.2	-	2	-	6.8	-
-	81.0	-	3	-	5.0
85.4	86.7	2	3	8.1	10.0
-	98.9	-	4	-	7.8
AVERAGE FOR ALL TESTS				*9.3*	*8.8*

TABLE 7.2: STATISTICAL SUMMARY OF RLT TESTING OF BORAL LOBETHAL AND PARA HILLS 20MM CRUSHED ROCK MATERIALS – RESILIENT MODULUS

For the Boral Lobethal (MT16-1 Project) and Boral Para Hills (MT16-2 Project) materials, at DDR = 98%, the 95th percentile Coefficient of Variation values of resilient modulus at a given target moisture content, are tabled (Table 7.2).

Having first tested the Boral Lobethal material, variations were found to be less than approximately 10% in nearly 90% of *all* stress levels (including repeat or duplicate points) for all of the target moisture content levels examined (see Figure 7.6). Only for some repeat points and those generally of a low mean normal and deviator stress levels, were CV values occasionally greater than 10%.

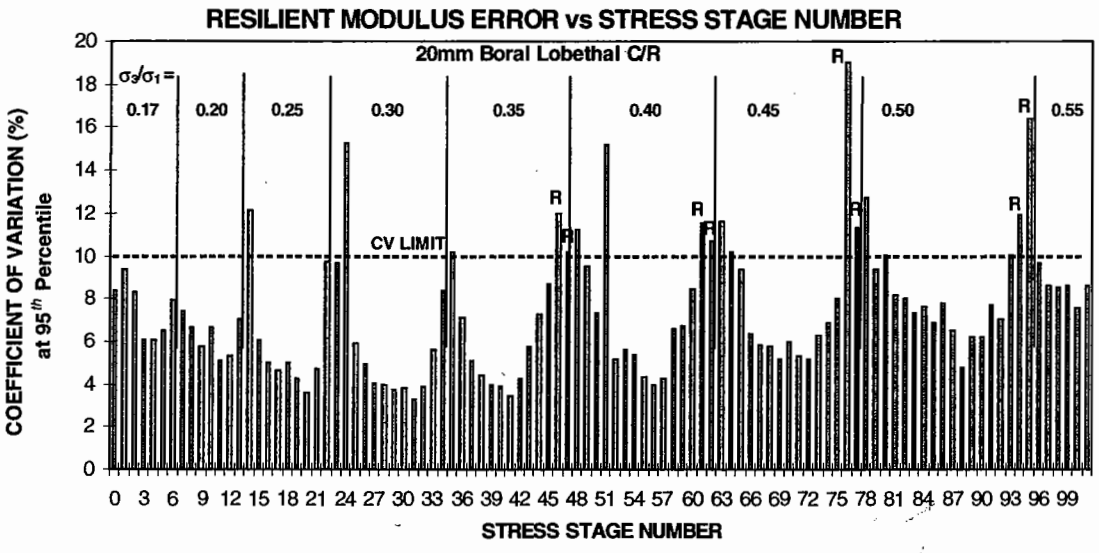

FIGURE 7.6: VARIATION IN RESILIENT MODULUS FOR EACH STRESS STAGE TESTED (20MM BORAL LOBETHAL C/R) – AVERAGE FOR ALL MOISTURE CONTENTS

For the second material tested, Boral Para Hills 20mm C/R, variations were again found to be less than approximately 10% in nearly 90% of *all* stress levels (including repeat or duplicate points) for all of the target moisture content levels examined (see Figure 7.7). However, a number of stress stage points between point number 76 and 102 (those having an inverse stress ratio, σ_3/σ_1, equal to 0.45 or greater) and some duplicate points were found to either border 10% repeatability or exceed it. These points correspond to stress combinations of low deviator stress for a range of mean normal stresses and also those of low deviator stress and low ranges of mean normal stress. These stress levels have been rejected in the newly proposed stress sequence proposed in §6.3.5.

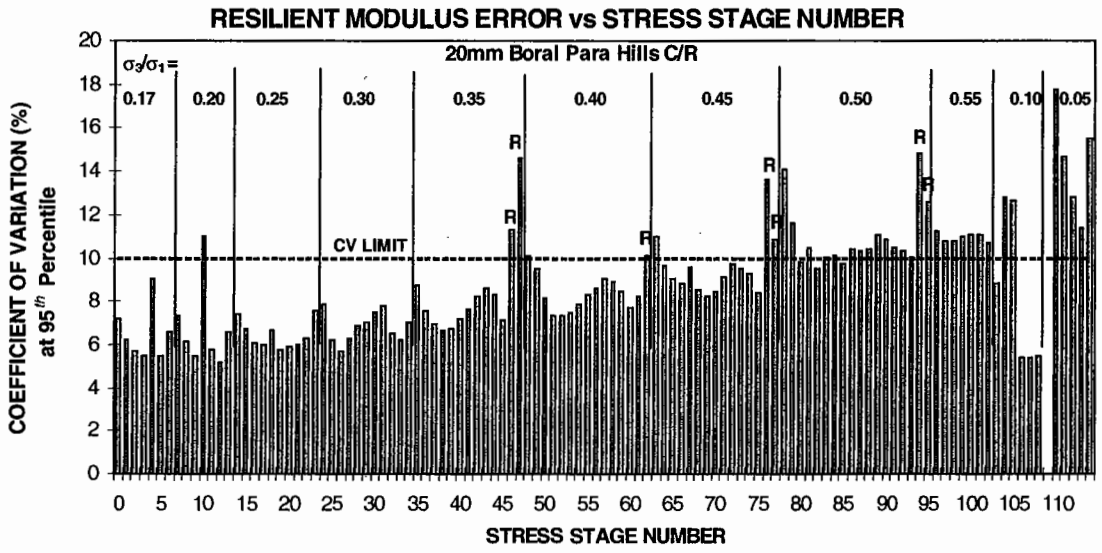

FIGURE 7.7: VARIATION IN RESILIENT MODULUS FOR EACH STRESS STAGE TESTED (20MM BORAL PARA HILLS C/R) – AVERAGE FOR ALL MOISTURE CONTENTS

NOTE: Point 109 with a stress combination of p = 25kPa and q = 65kPa was not tested for this material

7.2.3.3 Post-Test Grading

As part of this test program, all specimens had a post-test grading performed to investigate the magnitude of material breakdown, which varied from material to material due to geology, particle shape, moisture content, compaction density, resistance to crushing, etc. The post-test grading for the 20mm Boral Para Hills C/R, at a moisture content of approximately 80% of OMC, is presented in Figure 7.8 to examine the effect of compaction density in particular. Clearly, the specimens which were compacted to higher densities suffered higher levels of material breakdown. The grading for DDR = 98% somewhat follows the 'fine grading' curve shown in Figure 2.14, however, its curve falls inside of the upper grading limit for particles above approximately 0.8mm in size. It was shown in Figures 2.15 and 2.16, that materials exhibited improved performance (that is, low levels of permanent strain rate and high levels of resilient modulus) for fine gradings over a moisture range of up to 90% of OMC. However, this could vary from one product to the next. In §2.4.4 it was concluded that grading has an indirect effect on performance by controlling the impact of moisture and density of the system.

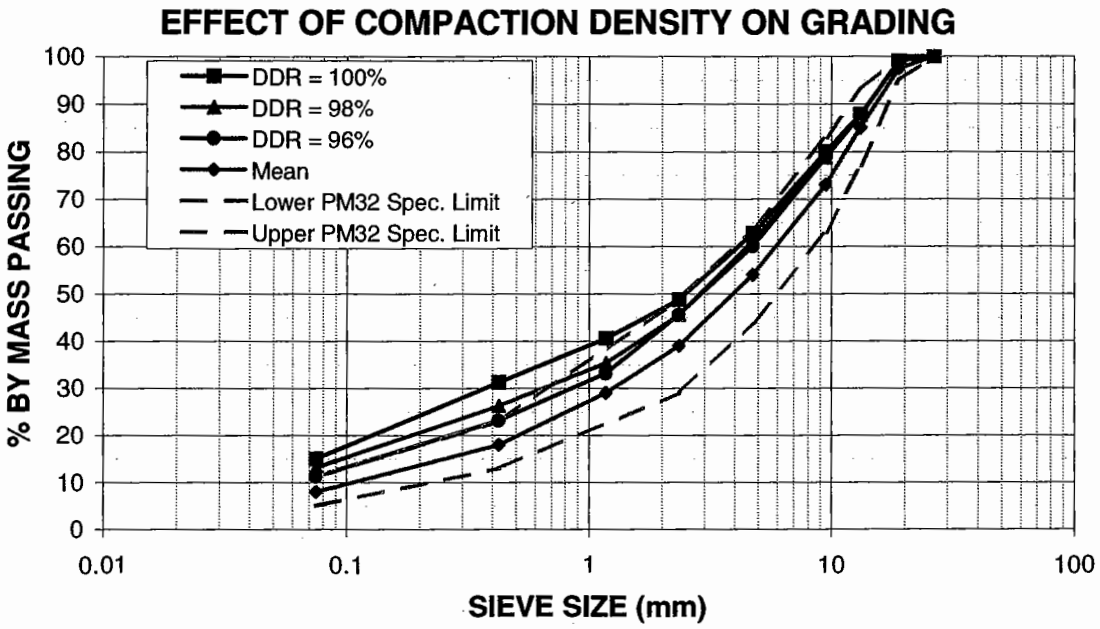

FIGURE 7.8: POST TEST GRADING FOR 20MM BORAL PARA HILLS C/R – VARYING COMPACTION DENSITIES

7.3 Consequences of the Testing Program

As a result of the TSA experimental testing program and the repeatability data obtained, the stress stage sequence to be performed for testing has been reviewed in order to further improve repeatability to within the target levels of 10% for resilient modulus. In addition, it is aimed to specify the stress combinations to be used in the test which are only necessary to spatially satisfy the Australian stress locus (see §5.4.1). The stress combinations targeted for removal are those:

- greater than approximately $\sigma_3/\sigma_1 = 0.35$ (or q/p less than approximately 1.25). Above this level the coefficient of variation begins to approach, then exceed, 10%.
- greater than approximately p = 325kPa, all q. This is to limit the confining pressure to 150kPa as recommended by the AGWRU (refer to limit line shown in Figure 6.5).

In addition, the order of the stress stage sequence has been modified to follow a path of increasing p within a stress ratio path of fixed q/p before moving to the next higher q/p value paths. Given that UGMs are not truly elastic, despite the

preconditioning phase of the test, it is considered important that, having followed a stress path of increasing q/p, the specimen is stress relieved along the same path at selected points. This approach involves selecting some of the same stress combinations when following decreasing p as were used for increasing p. Not all points need be selected, but those which provide a mean normal stress change of approximately less than 100kPa to restrict the magnitude of the change (that is, incremental change is sought).

The newly proposed stress sequences, one for basecourse high quality materials and one for lower quality sub-base materials, are as reported in §6.3.5.

7.4 Tests Performed with New Stress Sequences

Testing has been performed with the techniques used above, however, the newly proposed stress sequence (as reported in §6.3.5 and shown in Figure 6.5) was used.

The Boral Para Hills 20mm C/R material was again used for testing, although it was sampled at a latter date. One moisture content was targeted being RMC = 75%. It shall be noted that the specimens were compacted in the same manner as the testing reported above, however, the UMATTA test equipment used was a later model system than that previously used (as discussed in §6.2.1).

With reference to Figure 7.9, variations in resilient modulus were found to be low for all the basecourse stress levels tested, generally 4% or less. However, for two of the sub-base stress levels the variations were higher than the limit of 10% sought. These two stress combinations coincided with points deep into a fill layer, where very low q and p levels exist due to their remote stress location from the surface wheel load. As reported in §7.2.3.2, stress combinations with very low mean normal and deviatoric stresses provide small strains that are difficult to measure accurately. All repeat or duplicate points were found to either produce a repeatability less than 4%.

Whilst improvements in the UMATTA system are recognised as a contributing factor to the success of the results obtained, it is considered that the proposed method is of merit in determining resilient modulus results over a range of expected *in-situ* stress

conditions. Further testing by researchers using this stress sequence is recommended to further explore its benefits over existing approaches adopted worldwide. Consideration should be given to testing a wide range of materials, of varying quality, over a range of state conditions (density and moisture). The variety of materials used should cover those known to be of low to high shear strength and include alternative type materials such as recycled crushed concrete, incineration ash, blended products and the like.

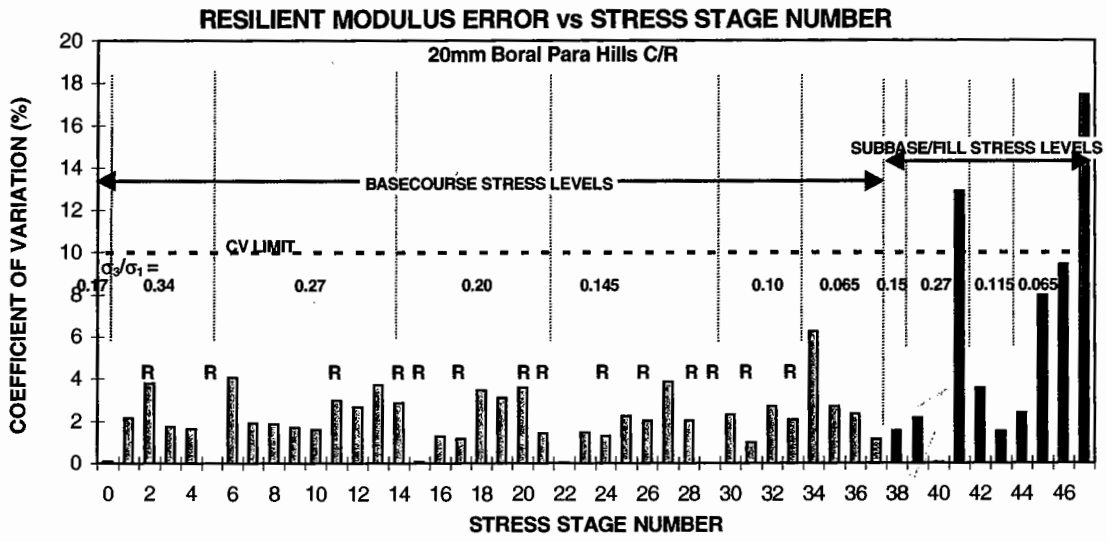

FIGURE 7.9: VARIATION IN RESILIENT MODULUS FOR EACH STRESS STAGE TESTED (20MM BORAL PARA HILLS C/R) – AVERAGE FOR ONE MOISTURE CONTENT

7.5 Summary

An overview of the testing program used by the Author in testing a range of materials was described, with the results of a select number to be presented in Chapter 8.

The results of two materials tested were statistically analysed in order to determine the repeatability of permanent strain rate and resilient modulus. Results illustrated that the coefficient of variation at the 95 percentile for strain rate was approximately 20% whilst for resilient modulus it was 9%. These levels of variation were below the target levels of 30% and 10% aimed for by the Author and supported by others (Barksdale and Alba).

Following the newly proposed stress levels and stress path for resilient modulus, lead to a further reduction in the coefficient of variation at the 95 percentile, with the value being 4% or less for the basecourse stress sequence. This is largely due to the removal of the less repeatable stress combinations, which are generally those with a high confining stress and low ratio of q/p, where recorded strains from testing materials are smaller and more difficult to measure accurately. The variation obtained for the sub-base stress combinations was expectedly higher for this very reason.

CHAPTER 8
KEY FINDINGS FROM LABORATORY TESTING PROGRAM

8.1 Introduction

The results of the materials investigation testing program, as discussed in Chapter 7, are presented here. The program aimed to better understand the performance of a range of unbound granular materials under conditions that are representative of those experienced in the field, namely environmental and load-induced, due to moving traffic wheel loads. The results allow pavement designers and material practitioners to more rigorously understand, and therefore predict, the material abilities in-service. Given that performance-based specifications have only recently been introduced into the South Australian materials industry (see Chapter 9), the MPIs can be used to compare materials which have been tested under the same conditions, according to predetermined density and moisture states.

The individual empirical and performance-based test results of a number of quarry-produced materials are examined in this Chapter. In particular, four 20mm crushed rock and two quarry rubble products, all sourced from local quarries, are examined. Both types of products are produced using a process of rock crushers and screen decks, working in combination, to influence product quality. All materials are known to satisfy local empirical pavement material supply and delivery specifications, PM32 (C/R) and PM21 (Q/R) (Department of Road Transport, 1990).

It is stated throughout the industry that "quarry rubble products are generally *believed* to be 'lower grade' materials than crushed rock products". This hypothesis shall be tested in §8.6.1. The statement is thought to be due to quarry rubble's having moderately higher plasticity, abrasion and fragmentation test values, resulting from a component of the source rock often being of lesser hardness, toughness and soundness than that used in the production of crushed rock products. The lower quality source rock is frequently extracted from a different 'bench' within the quarry

and may be blended with a higher quality rock in a proportion determined by local quarry practice in order to achieve the overall grade of product required. In addition, to produce the crushed rock, an additional screening process is employed to remove loose soil adhering to the rock. Consequently, this results in a cleaner product. This is reflected in more tolerance provided in specification values reported in Table 8.2.

A performance-based comparison (over a range of expected *in-situ* state conditions of density and moisture content) between the crushed rock and quarry rubble materials shall be made to test this hypothesis that "crushed rock material are superior in performance to quarry rubble materials". To do this, each material shall be assessed against MPI limiting criteria (shear strength, permanent strain rate and resilient modulus). In addition, the results of empirical tests shall be used to see if any parallels may be drawn.

If it is found that the performance of a quarry rubble is equal to or better than that of a crushed rock then considerable cost savings could be made in specifying these materials in the upper two base layers or a thin asphalt-surfaced pavement. Given the cost differential between the supply of a crushed rock and quarry rubble in Adelaide is A$4/tonne, the cost per kilometre of roadway (being 9m wide roadway, including 3.5m lane width and 1m shoulders, and considering the upper base layer to be 300mm in thickness) is of the order of $21,600/km (or £8640/km). Thus, considerable savings could be made if quarry rubble products could be used in place of the higher cost crushed rock.

8.2 Empirical Classification Assessment

The materials tested conformed to the grading envelopes for the products. The grading characteristics of the two product types are given below in Table 8.1, where it can be seen that the grading envelope for the quarry rubble is a little more broad and hence less 'tight' than that of the crushed rock.

Sieve Size (mm)	20mm Crushed Rock (% Passing)	20mm Quarry Rubble (% Passing)
26.5	100	100
19.0	95-100	90-100
13.2	77-93	74-96
9.5	63-83	61-85
4.75	44-64	42-66
2.36	29-49	28-50
0.425	13-23	11-27
0.075	5-11	4-14

TABLE 8.1: GRADING VARIATION BETWEEN A 20MM CRUSHED ROCK AND 20MM QUARRY RUBBLE

The following results were obtained for typical classification tests common used within the road construction industry for assessing the performance, empirically, of pavement materials. The four crushed rock and two quarry rubble products are named in Table 8.2. The wet and dry strength tests are Standards aggregate crushing tests performed on a 10-14mm particle size range, whereby the strength is determined based on the load applied to the specimen to generate 10% fines passing a 2.36mm sieve.

Product	Tests Performed										
	PI (%)	LL (%)	LS (%)	LA (%)	MDD (t/m^3)	OMC (%)	G_s	Ab (%)	Strength		
									Dry (kN	Wet (kN)	Var^n (%)
Boral Para Hills C/R	4	17	3	29	2.14	7.0	2.45	2.4	121	98	19
Linwood C/R	7	21	3	18	2.27	6.5	2.61	2.4	233	146	37.5
Boral Lobethal C/R	4	22	3	33	2.31	6.5	2.76	0.5	232	124	47
Stonyfell C/R	6	20	1	31	2.16	7.0	2.46	4.7	190	152	20
LIMITS (PM32)	6	25	3	30					-	100 (1) 80 (2)	35 (1)
Boral Para Hills Q/R	5	19	2	33	2.11	7.5	2.52	2.5	151	78	48
Boral Lobethal Q/R	5	24	1.5	18	2.30	5.5	2.72	0.7	220	130	41
LIMITS (PM21)	1/8	28	4	45					-	-	40

TABLE 8.2: CLASSIFICATION TEST RESULTS FOR THE SIX MATERIALS EXAMINED

PI = Plasticity Index, LL = Liquid Limit, LS = Linear Shrinkage, MDD = Maximum Dry Density, OMC = Optimum Moisture Content (modified Proctor compaction), LA = Los Angeles Abrasion, Ab = Water Absorption, N/T = Not Tested, C/R = crushed rock, Q/R = quarry rubble

NOTE: (1) base material, with < 50mm seal, (ESA > 4×10^6) - minimum limit = 100kN

(2) base material, with < 50mm seal, (10^5 < ESA < 4×10^6) - minimum limit = 80kN

By comparing the measured values given in Table 8.2 with the maximum (or minimum) limiting values, it can be stated that the materials are generally conforming to the conventional crushed rock base layer standards if, in some cases, a small tolerance is accepted.

8.3 Triaxial Shear Strength Assessment

This test is used to relate material shear strength to that required in thinly-surfaced pavement layer applications, resulting in high-quality base, marginal-quality sub-base and poor-quality fill material shear strength types (see Section §5.6). As discussed in §5.6, it is expected that this test will provide information regarding the *initial* suitability of a material to be used in a particular pavement layer, such that the material does not fail in shear under the applied wheel loads. This test is conducted before any 'more complex' RLT testing is undertaken, for it is an obvious statement that a material performing poorly in this test could not be expected to perform at a much higher level in the two phases (preconditioning and stress stage testing) of the RLT test. Although six different moisture levels were tested for, only two are illustrated here for each product, namely, a low and high moisture.

8.3.1 Crushed Rock Quarry Materials

8.3.1.1 Boral Para Hills

This material appears to have a shear strength applicable to a high-quality base material at all conditions, other than those of low density, DDR ≅ 96%, and moisture contents above approximately 65% of OMC (see Figure A.6.1). This figure was determined from an intermediate moisture content shear test not published here. The shear strength is moderately density-dependent.

8.3.1.2 Boral Lobethal

The Boral Lobethal material does not possess a sufficiently high shear strength associated with a high-quality base material, except at conditions of high compaction density, DDR ≅ 100% at both assessed moisture levels (see Figure A.6.2). As a result, this material is only deemed to be suitable for sub-base, or lower layer applications. The shear strength is only moderately density dependent.

8.3.1.3 Linwood

The Linwood quarry product possesses a shear strength that is highly dictated by moisture content changes for all density conditions. Figure A.6.3 illustrates that at low moisture content (RMC ≅ 50%) the material will well satisfy basecourse layer levels of loading for a density level of DDR ≅ 98% or greater. However, once the moisture level increases to above RMC ≅ 70% (as found from testing, referring to Figure 10.28), the material could only withstand stress combinations experienced by a sub-base layer. The shear strength is also very density-dependent.

8.3.1.4 Stonyfell

This product is only used in the metropolitan area of Adelaide when combined with a cement stabilising agent. The material has once been used in a 'semi' bound state (with the addition of 1½ to 2% cement) as a 70 and 120mm base layer for a pavement section of National Highway. The layer was found to 'de-bond' over time (due to its lack of thickness) to that of a 'modified' unbound material, with a high moisture content. This material had an inferior field (and laboratory-tested) performance, despite the pavement having a 115mm A/C20 asphalt base layer and a subsequent overlying 35mm OGFC surfacing layer. Both of these layers have failed several times within a four year period.

From Figure A6.4, it can be seen that the shear strength of this material is highly moisture sensitive at all density levels. At DDR ≅ 96 and 98%, the material could only withstand stress combinations experienced by a sub-base layer, at best. At these density levels, once the moisture content increases to in excess of 80% of OMC, the classification system would rank this material as being more suitable for use as fill, if used in a *thinly* surfaced pavement where stresses within these layers would be at the high end of the upper limits defined. The shear strength is very density-dependent.

8.3.2 Quarry Rubble Materials

8.3.2.1 Boral Para Hills

The quarry rubble product can be seen, with reference to Figure A6.5, to have very similar shear characteristics as the crushed rock product reported in §8.3.1.1 (compare with Figure A6.1).

8.3.2.2 Boral Lobethal

The quarry rubble product can be seen, with reference to Figure A6.6, to possess slightly lower shear strengths than the crushed rock product reported in §8.3.1.2. However, at a density level of DDR ≅ 96% and at high moisture content, the material possesses a lower shear strength than the comparable crushed rock product (compare with Figure A6.2).

8.4 Repeated Load Triaxial Permanent Strain Assessment

The tangential slope of the permanent strain-load cycle graph, as shown in §2.3.2, has been used to assess the susceptibility of UGMs to load-induced deformation or rutting. Materials can be ranked by this parameter.

The stress level used to assess the permanent strain rate is p_{max} = 133kPa and Δq = 250kPa, which is applicable to the approximate stress level at a depth of 110mm into the basecourse layer, beneath a very thin (35mm) surfacing. The coefficient of variation of strain rate at this stress level has been found to vary between 4% and 32% (average approximately 20%), with reference to §7.2.3.1.

By reference to performance data, to be discussed in detail in §10.2.6, a critical permanent strain rate has been set at $d\varepsilon_{1p}/dN = 2 \times 10^{-5}$ %/cycle for basecourse layer materials. The potential field performance of the materials examined below shall be assessed with respect to this laboratory-determined limit to gauge their permanent strain susceptibility and, hence, suitability for use within a pavement as a basecourse layer. From the performance data given in Figure 10.6 for a granular pavement with 30mm OGFC and 30mm dense mix A/C seal, this strain rate is seen to relate to a deflection curvature measure ($D_0 - D_{200}$) of approximately 0.15mm. Curvature function, which relates truly to dense graded asphalt mixes, is pictorially defined in §10.2.6.

The relationship between design curvature and design traffic is reproduced (see Figure 8.1) from the Austroads Pavement Design Guide, Figure 10.4 (Austroads, 1992). It has been found that the curvature function is influenced mainly by the properties of the basecourse. As mentioned, the curve is applicable to unmodified,

standard dense graded asphalt mixes and not to other mixes (open graded mixes with modifiers or high bitumen contents).

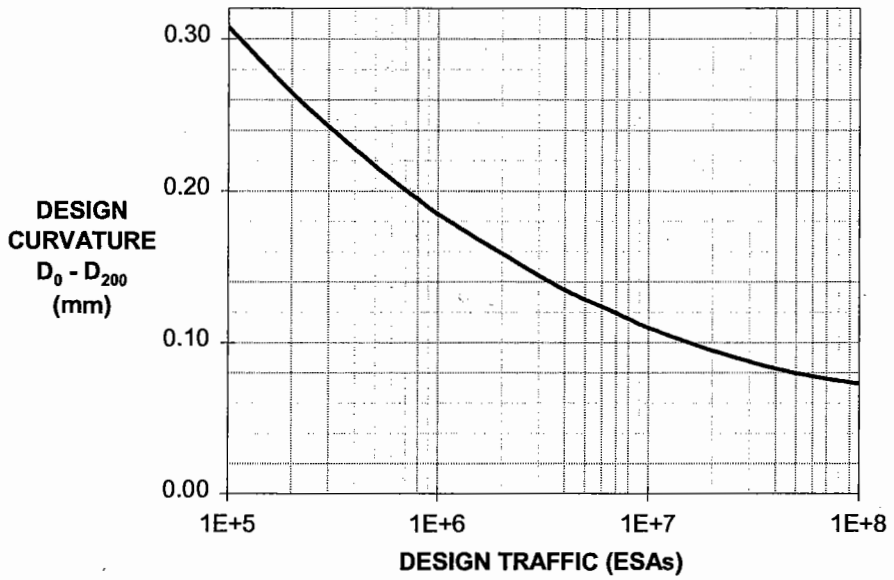

FIGURE 8.1: DESIGN CURVATURE FUNCTION VERSUS DESIGN TRAFFIC
[PRODUCED FROM AUSTROADS, 1992]

Thus, it is considered that a permanent strain rate of 2×10^{-5} %/cycle coincides to a curvature function of 0.15 (Inner Wheel Path, IWP) which is appropriate for a design traffic of 3×10^{6} ESAs. Obviously for higher design traffic to be carried by the pavement materials, a lower material strain rate would be required. For example, for a design traffic of 1×10^{7} ESA, a curvature function of 0.11 and hence a strain rate of approximately 1.3×10^{-5} %/cycle is sought. Further research may well show that the strain rate limit adopted for basecourse materials of 2×10^{-5} %/cycle should be slightly lowered to a level of 1.5×10^{-5} %/cycle. In addition, for sub-base materials, an estimate of acceptable performance for permanent strain rate shall to taken to be within the limit of $\leq 5 \times 10^{-5}$ %/cycle.

It shall be noted that all material density states were close to the nominal levels illustrated in tests for permanent strain rate and resilient modulus. Also, the curves drawn for all material density states reflect those of best fit through all the data points including those beyond the illustrated graphical scale limit displayed for each graph

of 7×10^{-5} %/cycle. This scale limit was selected to enable the reader to clearly see the development of strain increases with moisture levels, which may be sudden or slow depending of the moisture and density state tested.

8.4.1 Crushed Rock Quarry Materials

8.4.1.1 Boral Para Hills

The strain rate for this product (refer to Figure A6.7) increases at only minor rate when tested with increasing RMC or Sr for both density levels of DDR ≅ 98 and 100%. However, the lower density of DDR ≅ 96% produces a more rapid increase.

8.4.1.2 Boral Lobethal

The Boral Lobethal material can be seen, with reference to Figure A6.8, to be highly susceptible to permanent deformation at lower density levels of DDR ≅ 96 and 98% with increasing moisture content, with the 98% density level appearing to be the most sensitive to low level moisture increases. The strain curves become asymptotic at relative moisture levels of approximately 80 to 85% of OMC. However, it can be seen that when graphed with Sr, the rate of permanent strain increases at the same moisture level for both density states, with the 96% state being slightly worse at Sr > 63%. This indicates the necessity of assessment against Sr for this material. Once the strain rate limit of 2×10^{-5} %/cycle occurs, it is evident that very rapid increases in permanent deformation take place.

With reference to Figure A6.2, the preconditioning stress level of p_{max} = 133kPa and Δq = 250kPa is well below those at which shear failure of the material could be expected even at high relative moisture levels and lower density levels. Thus, the rapid increase in permanent deformation is not due to exceedence of the shear strength of the material. At a high compaction density of DDR ≅ 100%, the strain properties are very stable.

8.4.1.3 Linwood

The strain rate for this product (refer to Figure A6.9) is virtually unaffected by increasing moisture levels for all density levels. It is not until a moisture content of

90% of OMC that the rate of strain increases begin to accelerate for the DDR ≅ 96% state. However, when Sr is used as the abscissa, it can be seen that the lowest density state undergoes more rapid strain increases than the other states, commencing at Sr = 80%.

The preconditioning stress is quite a way lower than the nearest shear stress failure envelope, although the DDR ≅ 96% does approach this stress condition for the high RMC condition (refer to Figure A6.3).

8.4.1.4 Stonyfell

The Stonyfell material can be seen, with reference to Figure A6.10, to be highly susceptible to permanent deformation at all density levels with increasing moisture content. The strain curves become asymptotic at relative moisture levels of between approximately 80% and 95% of OMC. Interestingly, the highest density state of DDR ≅ 100% appears to perform the worst at the lower moisture states when considering strain rate with RMC. However, when Sr is used as the abscissa, it can be seen that the DDR ≅ 96 and 100% density state curves shift dramatically relative to the DDR ≅ 98% state curve. The more intuitive outcome of the low density state performing poorly and the high density state performing well prevails. Again, this result emphases very strongly the requirement that Sr should be used as the assessment 'moisture parameter'.

With reference to Figure A6.4, the preconditioning stress level is only slightly below the stress conditions which lead to shear failure of the DDR ≅ 96% and RMC = 86% material, whilst the other density level states are less critical. Thus, the responses in Figure A6.10 can only be partially explained by reference to the applied shear stress level.

8.4.2 Quarry Rubble Materials

8.4.2.1 Boral Para Hills

The quarry rubble product can be seen, with reference to Figure A6.11, to be very resistance to permanent deformation with increases in moisture content, for all density levels. These results are quite similar to the crushed rock product, although

at the lowest density level of DDR ≅ 96%, the resistance to permanent strain development is greater at high moisture levels, compared to the crushed rock product (Figure A6.11).

Once again, when Sr is used to interpret strain rate results, the shift in the DDR ≅ 96% and 100% level curves is apparent. The lowest density level now shows its more moisture sensitive nature.

With reference to Figure A6.5, the preconditioning stress level is well below the stress conditions that would lead to shear failure for all material conditions.

8.4.2.2 Boral Lobethal

The quarry rubble product can be seen, with reference to Figure A6.12, to show negligible susceptibility to permanent deformation at all density levels. This is in stark contrast to the crushed rock product (see Figure A6.8).

With reference to Figure A6.6, the preconditioning stress level is below the stress conditions that would lead to shear failure for all material conditions.

8.5 Repeated Load Triaxial Resilient Modulus Assessment

Resilient modulus, as defined in §2.3.1, is highly stress dependent as discussed in §2.4.6, to characterise this parameter in order to assess and 'rank' different products, a single stress level needs to be nominated for this purpose. The stress level used to report the resilient modulus here is p_{max} = 250kPa and Δq = 490kPa (ie. $\sigma_{1\ max}$ = 577kPa and σ_3 = 87kPa). This stress level is applicable to that experienced at the top of the basecourse layer under a very thin (35mm) surfacing (refer to Figure 5.7), as computed by non-linear elastic analysis, similar to the Example in Appendix 1. This is dependent somewhat on the stiffness levels adopted for the basecourse. It shall be noted that this is nearly the same stress level used to define the 'characteristic modulus, E_c' referred to in the European CEN test procedure for resilient modulus determination (CEN, 2000), with reference to §6.3.6. Given that this stress level is the highest one encountered under this type of surfacing, it is useful to assess the material for suitability as a base layer at this point. This is particularly so given the

modulus-stress dependence (see Figures 5.23 and 5.24). The coefficient of variation of resilient modulus at this stress level has been found to be of the order of 5 to 6%, with reference to §7.2.3.2.

For the satisfactory performance of a basecourse material, the magnitude of resilient modulus at this stress point (p_{max} = 250kPa and Δq = 490kPa) is considered to be 350MPa. The reasons for this are linked to the current Australian AUSTROADS design procedure for flexible pavements (NAASRA, 1987), where this is the minimum level of modulus specified in Table 6.4(a). This value has subsequently been adopted by a large number of practising pavement design engineers who apply the modular ratio methodology specified in this Guide. It has been generally found that by following this method, and accurately laboratory testing materials for resilient modulus at this stress level (using off-specimen strain measurement), that satisfactory pavement performance has resulted provided underlying layers do not vary in material quality nor *in-situ* condition of moisture. This statement is made considering that all other factors, such as drainage, compaction, traffic estimation, sound strength, stiffness and resistance to permanent deformation of lower pavement layers and subgrade, etc, have been successfully applied. The pitfalls of this method of design are described in some detail in §3.6.1; however, the modulus value nominated appears to be an adequate attempt at linking a laboratory ranking or assessment value to constructed pavement performance. This material 'ranking' is also supported in Europe, lead by the French (Paute, et al, 1994), and followed by others (EC, 2000, COURAGE Report pp. 45-46). In Europe, however, the minimum level of resilient modulus (measured by on-specimen techniques) is 500MPa, appropriate to a stress level of p_{max} = 250kPa and Δq = 500kPa (ie. $\sigma_{1\ max}$ = 583kPa and σ_3 = 83kPa) (refer to §3.6.5). The higher level demanded by the French in particular would largely be a requirement due to the higher local loadings imparted to the materials (refer to Table 3.1).

Considering that a sound material yields a resilient modulus of 350MPa at the stress level of p_{max} = 250kPa and Δq = 490kPa, additional moduli were determined by the Author for these materials but at two other stress combinations appropriate to the top of sub-base and fill layers (refer to Figure 5.7). By using the 'Resilient Modulus

Design Chart' for a number of sound materials, such as the one illustrated in Figure 5.24, this could be easily achieved. The values required for these layers were found to be:

- sub-base ≥ 240MPa (based on result at stress level of p_{max} = 105kPa and Δq = 260kPa)
- fill ≥ 175MPa (based on result at stress level of p_{max} = 50kPa and Δq = 130kPa)

The modulus figures presented above shall be used in §8.6.1 to rank the materials for suitability for use as particular pavement layers, according to four key MPIs of strain rate, resilient modulus, cohesion and angle of shearing resistance. The other two indicators of durability and permeability would also need to be addressed.

It shall be noted that all material density states were close to the nominal levels illustrated in tests for resilient modulus.

8.5.1 Crushed Rock Quarry Materials

8.5.1.1 Boral Para Hills

The Boral Para Hills material (refer to Figure A6.13) does not generate very high levels of modulus, which decreases with moisture content at all density levels greater than approximately 60% of OMC. The material does not appear very density dependent when assessed against RMC with all curves generally indicating the same result. However, when Sr is used as the moisture parameter, the performance shift of the lower density state of DDR ≅ 96% is most apparent at low moisture levels with a lower modulus of approximately 50MPa than the other two states resulting between Sr = 60 to 75%.

8.5.1.2 Boral Lobethal

The Boral Lobethal product (refer to Figure A6.14) is considered inferior with very low levels of modulus produced under expected traffic loading stress conditions. Optimum performance is again achieved around 60% of OMC, however, modulus levels become very low by 80% of OMC.

The results plotted against Sr show a shift in the performance of one density state to another, with the high density material performing the best at moisture contents above Sr ≥ 63%

8.5.1.3 Linwood

This product (refer to Figure A6.15) is considered a high performer if maintained dry of 70% of OMC, above which it is very moisture sensitive at all density levels. It is interesting to note that the lower density level of DDR ≅ 96% appears to out-perform the higher level of DDR ≅ 100% using this graphical interpretation.

The importance of specifying Sr is again highlighted in the results of this material. For Sr ≤ 70%, the material results show that a higher density state is associated with a higher level of performance, which is the converse to the results graphed with RMC. For Sr ≥ 70%, density has little perceived benefit with all density states exhibiting the same modulus.

8.5.1.4 Stonyfell

From Figure A6.16, it can be seen that the resilient modulus of this material is highly moisture sensitive at all density levels beyond approximately 68 to 76% of OMC. The modulus capability of the Stonyfell product is reduced by between 25 to 35%, beyond this moisture level up to optimum, depending on the density level. The highest density state of DDR ≅ 100% yields a much lower modulus than the other two density levels at relative moisture contents less than nearly 70% of OMC as was found with a number of other products.

The poor modulus performance of the DDR ≅ 96% density state with higher moisture content can only be seen with parameter Sr.

8.5.2 Quarry Rubble Materials

8.5.2.1 Boral Para Hills

The quarry rubble product can be seen, with reference to Figure A6.17, to perform in a similar manner to the crushed rock product of §8.5.1.1. However, it does yield higher moduli for the lower density level of DDR ≅ 96% at all moisture states,

particularly those beyond RMC = 60% although both products possess virtually the same shear strength at DDR ≅ 96% and RMC = 89% of OMC.

As for a number of the materials, poor performance of the lower density states with higher moisture content can only be seen with parameter Sr.

8.5.2.2 Boral Lobethal

This quarry rubble product can be seen, with reference to Figure A6.18, to show modulus levels that are not very dependent on density level with RMC but are more pronounced when graphed against Sr. If these results are compared with the crushed rock material (refer to §8.5.1.2), the modulus levels are much higher and are influenced by moisture content to a lesser degree.

8.6 Key Findings from Testing Program

Unstable permanent deformation or strain rate could be seen to occur in some of the materials tested. This was illustrated by high test result values including extremely rapid strain development at certain moisture levels. The main factors involved are considered to be due to (1) stress state, (2) relative moisture content or degree of saturation, (3) density or level and type of compaction and (4) quality of the material. It could be expected that considerable material instability might only *begin* to occur in materials tested beyond 3000 cycles. It is possible that, in some cases, the observation that a material is stable within 3000 cycles could be misleading regarding its long-term behaviour.

Optimum performance most often occurs at RMC = 60% of OMC (approximately Sr = 50% to 55% for most materials depending on the density level) or less. This level of moisture content cannot be directly translated for Sr, due to the parameter's strong dependence on density level. At this moisture level, all materials were found to yield very low permanent strain rates (generally around 0.2 to 1.0×10^{-5} %/cycle) and high resilient moduli (generally 330 to 390MPa) except for some materials at the highest density level of DDR = 100%. In contrast, at 85% of OMC, strain rates can range from 0.5 to 6.0×10^{-5} %/cycle and resilient moduli are lower at values of 220 to

350MPa. Large shear strength variations also occurred for materials at different densities and moisture contents.

8.6.1 Material Quality Summary

The materials tested can now be 'ranked' for suitability in a particular pavement layer, at a low (60% of OMC or Sr of 50%) and high moisture (85% of OMC or Sr of 75%), in accordance with the following criteria:

- shear strength classification system (see §8.3 and §5.6)
- permanent strain rate, based on p_{max} = 133kPa and Δq = 250kPa (see §8.4):
  - base $\leq 2 \times 10^{-5}$ %/cycle
  - sub-base $\leq 5 \times 10^{-5}$ %/cycle
- resilient modulus (see §8.5):
  - base $\geq$ 350MPa (based on result at stress level of p_{max} = 250kPa and Δq = 490kPa)
  - sub-base $\geq$ 240MPa (based on result at stress level of p_{max} = 105kPa and Δq = 260kPa)
  - fill $\geq$ 175MPa (based on result at stress level of p_{max} = 50kPa and Δq = 130kPa)

From the graphed material results presented for the four crushed rock and two quarry rubble materials in §8.3 to §8.5, with reference to Appendix 6, the following assessment can be made (see Table 8.3).

Assessment	C/R				Q/R	
	BPH	BLob	Lin	Stony	BPH	BLob
Shear Strength						
DDR ≅ 96, low MC	B	SB	SB	SB	B	SB
high MC	SB	SB	F	F	SB	Marg SB
DDR ≅ 98, low MC	B	SB	B	B	B	B
high MC	Marg B	SB	SB	F	Marg B	SB
DDR ≅ 100, low MC	B	B	B	B	B	B
high MC	B	B	SB	Marg B	B	Marg B
Perm Strain Rate	$\times 10^{-5}$ (%/cycle)					
DDR ≅ 96, low MC	0.8 B	0.3 B	0.6 B	0.9 B	0.4 B	0.3 B
high MC	2.3 SB	1.8 B	0.8 B	3.0 SB	0.7 B	0.5 B
DDR ≅ 98, low MC	0.6 B	0.5 B	0.5 B	0.9 B	0.5 B	0.3 B
high MC	1.1 B	5.8 F	0.9 B	2.05 SB	1.1 B	0.4 B
DDR ≅ 100, low MC	0.6 B	0.3 B	0.3 B	1.1 B	0.5 B	0.3 B
high MC	1.1 B	0.5 B	1.0 B	4.6 SB	0.9 B	0.3 B
Resilient Modulus	(MPa)					
DDR ≅ 96, low MC	350 B	300 SB	400 B	380 B	370 B	340 B #
high MC	270 SB	215 F	350 B	290 SB	325 SB	300 SB
DDR ≅ 98, low MC	340 B #	330 SB	380 B	380 B	365 B	330 SB
high MC	285 SB	220 F	330 SB	280 SB	275 SB	315 SB
DDR ≅ 100, low MC	320 SB	285 SB	370 B	320 SB	320 SB	340 B
high MC	270 SB	240 SB	290 SB	255 SB	290 SB	315 SB
Overall RESULT						
DDR ≅ 96, low MC		SB (1,3)	SB (1)	SB (1)		SB (1)
high MC	SB	F (3)	F (1)	F (1)	SB (1,3)	SB (1,3)
DDR ≅ 98, low MC		SB (1,3)				SB (3)
high MC	SB (3)	F (2,3)	SB (1,3)	F (1)	SB (3)	SB (1,3)
DDR ≅ 100, low MC	SB (3)	SB (3)		SB (3)	SB (3)	
high MC	SB (3)	SB (3)	SB (1,3)	SB (2,3)	SB (3)	SB (3)

TABLE 8.3: PERFORMANCE-BASED CLASSIFICATION OF THE FOUR CRUSHED ROCK AND TWO QUARRY RUBBLE MATERIALS ASSESSED, IN TERMS OF RMC

B = basecourse quality material, B = sub-base quality material, F = fill quality material

Marg. = marginal

1 = based on Shear, 2 = based on Permanent Strain Rate, 3 = based on Resilient Modulus

= within 10MPa tolerance

From these results, it can be seen that the materials are expected to perform as a basecourse material as follows:

- Boral Para Hills crushed rock material for density states of DDR ≅ 96 and 98%, and at low-end moisture levels (not greater than 62% of OMC)
- Linwood crushed rock material for density states of DDR ≅ 96 and 98%, and at low-end moisture levels (not greater than 72% of OMC)
- Stonyfell crushed rock material for a density state of DDR ≅ 98% only, and at low-end moisture levels (not greater than 67% of OMC)

- Boral Para Hills quarry rubble material for density states of DDR ≅ 96 and 98%, and at low-end moisture levels (not greater than 68% of OMC)
- Boral Lobethal quarry rubble material for a density states of DDR ≅ 100%, and at low-end moisture levels (not greater than 68% of OMC)

Given the importance of degree of saturation, particularly for the assessment of permanent strain rate and resilient modulus, the results in Table 8.3 are re-considered for this parameter (Table 8.4) to investigate whether the material usage in pavement is affected. The materials tested are 'ranked' for suitability in a particular pavement layer, at a low (Sr = 50%) and high (Sr = 75%) saturation.

Assessment	C/R				Q/R	
	BPH	BLob	Lin	Stony	BPH	BLob
Perm Strain Rate	$\times 10^{-5}$ (%/cycle)					
DDR ≅ 96, low Sr	0.6 B	0.4 B	0.5 B	0.8 B	0.4 B	0.5 B
high Sr	2.2 SB	40.0+ F	0.9 B	2.3 SB	0.9 B	1.0 B
DDR ≅ 98, low Sr	0.4 B	0.5 B	0.2 B	0.7 B	0.4 B	0.4 B
high Sr	0.9 B	7.0+ F	0.9 B	1.4 B	0.9 B	0.6 B
DDR ≅ 100, low Sr	0.4 B	0.3 B	0.2 B	0.3 B	0.4 B	0.3 B
high Sr	0.7 B	0.5 B	0.4 B	1.2 B	0.8 B	0.3 B
Resilient Modulus	(MPa)					
DDR ≅ 96, low Sr	350 B	300 SB	410 B	390 B	355 B	320 SB
high Sr	270 SB	275 SB	350 B	320 SB	275 SB	<240 F
DDR ≅ 98, low Sr	355 B	330 SB	420 B	375 B	365 B	325 SB
high Sr	300 SB	350 B	330 SB	300 SB	275 SB	275 SB
DDR ≅ 100, low Sr	350 B	285 SB	480 B	350 B	320 SB	340 B #
high Sr	315 SB	275 SB	335 SB	320 SB	300 SB	320 SB
Overall RESULT						
DDR ≅ 96, low Sr		SB (1,3)	SB (1)	SB (1)		SB (1)
high Sr	SB	F (1)	F (1)	F (1)	SB (1,3)	F (3)
DDR ≅ 98, low Sr		SB (1,3)				SB (3)
high Sr	SB (3)	F (2)	SB (1,3)	F (1)	SB (3)	SB (1,3)
DDR ≅ 100, low Sr		SB (3)			SB (3)	
high Sr	SB (3)	SB (3)	SB (1,3)	SB (3)	SB (3)	SB (3)

TABLE 8.4: PERFORMANCE-BASED CLASSIFICATION OF THE FOUR CRUSHED ROCK AND TWO QUARRY RUBBLE MATERIALS ASSESSED, IN TERMS OF SR

These results suggest the following changes to the classification of the materials:

- Boral Para Hills crushed rock at DDR ≅ 100%, reclassified to a base material
- Stonyfell crushed rock at DDR ≅ 100%, reclassified to a base material
- Boral Lobethal quarry rubble at DDR ≅ 96%, reclassified to a fill material

In all cases, this was due to the shift in the resilient modulus value with this alternative moisture parameter. It is apparent from these results that the degree of saturation allows the strain rate and modulus values to shift in a direction of reduced moisture level for DDR ≅ 96% materials and higher moisture level for DDR ≅ 100%. Consequently, the performance of DDR ≅ 96% materials appears to diminish, for DDR ≅ 98% performance remains virtually unchanged, whilst for DDR ≅ 100% material performance improves.

8.7 Summary

8.7.1 Shear Strength

Shear strength was found to greatly vary due to material geology, moisture content and density. The use of the new shear strength classification system, developed by the Author, showed that in certain materials some of these factors were much more dominant than in others. The new classification system provides a single analytical tool to 'rank' the quality of different materials (of varying state conditions) for suitability within a particular pavement layer.

8.7.2 Permanent Strain Rate

Permanent strain rate was found to be acceptably low (less than 1.1×10^{-5} %/cycle maximum) for all material density levels when the moisture content was low enough. However, at higher moisture levels above RMC = 75% (Sr = 65 to 70%), permanent strain rate was generally seen to increase at or near an exponential-type rate. For the Boral Lobethal and Stonyfell crushed rock products, the strain rate increased very rapidly with moisture content once a value of 2×10^{-5} %/cycle was exceeded. This tends to indicate that a level of $d\varepsilon_p/dN$ of 2×10^{-5} %/cycle (measured at p_{max} = 133kPa and Δq = 250kPa) is somewhat of a critical upper limit.

8.7.3 Resilient Modulus

Resilient modulus is a parameter that can be moderately dependent on compaction density. It is very moisture sensitive with optimum performance at approximately 60% of OMC (Sr = 50 to 55%) or less. By 85% of OMC (Sr = 75%), all materials displayed significant reductions in stiffness of generally up to 25%. One material,

Boral Lobethal crushed rock showed a reduction of 47%. From testing, it was apparent that greater modulus reductions occur for lower density levels (DDR ≅ 96 and 98%), however, the highest density state, DDR ≅ 100%, generally gave lower moduli at the lower moisture range and greater moduli at the higher moisture levels. A minimum modulus of 350MPa (measured at p_{max} = 250kPa and Δq = 490kPa) was adopted for obtaining acceptable stiffness performance of the material in the pavement.

8.7.4 General

These findings suggest that the hypothesis, presented in the Introduction to this Chapter, which states that "quarry rubble products are lower grade materials than crushed rock products" is not generally well founded. The results obtained from performance testing suggest that the Boral Para Hills quarry rubble is marginally better than the crushed rock, given its slightly reduced moisture sensitivity. With reference to Table 8.2, it should be noted that the empirical test results did not indicate much of a difference between these two products. Only a much greater wet/dry strength variation was apparent in the rubble which would see the material being 'out of specification' tolerances and, therefore, not suitable for use in a basecourse layer. The Boral Lobethal quarry rubble product far out-performed its crushed rock counterpart, the latter of which was only found to be of sub-base quality at best. These findings for the performance-based testing were only supported by one empirical test result, the LA test, which showed the rubble to be superior.

As a result, one must question the value of the empirical tests and/or their limiting acceptance values as detailed in empirical specifications. These empirical tests do not seem to produce results which lead to definitive outcomes for how materials should be used in the pavement. Given empirical tests do not use a fully graded material (only a component of the grading) and do not replicate the state conditions of density, moisture and stress, their use is somewhat limited in today's world where heavier and more frequent vehicle trips are made on pavements designed and constructed on leaner budgets. In addition, it is considered that for the pavements currently in-service that limited pavement capacity is available in reserve to accommodate the heavier and longer combination vehicles now using the road

network, especially considering that statutory axle masses have increased dramatically over the last 15 to 20 years. As a result, greater attention needs to be paid to pavement performance to ensure their sustainable management in future years resulting from the heavier loadings. Bridge structures, on the other hand, are considered the weak links, and certainly in Australia receive the funding required for capacity assessment on roads subject to high axle mass loadings, whereas pavements are more 'the forgotten infrastructure component'. However, we have seen a number of materials, under certain conditions, could well be close to their shear capacity limit.

It is apparent from the results that the degree of saturation allows the strain rate and modulus values to shift in a direction of reduced moisture level for DDR $\cong$ 96% materials and higher moisture level for DDR $\cong$ 100%. Consequently, the performance of DDR $\cong$ 96% materials appears to diminish, for DDR $\cong$ 98% performance remains virtually unchanged, whilst for DDR $\cong$ 100% materials performance improves.

To 'optimise' the performance of unbound granular materials it is imperative that the pavement layers not be sealed at higher level of moisture content, preferably not exceeding 60% of ΘMC (or degree of saturation not exceeding 50%). Chapter 9 discusses a practice adopted in a number of States in Australia to deal with this problem. In addition, the results of Chapter 8 suggest that key material performance indicators could well be specified in performance specifications to provide more knowledge concerning expected pavement material behaviour (refer to Chapter 9).

CHAPTER 9
CONSEQUENCES OF MATERIALS TESTING PROGRAM

9.1 Introduction

The results of the materials investigation testing program, as discussed in Chapter 8, illustrates clearly the effect on key MPIs of high moisture content. For some of the materials tested, higher moisture levels were found to produce high levels of permanent strain, along with lower levels of material strength and modulus for a given density state. As a result, measures need to be taken to ensure materials are initially sealed and subsequently maintained throughout their service life in a much drier state than OMC. This Chapter discusses a practice used when constructing many Australian pavements termed 'dry-back'.

In addition, performance-based specifications are described as a means of dealing with the problems associated with empirical-based specifications. As discussed in Chapter 8, empirical tests do not always produce results that lead to a clear distinction in the assessment of material quality. Preliminary work by the Author, along with further developments by others, is described in developing a South Australian specification.

9.2 'Dry-back' of Unstabilised Granular Pavement Layers

The pressure on road authorities and road operators to open newly constructed pavements to traffic as early as possible has sometimes resulted in premature failure requiring expensive rehabilitation and commuter delays. Where more marginal UGMs have been used, it is often due to inadequate 'dry-back' of the pavement layers prior to sealing.

Due to the strong sensitivity of some materials to the level of moisture content held within a granular pavement layer, a clause has been inserted in the TSA specifications regarding material placement. This is aimed at restricting the moisture

within a layer to levels that are known to be associated with near optimal laboratory performance and sound observed pavement performance.

The Boral Lobethal 20mm Crushed Rock proved to be one of the most moisture susceptible materials when tested at the mean of the 20mm Crushed Rock specification (refer to Figure 7.1). As a result, it was suggested in MTRD Report 16-4 (Mundy, 1996) that the crushed rock be compacted in the field to 98% Dry Density Ratio (DRR) or greater and 'dried back' to 60% (maximum) of the Optimum Moisture Content (OMC). This is to ensure that excessive permanent strain and/or static failure does not develop under standard axle loads.

Referring to Part 221 of the Specification concerning the Construction of Unstabilised Granular Pavement (Transport SA, 1997), the clause was inserted to read as follows:

3. *PLACEMENT*

"Placement of subsequent pavement layers shall not commence until the moisture content of the underlying pavement layer is less than 70% of OMC.

Areas to be sealed shall be tested for moisture content. The location of tests shall be selected by the Contractor for each lot on a stratified random basis. The number of strata shall be equal to the number of tests required for a given lot."

The upper limit on the moisture content of 70% of OMC is a little higher than should be allowed, particularly if one consults the resilient modulus and strain rate moisture sensitivity graphs presented in Appendix 6. These graphs show that peak material performance can generally be expected around 60% of optimum or 50 to 55% saturation level (as reported in § 8.8.3).

The contract clause is rather brief stating only the final result required, however, the approach used to achieve this result also needs to be considered. If a granular layer is dried back naturally without any intermediate interventions, the very top of the

layer can be much drier than at greater depth. The result often is a dry "puffy" surface which has reduced stiffness due to the very low moisture content and hence less capillary suction within the material. In preference, during the dry-back period, the layer should periodically have very light applications of water to its surface to enable an equilibrium value to stabilise throughout the entire layer thickness. In addition, the layer should be rolled during the early stages of dry-back to "squeeze out" water and bring moisture to the surface. The action of rolling will result in reduced 'dry-back' time and a stiffer pavement, given that it contains reduced air voids as water has left the pore spaces. By applying some water periodically at the surface, 'dry-back' time takes a little longer to achieve, but with very good results. 'Dry-back' tends to take 2-3 days during summer and 2-3 weeks in winter, provided only minor rainfalls occur. It should be noted that the pavement is not covered during periods of wet weather.

A similar clause has been inserted into Western Australian supply and delivery of pavement material contract documents, but choosing a moisture content of 60% (maximum) of OMC. This was in direct response to a considerable number of pavement failures between 1992 and 1996, which were attributed to, at large, the use of "marginal moisture sensitive basecourse materials". It was identified that "poorly performing sections had moisture contents exceeding 85% of optimum". Whilst the "moisture content for the basecourse materials which did perform satisfactorily were found to be generally lower than 60% of optimum" (Goh, 1994). Laboratory performance-based testing strongly supported these findings (Butkus, 1994, 1997). This case study is presented in detail in §10.2.

It should be noted that the importance of pavement dry-back is now recognised in the new draft Austroads Pavement Design Guide (Austroads, 2001) in §6.2.1.2. The Guide describes one of the major considerations relating to granular materials as the "extent of dry-back from the compaction moisture condition to the moisture condition at sealing and in-service." It is stated that "a dry-back period is required to reduce the moisture content to an acceptable level before sealing". The Guide does not, however, provide any guidance as to the target moisture content prior to sealing.

9.3 Australian Performance-based Specification for the Supply and Delivery of Pavement Materials

The successful implementation of a performance-based specification for unbound pavement materials relies upon a good deal of available laboratory performance data, such that limiting values of MPIs or acceptance criteria can be established based upon field experience. Until a large database of information becomes available, it is difficult to expect a performance-based specification to be the only quality measure. Instead, empirical-based specifications may be used as an *alternative* assessment tool in the interim period. This is the approach that TSA have adopted in the newly developed PM2000 – Standard Specification for the Supply and Delivery of Pavement Material (Transport SA, 2000).

However, it is anticipated that unless road authorities stipulate that the performance-based approach must be used, the road construction industry will opt for the 'easier to perform' and cheaper empirically based tests. In addition, overseas experience suggests that at a time when road builders also become responsible for the on-going maintenance of the constructed pavement, then they will also have an interest to keep maintenance interventions to levels in line with their tender bid to avoid penalties imposed by highway agencies. In design-build-fund-operate (DBFO) contracts of this type, if the road builder places a tender for a more cost-effective design this may well be associated with a higher risk assessment of the material's performance. To reduce this risk, performance-based laboratory testing is one form of treatment. This contract approach to road building and maintenance will better encourage the use of a performance-based assessment for higher risk designs, which may incorporate the use of marginal or alternative materials, over a more subjective empirically-based approach. Until this time occurs, less economic pavement designs incorporating conservative thicknesses of high quality / high cost materials will continue to occur, possibly even for lower trafficked roads.

It should be remembered that empirically based material specifications do not address the use of non-standard materials, changes in environmental conditions and traffic loadings. These specifications have evolved over many years of testing and experience – centring on the material properties of grading, plasticity and stone

hardness/durability. However their ability to truly evaluate material performance with certainty is questionable, as was found in Chapter 8 and will be discussed further in case studies presented in Chapter 10.

Performance-based testing has proved to be beneficial to quarry owners where new 'blended' products have been assessed according to expected field conditions. This has allowed known non-performing materials to be modified with alternative product types or additives in order to raise their performance to 'acceptable' levels (in keeping with those with a record of sound usage). In Australia, a wide range of composite material combinations has been tried in this fashion.
However, it was stated by Andrews (Andrews, 2000) that "key implementation issues (both technical and commercial) have been encountered in the implementation at a State level (by both road asset management authorities and product manufacturers)". One could equally expect this to be the case at a national level. These implementation issues have been summarised in terms of benefits and dis-benefits.

The benefits of performance-based specifications are considerable and present opportunities to many sectors of the community. In particular they provide:

- consideration to environmental and traffic-imposed effects on material performance
- a means for relationships to be developed between identified laboratory and field performance based parameters
- lower design risk of pavement failure with expected economic benefits through a more optimised design process
- options for the assessment and usage of alternative and more marginal materials resulting in:
  - reduced dependence upon higher quality quarried materials, leading to a more sustainable natural resource for future generations
  - reduced dumping of such materials to landfill or unwanted locations
  - benefits to industry in the removal and utilisation of industrial waste from demolition or plant sites

  - present strong business opportunities, backed by possible Government incentives, for utilisation of recycled or waste materials
- options for product manufacturers to blend materials and thereby create novel fit-for-purpose products, thereby reducing net quarried waste

The Author considers that the hindrances to performance-based specifications are:

- establishing 'universal' agreement to proposed conditions and limit values for the specification parameters
- lack of incentive and action to compel industry to commit to a new specification, possibly due to road authorities not moving down the path of DBFO contracts which force contractors to be more conscious of long-term pavement performance
- cultural change to occur in the market
- establishing site laboratories equipped to determine MPIs for products founded in remote, rural areas
- ability of the larger industry leaders to afford to undertake an extensive characterisation program compared to small or 'new market' producers
- no finalised national test procedure for determining material performance indicators, noting the:
  - cost of equipment and time required to perform a test
  - perceived 'technical complexity' of tests required to be performed in industry laboratories (which were established only to undertake simple empirical tests)

At present, the 'national standard' method is still being revised and is yet to be fully agreed to. The acceptance of a national 'standard' RLT testing procedure by SRAs, practitioners and industry is an essential first step before the adoption of performance-based material specifications. For this to occur, the method needs to be:

- clearly defined with transparent objectives
- applicable to *in-situ* environmental and stress conditions
- repeatable and reproducible in the results it achieves
- not too labour intensive or time consuming

- affordable
- applicable to a very wide range of materials

Finally, it is considered that 'controlled' field trials, in terms of construction conditions and axle loads, need to be conducted to verify the selection of MPIs used to assess laboratory performance against field performance.

9.4 Specification Changes for the Supply and Delivery of Pavement Materials – Transport SA

Due to the extensive materials characterisation testing program undertaken by Transport SA between 1990 and 1994/5, it has been possible to examine material performance under a wide range of potential *in-situ* conditions of density and moisture content. Key MPIs were determined for a wide range of materials. The material performance under laboratory test conditions has been continuously related back to field pavement performance, where the appropriate flexible pavements containing the various unbound granular materials have been constructed. This work has been undertaken to enable the introduction of performance-related unbound pavement material specifications that would encourage the efficient use of natural and waste or recycled materials. This specification permits products to be designed and manufactured to meet particular levels of in-service pavement performance.

9.4.1 Background

In 1993, the Author initially proposed that three MPIs that were most critical in the performance-based specification of UGMs (Mundy, 1993 - unpublished specification). The following criteria (see Table 9.1) were postulated for determination of acceptability, or otherwise, of a pavement material:

shear strength classification *(NEW)*, as reported in §5.6, (which embodies both cohesion, c and the angle of shearing resistance, ϕ) where material satisfies the required quality class, depending on layer usage of the material and pavement configuration.
rate of permanent strain, (determined at 3,000th cycle of a 3,000 cycle strain test, by modelling of the permanent strain curve from cycle 101 to cycle 3,000): ➢ strain rate, $d\varepsilon_p/dN \leq 2 \times 10^{-5}$ %/cycle (basecourse class 1) (see §8.4 and §8.6.1) ➢ strain rate, $d\varepsilon_p/dN \leq 5 \times 10^{-5}$ %/cycle (sub-base)
resilient modulus, determined during stress stage test: ➢ min $E_r \geq 350$MPa (basecourse class 1) (see §8.5 and §8.6.1) ➢ min $E_r \geq 240$MPa (sub-base) ➢ min $E_r \geq 175$MPa (fill)

TABLE 9.1: PERFORMANCE-BASED CRITERIA (MUNDY, 1993)

Conditions specified for testing are:

- specimens compacted using two layer static compaction,
- specimen conditions which satisfy the above criteria (performance rather than condition driven). As found in §8.6.1, the materials will generally need to be in a condition of at least DDR ≥ 98% of MDD and RMC ≤ 70% of OMC or Sr ≤ 60%, otherwise they will not be of the necessary quality to suit basecourse layer application,
- stress condition for determination of strain susceptibility was p_{max} = 133kPa and Δq = 250kPa (ie. $\sigma_{1\ max}$ = 300kPa and σ_3 = 50kPa) - the adopted preconditioning stress level,
- stress condition for determination of resilient modulus was p_{max} = 250kPa and Δq = 490kPa (ie. $\sigma_{1\ max}$ = 577kPa and σ_3 = 87kPa) - the adopted stress level from stress stage test appropriate to top of base layer under a thin 35mm dense-mix asphaltic concrete surfacing. For sub-base p_{max} = 105kPa and Δq = 260kPa and fill p_{max} = 50kPa and Δq = 130kPa.

The practical applicability of these specifications will be demonstrated in the case studies presented in Chapter 10.

9.4.2 Introduced Performance-based Specification

To introduce performance-related criteria, Transport SA has recommended in the newly developed "PM2000" specification (Transport SA, 2000) that the criteria should be adopted be in addition to the current empirical requirements for all material types (conventional and alternative). The current empirical parameters include grading, plasticity limits, LA and foreign material content (Department of Road Transport, 1990, summarised in Table 9.2).

"**grading-based**" criteria:
➢ Particle size distribution (grading) upper and lower-bound limits
➢ Liquid Limit limit, Plasticity Index limit, Linear Shrinkage limit
➢ Los Angeles Value limit, Foreign Material limits

TABLE 9.2: GRADING-BASED CRITERIA ("PM 2000" SPECIFICATION)

Where products are being manufactured and supplied under a performance-based specification, the material shall be supplied under *one* product specification, either "grading-based" – conventional specification - (see Table 9.2 for the criteria) or "performance-based" (see Table 9.3).

"**grading-based**" criteria:
➢ As per Table 9.2
angle of shearing resistance, ϕ, (triaxial test):
➢ min $\phi = 45^{o}$ (basecourse class 1, traffic loading > 5million ESAs)
➢ min $\phi = 45^{o}$ (basecourse class 2, traffic loading < 5million ESAs)
➢ min $\phi = 45^{o}$ (sub-base class 1, traffic loading > 5million ESAs)
➢ min $\phi = 40^{o}$ (sub-base class 2, traffic loading < 5million ESAs)
average rate of permanent strain, between the $20{,}000^{th}$ and $50{,}000^{th}$ cycles of a 50,000 cycle strain test. (Note: This is slightly different to the strain rate determined above by the Author which uses a mathematical model to model the "strain history", as illustrated by a strain curve developed over time, and then calculates the tangential strain rate at a specific cycle number)
➢ max average rate of permanent strain = 10^{-8} (basecourse class 1, traffic loading >

5million ESAs) ➢ max average rate of permanent strain = 10^{-7} (basecourse class 2, traffic loading < 5million ESAs) ➢ max average rate of permanent strain = 10^{-7} (sub-base class 1, traffic loading > 5million ESAs) ➢ max average rate of permanent strain = 10^{-6} (sub-base class 2, traffic loading < 5million ESAs)
resilient modulus, determined at the 50,000th cycle ➢ min E_r = 300MPa (basecourse class 1, traffic loading > 5million ESAs) ➢ min E_r = 250MPa (basecourse class 2, traffic loading < 5million ESAs) ➢ min E_r = 250MPa (sub-base class 1, traffic loading > 5million ESAs) ➢ min E_r = 220MPa (sub-base class 2, traffic loading < 5million ESAs)

TABLE 9.3: PERFORMANCE-BASED CRITERIA ("PM 2000" SPECIFICATION)

Since the work of the Author (Mundy, 1993 - unpublished specification), the same MPIs are still considered to be most important to adopt in a performance-based specification used by Transport SA, however, the same stress combination for the determination of both parameters has been utilised in the "PM2000" specification. This stress combination is in fact a higher one with applicability to bituminous spray-seal pavements. The "**performance-based**" conditions *now* specified in the "PM 2000" specification are given below.

Conditions specified for testing are:

- specimens compacted using eight layer dynamic compaction (hammer as described in AS1289 5.2.1),
- specimen conditions of DDR = 98% of MDD and RMC = 80% of OMC,
- stress condition for determination of the MPIs is p_{max} = 329kPa, Δq = 400kPa or $\sigma_{1\ max}$ = 596kPa and σ_3 = 196kPa (adopted stress level from stress stage test appropriate to stress levels at approximately 40mm depth into the top of the upper base layer under a bituminous spray sealed surfacing, refer to Figure 5.7)

Having assessed the newly proposed performance specifications, a number of comments are offered. The stress condition adopted for performance comparison is one of a material element located at 40mm into the top of a base of an unsealed granular pavement. However, vertical stress conditions here are well supported by a high level of confining stress, such that $\sigma_1/\sigma_3 = 3$. However, at slightly lower depths into the layer, the confining stress decreases rapidly. At a depth of 100mm, the stress ratio increases to about 10 (where $\sigma_{1\ max}$ = 420kPa and σ_3 = 40kPa). Thus, strain rates for permanent deformation would be very low for the proposed stress level and deemed 'not typical' for the performance of the layer as a whole. This may lead to a risky assessment based upon a more ideal *in-situ* stress condition, rather than a more conservative one. From the examination of case studies presented in Chapter 10, in which a number have thin surfacings of the order of 35mm, it is apparent that the stress level proposed will not be encountered in those type of pavement configurations.

In the proposed PM2000 specification, the friction angle, ϕ is well specified, however, the cohesion, c is not seen as a requirement or has perhaps been overlooked at this stage. As discussed in §2.3.6, both of these parameters together define the shear strength of a material, as can be seen in Equation 2.5. Further, σ_{1f} and σ_{3f} are related to c and ϕ according to Equation 9.2.

From Eq. 2.5 $\tau_f = c + \sigma_n \tan\phi$

and $$\sigma_n = \frac{1}{2}(\sigma_{1f} + \sigma_{3f}) + \frac{1}{2}(\sigma_{1f} - \sigma_{3f})\cos 2\theta \quad \ldots (9.1)$$

where $\theta = 45 + \frac{\phi}{2}$

thus, $$\sigma_{1f} = \sigma_{3f} \tan^2\left(45 + \frac{\phi}{2}\right) + 2c \tan\left(45 + \frac{\phi}{2}\right) \quad \ldots (9.2)$$

To illustrate the importance of including the cohesion term in the PM2000 specification, an example is given (Example 9.1) of the contribution of this parameter to the major principle failure stress at failure, σ_{1f}, for a level of confining stress which could be expected in the pavement of 30kPa.

EXAMPLE 9.1:

Determine the major principal stress at failure, σ_{1f} for a lateral stress, σ_{3f} of 30kPa and a friction angle, ϕ of 50° and cohesion, c of 58kPa (values obtained with reference to a common material in metropolitan Adelaide, as seen in Figures 2.10 and 2.11 for a DDR = 98% and RMC = 70% of OMC).

From Equation 9.2, substituting the values above gives σ_{1f} = 226 + 319kPa.

Thus, in Equation 9.2, the latter cohesion term contributes to the overall principal stress at failure by a very significant 59% and should not be neglected as a result. Knowledge of both the friction angle *and* cohesion are most important in determining the major principal stress at failure. Calculating the correct values of σ_{1f} and σ_{3f} are essential in determining material quality, and how it should be subsequently used in the pavement, according to the shear strength classification presented in §5.6.

In addition, the values of resilient modulus specified in "PM2000" are considered to be lower than should be for the high stipulated stress level. It has been discussed in §8.5 that satisfactory performance of a basecourse material can be obtained (given attention to other factors) if the magnitude of resilient modulus at the stress point of p_{max} = 250kPa and Δq = 490kPa is considered to be 350MPa. For the materials investigated in §8.5, and illustrated in Appendix 6, this generally corresponds to a material condition of DDR ≅ 98% and RMC ≅ 60% (or Sr ≅ 50 to 60%). If for these same materials one investigates the magnitude of resilient modulus which should be obtained at a stress point of p_{max} = 329kPa and Δq = 400kPa, but at RMC ≅ 80%, it has been found by the Author that the resilient modulus should be specified at 375MPa. It shall be noted that "PM2000" specifies a value of only 300MPa. Failure to specify a high enough level will result in insufficient material stiffness once the layer dries back to its equilibrium moisture level of around 40 to 60% of OMC for local conditions. Discussion with the Author of "PM2000" highlighted that testing a range of materials at the high moisture level of 80% of OMC produced resilient moduli of between 350 to 450MPa during the early stages of the test. However, as

testing proceeded to high cycle numbers (>5,000 to 10,000 cycles) the moduli of the materials, in most cases, decreased with time. It is expected that this is the result of gradual pore pressure build-up and accompanied by a subsequent reduction in effective stress within the material under continuous loading (refer to §2.4.1). This assessment moisture content is very conservative, given local equilibrium levels, and is most likely to lead to the under-specification of performance. A direct consequence of this may well be a decrease in pavement performance – more frequent pavement failures!

9.5 Summary

9.5.1 Field Performance

To 'optimise' the performance of unbound granular materials it is imperative that the pavement layers be 'dried-back' to a relative moisture content (RMC) not exceeding 60% of OMC (50 to 60% of saturation), prior to sealing or application of binder. The moisture content should be determined over the entire thickness of the layer, with samples taken from the top and bottom half. To ensure that the pavement materials are maintained in a low moisture state throughout their service life it is essential that adequate drainage of the road surface and sub-surface be achieved through well-designed systems.

Without adequate side-drains, unwanted water may infiltrate the unbound pavement layers and remain 'locked-in' for long periods of time, as discussed briefly in §2.3.4 and §2.4.1. Where strength and stiffness gain is difficult to achieve in countries of higher rainfall and lower temperatures, either:

- higher grade materials must be used, or
- thicker asphalt surfacing layer(s) or inclusion of a bituminous base layer to lower imparted stresses to the granular materials and, hence, reduce the strong stress to stiffness/strength dependence required

Alternatively, where uncertainty exists surrounding drainage requirements due to climate, terrain/topography, material types and extent of unsealed shoulders, the liberal use (low percentage by mass) of stabilising agents such as cement, lime/cement, foamed bitumen, or other proven additives should be strongly

considered. These products have been found to produce considerable improvement in strength, permanent strain rate and resilient modulus characteristics partially through reducing a material's susceptibility to moisture.

9.5.2 Specifications

Performance-based tests are considered to be a step forward in providing a meaningful assessment tool to better account for environmental and traffic-imposed effects than empirical-based tests. The Chapter presented benefits, such as the previous statement, and dis-benefits such as establishing 'universal' agreement to proposed limit values for the specification parameters. In addition, it was sited that a lack of incentive and action compelling industry to commit to a new specification could possibly result from road authorities not moving down the path of DBFO contracts. Contracts of this type somewhat force contractors to be more conscious of the risks associated with the goal of long-term pavement performance.

The MPIs adopted for the new Transport SA performance-based specification follows the recommendation of the Author, with permanent strain rate, resilient modulus and angle of shearing resistance selected. However, it was recognised that cohesion also must be specified to provide a complete picture of shear strength, in keeping with the classification system presented in §5.6. Without this parameter, material shear strength cannot be assessed which is of concern for thinly surfaced flexible pavements containing unbound granular materials. It is expected that the new Transport SA specification will need to be modified and then trialed for some time to examine the balance of the limits required to be attained with the field performance of the constructed pavement. Chapter 10 investigates the performance criteria limits specified by the Author (§9.3.1) in further detail, by examining the performance of a number of in-service pavements, to determine their suitability as an assessment tool.

CHAPTER 10
VALIDATION OF THEORETICAL ASSESSMENT APPROACH WITH FIELD PERFORMANCE

10.1 Introduction

A number of case studies will be discussed to highlight the merits of functional-type performance testing to characterise constituent pavement materials according to their field state and stress range conditions. Each study has been researched in terms of scientific testing to diagnose the 'cause of the failure' or produce evidence for successful performance. All studies are well supported by detailed field pavement evaluations and performance assessment.

10.2 Kwinana Freeway and Reid Highway (Western Australia)

10.2.1 Pavement History

The Kwinana Freeway was constructed in 1991. During 1992, concerns were raised regarding the suitability and performance of the crushed rock base material used following high curvature values measured during a deflection survey. The section surveyed was between South Street to the north and Forrest Road (Ch 18.83km) to the south (in the main south of Farrington Road), in the Perth Metropolitan area (Cray, 1992). This was the first test site where curvatures were found to exceed the design value. Other latter constructed pavement sections of the Kwinana Freeway in 1994 to the south of Forrest Road (Ch 18.83km), connecting to Thomas Road (Ch 30.46km), have also proved to be performing poorly with pavement failures occurring shortly after opening to traffic (Goh, 1994).

The material used predominantly as the crushed rock base on the Kwinana Freeway south of Farrington Road was a 20mm granitic material from the Boral company's 'Gosnell' quarry.

A section of the Reid Highway, between Ch 9.8km and 10.0km just west of Mirrabooka Avenue also used this material.

Other sections on both the Kwinana Freeway, between Forrest Road (Ch 18.83km) and Thomas Road (Ch 30.46km), also on the Reid Highway, both used a 20mm granitic material from the Pioneer Byford quarry in Armadale. These pavements have proved to possess slightly better performance with curvature values only slightly exceeding the design requirement. The limestone sub-base material was taken from Italias quarry.

The pavements for both the Kwinana Freeway and another road of interest, the Reid Highway, were of the flexible unbound granular type. The pavement configuration, used for both construction works undertaken in approximately 1991, was as shown in Figure 10.1.

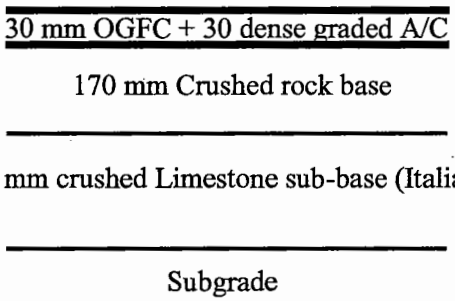

FIGURE 10.1: PAVEMENT CONFIGURATION FOR KWINANA FREEWAY & REID HIGHWAY

10.2.2 Design Requirements

The predicted ten-year design traffic loading of ESAs, N_{10}, was given by Main Roads Department, Western Australia as:

$$N_{10} = 8.0 \times 10^7 \text{ ESAs}$$

The corresponding design deflections and curvature values were determined to be:

$$D_o = 0.82\text{mm} \qquad D_0\text{-}D_{200} = 0.08\text{mm}$$

based on Austroads Design Guide Figures 10.3 and 10.4, respectively (Austroads, 1992).

10.2.3 Field Assessment

Concern was raised by the Main Roads Department – Western Australia with regard to the quality of the materials, which purportedly conformed to empirical

specifications (refer to §10.2.4). A deflectograph survey was performed to assess the Kwinana Freeway constructed of the Boral Gosnell Quarry and Italias materials. It was found that although the maximum deflections were within the design limit, the curvature function values were greater than twice the design curvature, suggesting a possible weakness in the pavement materials. Field deflection curvature function test results suggested poor pavement performance possibly due to:

- high moisture contents within the basecourse layer
- marginal quality basecourse materials which are moisture sensitive

Typical measured values of deflection and curvature for the southbound left lane of the Kwinana Freeway, between Chainage 14.25 to 14.63km were:

D_o = 0.54mm (OWP), 0.49mm (IWP), maximum = 0.60mm, CV = 7.8%
D_0-D_{200} = 0.19mm (OWP), 0.19mm (IWP), maximum = 0.26mm, CV = 16.5%

where OWP = outer wheel path and IWP = inner wheel path
and CV = coefficient of variation

10.2.4 Materials Testing

The unbound granular materials used for the constructed sections of the Kwinana Freeway and Reid Highway were derived from three separate quarries. The Boral Gosnell Quarry and the Pioneer Byford Quarry products, used as basecourse materials, are located 30km apart and utilise a geological granitic material formation. The Italias limestone, used as a sub-base material, is from a more remote quarry source.

Empirical Classification Testing

The classification test results from materials retrieved from test pits dug in the in-service pavements are given in Table 10.1. A comparison of test results is made with the "Technical Specification For Pavement Thicknesses and Crushed Rock Base" (Goh, 1994 – Appendix A).

Road	Material	Sample No.	PI (%)	LL (%)	LS (%)	LA (%)	FI (%)
Kwinana Freeway, south of Farrington Rd	Boral Gosnell	93M760	7.1	21.9	1.6	N/A	N/A
Reid Highway, west of Mirrabooka Ave	Boral Gosnell	93M701	7.4	21.8	2.4	N/A	31.9
Kwinana Freeway, Forrest Rd – Thomas Rd	Pioneer Byford	94M612	12.2	28.1	3.6	N/A	
		94M608	12.3	27.9	3.1	N/A	
LIMITS			None	25	> 1 < 3	40	35

TABLE 10.1: LABORATORY CLASSIFICATION TEST RESULTS FOR BASECOURSE MATERIAL

N/A = not available, but reported to be within specification

The Boral Gosnell material is within empirical specification limits at both pavement sites in which it was used, whilst the slightly better performing material, the Pioneer Byford product, is slightly out of specification. Comparing these specification limits with those used in South Australia (refer to Table 8.2), the LA value tolerated in Western Australia is much higher than for South Australia, being 40 compared to 30. In addition, no limit is specified for the plasticity index, compared to a value of 6 allowed in South Australia. All results in Table 10.1 exceed this value, but not by much for the two poorly performing pavements. So a dilemma exists for the materials assessed using this type of empirical specification, as their low-level of laboratory performance can not be clearly identified with pavement performance.

Repeated Load Triaxial Testing

At the request of the WA Main Roads Metropolitan Operations, a project was initiated in 1992 to assess the performance of these granular materials using deflection surveys on old and new works and to correlate the field performance with the repeated load key MPIs of resilient modulus and permanent strain. Resilient modulus testing was performed by DRT-SA in 1992, under the direction of the Author, who devised a testing program to highlight material performance issues. This type of testing provided information on the materials performance that was not pronounced by the classification test results for the two basecourse materials.

The stress levels adopted for testing were modelled upon those expected at the midheight of each basecourse sub-layer, with the pavement configuration as represented in §10.2.1. Sub-layer thicknesses adopted were 50mm, 50mm and

70mm, respectively, to account for non-linearity, in keeping with the discussion presented in §5.4.1. The vertical stresses applied to the different specimens of material were determined using the stress estimation charts (similar to those examples presented in Chapter 5) with conditions applicable to the "worst-case" material, the Boral Gosnell crushed rock product. Checks were also made by creating a mechanistic model of the pavement and analysing it using the program NONCIRL, a non-linear version of Australian linear-elastic computer program CIRCLY (Wardle, 2000). It should be noted that only the key performance indicators (strain rate and resilient modulus) are reported here for the stress combinations at the midheight of the top sub-layer (Table 10.2).

Product	DDR (%)	RMC (%)	$\sigma_{1\,max}$ (kPa)	σ_3 (kPa)	E_r (MPa) stress stage	Strain Rate at 15, 000 cycles $\frac{d\varepsilon_{1p}}{dN} \times 10^{-5}$	Max. ε_{1p} (%) at 15, 000 cycles
Boral Gosnell	98.0	78.5	285	28	182	10.3	4.70
	97.9	76.9	285	28	173	6.26	3.49
Pioneer Byford	97.4	82.5	285	28	220	0.60	0.87
	97.9	77.2	285	28	182	0.45	0.83
Italias	94.0	90.4	100	15	164	0.44	0.60
	94.2	88.7	105	10	118 *	13.7 *	3.08 *

TABLE 10.2: STRAIN AND RESILIENT MODULUS CHARACTERISTICS OF THE KWINANA FREEWAY AND REID HIGHWAY MATERIALS (TESTED IN DUPLICATE)

* stress levels lay just outside the elastic region as defined by the Mohr-Coulomb failure envelope. Thus, a failure condition exists.

If stress conditions were determined appropriate to those of each basecourse material, then direct comparison of the products would not be possible as stress is influenced by the stiffness of the sub-layer of material. From the example in Appendix 1, the vertical stress variation, $\Delta\sigma_{1\,max}$, was up to a maximum of 6.5% at the top of the base layer. In addition, the lateral stress will also vary depending on the stiffness and shear strength of the material, as discussed in §5.3. The materials were tested at their "in-service" conditions within the constructed pavement layers.

Boral Gosnell Crushed Rock - DDR = 98%, RMC = 80%

Pioneer Byford Crushed Rock - DDR = 98%, RMC = 80%

Italias Limestone - DDR = 94%, RMC = 100%

The permanent strain analysis clearly indicated the strain susceptibility of the Boral Gosnell product as compared to its Pioneer Byford counterpart when tested under the same stress regime. The Boral Gosnell product is very prone to plastic straining even at the tested moisture content, which is only 75% of optimum. The performance of this product would have been improved by sealing when the pavement materials were 60% dry of optimum (a condition requested in the compaction of pavement materials at TSA -SA), see §9.2. This recommendation to MRD-WA has now become a condition within their Contract documentation.

The Italias product was found to undergo high permanent strain rates when tested at stress levels just outside the elastic region where failure occurred (σ_1 = 105kPa, σ_3 = 10kPa). However, when tested within the elastic region (σ_1 = 100kPa, σ_3 = 15kPa) the material performed well, with very low strain rates recorded. It should be noted that this material was compacted at only 94% of the maximum dry density and at a high moisture content. This does not allow a direct performance comparison of its results with those of the basecourse materials, but does support the method of performance assessment. The particle size distribution of the Italias material indicated a very high proportion of fine material, which would tend to hold moisture, limit drainage, and cause plastic deformation under an applied load when tested near failure stresses.

Static Triaxial Testing

Drained, static triaxial testing was performed on each material to determine the material properties of cohesion and angle of shearing resistance (Table 10.3).

Product (Conditions)	Cohesion (kPa)	Angle of Shearing Resistance (deg)
Boral Gosnell (DDR=97.9%, RMC=73.8%)	20	50
Pioneer Byford (DDR=97.6%, RMC=78.9%)	40	47
Italias (DDR=93.8%, RMC=90.4%)	5	44

TABLE 10.3: PROPERTIES OF THE KWINANA FREEWAY AND REID HIGHWAY MATERIALS

In addition, static triaxial testing was to investigate how the materials 'rank' according to the newly proposed shear strength classification system, designed for material usage under a 40mm asphalt surfacing or less (refer to §5.6.2). In this case, the thickness of the surfacing is 60mm so some additional interpretation is necessary (refer to §5.6.3). The quality of the material, as illustrated by its ranking in the classification system, is given in Figure 10.2.

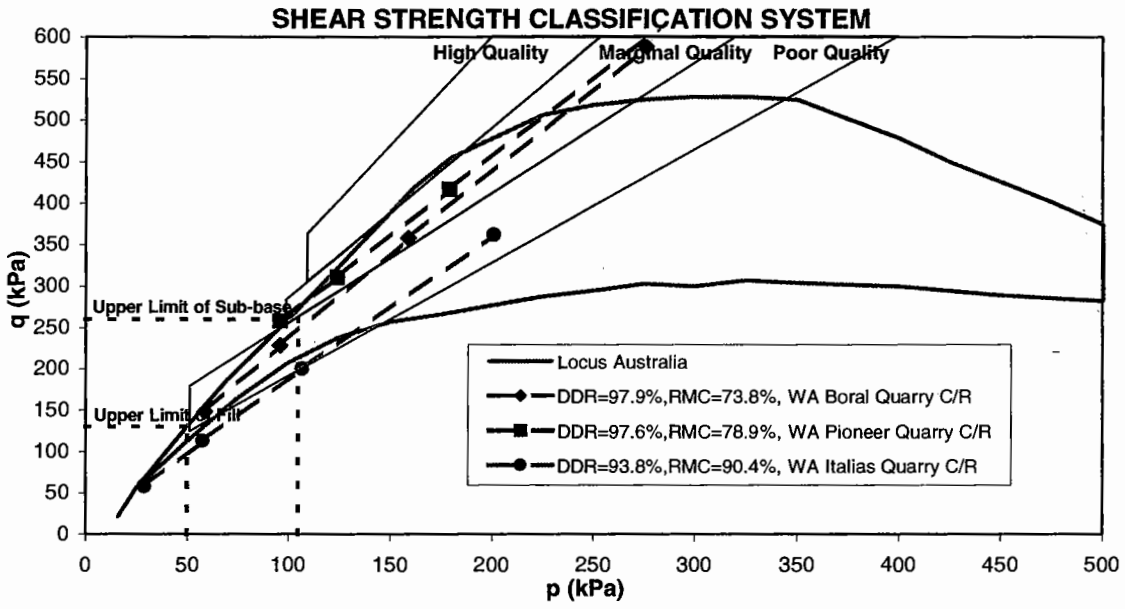

FIGURE 10.2: SHEAR STRENGTH CLASSIFICATION SYSTEM FOR THE KWINANA FREEWAY AND REID HIGHWAY MATERIALS

Due to the positions of the three different material shear strength envelopes, the following conclusions can be drawn:

- if the materials were to be used for thin surfacing applications (less than approximately a 40mm asphaltic concrete surfacing), their class would be:
  - Boral Gosnell material – very low-level, marginal quality and upper-level poor quality to use as a sub-base located at a reasonable depth or fill material.
  - Pioneer Byford material - mid-level, marginal quality to use for a sub-base material. The material is expected to border on low-level high quality if moisture level *in-situ* was reduced to approximately RMC = 60% of OMC.

- Italias material - very low-level, poor quality to use for a fill material if density was increased to DDR = 96%. It should be noted that this material is expected to improve greatly in strength with increasing density and by a natural cementing action, typical of many limestone materials, which develops with time.

Given that these materials were used for the construction of the Kwinana Freeway and Reid Highway, *which have thicker surfacings of 60mm A/C*, the layer application stress boundaries can shift, although their class is of-course unchanged. If the failure envelope for each material is compared to the expected stress path computed for the granular materials in the pavement, beneath the 60mm surfacing (refer to Figure 10.3), the Pioneer Byford material is expected to be marginally acceptable as a basecourse. On the other hand, the Boral Gosnell material will undergo failure according to this stress path since the envelope, which depicts its shear strength, crosses the expected stress path (refer to Figure 10.3). This material is not considered satisfactory for use as a basecourse layer.

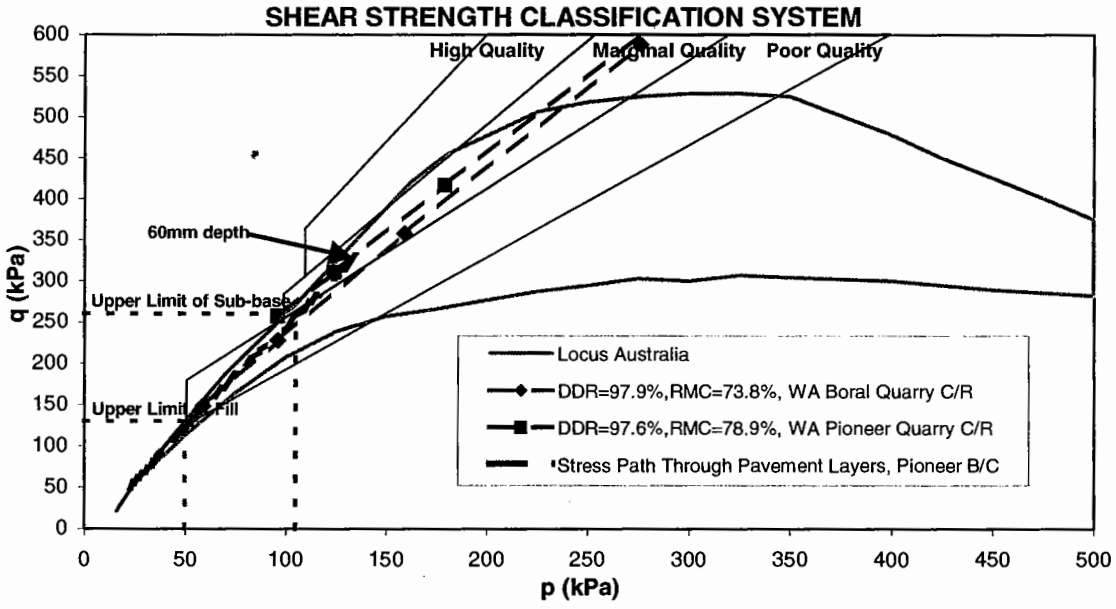

FIGURE 10.3: FAILURE ENVELOPES FOR THE BORAL GOSNELL AND PIONEER BYFORD MATERIALS COMPARED WITH THE COMPUTED STRESS PATH THROUGH THE PAVEMENT GRANULAR LAYERS

Follow-up Testing

Some 7 months following the above investigation of the pavement failure associated with the Boral Gosnell material, this product was modified by blending the original parent material size of approximately +4.75mm with a new source of fine material to improve the performance characteristics of the material. The 'Original' Boral Gosnell material (used in the failed Kwinana Freeway, south of Farrington Road) reportedly had a plasticity index of 7.1% (Table 10.1), which is considered high for a basecourse material, compared to the 'New' material which was found to be non-plastic. With reference to Table 10.4, the following results were obtained.

Product	DDR (%)	RMC (%)	$\sigma_{1\,max}$ (kPa)	σ_3 (kPa)	E_r (MPa) stress stage	Strain Rate at 15, 000 cycles $\frac{d\varepsilon_{1p}}{dN} \times 10^{-5}$	Max. ε_{1p} (%) at 15, 000 cycles
'Orig.' Boral Gosnell *	98.0	78.5	285	28	182	10.3	4.70
'Orig.' Boral Gosnell *	97.9	76.9	285	28	173	6.26	3.49
'New' Boral Gosnell	97.5	77.8	285	28	187	2.37	2.52

TABLE 10.4: COMPARISON BETWEEN STRAIN AND RESILIENT MODULUS CHARACTERISTICS OF THE 'ORIGINAL' AND 'NEW' BORAL GOSNELL PRODUCTS

* results as per Table 10.1.

The permanent strain analysis indicates that the 'New' Boral Gosnell product has an improved strain rate response compared to the 'Original' Boral Gosnell product, but which is still considered marginally too high for this stress condition. The resilient modulus has only very marginally increased. The static triaxial results (see Table 10.5) showed improvement in the cohesion value of the new product.

Product (Conditions)	Cohesion (kPa)	Angle of Shearing Resistance (deg)
'Orig.' Boral Gosnell (DDR=97.9%, RMC=73.8%)	20	50
'New' Boral Gosnell (DDR=96.8%, RMC=80.8%)	38	51

TABLE 10.5: PROPERTIES OF THE 'ORIGINAL' AND 'NEW' BORAL GOSNELL MATERIALS

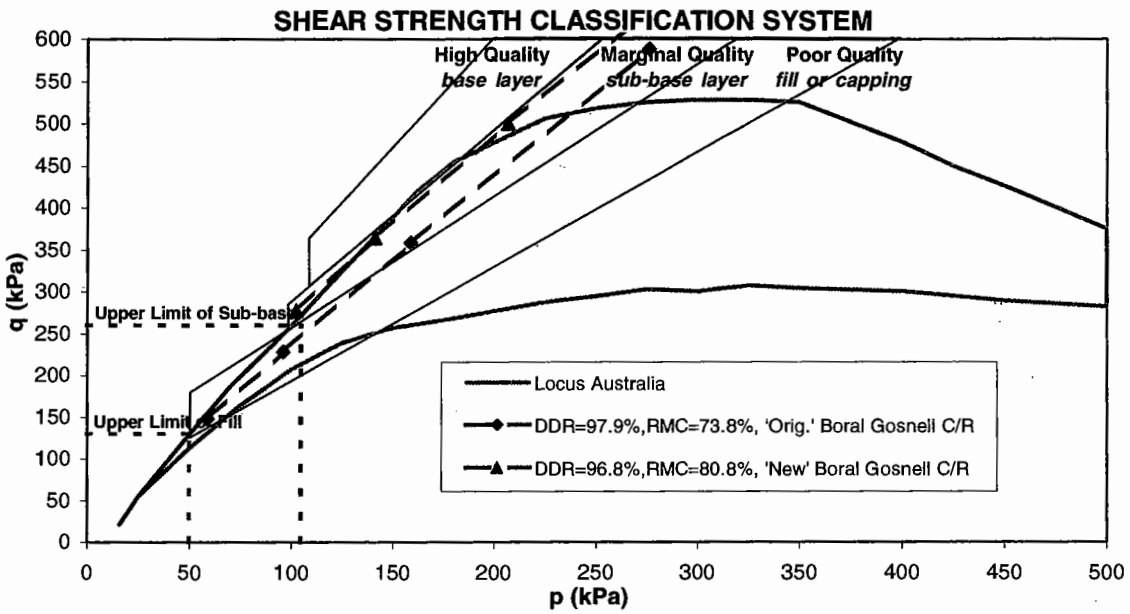

FIGURE 10.4: SHEAR STRENGTH CLASSIFICATION SYSTEM FOR 'ORIG' AND 'NEW' STOCKPILE BORAL GOSNELL QUARRY MATERIALS

Again, comparing how the 'Original' and 'New' Boral Gosnell materials compare according to the newly proposed shear strength classification system, designed for material usage under a 40mm asphalt surfacing or less, refer to Figure 10.4.

Due to the position of the shear strength envelope of the 'New' Boral product, the following conclusion is drawn:

- if the materials were to be used for thin surfacing applications (less than approximately a 40mm asphaltic concrete surfacing), its class would be:
  - 'New' Boral material – high-level, marginal quality for use as a sub-base. The material is expected to border on low-level, high quality if the moisture level *in-situ* was reduced to approximately RMC = 60% of OMC.

This new material shows satisfactory resistance to shear failure as a basecourse material under a 60mm surfacing. However, it must be remembered that the permanent strain rate was still quite high which adds some risk to its use as a basecourse material.

10.2.5 Pavement Evaluation and Rehabilitation

Acceptable deflections and lack of significant deformation indicates the pavement possessed adequate thickness to prevent subgrade failure. However, high curvature values compared to that of the design value, indicate poor stiffness within the upper granular layers. Treatment was to plane off the asphalt layers and dig out the crushed rock base and replace it with bitumen stabilised limestone basecourse compacted to DDR = 98% and dried back to a moisture content of 85% of OMC. This high moisture content could be tolerated given that the bitumen stabilised material is much less moisture sensitive than crushed limestone and has superior strain rate properties (four times lower) and resilient modulus (30 to 60% higher, depending on RMC) properties (Butkus and Goh, 1997, §5.2.4).

10.2.6 Summary

The testing program performed, as described in summary in §10.2.4, led to the following actions being undertaken by Main Roads, Western Australia, namely:

- a comprehensive materials characterisation program was performed by the Author and others on a range of raw and blended materials using the approach described.
- Main Roads, Western Australia, purchased a repeated load triaxial system (refer to §6.2.1) to perform further testing of materials (Butkus, 1994 and 1997). The Author has used these results to correlate field deflection-measured performance with laboratory assessed performance.
- Main Roads, Western Australia conducted repeated load triaxial performance testing on materials taken from five highway/freeway locations and concurrently measured deflection/curvature values at these sites. A correlation of two key MPIs, permanent strain rate and resilient modulus with measured deflection/curvature, has been undertaken by the Author to investigate the relationships using "real" data (see Figures 10.6 and 10.7). Correlations for both the inner and outer wheel paths are shown.

  Curvature function, determined from a deflection bowl which results from a load applied to the pavement surface, is defined in the Austroads Pavement Design Guide (1992), with reference to Figure 10.5 below.

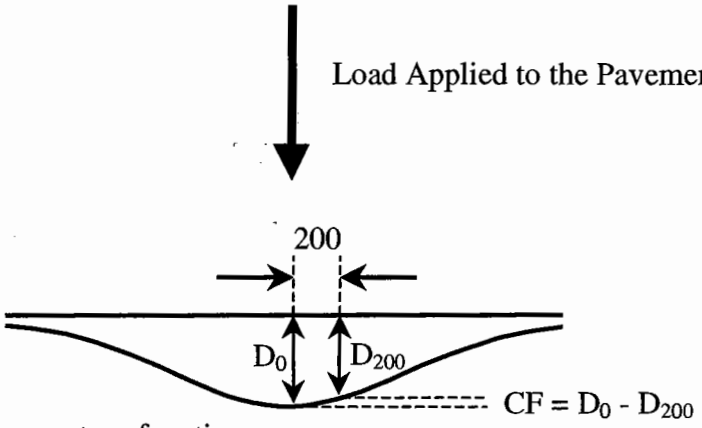

where CF is the curvature function

D_0 = central deflection of the bowl

D_{200} = is the deflection measured at 200mm perpendicular to the centre of the deflection bowl

FIGURE 10.5: CURVATURE FUNCTION

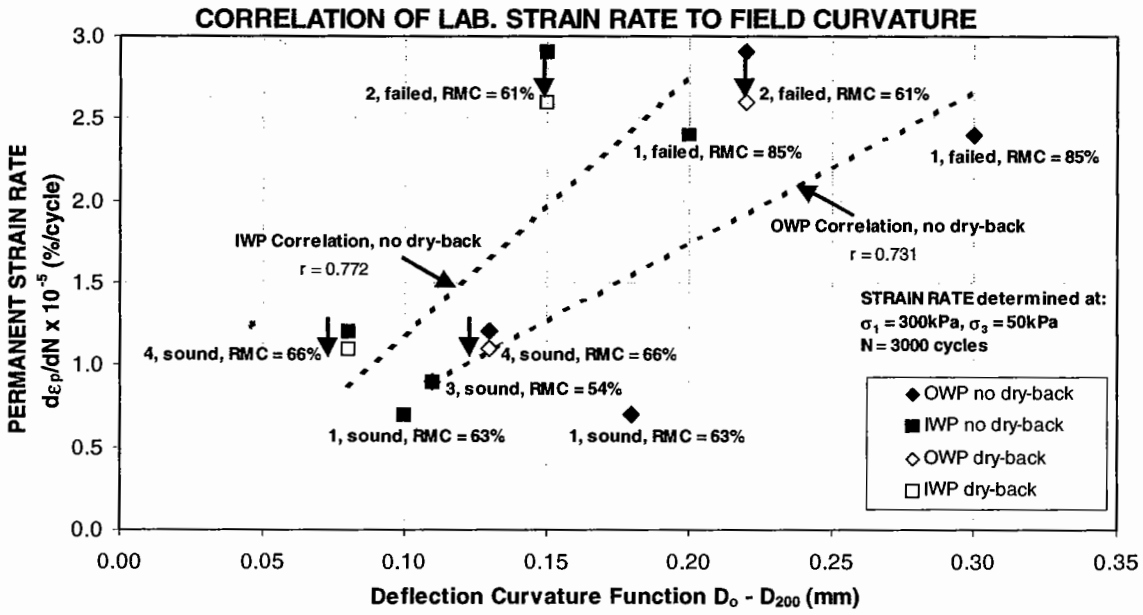

FIGURE 10.6: CORRELATION OF LABORATORY DETERMINED PERMANENT STRAIN RATE PARAMETER WITH FIELD DEFLECTION CURVATURE FUNCTION VALUES (FROM SURVEYS OF FOUR WA FREEWAY/HIGHWAY ROADS)

OWP = outer wheel path, IWP = inner wheel path

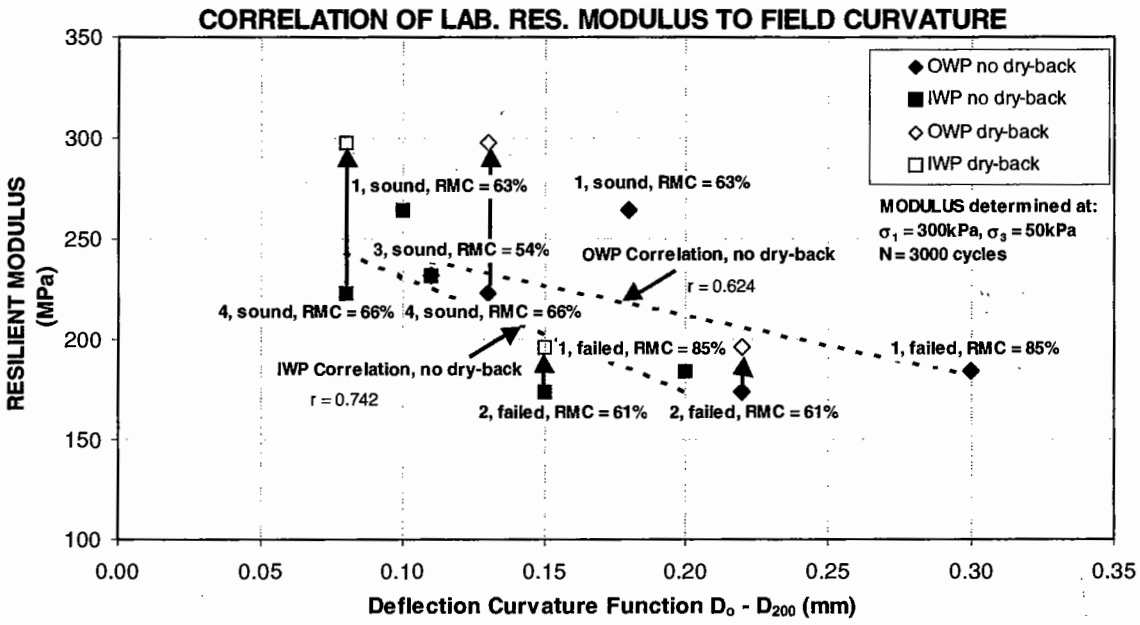

FIGURE 10.7: CORRELATION OF LABORATORY DETERMINED RESILIENT MODULUS WITH FIELD DEFLECTION CURVATURE FUNCTION VALUES (FROM SURVEYS OF FOUR WA FREEWAY/HIGHWAY ROADS)

OWP = outer wheel path, IWP = inner wheel path

It can be seen from these results that laboratory-determined permanent strain rate shows a strong increase, and resilient modulus a decrease, as the field-measured curvature function increases (refer to Figures 10.6 and 10.7). In addition, it can be observed that "dry-back" of the material acts to further improve laboratory-determined performance, however, the corresponding field measured curvature values were not determined by Main Roads Western Australia.

It was hoped to gain an appreciation of the critical upper limit on permanent strain rate, which might be specified, by examining the correlation with curvature function, given the design curvature. This is discussed below.

The results presented in Figure 10.6 and 10.7 illustrate that a reasonable correlation does exist between permanent strain rate and curvature function and it is dependent on whether the measurements are taken within the inner or outer wheel path. Generally, the outer wheel path materials can be found to be in a higher moisture state due to the ingress of water from the pavement shoulders. In

addition, the materials can be less compacted in the outer wheel path due to less material confinement provided by the shoulders.

To consider this further, Figure 10.6 is reproduced with a 'LIMIT ZONE' added (see Figure 10.8). This zone represents a region in which a potential critical level of permanent strain rate is considered to exist. A strain rate above this range has resulted in non-performing materials both in the field (as assessed by curvature function) and in the laboratory (as assessed by permanent strain rate). With reference to Figure 10.8, the critical permanent strain rate has been set at $d\varepsilon_{1p}/dN = 2 \times 10^{-5}$ %/cycle for basecourse layer materials, which corresponds to a deflection curvature ($D_0 - D_{200}$) of approximately 0.15mm.

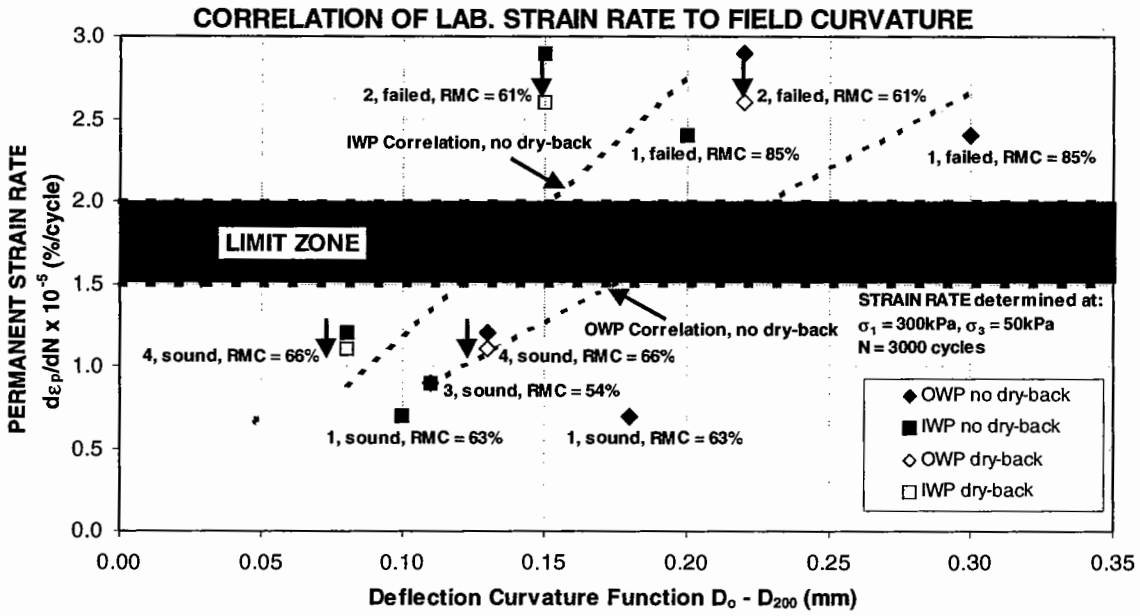

FIGURE 10.8: PERMANENT STRAIN RATE VS DEFLECTION CURVATURE FUNCTION – A LIMIT ZONE IN WHICH A CRITICAL STRAIN RATE EXISTS

A report by Butkus (1994) concluded that: "when tested using the UMATTA (a specific make of RLT), all Metropolitan CRB (crushed road base) products show a marked improvement in resilient modulus and permanent strain as moisture is reduced. This moisture sensitivity has not been recognised in the past". "The practical effect of this improvement on field performance was demonstrated by the drastic reduction in deflection and curvature as field moisture was reduced".

> Further, it is concluded that "poor pavement performance of CRB, which can be predicted by high deflection and curvature values, invariably appears to be associated with field moisture values above 60% RMC. If the CRB cannot be maintained at less than 60% RMC then it should not be used." The report then states "It has been shown that moisture remains in a pavement for very long periods and it is therefore considered essential that the CRB is dried back prior to sealing. The entire CRB layer thickness should be drier back to below 60% RMC. A mean layer moisture content of 60% RMC which incorporates a wetter CRB sub-layer may not be adequate".

These outcomes, which are derived from the Author's initial testing work, with the consequences of material field moisture sensitivity summarise in §9.2. The key points are reinforced by subsequent testing at Main Roads WA and serve to illustrate the substantial practical impact of this work upon the business activities of a State road authority. It shall be noted that the empirical classification test results did not provide any conclusive information highlighting material performance or otherwise. In particular, the dramatic pavement failure associated with the Kwinana Freeway south of Farrington Road was not detected through traditional testing methods, due to the Boral Gosnell material's compliance with specifications. In comparison, the performance based testing, coupled with field deflection testing, has delivered quite specific scientific findings.

10.3 Kings Road (South Australia)

10.3.1 Pavement History

In 1994, Kings Road between the Salisbury Highway (maintenance marker - MM3.52km) to Cross Keys Road (MM4.69km) was upgraded to provide one additional lane (hence two lanes) in each direction (Figure 10.9).

Road layout:

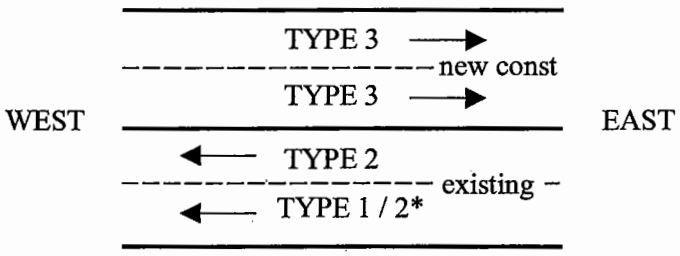

FIGURE 10.9: ROAD LAYOUT FOR KINGS ROAD

* between 145m east of the railway crossing and Cross Keys Road

This was achieved by the construction of an 'upside-down' pavement as the eastbound carriageway (see Figure 10.10B), with the original pavement retained on the westbound carriageway which was an 'upside-down' pavement along the outer lane between Salisbury Highway and a point 145m east of the railway crossing. Elsewhere the pavement was unbound granular (see Figure 10.10A). Pavement distress along this road became severe in 1997-1998, after nearly four years of service. As a result, an investigation was conducted to determine the cause of failure and determine its rehabilitation (Poli, 1999)

The pavement configurations were:

existing 'upside-down' pavement (TYPE 1) (westbound carriageway - outer lane) of new road between Salisbury Highway and a point 145m east of the railway crossing

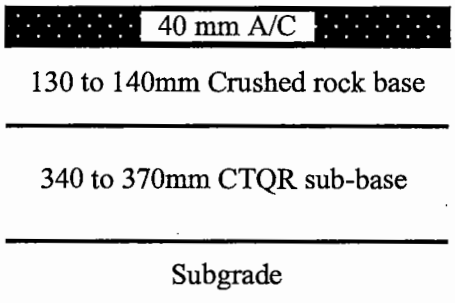

existing granular pavement (TYPE 2)
(westbound carriageway - inner lane) of new road
(westbound carriageway - outer lane) of new road
between point 145m east of railway crossing to
Cross Keys Rd

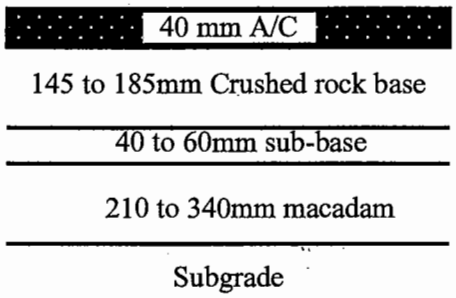

FIGURE 10.10A: PAVEMENT CONFIGURATIONS FOR THE WESTBOUND CARRIAGEWAY OF KINGS RD

It should be noted that the entire westbound carriageway was levelled with a granular overlay, prior to sealing with a thin (40mm) asphaltic concrete surfacing.

new construction upside-down pavement (TYPE 3)
(eastbound carriageway)

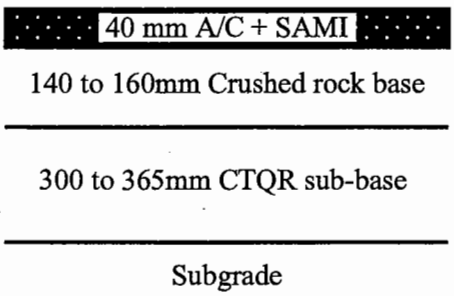

FIGURE 10.10B: PAVEMENT CONFIGURATION FOR THE EASTBOUND CARRIAGEWAY OF KINGS RD

The terrain in the vicinity of the roadworks is very flat. It was reported by staff associated with the construction works at the time that the verges of the pavement often contained large sheets of ponded water, unable to drain away. No deep side-drains were installed along the length of the pavement to trap the water which could, therefore, permeate through into the unbound granular layer from the verges. In addition, the wide median constructed to separate the two carriageways was of unbound granular material with no moisture barrier placed to prevent the ingress of water during periods of rainfall. Thus, moisture entry post construction is seen as a significant problem. The construction staff did consider that adequate dry-back of the UGMs occurred prior to placement of the dense mix asphalt concrete wearing course layer.

The design recommendation in 1992 was for either a fully bound composite pavement comprising a 135mm A/C and 275mm CTQR, including a SAMI. The lower cost option, but higher risk alternative 'upside-down' pavement comprising a 35mm A/C, 150mm quartzite C/R base and 300mm CTQR sub-base upon a sandy clay subgrade (E = 50MPa) was adopted for construction, which occurred in 1994. Design calculations pre and post construction used the AUSTROADS modular ratio approach (refer to §3.6.1) with an "$E_{top\ of\ base}$" = 350MPa being assumed.

10.3.2 Design Requirements

The design traffic loading was based on a 1997 AADT of approximately 13,650 vehicles / day with 6.2% (westbound) and 5.8% (eastbound) commercial vehicles and a growth rate of 9% (west) and 6% (east), with 1.6 ESAs / commercial vehicle: -

this provides a predicted 10 year traffic loading of ESAs, N_{10}, of:

$$N_{10} = 3.6 \times 10^6 \text{ (westbound) and } N_{10} = 2.8 \times 10^6 \text{ (eastbound)}$$

Design deflections and curvature values were dependent on the pavement configuration (based on Austroads Pavement Design Guide Figures 10.3 and 10.4, respectively, Austroads, 1992). The values determined were:

Eastbound	Inner*	$D_o = 0.44$mm	D_0-$D_{200} = 0.14$mm
	Outer	$D_o = 0.40$mm	D_0-$D_{200} = 0.12$mm
Westbound	Inner	$D_o = 0.90$mm	D_0-$D_{200} = 0.14$mm
	Outer	$D_o = 0.40$mm (w)/0.85mm (e)	D_0-$D_{200} = 0.12$mm

where (w/e) = west/east of rail crossing

10.3.3 Field Assessment

A visual assessment of the pavement's surface, undertaken in November 1998, showed fatigue of the asphaltic concrete was the main form of distress affecting approximately 35% of the surface (after a 4 year life). Crazing of the surface was very severe along the entire outer granular westbound lane (Type 2 pavement) at MM4.62, 4.69km (between Cross Keys Road and the railway crossing) and at least 50% of the adjacent inner lane (Type 2 pavement) (see Figure 10.11).

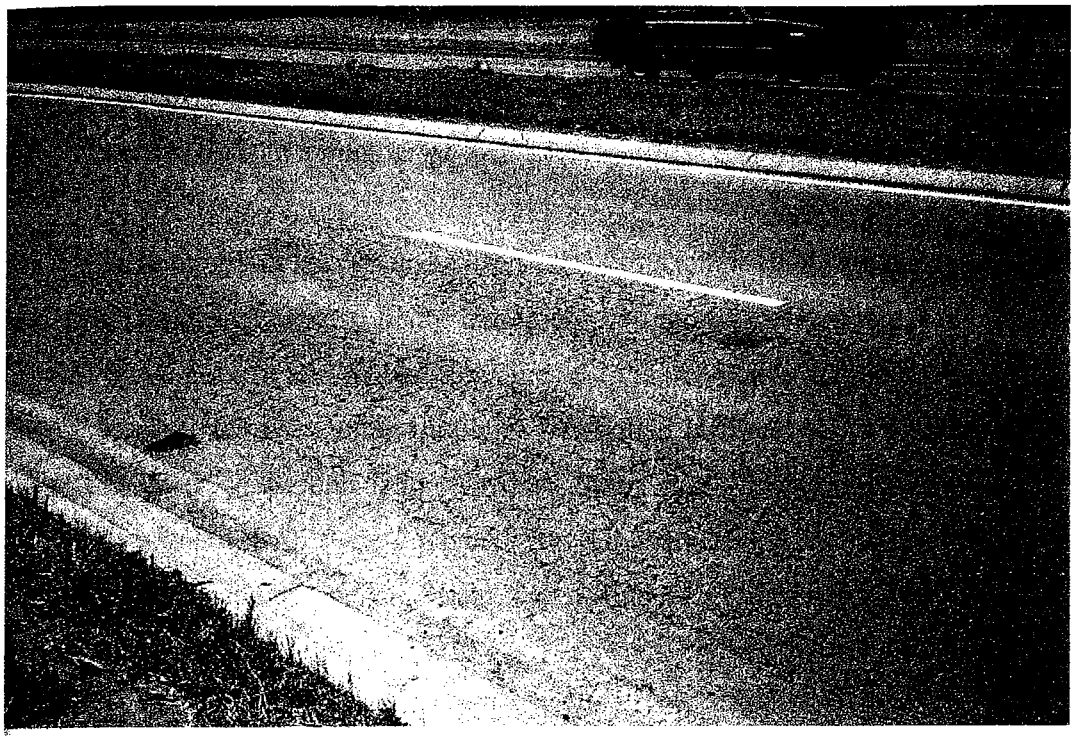

FIGURE 10.11: CRAZING OF SURFACING (CH. 1.1KM, WESTBOUND CW, OUTER LANE – TYPE 2 PAVEMENT)

FIGURE 10.12: CRAZING AND PUMPING OF BASECOURSE FINES (CH. 950M, EASTBOUND CW, OUTER LANE - TYPE 3 PAVEMENT)

In addition, the new eastbound carriageway outer lane (Type 3 pavement) displayed areas of severe crazing at two locations, MM3.88km and 4.25km, with pumping of the basecourse fines in a number of locations (see Figure 10.12).

From a deflectograph survey conducted on 28th October 1998, all deflections were less than the design values, being extremely low along the eastbound carriageway (upside-down pavement). Curvature values for the unbound granular pavement were double the design values along the inner westbound lane and triple the design value along the outer westbound lane (between 145m east of the railway crossing and Cross Keys Road), both Type 2 pavements. All characteristic curvature values were less than the design value all along the upside-down pavement (Type 1 and 3 pavements).

10.3.4 Materials Testing

The unbound granular material is a 20mm crushed rock quartzite originally sourced from the Boral Para Hills quarry for the construction of the Kings Road pavement. The material tested has been subsequently retrieved from several test pits dug into failed sections of the pavement on both the east and west carriageways.

Empirical Classification Testing

A comparison of test results (presented in Table 10.6) is made with the "Standard Specification for Supply and Delivery of Pavement Material" (Department of Road Transport, 1990).

From Atterberg Limits testing, the material was found to have a plasticity index of between 2 and 7% (averaging 6%) which is bordering on the tolerance of acceptance for a basecourse material. All other results were well within specification limits. It should be noted that the Boral Para Hills material tested under the characterisation program discussed in Chapters 7 and 8, was found to have a plasticity of only 4%.

Carriageway		Test Pit No.	PI (%)	LL (%)	LS (%)	LA (%)
East		TP1-4	5 - 7	18 - 22	1 - 3	N/T
West	Type 1 – outer lane	TP9	7	24	2	N/T
West	Type 2 – inner lane	TP5-8	2 - 7	19 - 23	1.5 - 3	N/T
LIMITS			**6**	**25**	**3**	**30**

TABLE 10.6: LABORATORY CLASSIFICATION TEST RESULTS FOR BASECOURSE MATERIAL

N/T = not test but reported to be within specification

In addition, modified Proctor compaction testing provided the following results:

$$OMC = 6.5\%, MDD = 2070kg/m^3$$

Repeated Load Triaxial Testing

Resilient modulus testing was performed to determine the materials' strain characteristics (both resilient and permanent) under one or a number of imposed stress conditions.

The permanent strain analysis for the material, illustrated in Figure 10.13, highlights the low level of susceptibility to moisture of the material's strain response (at DDR = 98.7%) and preconditioning stress conditions of $\sigma_{1\ max}$ = 300kPa and σ_3 = 50kPa.

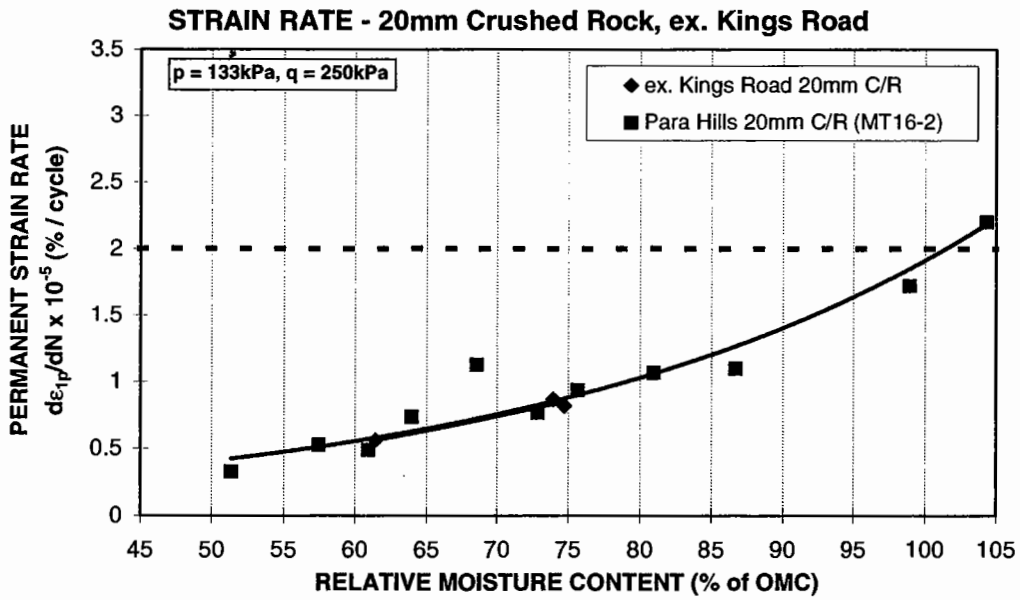

FIGURE 10.13: STRAIN RATE CHARACTERISTICS OF THE KINGS ROAD MATERIAL

The strain rate developed is considered to be very low at both RMC levels tested, namely 62% and 74%, where $d\varepsilon_p/dN$ = 0.53 and 0.84 × 10^{-5} %/cycle (average), respectively. These values are virtually identical to those found from testing as part of the materials characterisation program described in Chapter 8. The 'similar' product, a Boral Para Hills C/R sampled in August 1990, but with a plasticity index of 4% (compared to the Kings Road material of 2 to 7% - 6% average), was found to show the same strain characteristics (as illustrated in Figure 10.13).

The stress levels adopted for resilient modulus determination followed the stress path sequence as presented in Figure 5.13. A graph of the variation of resilient modulus with moisture content (Figure 10.14) is illustrate for the stress condition at the top of the basecourse layer under a 35mm asphalt surfacing ($\sigma_{1\ max}$ = 577kPa, σ_3 = 87kPa), which is appropriate for the constructed pavement configuration of Kings Road.

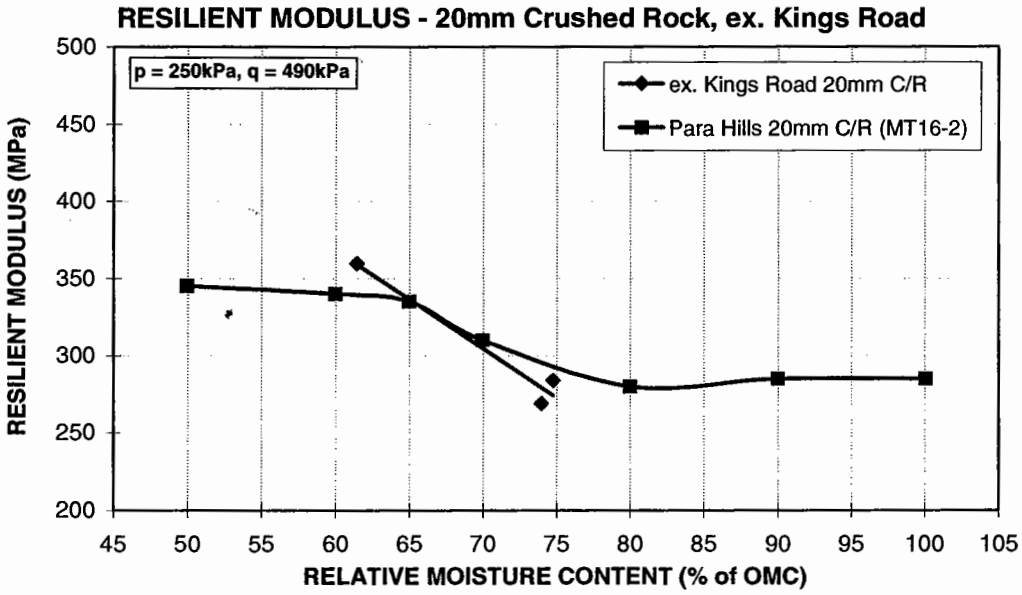

FIGURE 10.14: RESILIENT MODULUS CHARACTERISTICS OF THE KINGS ROAD MATERIAL

The level of stiffness developed is considered to be very low at a moisture level of RMC = 74%, where E_r = 277MPa (average), and is notably lower than that found from testing as part of the materials characterisation program described in Chapter 8. The 'similar' product, a Boral Para Hills C/R sampled in August 1990, but with a plasticity index of 4% (compared to the Kings Road material of 2 to 7% - 6% average), was found to yield E_r = 295MPa at this level of moisture content. At a

moisture level of RMC = 60%, the material of 1990 was found to have a E_r = 340MPa, which would be considered within tolerance of the 350MPa value specified in §8.5. Lower levels of moisture content see a dramatic increase in modulus of the Kings Road material, above this value, to that of 360MPa. Given that the pavement for Kings Road was supposedly sealed to a 'dry-back' moisture content of the granular layers of RMC = 60% of OMC, the levels of strain and stiffness would have been satisfactory if this were maintained as the equilibrium value. In practice, however, the materials became much wetter than this due primarily to the absence of sub-surface drainage provide along this road, as mentioned previously §10.3.1. It is evident from these results that higher moisture content levels produce a very diminished surfacing life expectance due to the very significant loss of stiffness (25% stiffness reduction on the basis of Figure 10.14).

Static Triaxial Testing

Drained, static triaxial testing was performed on the Kings Road material to determine the material properties of cohesion and angle of shearing resistance. The following results were obtained:

Conditions	Cohesion (kPa)	Angle of Shearing Resistance (deg)
DDR=98.6%, RMC=60% (static compaction)	95	42.3
DDR=99.0%, RMC=77% (static compaction)	90	47.7
DDR=98.6%, RMC=77% (dynamic compaction)	115	46.6

TABLE 10.7: PROPERTIES OF THE KINGS ROAD MATERIAL

In addition, static triaxial testing was used to investigate how the materials 'rank' according to the newly proposed shear strength classification system, designed for material usage under a 40mm asphalt surfacing or less. This pavement required a 35mm asphalt surfacing.

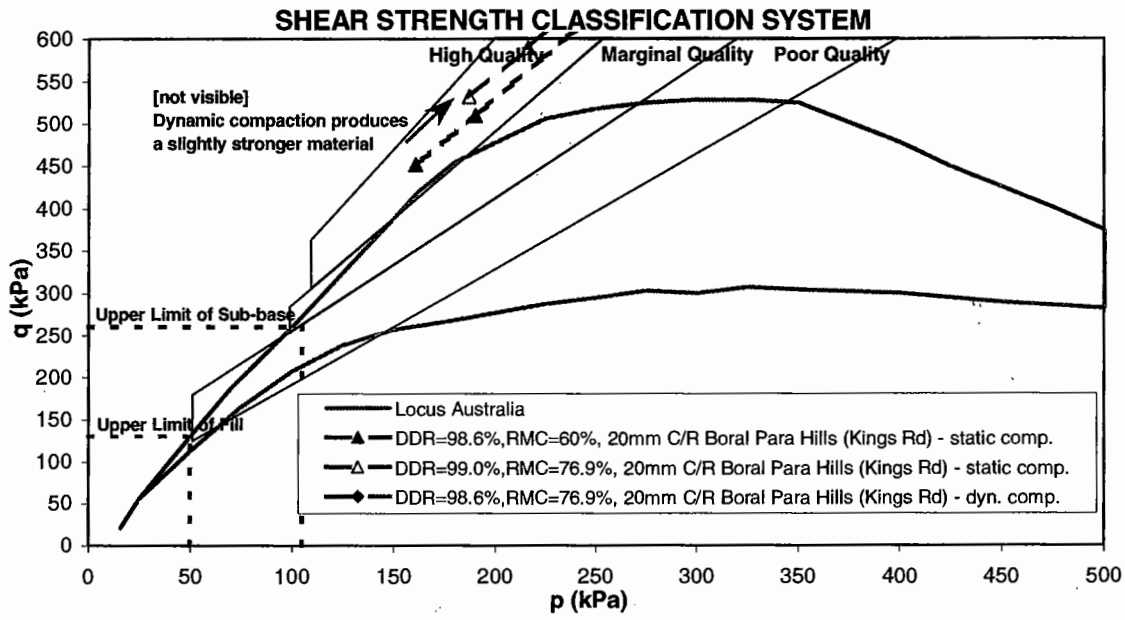

FIGURE 10.15: SHEAR STRENGTH CLASSIFICATION SYSTEM, 20MM C/R BORAL PARA HILLS MATERIAL AS USED IN THE CONSTRUCTION OF KINGS ROAD

Two shear strength envelopes were determined corresponding to two different levels of moisture content, both at approximately DDR = 99% (see Figure 9.16). Given the position of each of the envelopes, the following conclusions can be drawn:

- given the material was used beneath a thin surfacing (of approximately 35mm asphaltic concrete surfacing), its class is:
  - RMC <~77% – high quality, satisfactory for use as a basecourse material. The material's shear strength performance is high over the moisture range anticipated to exist *in-situ*. Interestingly, a slight increase in shear strength occurs for the higher moisture level, which has a very similar cohesion but a higher angle of shearing resistance. Given that the angle of shearing resistance should not exhibit variation with moisture content (as discussed in §2.3.6 and illustrated in Figure 2.11), it is considered that a discrepancy in this value may exist between the two statically compacted specimen test results. This is expected to be somewhat operated-influenced (possibly by material segregation or extent of material tamping process prior to the static compaction of each layer).

It should be stated that a static triaxial test was also performed at an RMC level of 77% of OMC, however, being initially prepared using 8-layer dynamic compaction. When compared to the statically prepared material, it was found to possess a higher shear strength (of the order of 8-9% higher). It is considered that this compaction technique allows a higher preferential orientation of the particles and more localised compaction within each layer, thereby, providing a higher strength material.

10.3.5 Pavement Evaluation and Rehabilitation

"Unbound Pavement"

Acceptable deflections and lack of significant deformation indicates the pavement possessed adequate thickness to prevent subgrade failure. However, extremely high curvature values indicate "poor stiffness within the granular overlay" (Poli, 1999) of the macadam material. Treatment was to plane off the A/C and *in-situ* stabilise to 200mm depth with 2% of 1:2 lime:flyash blend, resealing with 35mm of A/C10 modified.

"Upside-down Pavement"

Deflection values indicate the pavement is of the right thickness. Generally, curvature values were below the design value, although many individual values were above it. The stiffness of the granular layer is questionable, particularly in the winter months when moisture ingress can readily occur due to the highlighted drainage problems, and after opening to traffic. It should be remembered that the designer assumed a sound level of modulus at the top of the basecourse of 350MPa. Treatment was to plane off A/C and *in-situ* stabilise to 150mm depth with 3% of 1:2 lime:flyash blend, reseal with 35mm of A/C10 modified.

10.3.6 Summary

Performance-based laboratory testing has highlighted the sensitivity of the Kings Road material to increases in moisture content, with the layer stiffness being primarily effected. This was well supported by high curvature values which were double the design values along the inner westbound lane and triple the design value along the outer westbound lane (between 145m east of the railway crossing and Cross Keys Road), both Type 2 granular pavements. The shear strength and

permanent strain susceptibility of the material was found not to be of concern. Empirical laboratory testing failed to indicate any material deficiencies when compared with accepted specification limits.

The use of unstabilised quartzite materials as unbound granular base layers in a pavement should be viewed with caution, based upon their poor field performance history under high traffic loadings and within high moisture environments. Evidence of their marginal is supported by laboratory-based performance testing. This study clearly illustrates the need to provide deep side drains to prevent moisture entry into the UGMs from the verges. The permeable nature of the wide median also provides a transfer mechanism into the pavement.

10.4 Gawler Bypass – Stage II (South Australia)

10.4.1 Pavement History

The four lane divided carriageway Gawler Bypass, located approximately 40km north of Adelaide, was realigned in 1986 – 1992 with the new construction performed in four Stages. The road carries heavy traffic from the Clare Valley wine district and Riverland Region of South Australia, as well as interstate traffic from New South Wales and Victoria. One section of construction of 3.4km in length running from the Gawler Trotting Track to Chamberlain Road, referred to as Stage II, failed structurally within two months of opening to traffic in late 1987. The pavement constructed for Stage II was an "inverted" type (defined in §1.1.1), with the configuration shown in Figure 10.16.

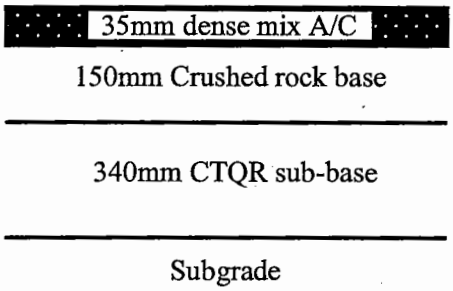

FIGURE 10.16: PAVEMENT CONFIGURATION FOR GAWLER BYPASS STAGE II

All of the 20mm crushed rock and quarry rubble materials met the Standard Specification pavement material limits, employing 'simple' empirical-based tests (grading, plasticity indices, Los Angeles Abrasion). The cement treated sub-base layer, stabilised with 3.5% cement, was placed on a sandy clay subgrade, of resilient modulus (estimated from CBR testing, refer to §3.5.1) varying from 30MPa to 70MPa throughout this Stage. As a result, the sub-base thickness varied between 340 to 280mm from mechanistic design computations.

10.4.2 Design Requirements

The design traffic loading was based on an AADT of 10,900 vehicles / day with 10% commercial vehicles and a growth rate of 2%, with 2 ESAs / commercial vehicle. Hence, the predicted twenty-year design traffic loading of ESAs, N_{20}, was

$$N_{20} = 1.2 \times 10^7$$

Design deflections and curvature values were:

$D_o = 0.86mm$ $D_0\text{-}D_{200} = 0.10mm$

based on NAASRA Pavement Design Guide (NAASRA, 1987).

10.4.3 Field Assessment

The type of failure observed was generally cracking confined to vehicle wheelpaths of the outer lanes and occurring in areas usually less than 10m in length.

The fatigue cracking was observed to commence within two months of opening the road to traffic. Fine hairline cracks appeared which developed into a state of severe crazing, with pumping of basecourse fines, within a period of 12 months. In most severe cases, rut depths of 5-7mm were observed and small blocks of crazed asphaltic concrete were at or near the stage of dislodgment by traffic.

The extent of distress was progressing rapidly with time. Initially, one or two small localised areas of cracking were observed in September/October 1988. In the 12 months following, many other localised zones appeared within a 3km length of the carriageway.

In October 1988, both deflectograph and FWD surveys were undertaken to investigate the cause and extent of the pavement failures. No definite conclusions were drawn at the time from these investigations. However, further zones of cracking occurred during 1989.

The cement treated sub-base layer is considered to be most sound and is expected to see a service life in excess of the design life of 20 years. Surveys, which involved digging a number of test pits to expose the surface of the stabilised layer, revealed this layer to be performing well with no cracking observed.

10.4.4 Materials Testing

The unbound granular material is a blue/grey dolomitic limestone from Boral Lobethal quarry.

Five basecourse samples (see Table 10.8) were taken from the newly constructed pavement in July 1989 at different locations along the road (both sound and failed sites). It is unclear, from the historical records available, whether site TP5 was in fact beginning to fail due to the high moisture content and why site TP4 had such a low moisture content for a failed site.

Test Pit No.	Condition	Field M.C. (RMC, % of OMC)	Field DDR (%)
TP1	sound	3.9 (57.4)	99
TP2	failed	4.8 (70.6)	103
TP3	failed	4.9 (72.1)	105
TP4	failed	3.6 (52.9)	101
TP5	sound	5.3 (77.9)	98.5

TABLE 10.8: BASECOURSE LAYER SAMPLES TAKEN FROM THE PAVEMENT FOR GAWLER BYPASS STAGE II

Note: OMC = 6.5% (modified compaction), MDD = 2270kg/m^3 (modified compaction)

It should be noted that the high densities greater than DDR = 99% at the three failed sites are likely to be due to the nominal 7mm of rutting which has further densified the compacted layer material. If one considers a unit volume of material, theoretical calculations show that if a 150mm layer was compacted to DDR = 98%, it is expected that 7mm of subsequent traffic-induced rutting (causing a decrease in the unit volume) could increase the density of that layer to approximately DDR = 102.5%. Further, 10mm of rutting yields a density of approximately DDR = 104.5%.

Empirical Classification Testing

A comparison of test results (presented in Table 10.9) is made with the "Standard Specification for Supply and Delivery of Pavement Material" (Department of Road Transport, 1990). In addition, the results for the same material, but sampled later in March 1992 as part of the MT16-4 research program, are shown. All results for the basecourse material used in the Gawler Bypass II pavement were found to be within

specification limits, whilst the material used in the research program was only slightly out of specification on LA.

Road	Material	Sample No.	PI (%)	LL (%)	LS (%)	LA (%)
Galwer Bypass, Stage II (1989)	Boral Lobethal	Many	6	21	1	20
MT16-4 (March 1992)	Boral Lobethal	NFD9192 - 4388	4	22	3	33
LIMITS			6	25	3	30

TABLE 10.9: LABORATORY CLASSIFICATION TEST RESULTS FOR BASECOURSE MATERIAL

Repeated Load Triaxial Testing

The resilient modulus of the basecourse material, with a moisture content of 60% of OMC, was found to have a value of only 280MPa. By using this value in the mechanistic analysis model of the pavement (which followed the modelling principles discussed in previous Chapters), it was found that the life of the asphalt surfacing would be less than two months, compared to the anticipated design life of 10 years.

Following the Gawler Bypass pavement failure investigation, it was decided to monitor the performance of this product over a four-year period. Samples of material used in the construction of the Bypass were taken from the failed pavement in June 1989. In addition, samples were taken from the 20mm crushed rock product stockpiles at the Lobethal quarry in June 1990, March 1992 and again in October 1993.

So that each product was assessed in an "unbiased" manner (given that §2.3.3 showed that grading changes significantly effect performance), the grading for each sample of the material was "adjusted" to one central of the supply specification for a 20mm crushed rock. This allowed the research to concentrate on the difference arising from material geology. In addition, all products were tested at a nominal DDR of 98% of Proctor modified dry density. The results are presented in Figures 10.17 and 10.18 in terms of two key MPIs, discussed in §2.3, namely strain rate and resilient modulus.

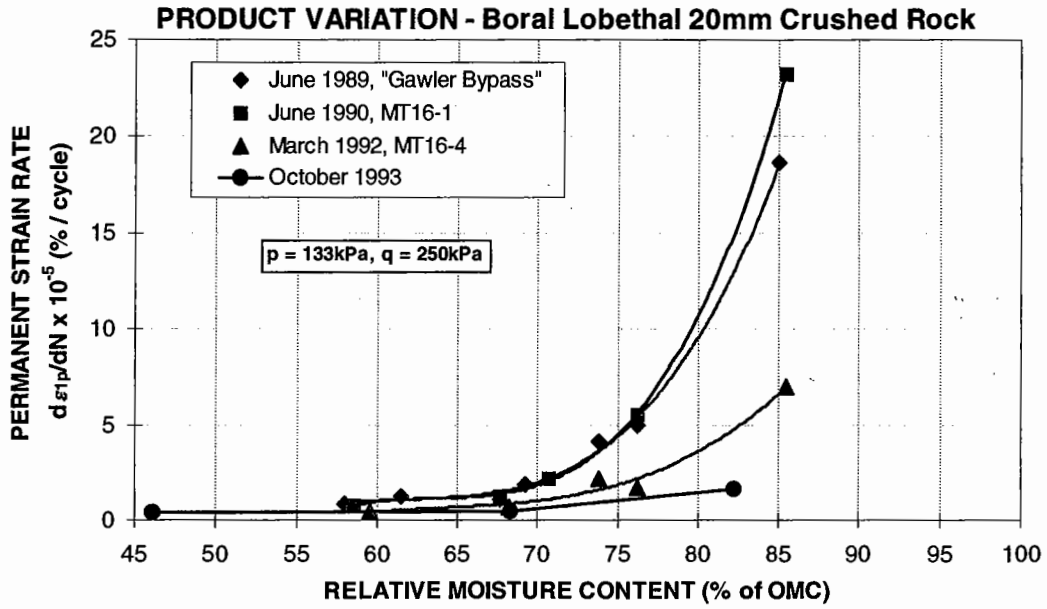

FIGURE 10.17: STRAIN RATE VARIATION WITH RMC - BORAL LOBETHAL PRODUCT

The strain rates of the 1989 and 1990 products are much greater, at high moisture levels, than the products of later years. As a result, the material is expected to exhibit strong susceptibility to rutting, particularly when subjected to even higher stress levels typical of those directly under the 35mm asphalt surfacing.

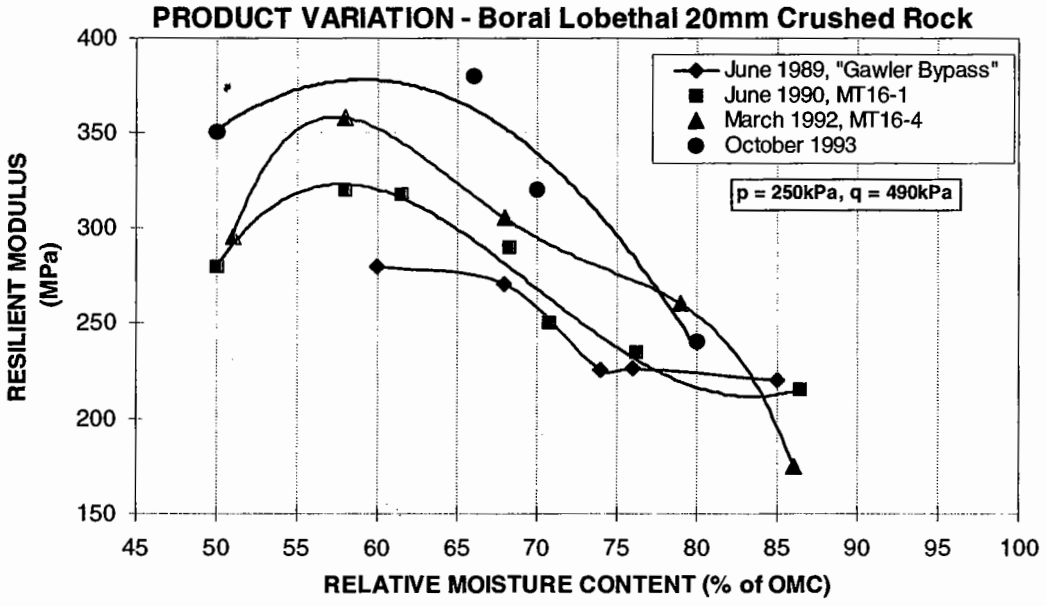

FIGURE 10.18: RESILIENT MODULUS VARIATION WITH RMC - BORAL LOBETHAL PRODUCT

It can be seen that in all cases the resilient moduli of the three products are very sensitive to moisture increases. However, the materials sampled in 1992 and 1993

appear to posses a higher stiffness (350 to 370MPa) at the lower moisture content range of 55 to 62% of OMC. In comparison, the poor performance of the 1989 and 1990 products can be seen.

The large variation in strain rate and modulus with time, as shown from the testing results, strongly indicates that regular product laboratory performance monitoring is required (particularly for 'high risk' designs such as the one adopted). Incidentally, the quarry manager in conversation reported that during the construction of the Bypass in the very late 1980s, the material was extracted from a previously untouched face of the quarry. It is expected that the geology of the material in this new 'zone' was altered, as indicated by the poor results obtained from laboratory testing. However, it is noted that the material satisfied all empirically based classification tests undertaken at the time, which further strengthens the need for performance-based testing of materials. A further example, which highlights the need for regular quality control testing, is given in Appendix 7 for the Solomon 20mm crushed rock material. Here, the material varied greatly in quality due to its extraction from two differently located open pit mines.

Static Triaxial Testing

To provide an indiçation of the quality of the material used for Gawler Bypass Stage II pavement, it shall be compared with the "better" quality material sampled in March 1992, tested as part of MT16-4 research project. The material properties of cohesion and angle of shearing resistance have been examined using drained, static triaxial testing. Moisture conditions to be used for testing were targeted for near 60% and 80% of OMC. This testing was not performed on the poor quality basecourse material of 1989. The following results were obtained:

Conditions	Cohesion (kPa)	Angle of Shearing Resistance (deg)
DDR=98%, RMC=80% (1989)	3	43.7
DDR=97.4%, RMC=52% (1992)	50	49.5
DDR=97.6%, RMC=80% (1992)	42	49.2

TABLE 10.10: PROPERTIES OF THE BORAL LOBETHAL MATERIAL (1989 & MARCH 1992)

In addition, static triaxial testing was performed to investigate how the materials rank according to the newly proposed shear strength classification system, designed for material usage under a 40mm asphalt surfacing or less. In this case, the thickness of the surfacing was a 35mm dense mix asphalt.

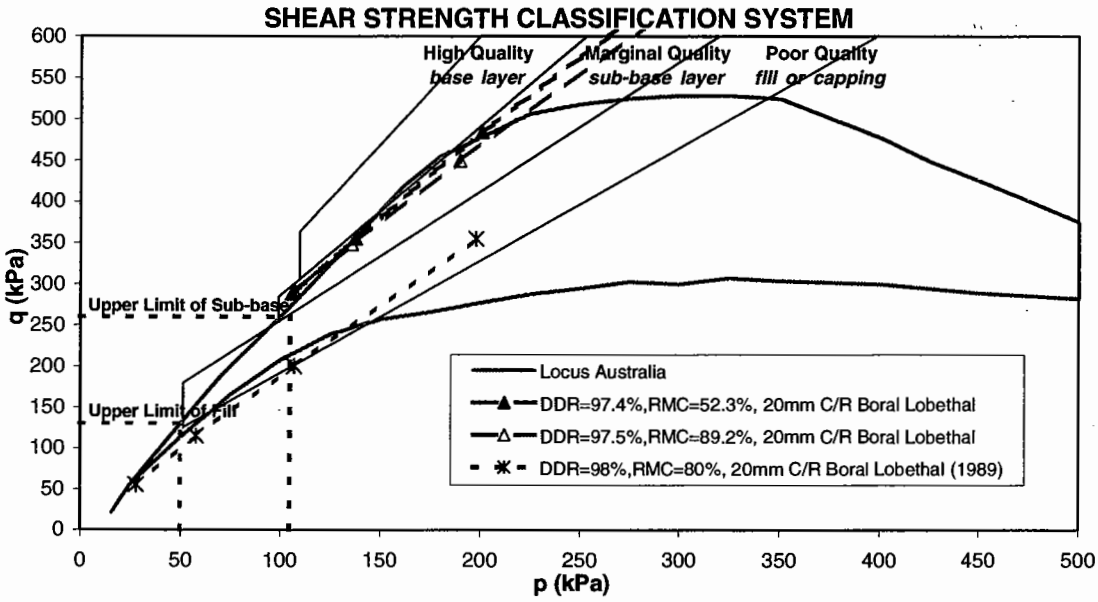

FIGURE 10.19: SHEAR STRENGTH CLASSIFICATION SYSTEM FOR THE BORAL LOBETHAL MATERIAL (MARCH 1992) AND FAILED PAVEMENT (1989)

Due to the positions of the material shear strength envelopes in Figure 10.19, the following conclusions can be drawn:

- if the materials were to be used for thin surfacing applications (less than approximately a 40mm asphaltic concrete surfacing), their class would be:
  - 1992 Boral Lobethal material – mid to upper-level marginal quality to use as a sub-base material. At a very low moisture content, one could possibly consider as a low-level high quality basecourse material.
  - 1989 Boral Lobethal material – not of suitable quality for use in the pavement at any level. This result is comparable with the strain rate and resilient modulus results.

10.4.5 Pavement Evaluation and Rehabilitation

The cause of the failure was reported (Highways Department, 1989) to be due to a combination of:

- over-estimation of the stiffness of the crushed rock material used in the base layer
- lack of bond between the asphalt and the base layer

In addition, the Author's investigation, which was conducted soon after the pavement failures were apparent, highlighted a poor quality source material was utilised in construction compared to that usually supplied by that quarry. This was later found to be due to the material for this job being extracted from a new 'face' of the quarry, thus, the material was mechanically unproven.

The pavement was designed according to the materials and design technology available to the then Highways Department in 1985. Early forms of the NAASRA Pavement Design Guide (1987), which used similar principals as the method in the Austroads Guide (1992), were adopted. The modular ratio design concept was applied, as discussed in §3.6.1, with a value of 'E_{top}' of 450MPa (presumptive Austroads Design Guide value, Table 6.4a) assumed for the resilient modulus at the top of the base layer. However, post-construction RLT testing results showed that, for a low moisture content, the resilient modulus at this stress condition would be, at best, 280MPa. As a result, the design life reduced to less than 3 years. 'Inverted' pavements are known to be highly sensitive to design basecourse modulus levels (Poli, 1999). This can be readily established by mechanistic design computations.

The remedial treatment applied during 1990 was to cold plane off the 35mm asphalt surfacing and place a SAMI then reinstate the surfacing with a 35mm open graded friction course (OGFC) 14mm asphaltic concrete with modified binder. An expected design life of 7 years was anticipated. Since the time in which the pavement treatment was applied, only limited maintenance has been required until the end of 1998.

For the following section of roadworks (referred to as Stage III), where the base layer was yet to be placed, the base material was *in-situ* stabilised with approximately 2%

cement in order to 'modify' the material and increase its stiffness. Maintenance of Stage III has comprised extensive crack sealing of transverse shrinkage reflection cracks through the thin asphaltic surfacing. In addition, pumping of "cemented" basecourse fines through these transverse cracks is a concern particularly during wet weather. This is due to erosion of the low cement content modified base layer.

For Stage IV, a 135mm asphalt / 315mm cement treated sub-base composite pavement was constructed.

10.4.6 Summary

The Boral Lobethal crushed rock material was found to be highly variable in its permanent strain and resilient modulus properties. The large variation in strain rate and modulus of the products sampled at different time periods, as shown from the testing results, strongly indicates that regular product laboratory performance monitoring is required prior to material selection (at the preliminary design stage) and during the course of construction. Rigorous attention to quality control is particularly important where the designer has opted for a 'high risk' pavement design to be constructed, such as an 'inverted' pavement type where the granular layer is 'sandwiched' between two stiff layers which can 'lock' moisture into the unbound material layer. The shear strength of the base material was assessed as being most unacceptable for the Gawler Bypass Stage II material.

Empirical laboratory testing failed to indicate any material deficiencies when compared with accepted South Australian road construction specification limits.

10.5 Bass Highway (Tasmania)

10.5.1 Pavement History

In 1990, a pavement investigation of the Bass Highway from the Forbes Street Overpass (Davenport end) in the east (Chainage 0.60km) to the Don River Bridge (Ulverstone end) in the west (Chainage 4.25km) was conducted (Walker, 1990). The Highway is a dual carriageway, which was mainly constructed during 1974 to 1977 as just a spray seal surfaced flexible unbound granular pavement. An asphalt overlay was applied between 1980 and 1985, which after only a six year period suffered severe, premature distress.

The pavement configurations was as shown in Figure 10.20:

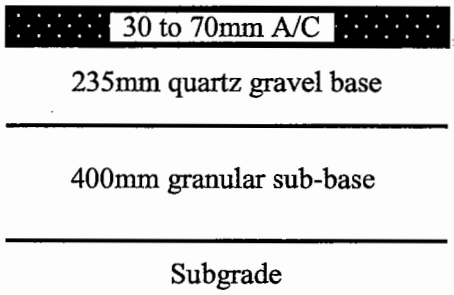

FIGURE 10.20: PAVEMENT CONFIGURATION FOR BASS HIGHWAY

The measured asphalt thickness varied from 30 to 70mm, being 30 to 50mm from Ch. 00 to 1.65km and then 60 to 70mm for the remainder of the section. The basecourse was a natural silty quartz gravel extracted from Nook Pit. The material was generally non-plastic and very high in the fine sieve content and deficient in the coarser fraction. The quartzite was out of specification below the 19mm sieve size, being up to 20 to 25% too fine at the 0.425mm to 9.5mm sieves. The sub-base was a coarse river washed gravel between Ch. 00 to 1.5km, with the remainder of the section being a micaceous quartz gravel. The subgrade was a clay of resilient modulus (estimated from CBR testing) to be E = 30MPa.

10.5.2 Design Requirements

The design traffic loading in 1989 gave an AADT of approximately 7,260 (east end) and 10,320 (west end) vehicles / day with 11.7% commercial vehicles and an annual

growth rate of 2%, giving a predicted ten-year design traffic loading of ESAs, N_{10}, as:

$$N_{10} = 3.0 \times 10^6$$

Design deflections and curvature values for the 10 year life of asphalt overlay were:

$$D_o = 0.98\text{mm} \qquad D_0\text{-}D_{200} = 0.145\text{mm}$$

10.5.3 Field Assessment

A visual assessment of the pavement's surface revealed it is severely distressed in the 'slow lanes' for the majority of the section, showing extensive cracking, deformation or rutting (low to moderate) and patching. The 'fast lanes' are basically intact. The fast Davenport-bound lane between Ch. 2.95 and 3.6km are distressed due to major traffic movements in this lane bound for the Victoria bridge.

From a deflection survey, total deflections were found to be very low which was consistent with the 600+mm of pavement depth, with a number of segments being marginal or greater than the design curvature function criteria. Generally, large variations in curvature function were found and in a number of cases low values were associated with high levels of distress. Curvature functions of 0.20mm and greater were continuously recorded in the slow lane between Ch. 0.4 to 1.65km (Devonport bound carriageway) and in the slow lane between Ch. 1.4 to 3.3km (Ulverstone bound carriageway).

10.5.4 Materials Testing

The unbound granular material is a silty quartzite from a local Pit, with a very fine grading passing 37.5mm and a particle density of 2.76t/m^3. The percentage passing all sieve sizes less than 19mm is much greater than current base 'B' limits of the specifications for natural gravel basecourse materials (see Figure 10.21).

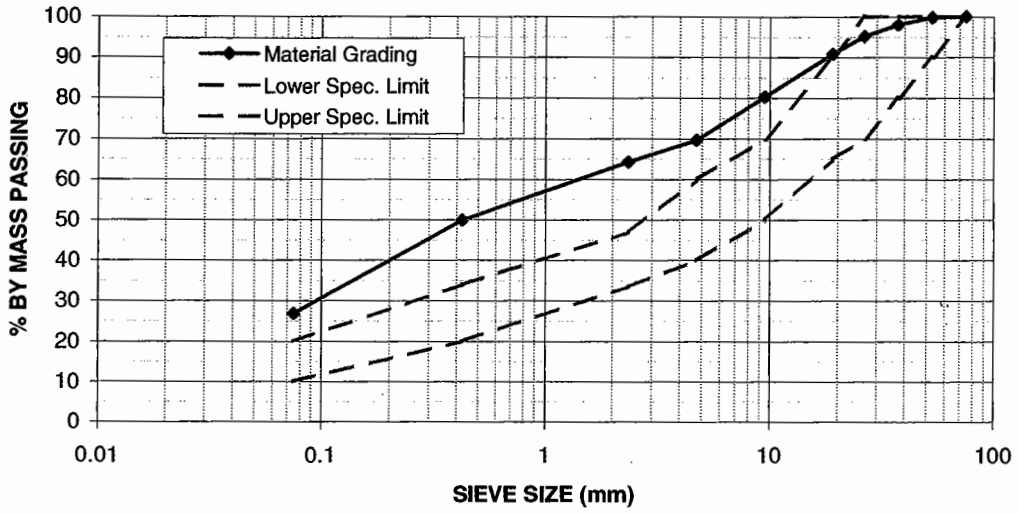

FIGURE 10.21: GRADING OF THE BASECOURSE MATERIAL USED FOR THE BASS HIGHWAY

Empirical Classification Testing

Atterberg limits testing of the basecourse material resulted in its classification being non-plastic, with the linear shrinkage test producing a null result. Other simple empirical-type tests conducted on the material by DoT-Tasmania (Walker, 1990) were permeability, dry compressive strength, CBR and Texas triaxial. From the latter two tests, Walker stated that the material would have acceptable strength if compacted well and to a moisture content below 6%.

It was found that materials taken from a number of test pits showed a moisture content of between 4.1 to 8.5% (mean 5.5%). The moderately deformed and highly cracked asphalt areas have base materials with moisture contents in the range of 6.2 to 8.5% (RMC = 88.6 to 121.4% of OMC).

Modified compaction testing provided the following results:

$$OMC = 7.0\%, MDD = 2100kg/m^3$$

In-situ measured densities ranged from DDR = 89 to 103% (mean 97.2%). Deformation was noted to occur prior to the onset of cracking in the majority of distressed locations. Lower densities were measured in non-deformed locations, indicating that inadequate compaction may be a factor, thereby leading to shear deformation (rutting). Information also suggested that the asphalt was placed in the mid 1980s to correct deformations which developed in the wheelpaths, indicating

prior problems with the granular materials whilst the pavement had only a bituminous spay seal treatment.

Repeated Load Triaxial Testing

Resilient modulus testing was performed to determine the materials' strain characteristics (both resilient and permanent) under one or a number of imposed stress conditions.

The stress levels adopted for testing were modelled upon those expected at the very top of the base layer and midheight of each 50mm basecourse sub-layer, with the pavement configuration as represented in §10.5.1. The vertical stresses applied to the different specimens of material were determined using the stress estimation charts (similar to those examples presented in Chapter §5.2) with conditions applicable to the "worst-case" material conditions. Checks were also made by creating a mechanistic model of the pavement and analysing it using the program NONCIRL.

For the preconditioning stage of the RLT test, the stress combination used was $\sigma_{1\ max}$ = 300kPa and σ_3 = 50kPa for comparing the permanent strain characteristics of the different material state conditions.

A range of density conditions, with 'higher-end' moisture contents (near OMC and typical of 'average' field conditions), were tested. In addition, one low moisture condition was examined at the mid density condition, DDR = 98%, to determine the moisture sensitivity of the material. Results appear in Table 10.11 below.

Product	DDR (%)	RMC (%)	σ_1 (kPa)	σ_h (kPa)	E_r (MPa) stress stage	Strain Rate at 3,000 cycles $\frac{d\varepsilon_{1p}}{dN} \times 10^{-5}$	Max. ε_{1p} (%) at 3,000 cycles
7	95.0	100.0	300	50	132	19.20	2.37
8	97.6	97.2	300	50	143	9.20	1.70
9	99.9	94.4	300	50	164	3.14	1.14
10	97.6	56.9	300	50	176	1.10	0.63

TABLE 10.11: STRAIN AND RESILIENT MODULUS CHARACTERISTICS OF THE DIFFERENT BASECOURSE MATERIAL STATE CONDITIONS

The permanent strain analysis clearly indicated the very high level of strain susceptibility of the lower density quartzite material. In addition, the influence of moisture content is severe when comparing the strain rate of product 8 (RMC = 97.2%) to product 10 (RMC = 56.9%).

As a further indicator of material quality, measured values of resilient modulus are reported in Table 10.12 below for the stress condition computed at the top of the basecourse layer under a 30mm asphalt surfacing using NONCIRL.

Product	DDR (%)	RMC (%)	$\sigma_{1\,max}$ (kPa)	σ_3 (kPa)	E_r (MPa) stress stage
7	95.0	100.0	595	90	184
8	97.6	97.2	595	90	205
9	99.9	94.4	595	90	220
10	97.6	56.9	595	90	258

TABLE 10.12: RESILIENT MODULUS CHARACTERISTICS OF THE DIFFERENT BASECOURSE MATERIAL STATE CONDITIONS

These levels of stiffness are considered to be very low compared to those of local (South Australian) quarry materials, even at a low moisture content (refer to Appendix 6). As a result, inadequate support is provided to the asphalt surfacing from this material when used as a basecourse layer. This fact, combined with the low annual pavement temperature in Tasmania, would accelerate fatigue of the surfacing. Thus, the performance of this material is greatly effected by the

conditions of density and moisture content which may be exacerbated by the excessively high fines content.

Static Triaxial Testing

Drained, static triaxial testing was performed on the quartzitic basecourse material to determine the material properties of cohesion and angle of shearing resistance. Moisture conditions near OMC, typical of those measured *in-situ*, were replicated. The following results were obtained:

Conditions	Cohesion (kPa)	Angle of Shearing Resistance (deg)
DDR=97.7%, RMC=104.3%	28	43
DDR=99.1%, RMC=107.1%	35	44

TABLE 10.13: PROPERTIES OF THE TASMANIAN MATERIAL

In addition, static triaxial testing was to investigate how the materials 'rank' according to the newly proposed shear strength classification system, designed for material usage under a 40mm asphalt surfacing or less. In this case, the thickness of the surfacing is between 30mm to 70mm, with the worst performing sections being of thinner surfacing, 30 to 50mm between Ch. 00 to 1.65km (see Figure 10.22).

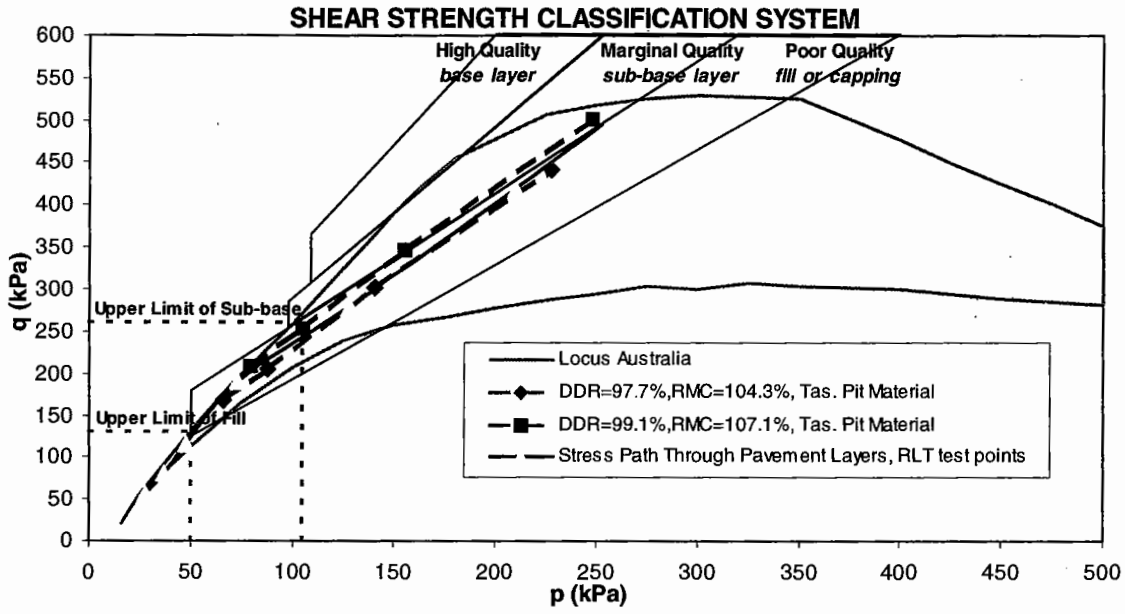

FIGURE 10.22: SHEAR STRENGTH CLASSIFICATION SYSTEM FOR THE TASMANIAN MATERIAL

Due to the positions of the two different material shear strength envelopes, the following conclusions can be drawn:

- if the materials were to be used for thin surfacing applications (less than approximately a 40mm asphaltic concrete surfacing), their class would be:
  - DDR = 97.7% – mid to upper-level, poor quality to use for a fill material.
  - DDR = 99.1% – low-level, marginal quality to upper-level poor quality for possible use as, at very best, a sub-base located at a reasonable depth or fill material. The material shear strength performance is expected to increase considerably, possibly bordering on mid-level marginal quality if moisture level *in-situ* was reduced to approximately RMC = 60% of OMC.
- The basecourse material will undergo shear failure according to the upper level pavement stress combinations imposed by heavy traffic and, as a result, develops a different line of stresses through this process. This material is not considered satisfactory for use as a basecourse layer.
- For surfacing of approximately 70mm thickness, the higher density/moisture condition material shear strength would be adequate given the much lower stress conditions throughout the basecourse layer. Hence, the more acceptable

performance of the Bass Highway is reported under these conditions, *provided* adequate stiffness is generated.

10.5.5 Pavement Evaluation and Rehabilitation

Acceptable deflections, over a great thickness of pavement, indicate adequate thickness to prevent subgrade failure. However, it was considered that the major cause of the distress, stated by Walker (1990), was "insufficient pavement stiffness for the asphalt quality provided". "It was evident that in higher trafficked locations of the pavement the curvature functions were generally higher, which suggested weakening of the upper pavement, ie, basecourse and or asphalt." In addition, inadequate compaction and moisture control were sited as possible contributing factors, along with the very high fines content of the material. Treatment options proposed were to either plane off the A/C and overlay with a minimum thickness of 60mm asphalt and SAMI; or mechanically *in-situ* stabilise to 150mm depth; or remove the asphalt and place a 150mm granular overlay.

The option chosen for rehabilitation was to mill and pulverise the existing asphalt layer then incorporate this material into the new basecourse layer, formed by *in-situ* cement stabilisation (2% cement) to a depth of 175mm. A primer seal overlain by a 5mm slurry seal provided the surfacing. In severely deteriorated sections, a geofabric was used under a 14mm polymer modified binder (PMB) spray seal. Eight years of monitoring this road has shown the treatment option to be satisfactory, although the road has required increased surface patching in more recent years. However, a deflection survey of August 1998 indicated that the curvature function was still quite high in many sections.

10.5.6 Summary

The crushed rock material used in the Bass highway pavement was found to be most unsatisfactory, generating high levels of permanent strain and low levels of resilient modulus. This was found to occur even at density and moisture levels which, in the main, are considered to allow optimal material performance to be displayed. In addition, the shear strength classification system illustrated the material to be of poor quality. The high permanent strain susceptibility of the material encouraged

considerable wheel path deformation to occur, which eventually lead to cracking of the asphaltic surfacing.

A selection of simple empirical laboratory tests, conducted by DoT-Tasmania, suggested that the material would have acceptable strength if compacted well and to a moisture content below 6% (RMC = 85.7% of OMC). History shows that this was far from the truth. The only empirical indicators which may have prompted some concern regarding the material's ability to perform was the material's non-plastic nature and its very fine grading, approximately 10 to 20% finer than the upper specification limit. However, in §2.4.4 we saw the results of two materials with a fine grading which performed very well, with low levels of permanent strain rate and high levels of modulus. In addition, purely quartzitic materials, that is, those not blended with geologically different materials have been found in South Australia to exhibit performance deficiencies particularly at higher moisture contents (refer to the results in Appendix 6). Such an example is the Stonyfell 20mm crushed rock. The Boral Para Hills material performs a little better given it is blended with a siltstone finer than the 4.75mm sieve.

10.6 Flagstaff Hill Road (South Australia)

10.6.1 Pavement History

In 1991, a section of Flagstaff Hill Road, between 300m north of Bonneyview Road to Black Road, was reconstructed. It was proposed that the road be widened to provide divided dual lane carriageways to enable easier access to a growing population emerging in new residential areas. From Chainage 0.55km, the existing thin asphaltic concrete surfaced granular pavement (prior to the reconstruction), which was sealed in 1986, was found to have crazing (with pumping of fines in areas), longitudinal cracking and patching. This section had a limited life of the surfacing of less than 5 years.

The reconstruction was achieved with a full depth unbound granular pavement, having a thin asphaltic concrete surfacing from Chainage 0.55km to 2.3km (see Figure 10.23). This pavement is still performing very well.

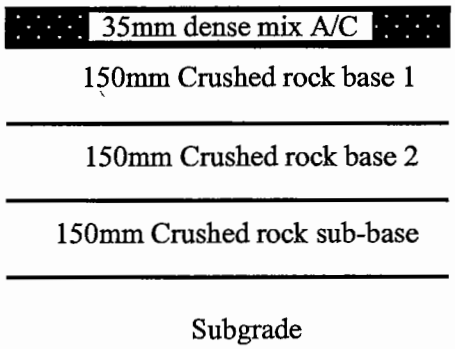

FIGURE 10.23: PAVEMENT CONFIGURATION FOR FLAGSTAFF HILL ROAD

The design recommendation in 1991 was for the construction of a granular pavement comprising a 35mm A/C wearing course, two 150mm dolomitic limestone C/R basecourse layers and one 150mm granular sub-base (both supplied from the Linwood quarry). This pavement, constructed in 1992, overlaid a sandy clay subgrade of minimum resilient modulus, determined from RLT testing, of E_r = 50MPa. Design calculations pre- and post- construction used the AUSTROADS modular ratio approach with an "$E_{top\ of\ base}$" = 350MPa being assumed. It should be noted that the use of cement-treated sub-base layers was avoided due to the rather

expansive subgrades encountered in some locations during the initial evaluation investigation. In addition, it was recommended that moisture conditions be stabilised in the outer wheel path by sealing the shoulders or verges for a width of 1.0 to 1.5m from the edge of the outer lane.

10.6.2 Design Requirements

The design traffic loading in 1990 gave an AADT of approximately 19,000 vehicles / day with 3.7% commercial vehicles and an annual growth rate of 2.0% in the first 10 years, with 1% anticipated in the remaining 10 years. This traffic volume falls into the low to moderate range for Adelaide urban arterial roads. The route caters primarily for commuter traffic, concentrated during peak periods, and bus movements. The predicted ten-year design traffic loading of ESAs, N_{10}, was:

$$N_{10} = 1.4 \times 10^6$$

It should be noted that traffic volume increases from the time of construction up to March 1998 have been much higher, of the order of 5.5 to 6.3% per year, with the total number of commercial vehicles remaining somewhat constant at around 560 to 580 per day.

From the NAASRA Pavement Design guide (1987), design deflections and curvature values for a 35mm asphalt surfacing were:

D_o = 1.10mm (20 year life) D_0-D_{200} = 0.22mm (10 year life)

Following the lessons from previous pavement failures attributed to the low quality unbound granular materials and the results of laboratory repeated load triaxial testing, the pavement design report (Mathias, 1991) recommended the following:

- compaction densities of UGMs to 98% relative modified compaction,
- "granular layers require a high degree of stiffness when an asphaltic concrete surfacing is used. Moisture contents well dry of OMC, preferably less than 60% of OMC, should be achieved before placing the next layer".

10.6.3 Materials Testing

The unbound granular material is a 20mm Linwood quarry crushed rock; a blue-grey dolomitic limestone which conformed to the "Standard Specification for Supply and Delivery of Pavement Material" (Department of Road Transport, 1990) in terms of grading, Atterberg limits and Los Angeles abrasion. Modified Proctor compaction testing provided the following results:

$$OMC = 6.3\%, MDD = 2270kg/m^3$$

In-situ measured densities were consistently around DDR = 98%.

Repeated Load Triaxial Testing

Resilient modulus testing was performed to determine the materials' strain characteristics (both resilient and permanent) under one or a number of imposed stress conditions.

The permanent strain analysis for the 20mm Linwood crushed rock, illustrated in Figure 10.24, highlights the low level of moisture susceptibility of the material (at DDR = 98%) and preconditioning stress conditions of $\sigma_{1\ max}$ = 300kPa and σ_3 = 50kPa.

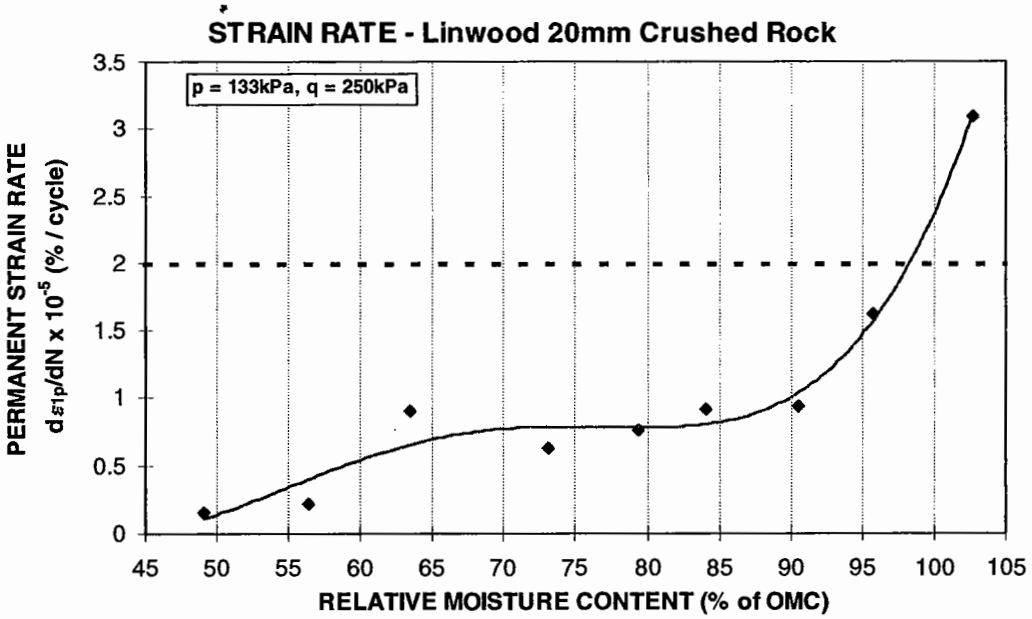

FIGURE 10.24: STRAIN RATE CHARACTERISTICS OF THE 20MM LINWOOD CRUSHED ROCK

The material is relatively insensitive to moisture content until approximately RMC = 90%, which is well above the *in-situ* moisture content. Thus, from laboratory performance-based testing, satisfactory field performance is expected according to this parameter.

To gain further knowledge concerning expected field performance, falling weight deflectometer (FWD) testing was organised shortly after the completion of roadworks. It was aimed to measure the curvature function at a number of locations along the outer wheel path (OWP) and graphically represent the average result on Figure 10.6, which illustrates a relationship between permanent strain rate and curvature function. The FWD measured a curvature value of 0.134mm with a small variation about this mean. From the moisture content of the layer, which was generally measured to be 70% of OMC or less, a value of $d\varepsilon_p/dN = 0.75 \times 10^{-5}$ % / cycle is obtained from Figure 10.24. This data point is plotted on Figure 10.6 and reproduced as Figure 10.25. The new data point (Flagstaff Hill Rd) lay in the zone associated with sound material and pavement performance and is positioned in-keeping with the other points used in the correlation.

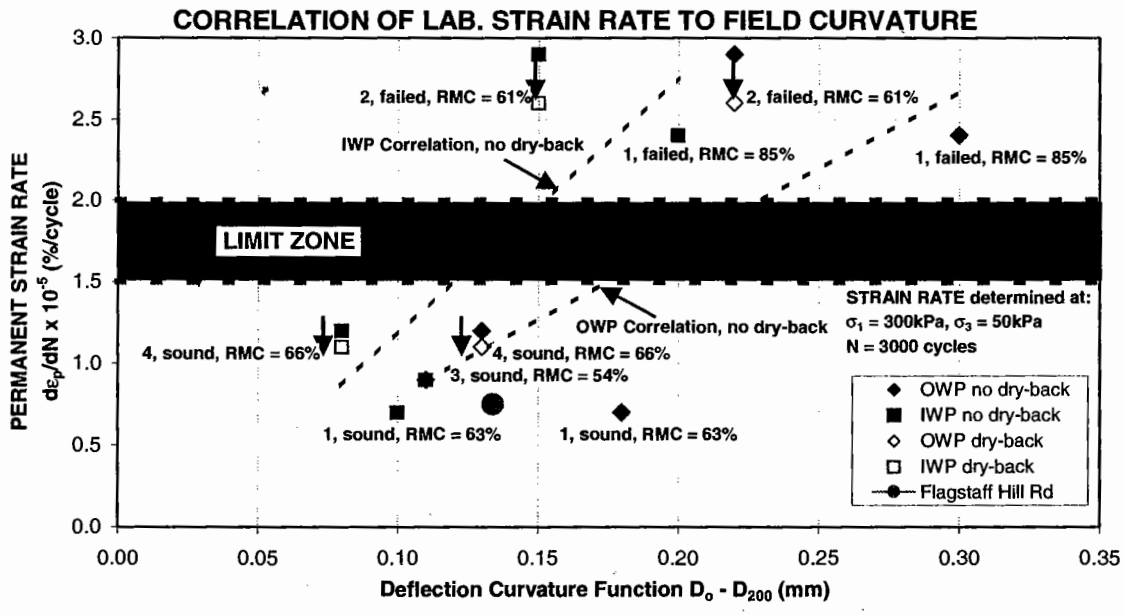

FIGURE 10.25: THE AVERAGE RESULT FOR THE LINWOOD C/R USED IN FLAGSTAFF HILL RD IS ADDED TO THE STRAIN RATE / CURVATURE FUNCTION CORRELATION

The stress levels adopted for resilient modulus determination followed the stress path sequence as presented in Figure 5.13. A graph of the variation of resilient modulus with moisture content (Figure 10.26) is illustrated for the stress condition at the top of the basecourse layer under a 35mm asphalt surfacing ($\sigma_{1\ max}$ = 577kPa, σ_3 = 87kPa), which is appropriate for the constructed pavement configuration of Flagstaff Hill Road.

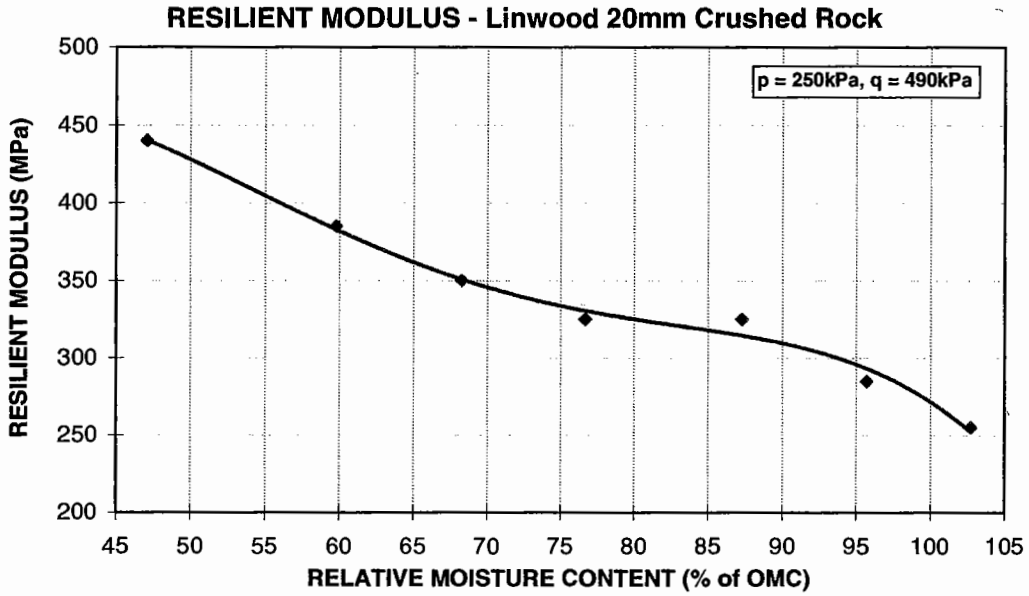

FIGURE 10.26: RESILIENT MODULUS CHARACTERISTICS OF THE 20MM LINWOOD CRUSHED ROCK

These levels of stiffness developed are considered to be quite satisfactory up to a moisture level of approximately RMC = 70%, where E_r = 350MPa. Lower levels of moisture content see a significant increase in modulus above this value. Given that the pavement for Flagstaff Hill Road was primarily constructed through the summer period, dry-back of the granular layers to a moisture content of RMC = 60% of OMC was easily achieved. As mentioned, the equilibrium moisture content has been measured to be 70% of OMC or less. As a result, strong support would be provided to the asphalt surfacing from this material when used as a basecourse layer. In addition, the testing program concluded that resilient modulus for the Linwood material was not found to be density dependent for the tested density levels of 96%, 98% and 100% DDR applicable to construction (refer to Appendix A6.3). So, if some areas of the pavement were found to be of a lower density than DDR = 98%, resilient modulus would not be greatly affected.

Once again, to gain further knowledge concerning expected field performance, the resilient modulus, measured at the end of the preconditioning test, was compared with the curvature function measured by the FWD. The resulting point of data is added to the data shown in Figure 10.7 and reproduced as Figure 10.27. A value of E_r = 230MPa was obtained from RLT testing at the end of the preconditioning test, corresponding to a moisture content of approximately 70% of OMC (note different stress level to the values shown in Figure 10.26). From this result, it can be seen that the new data point (Flagstaff Hill Rd) lay in the zone associated with sound material and pavement performance and is positioned in-keeping with the other points used in the correlation.

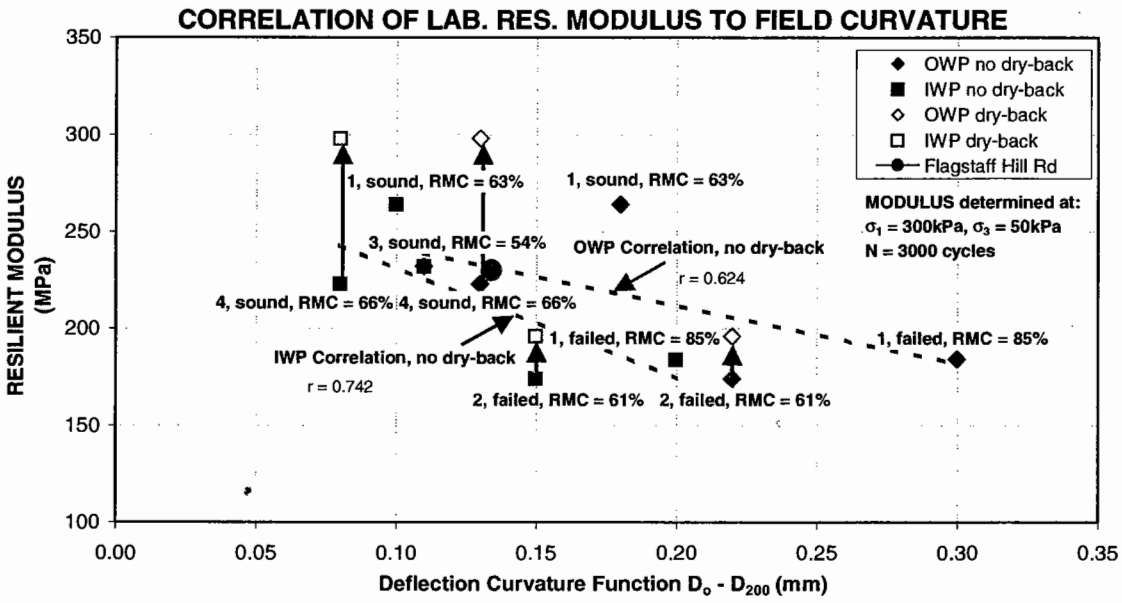

FIGURE 10.27: THE AVERAGE RESULT FOR THE LINWOOD C/R USED IN FLAGSTAFF HILL RD IS ADDED TO THE RESILIENT MODULUS / CURVATURE FUNCTION CORRELATION

Static Triaxial Testing

Drained, static triaxial testing was performed on the Linwood dolomitic limestone basecourse material to determine the material properties of cohesion and angle of shearing resistance. The following results were obtained:

Conditions	Cohesion (kPa)	Angle of Shearing Resistance (deg)
DDR=97.9%, RMC=52.4%	80	50
DDR=98.1%, RMC=87.3%	28	46

TABLE 10.14: PROPERTIES OF THE LINWOOD MATERIAL

In addition, static triaxial testing was to investigate how the materials 'rank' according to the newly proposed shear strength classification system, designed for material usage under a 40mm asphalt surfacing or less. From §10.6.1, this pavement was designed for a 35mm asphalt surfacing.

Three shear strength envelopes were determined corresponding to three different levels of moisture content, and all at approximately DDR = 98% (see Figure 10.28). Given the position of each of the envelopes, the following conclusions can be drawn:

- if the materials were to be used for thin surfacing applications (less than approximately a 40mm asphaltic concrete surfacing), their class would be:
  - RMC < 70% – high quality, satisfactory for use as a basecourse material.

    The material shear strength performance is seen to increase considerably, as the moisture level *in-situ* is reduced to approximately RMC = 60% or less of OMC, which satisfies the strength criterion for the measured *in-situ* moisture content level in service.
  - RMC > 70% – mid-level, marginal quality for use as a sub-base material due to the rapidly increasing moisture sensitivity of the material (as can also be seen in the resilient modulus above this moisture level).

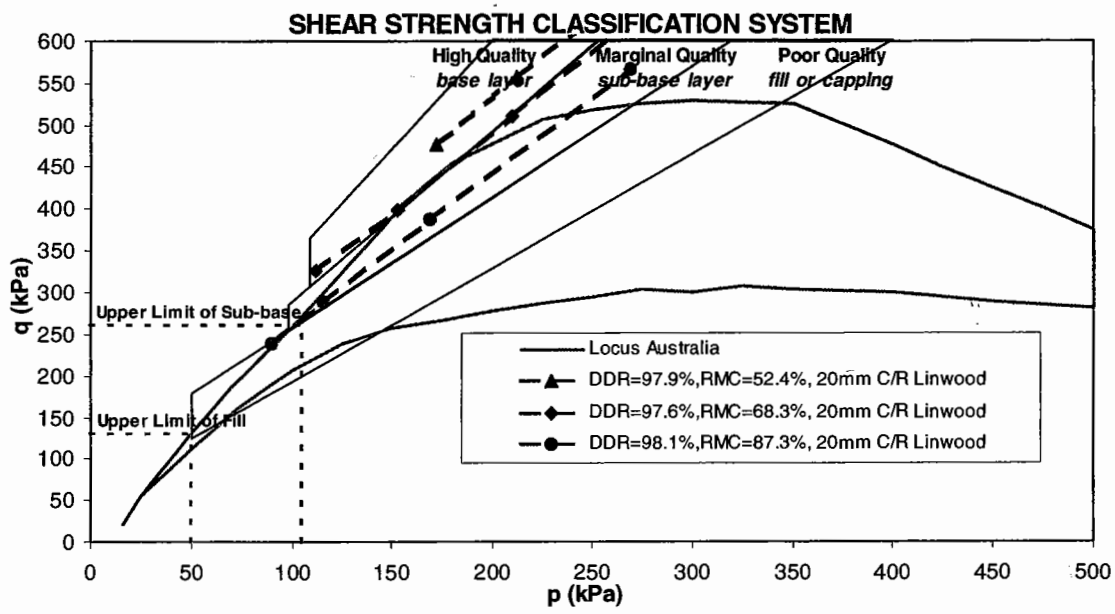

FIGURE 10.28:SHEAR STRENGTH CLASSIFICATION SYSTEM, 20MM C/R LINWOOD MATERIAL

10.6.4 Field Assessment

A visual assessment of the pavement's surface revealed the pavement is performing very well with little or no maintenance being applied to the constructed section of road. Sound drainage along this road is sited to be a key contributing factor.

10.6.5 Summary

This case study clearly illustrated the qualities required for a successful service life of a granular pavement. All parameters were found from laboratory and field testing to yield performance-based test results within the limits discussed in Chapters 8 and 9. Thus, sound performance of the pavement could be achieved providing the *in-situ* moisture content pertaining to the parent material, Linwood quarry 20mm crushed rock, remains below 70% of OMC, ideally at 60% of OMC.

10.7 Summary

From these studies, it can be stated that relationships *do* appear to exist between key MPIs (resilient modulus, permanent strain rate and shear strength parameters) measured from laboratory RLT testing and observed and measured field pavement performance (deflection curvature). The critical limits required of these parameters for satisfactory field performance varies according to the application assigned to the

materials in the pavement (viz, basecourse 1, basecourse 2, sub-base or fill/capping layers). It can be expected that higher limits of resilient modulus and shear strength, whilst low levels of permanent strain rate, will be required of the materials when used higher up in the pavement structure, where *in-situ* stresses are greater.

Correlations of the permanent strain rate and resilient modulus with deflection curvature function appear to show great promise. The collection of more field and laboratory data, where materials tested in the laboratory replicate those conditions *in-situ*, will further validate not only the apparent relationships that exist but also the processes applied in diagnostic investigations. This in turn will lead to well researched limits for the key MPIs, which can be applied at the quality assessment phase *prior* to and during pavement construction. This implies a performance-based specification for material assessment. By pursuing this path, pavements can be constructed of sound fit-for-purpose materials, being of standard, naturally occurring source rock or alternatively processed materials (waste products). Attention should be given to the separation of inner and outer wheel path deflection curvature data when assessing any correlations with strain rate and resilient modulus.

As reported §8.8.4, the empirical test results of the individual case studies did not suggest the poor levels of service that were found to occur. Only in the case of the Bass Highway pavement did the excessively fine grading suggest a cause for concern. However, we saw in §2.4.4 that two materials with a fine grading performed soundly with low levels of strain rate and high levels of modulus so a prediction based on grading cannot always be absolute.

In the Gawler Bypass II study, all of the empirical test indicators did not illustrate the dramatic difference in material performance found from functional testing over a four year period. Given that functional testing was not available to the road authority at the time, pavement layer stiffness predictions were made based upon empirical test results and assumed values of resilient modulus, coupled with knowledge derived from experience. On reflection, this could possible be sited as a recipe for disaster. In addition, the need for quality control performance-based testing was clearly evident from this study.

CHAPTER 11
CONCLUSIONS

11.1 Post Summary

Roads are an integral part of life and the well established networks worldwide represent an asset which, in economic and strategic terms, is irreplaceable. This asset, however, will deteriorate with time through environmental and heavy vehicular impacts. Consequently, current design techniques must continue to develop and utilise the growing "warehouse" of laboratory and field material performance-based data to provide more certainty in the assessment of pavement life, with lower associated risk of more frequent maintenance interventions and treatments. Mechanistic design methods make it possible to adopt designs to the particular conditions.

It was demonstrated in Chapter 10 that a definite relationship exists between key material performance indicators, MPIs (permanent strain rate, resilient modulus and shear strength) of RLT test results and observed relative field performance (deflection curvature and stiffness).

11.2 Conclusions

The work of the Author has focussed on MPIs, which can be directly linked to the in-service performance of materials within a loaded pavement structure. The MPIs found to be most influential in predicting material behaviour, by varying the *in-situ* state conditions (moisture, density, stress, grading, suction forces, etc) and geology were permanent strain rate, resilient modulus, cohesion and angle of shearing resistance. Durability and permeability also play a key role in influencing this response by facilitating, or otherwise, both material degradation and the ability to shed (or store) moisture from (or within) the aggregate skeleton. Given the very high dependence of all the MPIs upon moisture (other than angle of shearing resistance), the need for free-draining, permeable materials is a necessity and frequently overlooked by pavement designers.

Analytical modelling of pavements:

Many analytical pavement design modelling procedures have remained virtually unchanged since their inception in the late 1980s. The detail presented in their methodology upon introduction was in keeping with the level of knowledge at the time. Improved analytical modelling of pavements is now seen as a requirement to more accurately calculate critical stresses and strains and thereby reduce the likelihood of poor pavement performance. The procedure should require designers to adequately examine the dependence of a material's performance linked to *in-situ* state conditions and apply sound mechanistic modelling principals. It was found that virtually all the methods used around the world did not achieve this. In particular the methods were found to exhibit shortcomings in the following areas where they did not:

- assess the shear strength of the constituent materials – a necessity where thinly surfaced pavements (with surfacing less than 80mm) are used.
- account for non-linearity of the UGMs (where stress change gradients within the layers were significant, particularly for pavements within a bituminous surfacing of less than 80mm in thickness) by adequately sub-layering the total thickness of UGMs.
- account for different material seasonal variations which are associated with a unique set of properties, largely controlled by moisture.
- account for overburden and residual stresses.
- harmonise stress / modulus through iterative techniques and apply meaningful mathematical material modelling relationships or graphical representation (such as 'Resilient Modulus / Stress Design Charts').
- consider the influence of plastic strain behaviour and its impact on pavement performance, given that 'real' pavements are not solely elastic in their response to continuous heavy vehicle axle loading.

To overcome the issue of non-linearity of UGMs, the Author recommends modelling in sub-layers to a depth of at least 260mm for a BST pavement, 215mm for a 35mm surfaced pavement and 160mm where an 80mm surfacing is used. A number of 50mm and 75mm sub-layers are to be used to achieve this outcome.

Analytical methods need to 'accurately' determine the stress conditions which exist in the pavement due to the combination of compaction processes, overburden, material failure criteria and traffic loading. It is important that strains determined from mechanistic analysis use the 'correct' stresses resulting from the interaction of all these conditions, otherwise the strains calculated could be unnecessarily excessive.

Moisture control:

The *in-situ* monitoring of the UGM condition in pavements, as part of the COURAGE project, has revealed that the moisture content of the UGM layers vary considerably with the season. In base layers (those immediately beneath the bound surfacing), the variation was found to be between 40 and 90% of optimum moisture content. For the lower sub-bases, an even greater variation of between 30 and >100% of optimum moisture content was measured.

The research conducted herein has clearly demonstrated the dramatic reduction in material performance which can result if thinly surfaced pavements are sealed with high 'locked in' levels of moisture.

In the pavement, moisture should be removed from the materials through controlled drying back of the layers immediately following placement and compaction. The level of moisture targeted in the UGMs should not exceed 60% of OMC (50 to 60% of saturation), prior to sealing or application of binder. In addition, adequate surface and sub-surface road drainage systems should be designed for in climatic regions where rainfall and temperature conditions are considered detrimental to performance, especially when coupled with material geology and terrain. It has been demonstrated that wetting up of the pavement materials will act to significantly reduce the pavement's service life.

Where the attainment of satisfactory material strength and stiffness is difficult to achieve in countries of higher rainfall and lower temperatures, it is recommended to use either:

- higher grade materials to encourage load spreading, or

- thicker asphalt surfacing layer(s) or inclusion of a bituminous base layer to lower imparted stresses to the granular materials and, hence, reduce the strong stress to stiffness/strength dependence, or
- liberal percentages by mass of stabilising agents such as cement, lime/cement, foamed bitumen, or other proven additives. These products have been found to produce considerable improvement in strength, permanent strain rate and resilient modulus characteristics partially through reducing a material's susceptibility to moisture.

It was shown from the research conducted that degree of saturation is more meaningful in illustrating material performance, given that it accounts for, and highlights, a materials' density dependence. This parameter is most important when analysing material performance at higher or lower modified Proctor compaction levels than DDR = 98%, where data shifts to higher or lower moisture states as a result. A material's degree of saturation provides a better understanding of the moisture within the pore spaces of a compacted material than the relative moisture content. However, it is felt that the construction industry may struggle to comprehend the true meaning of this more geotechnical-based parameter, compared with the simple and long used parameters of moisture content and OMC.

From the thinly surfaced pavement analysed for two different seasonal conditions of winter and summer (higher stiffness), it was apparent that UGM layer stiffness can increase by up to 40 to 50% for the drier moisture state, depending on the material product type and ability of the drainage system.

A higher moisture state (encountered during winter) was found to dramatically reduce the asphalt surfacing fatigue life by a factor of 9 and increase the vertical compressive stress at the top of the base layer by 35%. Thus, pavements should be analysed for a number of different seasonal periods throughout the year.

Stress regimes:

Experimental research has found that vertical stress regimes within UGMs can vary very significantly depending on the quality of the layer materials. Those materials of

high quality tend to act as an effective load-spreading medium with a high degree of stress reduction achieved at the bottom of the layer (depending on its overall thickness). Research has shown that existing theory may tend to over-estimate the magnitude of vertical stress at a point within an UGM layer, if the material is of high quality.

It was found that the magnitude of vertical stress was relatively insensitive to variations in the subgrade modulus. In addition, vertical stresses within UGMs are not greatly affected by changes in sub-layer resilient modulus, particularly at stress levels below about 150kPa (at a depth of approximately 200mm into the pavement).

An apparent tensile stress of 14kPa was found to exist for a granular material of low compaction level (93% MDD standard compaction) having dried the material out of 50% of OMC. It could be expected that higher stresses could be obtained when testing materials at higher compaction densities more in line with those encountered in constructed pavements.

In addition, residual stresses have been measured by a number of researchers and found to be dependent of the magnitude of applied vertical stress. The Author presented theory to estimate the magnitude of residual stresses with the view to correcting lateral stresses computed by non-linear elastic theory. It makes use of a minimum stress ratio to account for unloaded state lateral stress contributions from residual stresses *and* overburden stresses only. The theory requires knowledge of the vertical stress imparted at depth z in the layer resulting from compaction apparatus working at the final passage of the roller. It was demonstrated that 'Lateral Stress Correction Charts' could be derived for use in this process. In doing so, theoretically computed strains within the pavement UGMs can be greatly reduced, thereby improving the predicted life of pavements to some degree, which is dependent on the likely failure mode.

Shear strength classification system:

The research conducted showed the importance of assessing the shear strength of a pavement material to determine its capability to support applied traffic stresses. This

in turn affects the position in which the material may be placed in the pavement structure. A new classification system has been proposed which can be directly incorporated into pavement design procedures. Three material quality zones were formed which, for thinly surfaced pavements (with a seal of less than 40mm) relate to base, sub-base and fill layer stress zones. This system is the *first* means of assessment to determine how a material could be used in the pavement. If the material is found to posses sufficient shear strength, in excess of the shear generated by imposed traffic loadings, then this will act to assist in the control of permanent deformation (and hence rut) development. The new classification system provides a single analytical tool to 'rank' the quality of different materials (of varying state conditions) for suitability within a particular pavement layer

Rationalisation of stress levels for RLT testing:

By theoretically modelling a wide range of pavements subjected to applied design standard axle traffic loadings, a stress locus was derived which encompassed all stress combinations expected within the UGMs of any loaded pavement configuration. From this information, the Author has derived a new set of stress conditions that can be applied to the RLT test to determine moduli for design purposes. The benefits of the new stress levels include their separation into those encountered in basecourse (high quality material) and sub-base/fill (marginal/poor quality material) layers. Small Δp and Δq steps were devised in the testing sequence to improve the continuity of modulus test results for graphical presentation or modelling purposes.

On applying the new stress sequence to testing a material, it was found that the variation in resilient modulus for repeat testing was 4% or less for the basecourse stress sequence. This is largely due to the removal of the less repeatable stress combinations, which are generally those with a high confining stress and low ratio of q/p, where recorded strains from testing materials are smaller and more difficult to measure accurately. The variation obtained for the sub-base stress combinations was expectably higher for this very reason.

Given that granular materials are most stress dependent, materials must be assessed at stress conditions representative of those *in-situ*, under applied design traffic loadings. This is particularly important given that resilient modulus and permanent strain rate are very sensitive to the applied stress conditions experienced by a material element (ie, stress-dependent).

Optimising the performance of UGMs:

The optimal use of unbound granular materials, UGMs, depends on the:

- geological nature of the raw material (totally non-plastic materials were found to perform poorly, whilst materials of modestly higher plasticity than allowed under specification were found to perform satisfactorily).
- stable and low equilibrium levels of moisture content or saturation levels (generally found to be around 60% of optimum moisture content or a 50 to 60% saturation).
- density level (generally requiring 98% to 100% of modified Proctor compaction, in some cases a lower level may produce acceptable performance).
- imposed stress conditions, resulting from heavy vehicular axle loadings.
- satisfactory shear strength in keeping with the classification system proposed by the Author and in line with the application of the material (to which layer and at what depth) in the pavement, which will be influenced by the stresses generated within that layer.
- acceptable rate of permanent strain, which for base materials was found to be a maximum level of 2×10^{-5} % / cycle at a stress combination of p_{max} = 133kPa and Δq = 250kPa, which is applicable to the approximate stress level at a depth of 110mm into the basecourse layer beneath a very thin (35mm) surfacing. For a sub-base material, an upper limit of 5×10^{-5} % / cycle is proposed.
- limiting the vertical compressive strain to 1600 microstrain at the top of the base layer under a thin 35mm asphalt surfacing. This value should be used in design practice until further research can refine this. In addition, a value of 900 microstrain could be used at the top of the second base layer.
- acceptable resilient modulus for base materials was found to be 350MPa at a stress combination of p_{max} = 250kPa and Δq = 490kPa, applicable to that

experienced at the top of the basecourse layer under a very thin (35mm) surfacing. For sub-base and fill materials, acceptable levels of resilient modulus are considered to be 240MPa (based on the result at stress level of p_{max} = 105kPa and Δq = 260kPa) and 175MPa (based on the result at stress level of p_{max} = 50kPa and Δq = 130kPa), respectively.

- regular product monitoring through performance-based testing as a means of quality control assessment prior to, and throughout the course of, construction.

Empirical vs Performance testing:

From testing conducted, empirical test results did not indicate much of a difference between quarry rubble and crushed rock products. In one case, the quarry rubble product far out-performed its crushed rock counterpart using performance-based testing, the latter of which was only found to be of sub-base quality at best. As a result, one must question the value of the empirical tests and/or their limiting acceptance values as detailed in empirical specifications. These empirical tests do not seem to produce results that lead to definitive outcomes for how materials should be used in the pavement. Given empirical tests do not use a fully graded material (only a component of the grading) and do not replicate the state conditions of density, moisture and stress, their use is somewhat limited in today's world where heavier and more frequent vehicle trips are made on pavement designed and constructed on leaner budgets.

Performance-based tests are considered to be a step forward in providing a meaningful assessment tool beyond empirical-based tests to better account for environmental and traffic-imposed effects. A lack of incentive and action compelling industry to commit to a new specification could possibly result from road authorities not moving down the path of Design-Build-Fund-Operate (DBFO) contracts. Contracts of this type somewhat force contractors to be more conscious of the risks associated with the goal of long-term pavement performance.

The MPIs adopted for the new Transport SA performance-based specification follow the recommendation of the Author, with permanent strain rate, resilient modulus and angle of shearing resistance selected. However, it has been recognised that cohesion

also must be specified to provide a complete picture of shear strength, in keeping with the classification system presented by the Author.

Field and laboratory material performance:

It was concluded in the European ALT-MAT project (European Commission, 2000) that "alternative materials often give better mechanical performance in the field than would be expected from the results of tests such as the Los Angeles or Micro-Deval. Design should therefore be based on performance-related tests such as cyclic-load triaxial or gyratory compaction. Work needs to be done to relate these tests to measurements of field performance made with the FWD and similar tests".

From a number of case studies examined in the Author's research, relationships *do* appear to exist between key MPIs (resilient modulus, permanent strain rate and shear strength parameters) measured from laboratory RLT test results and observed field pavement performance (stiffness and deflection curvature).

Correlations of the permanent strain rate and resilient modulus with deflection curvature function appear to show great promise. The collection of more field and laboratory data, where materials tested in the laboratory replicate those conditions *in-situ*, will further validate not only the apparent relationships that exist but also the processes applied in diagnostic investigations. This in turn will lead to well researched limits for the key MPIs, which can be applied at the quality assessment phase *prior* to and during pavement construction. This implies a performance-based specification for material assessment. By pursuing this path, pavements can be constructed of sound fit-for-purpose materials, being of standard, naturally occurring source rock or alternatively processed materials (waste products). Attention should be given to the separation of inner and outer wheel path deflection curvature data when assessing any correlations with strain rate and resilient modulus.

Given that material properties (such as moisture content, grading, suction forces developed through dry-back of the materials, and density) could vary dramatically within the constructed length of a road pavement, it is essential that their influence on pavement performance be established prior to design and construction. It is

recommended that this be done by monitoring the resulting changes in the key material performance indicators listed through selectively testing for material property variations under conditions within limits expected *in-situ*.

In addition, it is considered that for the pavements currently in-service that limited pavement capacity is available in reserve to accommodate the heavier and longer vehicle combinations now using the road network. This statement is supported by the fact that statutory axle mass limits have increased dramatically over the last 15 to 20 years and now, in many countries, exceed the design axle loading. In Australia, a 10t limit is allowed for certain buses (representing a 22% overloading beyond the design value of 8.2t), whilst in the United Kingdom a 11.72t maximum loading is permitted for certain vehicles (representing a 44% overloading beyond the design value of 8.15t). This situation should be addressed immediately to achieve better compatibility between operating conditions and design. In addition, greater attention needs to be paid to pavement performance to ensure their sustainable management in future years resulting from the heavier loadings.

CHAPTER 12
FUTURE RESEARCH

Further work is recommended to examine a number of issues, which are detailed below.

At present, pavement design deflection curvature is only reported against anticipated levels of design traffic equivalent standard axle loadings and does not account for pavement type and variations in material and geology, state conditions. Further examination of the relationship between field-assessed deflection curvature and permanent strain rate is required to consolidate the interpretation derived from existing experimental data. The acquisition of new data would be useful to further validate, or modify, the strain rate limits recommended in this study. As permanent strain rate is strongly influenced by material moisture content, this information can be influential in determining the upper moisture limit which should be specified in the constructed pavement. This in turn will either ensure that the Clauses in current pavement construction specifications concerning material dry-back are either maintained or relaxed, depending on the findings and how broadly they can be applied. More certainty in this area is critical to the business of asset managers, who require knowing "what levels of deflections in pavements are tolerable". This will generally vary from pavement to pavement and between different climate zones.

Simulate wheel loading tests, using an equivalent standard axle loading, are considered valuable in determining the relationship of laboratory MPIs (particularly permanent strain rate and resilient modulus) with field performance.

Further work is required to develop a more rigorous pavement design methodology, although the Author has outlined the key factors which should be accounted for in the procedure. The Author has highlighted a rationale for sub-layering UGMs under thin bituminous surfacings of approximately 80mm or less.

Information from this and other studies is sufficient to prepare a state-of-the-art practitioners' guide for the successful use of unbound granular materials in pavements, which covers newly designed pavements and those requiring rehabilitation.

REFERENCES

AASHTO (1993),

"AASHTO Guide For Design of Pavement Structures"

Published by the American Association of State Highway and Transportation Officials, Washington.

ABS (2000),

"2000 Year Book Australia"

Australian Bureau of Statistics.

Al-Khafaf S, Hanks R J (1974),

"Evaluation of the Filter Paper Method For Estimating Soil Water Potential"

Soil Science. Volume 117, Number 4, pp. 194-199.

Andrews R C (April 1997),

"Performance Comparisons of Granular Basecourse Materials Using Repeated Load Triaxial Testing"

MTRD Report No. 16-10. Department of Road Transport-SA.

Andrews R C, Mundy M J (1993),

"Solomon Crushing Contract Material Evaluation"

Materials Services Section, Department of Road Transport. Report Number RM-Soll, 15th December 1993.

Andrews R C, Vuong B T (2000),

"Performance Based Specifications: WHY-WHAT and HOW. An Overview of Australian Developments and Implementation Strategies"

Paper from UNBAR5, June 2000, Unbound Aggregates in Roads, University of Nottingham, UK.

APRG (1993),

"Characterisation of Unbound Pavement and Subgrade Materials Using Repeated Load Triaxial Testing"

APRG Report No. 8, 1993, ISBN 0 86910 532 9.

Askegaard V (1978),

"Stress and Strain Measurement in Solid Materials"

Structural Research Laboratory, Technical University of Denmark, Report No R92, 1978.

AUSTROADS (2001),

"2001 Austroads Pavement Design Guide (final draft), for public comment"

November 2001. Austroads, Sydney.

AUSTROADS (2000),

"Facts and Figures"

Austroads Publication. Austroads, Sydney.

AUSTROADS (2000),

"Weigh-In-Motion Technology"

Austroads Publication No. AP-R168/00. Austroads, Sydney.

AUSTROADS (1992),

"Pavement Design: A guide to the Structural Design of Road Pavements"

Austroads, Sydney.

Baker H B, Buth M R, Van Deusen D A (1994),

"Minnesota Road Research Project, Load Response Instrumentation Installation and Testing Procedures"

Minnesota Department of Transportation, Report No. MN/PR-94/01, March 1994. Final Report 1992-1994.

Balay J, Gomes Correia A, Jouve P, Hornych P, Paute J-L (July 1998),

"Étude Expérimentale et Modélisation du Comportement Mécanique des graves non traitées et des Sols Supports de Chaussées, Dernières Avancées"

Bulletin Des Laboratoire central des Ponts et Chausées - 216 - July-August - Ref. 4182, pp. 3-18.

Barksdale R D, Alba J, Khosla N P, Kim R, Lambe P C, Rahman M S (June 1997),

"Laboratory Determination of Resilient Modulus for Flexible Pavement Design"

Final Unpublished Report. Prepared for National Cooperative Highway Research Program, Transport Research Board, National Research Council. Georgia Institute of Technology. Georgia Tech Project E20-634.

Bjarnason G, Erlingsson S, Petursson P (1999),

"Aggregate Resistance to Fragmentation, Weathering and Abrasion – Comparison of Different Test Methods"

Public Roads Administration, Iceland. Document No. 8/8, September 1999.

Boussinesqu J (1885),

"Application des Potentiels á l'etude de l'equilibre et du mouvement des solides élastique"

Public Roads Administration, Iceland. Document No. 8/8, September 1999.

Boyce H R (1980),

"A Non-linear model for the Elastic Behaviour of Granular Materials Under Repeated Loadings"

Proceedings International Symposium on Soils Under Cyclic and Transient Loading, Swansea, U.K. Volume 1, pp. 285-294.

Brown S F (1977),

"State-of the-Art Report on Field Instrumentation for Pavement Experiments"

Transportation Research Record, 640, Multiple Aspects of Soil Mechanics, Transport Research Board, National Research Council, Washington D.C., pp. 13-28.

Burmister D M (1945),

"The General Theory of Stresses and Displacements in Layered Soil Systems"

Journal of Applied Physics. Volume 16, pp. 84-94, 126-127, 296-302.

Butkus F (1994),

"Crushed Rockbase Investigation"

Materials Engineering Report No. 94/15 M. March 1994, Main Roads, Western Australia.

Butkus F, Goh A L (1997),

"Pavement Moduli Project. A Review of Repeated Load Triaxial Test Results (Volume 1)"

Materials and Pavement Technology Engineering Report No. 97/4 M. February 1997, Main Roads, Western Australia.

Collins R, Lee K J, Lilly G P, Westmann R A (1972),
"Mechanics of Pressure Cells"
Experimental Mechanics, Volume 12, Number 11, pp. 514-519.

Comité Européen de Normalisation (CEN) (2000),
"Unbound and Hydraulic Bound Mixtures for Roads - Test Methods - Cyclic Load Triaxial Test"
WI 00227413. October 2000.

Corté J-F, Goux M-T, et al (May 1997),
"French Design Manual for Pavement Structures"
Guide technique LCPC-SETRA. May 97. Book of Laboratoires des Ponts et Chaussées.

Craig R F (1987),
"Soil Mechanics"
Van Nostrand Reinhold (UK) Co. Ltd, 4th Edition.

Cray A (1992),
"Evaluation of Pavement Deficiency, Kwinana Freeway 13.20-19.08 SLK"
Materials Engineering Report No. 92/93 M. September 1992, Main Roads, Western Australia.

De Boissoudy A (1996),
"Summary"
Flexible Pavements. Edited by A. Gomes Correia. Balkema 1996, Rotterdam. ISBN 90 5410 523 2.

Dawson A R (1999),
"Implications of Granular Material Characteristics on the Response of Different Pavement Constructions"
Unbound Granular Materials – Laboratory Testing, In-situ Testing and Modelling. Edited by A. Gomes Correia. Proceedings of an International Workshop on Modelling and Advanced

Testing for Unbound Granular Materials. Lisbon, 21-22 January 1999. Balkema 1999, Rotterdam. ISBN 90 5410 491 0.

Djärf J, Wiman L G, Carlsson H (1996),
"A New Flexible Pavement Design Method"
Meldelande 778A. VTI Swedish National Road and Transport Research Institute. Linköping, Sweden.

Department of Road Transport (1990),
"Standard Specification for Supply and Delivery of Pavement Material"
Pavement Material (PM) Specifications.

Department of Road Transport (January 1991),
"Test Procedure DRT 107.14. Determination of Resilient Modulus of Granular Unbound Pavement Materials Using Pneumatic Apparatus"
Manual of Test Procedures.

Dunnicliff J (1988),
"Geotechnical Instrumentation for Monitoring Field Performance"
John Wiley and Sons, New York, 1988.

ECMT (1998),
"Statistical Trends in Transport 1965-1994"
European Conference of Ministers of Transport. OECD Publication Series.

European Commission (2000),
"ALT-MAT: ALTernative MATerials in road construction "
Final Project Report, RTD 4th Framework Programme (1994 – 1998). European Commission, Brussels. Contract No. RO-97-SC.2238.

European Commission (2000),
"AMADEUS: Advanced Models for Analytical Design of European Pavement Structures"
Final Project Report, RTD 4th Framework Programme (1994 – 1998). European Commission, Brussels. Contract No. RO-97-SC.2137.

European Commission (December 1999),

"Construction with Unbound Road Aggregates in Europe - COURAGE"

Final Project Report, RTD 4th Framework Programme (1994 – 1998). European Commission, Brussels. Contract No. RO-97-SC.2056. Prepared by the University of Nottingham.

European Commission (2000),

"Development of a New Bituminous Pavement Design Method – COST 333"

Final Project Report, RTD 4th Framework Programme (1994 – 1998). European Commission, Brussels.

Fuller , Thompson (1907),

as referenced by Lay, 1998

Galjaard P J, Paute J –L, Dawson A R (1996),

"Comparison and Performance of Repeated Load Triaxial Test Equipment for Unbound Granular Materials"

Proceedings of the European Symposium Euroflex 1993, Lisbon/Portugal, September 1993.

Gardner R (1937),

"A Method of Measuring the Capillary Tension of Soil Moisture Over a Wide Moisture Range"

Soil Science. Volume 43, Number 4, pp. 277-283.

Gerritsen A H, Koole R C (1986),

"Seven Years Experience with the Structural Aspects of the Shell Pavement Design Manual"

Proceedings of the 6th International Conference on the Structural Design of Asphalt Pavements, pp. 94-106.

Goh A L (1994),

"Kwinana Freeway Contract No. 140/92, Forrest Road to Thomas Road. Pavement Investigation"

Materials Engineering Report No. 94/95 M. October 1994, Main Roads, Western Australia.

Goode J (1993),

"Pavement Design and Development of the Falling Weight Deflectometer"

Thesis for the Degree of Master of Engineering, University of South Australia, February 1993.

Haynes J H , Yoder E J (1963),

"Effect of Repeated Loading on Gravel and Crushed Stone Base Course Materials used in the ASSHO Road Test"

Highway Research Board Record, No. 39. Highway Research Board.

Hazell D (1998),

"Pavement Rehabilitation Report – RN7200 Gawler By-pass, MM27.5 – MM36"

Materials Technology Section, Transport SA, Document No. 7200-98-DCH1. October 1998.

Herner R C (1955),

"Effect of Base-Course Quality on Load Transmission Through Flexible Pavements"

Proceedings of Highway Research Board, 1955.

Hicks G R, Monismith C L (1970),

"Factors Influencing the Resilient Response of Granular Materials"

Highway Research Record, No. 345, pp. 15-31.

Highways Agency (1994),

" Design Manual for Roads and Bridges"

United Kingdom Highway Agency. Volume 7 - Pavement Design and Maintenance, Section 2 - Pavement Design, Part 3, HD26/94.

Highways Department of South Australia (1989),

"Discussion Paper – Gawler Bypass Pavement, 19 October 1989"

Materials Services Section, Highways Department of South Australia. Document Number 4833R, 19th October 1989 and Document Number 7964Q, undated.

Hornych P, Kazai A, Quibel A (2000),

"Modelling of a Full Scale Experiment on Two Flexible Pavement Structures with Unbound Granular Bases"

Proceedings, International Symposium on Unbound Aggregates on Roads (UNBAR5), June 2000, Unbound Aggregates in Roads, University of Nottingham, UK.

Hornych P, Kazai A, Piau J-M (1998),

"Study of the Resilient Behaviour of Unbound Granular Materials"

Proceedings 5th International Conference Bearing Capacity of Roads & Airfields, Volume 3, pp. 1277-1287, Norwegian Univ. of Science & Technology, Trondheim, Norway, 1998.

Hornych P, Salasca S (February 1999),

"COURAGE WP4 Interim Report. Presentation of Results of the LCPC Full Scale Experiment"

Document Laboratoires des Ponts et Chaussées - WP4/8.

Hvorslev M J (1976),

"The Changeable Interaction Between Soils and Pressure Cells; Tests and Reviews at the Waterways Experiment Station"

Technical Report S-767, U.S. Army Waterways Experiment Station, Vicksburg, Mississippi, 1976.

Jones H A, Jones R H (1989),

"Horizontal Permeability of Compacted Aggregates"

Proceedings, International Symposium on Unbound Aggregates on Roads (UNBAR3), April 1989, Unbound Aggregates in Roads, Edited by R.H. Jones and A.R. Dawson, Part of Reed International Publishing, UK, pp. xxx-xxx.

Jones R H, Jones H A (1989),

"Granular Drainage Layers in Pavement Foundations"

Proceedings, International Symposium on Unbound Aggregates on Roads (UNBAR3), April 1989, Unbound Aggregates in Roads, Edited by R.H. Jones and A.R. Dawson, Part of Reed International Publishing, UK, pp. xxx-xxx.

Karol R H (1960),

"Soils and Soils Engineering"

Prentice-Hall, New Jersey, p. 11.

Laaksonen R, Huhtala M, Koskinen J, Petäjä S (1999),
"Variability of In-situ Condition (WP3) VTT Final Report, Courage WP3 Report"
RTD 4th Framework Programme (1994 – 1998). European Commission, Brussels. October 1999.

Lämsä P, Ehrola E, Belt J (1999),
"Wheel Tracking Tests. UOulu Final Report. October 1999"
University of Oulu. Road and Traffic Laboratory.

Lay M G (1998),
"Handbook of Road Technology"
Volume 1: Planning and Pavements, Third Edition.

Liddle W J (1962),
"Application of ASHO Road Test Results to the Design of Flexible Pavement Structures"
Proceedings International Conference on the Structural Design of Asphalt Pavements, Ann Arbor, Michigan, 1962, pp. 42-51.

McMahon T F, Yoder E J (1960s),
"Design of a Pressure-Sensitive Cell and Model Studies of Pressure in a Flexible Pavement Subgrade"
Source and exact date unknown.

Mathias C L (1991),
"RN 4601 Flagstaff Road, Bonneyview Road – Black Road, Pavement Design"
Materials Services Section, Department of Road Transport. 8th March 1991.

Mundy M J (1991),
"Resilient Modulus Characterisation of Granular Unbound Pavement Materials, Report No.1 "
MTRD Report No. 16-1. Department of Road Transport-SA.

Mundy M J (May 1991),
"Specification for the Supply of a Repeated Load Triaxial Testing Machine"
Department of Road Transport, SA. Internal Report. 21st May 1991.

Mundy M J (January 1992),

"Equipment and Data Acquisition Development for Dynamic Testing of Pavement Materials, Report No. 1, Asyst Software"

MTRD Report No. 8-1. Department of Road Transport-SA.

Mundy M J (1992),

"Equipment, Test Procedure and Material Evaluation for Resilient Modulus Determination of Subgrade Materials"

MTRD Report No. 66-1. Department of Road Transport-SA.

Mundy M J (September 1992),

"The Application of Non-Linear Material Model Parameters into Pavement Design Models, Report No.1"

MTRD Report No. 79-1. Department of Road Transport-SA.

Mundy M J (1993),

"Performance-Based Pavement Materials Specification"

Draft - unpublished. Department of Road Transport-SA.

Mundy M J (September 1994),

"The Influence of Density and Moisture Content on the Elastic and Plastic Properties of Pavement Materials, Boral Para Hills 20mm Crushed Rock, Report No.2"

MTRD Report No. 16-2. Department of Road Transport-SA.

Mundy M J, deVos K (1991),

"Draft Specification – Pneumatic Repeated Load Triaxial Testing Machine For Unbound Materials"

Produced in cooperation between Department of Road Transport-SA and Industrial Process Controls Limited, Revision 23 July, 1991.

NAASRA (1987),

"Pavement Design, A Guide to the Structural Design of Road Pavements"

1987.

Norman G M, Selig E T (1983),

"Ballast Performance Evaluation With Box Tests"

Bulletin American Rly Engineering Association, Number 692, Volume 84, May 1983, pp 207-239.

Paute J L, Hornych P, Benaben J P (1993),

"Repeated Load Triaxial Testing of Unbound Granular Materials in the French Network of Laboratoires des Ponts et Chaussées"

Euroflex 1993, Session 1, Lisbon, Portugal.

Paute J L, Hornych P, Benaben J P (1994),

"Comportement Mécanique des Graves Non Traitées"

Bulletin Liaison Laboratoires des Ponts et Chaussées 190, pp 27-38.

Plaistow C L, Dawson A R (1994),

"Non-Linear Behaviour of some Pavement Unbound Aggregates"

M.Sc. Thesis. Department of Civil Engineering, University of Nottingham, 1994.

Plaistow C L, Dawson A R (1996),

"Parametric Study – Flexible Pavements"

Flexible Pavements. Edited by A. Gomes Correia. Balkema 1996, Rotterdam. ISBN 90 5410 523 2.

Poli D (1999),

"Pavement Investigation Report, RN 5403 Kings Road, Salisbury Highway – Cross Keys Road (MM3.52 to 4.69km), Pavement Rehabilitation"

Materials Technology Section, Transport SA. Report Number 5403/0699, 9th June 1999.

Raad L, Figueroa J L (1980),

"Load Response of Transportation Support Systems"

Journal of the Transportation Engineering Division, ASCE, Volume 106, Number TE1, January 1980, pp. 111-128.

Selig E T (1987),

"Tensile Zone Effects on Performance of Layered Systems"

Geotechnique, Volume 37, Number 3, pp. 247-254.

Selig E T, Roner C J (1988),

"Tensile Zone Effects on Performance of Layered Systems"

Transportation Research Record, 1131, Transport Research Board, National Research Council, Washington D.C., pp. 1-6.

Selig E T (1989),

"In Situ Stress Measurements"

Proceedings, Conference on State of the Art of Pavement Response Monitoring Systems for Roads and Airfields, U.S. Army Cold Regions Research and Engineering Laboratory, Hanover, New Hampshire, pp. 162-169.

Shell International Petroleum Co. (1995),

"BISAR-PC Users Manual"

Shell International Petroleum Company, London, UK, 1995.

Shell International Petroleum Co. (1978),

"Shell Pavement Design Manual – asphalt pavements and overlays for road traffic"

Shell International Petroleum Company, London, UK, 1978.

Shook J F, Finn F N, Witczak M W, Monismith C L (1982),

"Thickness Design of Asphalt Pavements – The Asphalt Institute Method"

Fifth International Conference on the Structural Design of Asphalt Pavements, Proceedings Volume 1, Delft University of Technology, The Netherlands, pp. 17-44.

SHRP (1992),

"Interim Method of Test for Resilient Modulus of Unbound Granular Base/Subbase Materials and Subgrade Soils"

SHRP Protocol P46 (AASHTO Designation: T294-92I).

Standards Australia (1995),

"Methods of Testing Soils for Engineering Purposes. Method 6.8.1: Soil Strength and consolidation Test - Determination of the Resilient Modulus and Permanent Deformation of Granular Unbound Materials"

AS1298.6.8.1.

Stewart E H, Selig E T, Norman G H (1985),

"Failure Criteria and Lateral Stresses in Track Foundations"

Transportation Research Record, 1022, Transport Research Board, National Research Council, Washington D.C., pp. 59-64.

Sweere G T H (1989),

"Keynote paper. Design Philosophy"

Proceedings, International Symposium on Unbound Aggregates on Roads (UNBAR3), April, Unbound Aggregates in Roads. Edited by R.H. Jones and A.R. Dawson, Part of Reed International Publishing, UK, pp. 239-252.

Sweere G T H, Penning A, Vos E (1987),

"Development of a Structural Design Procedure for Asphalt Pavements with Crushed Rubble Base Courses"

Proceedings, International Conference of Structural Design of Asphalt Pavements. Volume 1, Michigan 1987, pp. 34-49.

Thom N H (1988),

"Design of Road Foundations"

Ph. D. Thesis, Department of Civil Engineering, University of Nottingham, 19888.

Thom N H, Brown S F (1988),

"The Effect of Grading and Density on the Mechanical Properties of a Crushed Dolomitic Limestone"

Proceedings 14th ARRB Conference, Part 7, 1988, pp. 94-100.

Thompson R J, Visser A T (1998),

"Pavement Design for Ultra-Heavy Mine Trucks"

Proceedings 5th International Conference Bearing Capacity of Roads & Airfields, Volume 3, pp. 649-661, Norwegian Univ. of Science & Technology, Trondheim, Norway, 1998.

Transport SA (1997),

"Construction of Unstabilised Granular Pavement"

Specification Part 221. Transport SA, November 1997.

Transport SA (1999),

"Higher Mass Limits for Vehicles Fitted with Road Friendly Suspensions"

Transport SA Information Bulletin. Transport SA, December 1999.

Transport SA (2000),

"PM 2000 - Standard Specification for Supply and Delivery of Pavement Material"

Pavement Material (PM) Specifications. Transport SA.

Tritt B (1991),

"Background, Status and Costs of UMATTA Systems"

Detailed Memorandum Document to Members of the APRG Working Group on Testing Unbound Materials. 15th October 1991. Industrial Process Controls Ltd.

Ullidtz P, Askegaard V, Sjølin FO, (1996),

"Normal Stresses in a Granular Material Under FWD Loading"

75th Annual Meeting of the Transportation Research Record, Washington D.C., 1996.

Uzan J (1985),

"Characterization of Granular Materials"

Transportation Research Record, Number 1022, Symposium on Mechanics of Granular Materials, Transport Research Board, National Research Council, Washington D.C., pp. 52-59.

Vallerga B A, Seed H B, Monismith C L, Cooper R S (1956),

"Effect of Shape, Size and Surface Roughness of Aggregate Particles on Strength of Granular Materials"

Special Technical Publication 212: Road and Paving Materials, ASTM, pp. 63-76.

Van Deusen D A (1991),

"Laboratory and Field Performance of Soil-Stress Cells"

Thesis for Master of Science, University of Minnesota, Minneapolis, Minnesota, February 1991.

Vuong B (January 1999),

"Special Lecture: Precision Studies of Resilient Modulus and Permanent Strain Testing"
Lisbon Workshop on Modelling and Advanced Testing for Unbound Granular Materials, 21-22 January 1999. IST, Lisbon, Portugal.

Walker B J (1990),

"Bass Highway, Forbes St Overpass – Don River Bridge, Pavement Investigation"
Department of Roads and Transport. Report Number 90/126, 12th September 1990.

Walker P J (1997),

"Measurement of Total Suction and Matric Suction in Pavement Materials at Dandenong ALF Site"
Road and Transport Research. A Journal of Australian and New Zealand Research and Practice. Volume 6, Number 4, December 1997.

Wallace K (1998),

"The Tensile Response of an Unbound Granular Pavement"
Road and Transport Research, A Journal of Australian and New Zealand Research and Practice. Volume 7, Number 3, September 1998.

Wardle L (2000),

"Circly"
Minicad Systems, Australia.

Witczak M W, Uzan J (1998),

"The Universal Airport Pavement Design System: Report I of IV: Granular Material Characterization"
University of Maryland, Maryland, USA.

Zeilmaker J, Henny R J (1989),

"The Measurement of Residual Stresses Due to Compaction in Granular Materials"
Proceedings, International Symposium on Unbound Aggregates on Roads (UNBAR3), April, Unbound Aggregates in Roads, Edited by R.H. Jones and A.R. Dawson, Part of Reed International Publishing, UK, pp. 159-168.

APPENDIX 1

Modelling the Effects of Seasonal Moisture Variation in a Pavement

It was discussed in §2.3.1 that work conducted as part of the European RTD COURAGE project (European Commission, 1999) has provided useful information concerning the variation of moisture levels over the seasonal cycles occurring within a year. The results suggested that pavements should be analysed according to their average moisture state within each seasonal period, particularly given the high level of moisture sensitivity of permanent deformation and resilient modulus for many materials and its subsequent effect on pavement design performance criteria. The modelling of the environmental moisture cycle in the laboratory is very important, but is a usually neglected practical aspect of pavement design.

Calculations are presented for a thinly surfaced flexible pavement, to demonstrate the importance of using a methodology that allows for estimating the modulus of all unbound layers for different seasons. The use of layer moduli for different seasons will allow the designer to determine more accurately assess the damage induced by traffic loads within each season.

Through modelling different seasonal pavements, it is aimed to examine the variations obtained in compressive (resilient) vertical strains and stresses with depth throughout the total thickness of UGMs and the tensile strain at the bottom of the asphalt. Linear elasticity is used to model the pavement properties representative of two seasonal pavements. A non-linear analysis has been applied to account for the rapid variation of resilient modulus with stress conditions, predominantly within the upper 150mm of the UGMs. The stresses and strains in the pavement layers are calculated using a multi-layer non-linear elastic pavement analysis program (program NONCIRL, based on the Burmister model). The standard axle load is a dual wheel axle load of 80kN.

Two Seasonal Pavements examined:

Case 1: ***summer conditions*** in UGMs, represented by:

DDR = 98%, RMC = 50% of OMC, Linwood crushed rock – local product

Shear strength parameters, $\phi = 50^{o}$, cohesion = 80kPa

Case 2: ***winter conditions*** in UGMs, represented by:

DDR = 98%, RMC = 85% of OMC, Linwood crushed rock – local product

Shear strength parameters, $\phi = 48^{o}$, cohesion = 35kPa

The resilient modulus values used in the two pavement response models analysed are illustrated in Figure A1.1. The pavement consists of a thin 35mm asphalt surfacing, two 150mm thick 'high' quality basecourse material layers, one 150mm thick sub-base layer, overlying a sandy clay subgrade. The layers of UGM have been further sub-divided into sub-layers to better account for the non-linear behaviour of the materials with applied stress. The influence of this affect is greatest in the top basecourse layer, where the stress changes with depth are the most severe. This shall be further discussed in Chapter 5.

It shall be noted that the modulus of the asphalt are subgrade materials was held constant so that differences in the stresses and strains, due purely to the variation in UGM properties, could be examined.

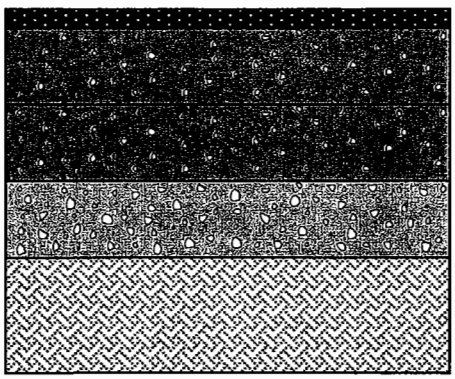

Values of Resilient Modulus for sub-layers
Case 1, 50% OMC : Case 2, 85% OMC

		Sub-layer t	2800MPa	2800MPa
A/C	35mm			
		50mm	370	260
B/C1	150mm	50mm	307	205
		50mm	297	201
		75mm	286	197
B/C2	150mm			
		75mm	276	193
		75mm	268	190
S/B	150mm			
		75mm	263	188
	2515mm		80	80
S/G				
	~ mm		10000	10000

FIGURE A1.1: PAVEMENT RESPONSE MODELS USED FOR COMPARISON OF SUB-LAYER UGMS OF TWO SEASONAL MOISTURE CONTENTS

Analysis of the results obtained from the two pavement models is presented below. Figure A1.2 shows the differences between the vertical stress distributions with

depth into the UGM layers. It can be seen that the stronger, drier, summer pavement yields slightly higher stresses at the same depth compared with the weaker, wet, winter pavement. However, this is only occurs to a depth of 200mm into the UGM. The vertical stress variation, $\Delta\sigma_{1\ max}$, is up to a maximum of 6.5%, at the top of the base layer, which decreases to zero at 200mm depth. Below this depth the stresses in the weaker pavement begin to exceed those of the stronger pavement, but only up to 13% at the base of the UGM, which equates only to about 5kPa in 40kPa. It should be noted that the modulus increase within the UGM sub-layers from the winter to the summer condition is between 40 to 50% (refer to Figure A1.1).

Thus, significant changes in the resilient moduli within the UGM sub-layers only results in relatively minor alterations in the vertical stress distribution from one seasonal condition to another.

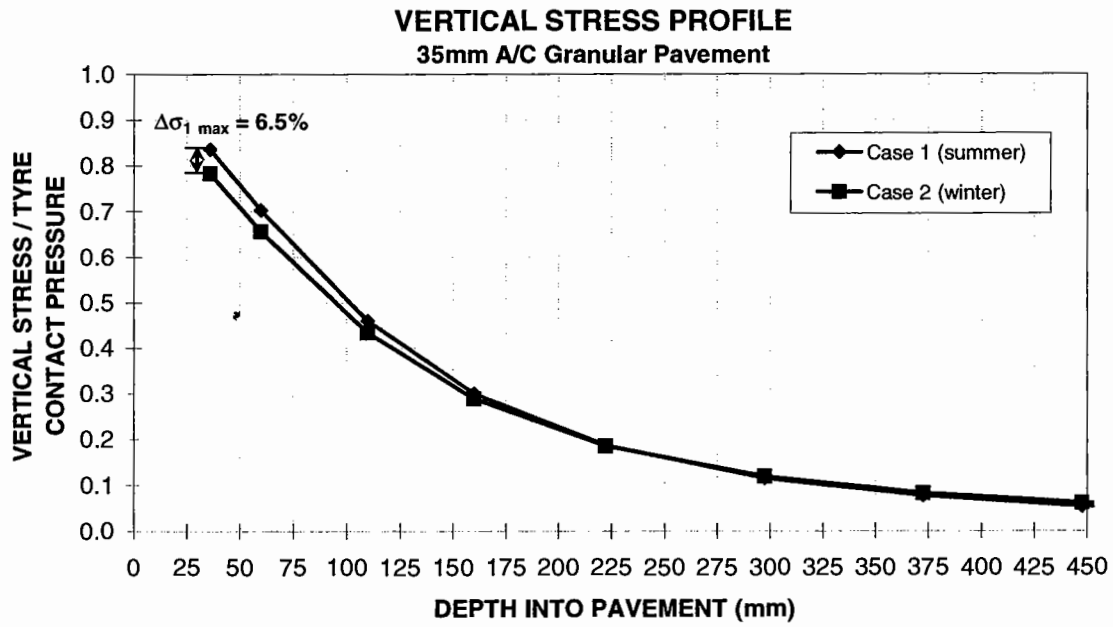

FIGURE A1.2: VERTICAL STRESS VARIATION WITH DEPTH FOR A 35MM ASPHALT-SEALED PAVEMENT

In order to determine the principal vertical and lateral strains, at selected positions within the pavement, the appropriate vertical stresses and corrected lateral stresses (according to the discussion presented in §5.3) were used along with the corresponding resilient moduli.

The principal strains have been determined according to the generalised Hooke's Law:

$$\varepsilon_1 = \frac{1}{E}[\sigma_1 - \nu(\sigma_2 + \sigma_3)] \qquad \varepsilon_2 = \frac{1}{E}[\sigma_2 - \nu(\sigma_1 + \sigma_3)] \qquad \varepsilon_3 = \frac{1}{E}[\sigma_3 - \nu(\sigma_1 + \sigma_2)]$$

... (A1.1 to A1.3)

where:

E = elastic modulus

ν = Poisson's ratio

1,2,3 = indication of principal stress and strain directions

The profiles of compressive strains with the total depth of UGM were calculated using equation A1.1, with the results presented in Figure A1.3. The results show solid profile lines that represent the differences in strains between the summer and winter pavement conditions.

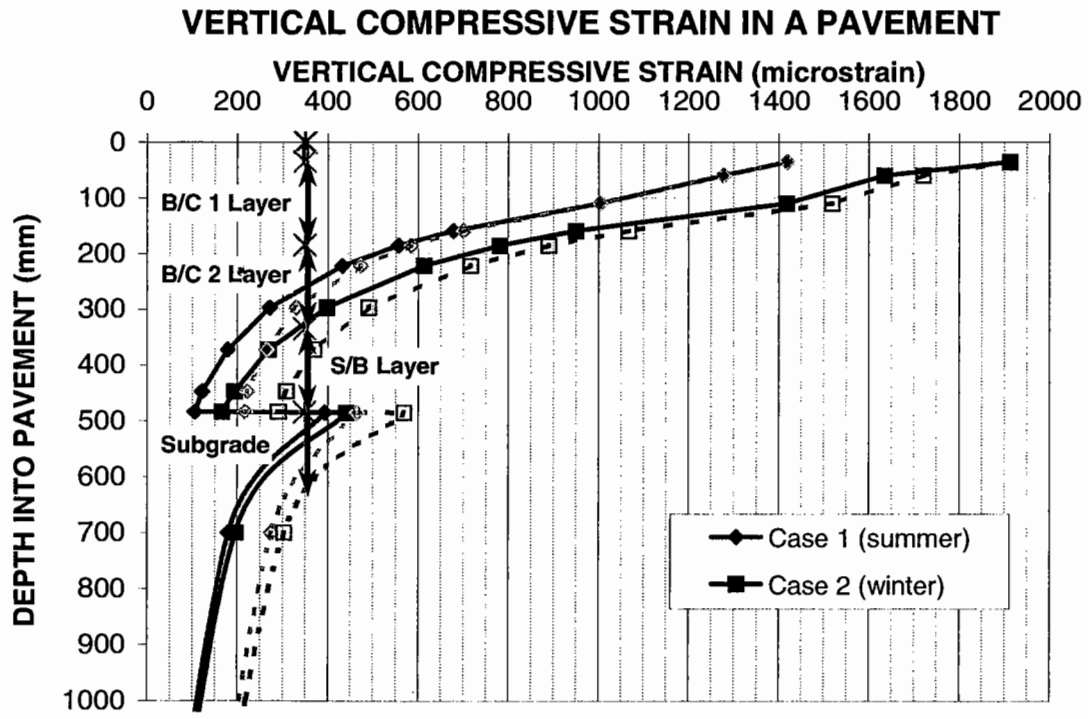

FIGURE A1.3: COMPARISON OF THE VERTICAL COMPRESSIVE STRAINS IN THE UGMS PREDICTED IN THE 'SUMMER' AND 'WINTER' PAVEMENTS ANALYSED

It can be seen from Figure A1.3 that the compressive strains are very substantially lower in the summer condition than in the winter condition, by up to a maximum of

41% at a depth of 65mm into the UGM base layer. This seems to be a critical depth as the confining pressure is quite low relative to the vertical stress at this point. From Figure A1.2, given that the differences in the vertical stress profiles between the summer and winter conditions are not that significant, the large resulting differences in the strain profiles are primarily due to the variations in sub-layer resilient moduli, by equation A1.1.

The dotted lines in Figure A1.3 illustrate the summer and winter strain profiles obtained if the lateral stresses within the UGM layers are not corrected according to the considerations discussed in §5.3. Thus, very small compressive or tensile lateral stresses, calculated by linear elastic pavement modelling software, without correction, will over-estimate the magnitude of strains predicted particularly deeper into the UGM layer (greater than 150mm).

The results of critical strains for the two pavements analysed are summarised in Table A5.1. The design values of strain considered in the table have been determined at the interface of the pavement layers ($\varepsilon_{t\ A/C}$ right at the bottom of the asphalt layer, $\varepsilon_{zz\ top\ of\ UGM}$ right at the top of the granular layer and $\varepsilon_{zz\ top\ of\ S/G}$ at the top of the subgrade).

Design Criterion	Modelling Approach	Seasonal Condition			
		Case 1 (summer)		*Case 2 (winter)*	
		strain (μstrain)	NE (1)	strain (μstrain)	NE (1)
$\varepsilon_{t\ A/C}$	corrected stresses	225	1.99×10^6	349	2.21×10^5
	stresses not corrected	228	1.86×10^6	354	2.06×10^5
$\varepsilon_{zz\ top\ of\ UGM}$	corrected stresses	1420	N/A (2)	1914	N/A (2)
	stresses not corrected	1420	N/A (2)	1914	N/A (2)
ε_{zz} 151mm into UGM (top of B/C2 layer)	corrected stresses	711	N/A (2)	1020	N/A (2)
	stresses not corrected	737	N/A (2)	1138	N/A (2)
$\varepsilon_{zz\ top\ of\ S/G}$ (3)	corrected stresses	393	3.15×10^9	443	1.34×10^9
	stresses not corrected	507	5.10×10^8	571	2.18×10^8

TABLE A1.1: CALCULATED STRAINS AT CRITICAL LOCATIONS WITHIN THE 'SUMMER' AND 'WINTER' PAVEMENTS ANALYSED

(1) NE = number of equivalent standard axle loads (80kN)

(2) N/A = no applicable performance criteria at present for calculating the number of equivalent standard axle loads

(3) The position of critical strain for the subgrade is determined at the midpoint between the dual wheels

The results of maximum surface deflection for each of the pavement types analysed showed that for Case 1: Summer Condition, d_{max} = 0.53mm, whilst for Case 2: Winter Condition, d_{max} = 0.66mm. This represents a variation of 25% from the summer condition.

The design calculations (Table A1.1) show that the:

- failure is governed by the asphalt strain criterion under both seasonal conditions, given that no UGM strain criterion currently exists.
- winter condition, which results in a dramatic reduction the stiffness of the UGM sub-layers, significantly reduces the asphalt life (ratio of 9), which represents only 88.9% of the summer condition fatigue life.
- winter condition, which results in a dramatic reduction the stiffness of each UGM sub-layer, significantly increases the vertical strain at the top of the granular layer (by 35% from the summer condition).

The design calculations presented here serve to illustrate the importance of considering the moisture content of the granular material (which depends strongly on the climatic and drainage conditions). A summary of the data analysis is presented on the next page.

SEASONAL PAVEMENT

SUMMARY OF ANALYSIS:

Linwood 20mm C/R

DDR 98 % p = 700 kPa

RMC 50 % of OMC

phi 50 deg c 80 kPa **Case 1 (summer)**

Iteration values

	σ_1	σ_1 / p	σ_3 corrected	Er	ε_1 corrected	σ_3 noncirl	ε_1 calc noncirl	ε_1 noncirl		ε_1 corrected	ε_1 noncirl
36	585	0.84	85	370	1.420E-03	85	1.420E-03	1.42E-03		1420	1420
60	491	0.70	25	370	1.280E-03	25.3	1.279E-03	1.28E-03		1280	1279
110	322	0.46	19	307	1.006E-03	19	1.006E-03	9.74E-04		1006	1006
160	210	0.30	12	297	6.788E-04	2.4	7.014E-04	6.90E-04		679	701
186	170	0.24	11	291	5.577E-04	-0.8	5.861E-04	5.93E-04		558	586
222.5	131	0.19	10	286	4.336E-04	-6.7	4.744E-04	4.72E-04		434	474
297.5	81	0.12	8	276	2.732E-04	-15	3.315E-04	3.31E-04		273	332
372.5	54	0.08	8	268	1.806E-04	-24.6	2.657E-04	2.60E-04		181	266
447.5	38	0.05	8	263	1.232E-04	-29.6	2.233E-04	2.24E-04		123	223
484	33.7	0.05	8	263	1.068E-04	-34.1	2.189E-04	2.19E-01		107	219
486	37.1	0.05	8	80	3.938E-04	-0.25	4.659E-04	5.07E-04		394	466
700	20.1	0.03	8	80	1.813E-04	-2.9	2.766E-04	2.76E-04		181	277
1743	5	0.01	9	80	-1.625E-05	-0.5	6.688E-05	6.76E-05		-16	67
3001	2	0.00	12	10000	-6.400E-07						

Critical values

Fatigue Life

	σ_1	σ_1 / p	σ_3 corrected	Er	ε_2 corrected	ε_2 noncirl	ε_2 corrected	V_b vol bit	$K_{A/C}$
a/c	587	0.84	-644	2800	-2.249E-04	-2.28E-04	-225	11	4169
								n	N
								5	1.99E+06
					ε_1 corrected	ε_1 noncirl	ε_1 corrected		$K_{S/G}$
s/g	37	0.05	8	80	3.925E-04	5.07E-04	393		8511
								n	N
								7.14	3.15E+09

Linwood 20mm C/R

DDR 98 %

RMC 85 % of OMC

phi 48 deg c 35 kPa **Case 2 (winter)**

Iteration values

	σ_1	σ_1 / p	σ_3	Er	ε_1 corrected	σ_3 noncirl	ε_1 calc noncirl	ε_1 noncirl		ε_1 corrected	ε_1 noncirl
36	548	0.78	72	260	1.914E-03	72	1.914E-03	1.92E-03		1914	1914
60	459	0.66	48	260	1.636E-03	16	1.722E-03	1.72E-03		1636	1722
110	304	0.43	19	205	1.418E-03	-10.9	1.520E-03	1.52E-03		1418	1520
160	203	0.29	17	201	9.507E-04	-16.7	1.068E-03	1.07E-03		951	1068
186	167	0.24	15	200	7.825E-04	-16.1	8.914E-04	9.06E-04		783	891
222.5	130	0.19	13	197	6.137E-04	-16.1	7.171E-04	7.18E-04		614	717
297.5	84	0.12	10	193	3.990E-04	-15.8	4.925E-04	4.92E-04		399	493
372.5	58	0.08	9.5	190	2.703E-04	-17.7	3.705E-04	3.70E-04		270	370
447.5	43	0.06	9	188	1.952E-04	-21.7	3.095E-04	3.07E-04		195	310
484	37.7	0.05	9	188	1.670E-04	-24.6	2.921E-04	2.93E-04		167	292
486	41.7	0.06	9	80	4.425E-04	-5.6	5.703E-04	5.71E-04		443	570
700	22.1	0.03	9	80	1.975E-04	-3.2	3.043E-04	3.04E-04		198	304
1743	5	0.01	9	80	-1.625E-05	-0.55	6.731E-05	7.03E-05		-16	67
3001	2	0.00	12	10000	-6.400E-07						

Critical values

Fatigue Life

	σ_1	σ_1 / p	σ_3	Er	ε_2 corrected	ε_2 noncirl	ε_2 corrected	V_b vol bit	$K_{A/C}$
a/c	551	0.79	-1120	2800	-3.492E-04	-3.54E-04	-349	11	4169
								n	N
								5	2.20E+05
								% Reduction life	
								88.9	
					ε_1 corrected	ε_1 noncirl	ε_1 corrected		$K_{S/G}$
s/g	41.7	0.06	9	80	4.425E-04	5.71E-04	443		8511
								n	N
								7.14	1.34E+09
								% Reduction life	
								57.5	

APPENDIX 2

Determination of Vertical Stress at Depth z in UGM under a Vibratory Roller

Calculations are presented to examine the work of Barksdale (1997) to determine vertical stresses at depth z into the UGM under the centre of a vibratory roller, of diameter 60in (1.52m) and the length of 84in (2.134m).

Vertical stresses at depth z can be estimated by superposition using Fadum charts (Craig, 1987) to determine the values under the centre of the roller drum where the residual stresses were measured, ie, 5in (127mm) and 11in (279mm).

Barksdale suggests measurements were taken for an embedment depth of 0.05in to which he equated the estimated width of roller contact area as being approximately "2 to 3 in at the completion of rolling" [in recent e-mail correspondence] (the value determined by the Author being 3.5in, see below).

Parameters:

Unit weight of UGM = 18kN/m^3

Roller radius = 0.762m

Roller length = 2.134m

Embedment of roller into the granular material = 0.05in = 1.27mm = 0.00127m

Maximum dynamic force = $F_{dynamic}$ = 199.24kN or 93.4kN/m length

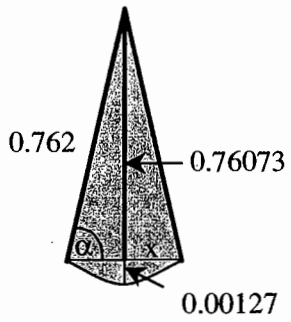

FIGURE A2.1: ELEVATED VIEW OF A PORTION OF THE EMBEDDED ROLLER

$$\sin\alpha = \frac{0.76073}{0.762} = 0.99833$$

$$\text{Thus, } \alpha = 86.692°$$

$$x = 0.04398\text{m and } 2x = 0.08795\text{m } (= 3.46\text{in} \cong 3.5\text{in})$$

Thus, the dynamic pressure imparted by the vibratory roller, which acts over an area of 2.13m by 0.08795m, is:

$$p = \frac{F_{dynamic}}{\text{Area}} = \frac{199.24\text{kN}}{2.13\text{m} \times 0.08795\text{m}} = 1062\text{kPa}$$

The vertical stress shall be estimated by using Fadum Charts based on summation of the contribution of the four equal area pressure pads (see Figure A2.2).

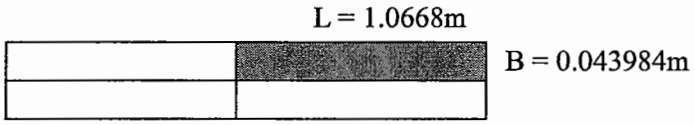

FIGURE A2.2: PLAN VIEW OF ROLLER IMPRINT

For depth required of z = 5in = 0.127m

$$m = \frac{B}{z} = 0.346\,,\ n = \frac{L}{z} = 8.400 \quad \Rightarrow I_\theta = 0.105$$

Thus, $4I_\theta = 0.420\,,\ \sigma_v = 0.420 \times 1062 = 446\text{kPa}$

where I_θ = influence factor for vertical stress determination under a pressure pad

For depth required of z = 11in = 0.279m

$$m = \frac{B}{z} = 0.158\,,\ n = \frac{L}{z} = 3.824 \quad \Rightarrow I_\theta = 0.050$$

Thus, $4I_\theta = 0.200\,,\ \sigma_v = 0.200 \times 1062 = 212\text{kPa}$

APPENDIX 3

AWGRU (1999) Proposed Stress Combinations for RLT resilient modulus Stress Stage testing.

Stress Level	p (kPa)	q (kPa)	σ_1 (kPa)	σ_3 (kPa)	q/p
0 prec	83	100	150	50	1.2
1	83	100	150	50	1.2
2	125	150	225	75	1.2
3	167	200	300	100	1.2
4	208	250	375	125	1.2
5	250	300	450	150	1.2
6	100	150	200	50	1.5
7	150	225	300	75	1.5
8	200	300	400	100	1.5
9	250	375	500	125	1.5
10	300	450	600	150	1.5
11	82	125	165	40	1.5
12	63	100	130	30	1.6
13	90	150	190	40	1.7
14	117	200	250	50	1.7
15	175	300	375	75	1.7
16	233	400	500	100	1.7
17	292	500	625	125	1.7
18	175	300	375	75	1.7
19	72	125	155	30	1.7
20	53	100	120	20	1.9
21	80	150	180	30	1.9
22	107	200	240	40	1.9
23	133	250	300	50	1.9
24	200	375	450	75	1.9
25	267	500	600	100	1.9
26	88	175	205	30	2.0
27	150	300	350	50	2.0
28	225	450	525	75	2.0
29	150	300	350	50	2.0
30	62	125	145	20	2.0
31	123	250	290	40	2.0
32	97	200	230	30	2.1
33	132	275	315	40	2.1
34	167	350	400	50	2.1
35	250	525	600	75	2.1
36	70	150	170	20	2.1
37	140	300	340	40	2.1
38	183	400	450	50	2.2
39	148	325	365	40	2.2
40	113	250	280	30	2.2
41	78	175	195	20	2.2
42	157	350	390	40	2.2
43	200	450	500	50	2.3
44	122	275	305	30	2.3
45	165	375	415	40	2.3

46	138	325	355	30	2.3
47	95	225	245	20	2.4
48	190	450	490	40	2.4
49	103	250	270	20	2.4
50	207	500	540	40	2.4
51	163	400	430	30	2.4
52	120	300	320	20	2.5
53	180	450	480	30	2.5
54	240	600	640	40	2.5
55	197	500	530	30	2.5
56	137	350	370	20	2.6
57	213	550	580	30	2.6
58	145	375	395	20	2.6
59	222	575	605	30	2.6
60	187	500	520	20	2.7

TABLE A3.1: AWGRU (1999) MATERIAL RLT TEST STRESS LEVELS

APPENDIX 4

New Stress Combinations proposed for RLT resilient modulus stress stage testing

Stress Level	p (kPa)	q (kPa)	σ_1 (kPa)	σ_3 (kPa)	q/p
0 prec	133	250	300	50	1.88
1	124	155	227	72	1.25
2	164	205	300	95	1.25
3	207	260	380	120	1.26
4	248	310	455	145	1.25
5 R	164	205	300	95	1.25
6	60	90	120	30	1.50
7	90	135	180	45	1.50
8	119	178	238	60	1.50
9	155	233	310	77	1.51
10	198	295	395	100	1.49
11	238	355	475	120	1.49
12	275	412	550	138	1.50
13	315	473	630	157	1.50
14 R	238	355	475	120	1.49
15	148	258	320	62	1.74
16	185	323	400	77	1.75
17	224	392	485	93	1.75
18	260	455	563	108	1.75
19	300	525	650	125	1.75
20 R	224	392	485	93	1.75
21 R	148	258	320	62	1.74
22	82	163	190	27	1.99
23	109	219	255	36	2.00
24	140	280	327	47	2.00
25	175	350	408	58	2.00
26	213	425	496	71	2.00
27	250	500	583	83	2.00
28 R	213	425	496	71	2.00
29 R	140	280	327	47	2.00
30	132	297	330	33	2.25
31	167	375	417	42	2.24
32	204	460	510	50	2.26
33 R	167	375	417	42	2.24
34	48	120	128	8	2.50
35	75	187	200	13	2.48
36	99	248	265	17	2.50
37	125	314	335	21	2.51

TABLE A4.1: BASE MATERIAL RLT TEST STRESS LEVELS

R = Repeat or duplicate test conditions

Stress Level	p (kPa)	q (kPa)	σ_1 (kPa)	σ_3 (kPa)	q/p
1 prec	82	162	190	28	1.98
2	95	142	190	48	1.49
3	60	90	120	30	1.50
4	30	45	60	15	1.50
5	55	110	128	18	2.01
6	82	163	191	28	1.98
7	75	188	200	12	2.52
8	48	120	128	8	2.50
9	34	84	90	6	2.47
10	16	40	43	3	2.45

TABLE A4.2: SUB-BASE MATERIAL RLT TEST STRESS LEVELS

APPENDIX 5

Boyce Model - data comparison by modelling all q/p ratios against selected q/p ratios

Materials analysed are the French Gneiss, Portuguese Granite and Solvenian Limestone tested by RLT testing using the CEN Method A as part of the COURAGE Project.

Select stress ratios are either:
q/p = all (0, 0.5, 1.0, 1.5, 2.0, 2.5), or
q/p = 1.0, 1.5, 2.0, or
q/p = 1.5, 2.0, 2.5

Reported in the tables are:
the Boyce parameters K_a, G_a, n, γ

the measure of fit, ρ , given by:

$$\rho = 1 - \sqrt{\frac{1}{2}\left\{\left[\frac{\Sigma\left(\varepsilon_{v\,meas} - \varepsilon_{v\,calc}\right)^2}{\Sigma\left(\varepsilon_{v\,meas} - mean\varepsilon_{v\,meas}\right)^2}\right] + \left[\frac{\Sigma\left(\varepsilon_{q\,meas} - \varepsilon_{q\,calc}\right)^2}{\Sigma\left(\varepsilon_{q\,meas} - mean\varepsilon_{q\,meas}\right)^2}\right]\right\}}$$

the elastic, isotropic derived E_v and ν, based upon the Hooke's law equations

the average variation of elastic modulus (via Hooke) determined from equation:

$$\%E_r \text{ variation} = \frac{\Sigma\sqrt{\left\{\frac{\left[E_{meas} - E_{calc}\right]}{E_{meas}}\right\}^2}}{N}$$ within each of the stress ratio sets examined

where:

E_{meas} = elastic modulus determined for the stress stages considered, using measured elastic strains (ε_v and ε_q)

E_{calc} = elastic modulus determined for stress stages considered, using elastic strains (ε_v and ε_q) calculated from Boyce equations for each of the stress ratio sets examined

N = number of samples within the stress ratio set examined

the Boyce derived E_v and ν, based upon the Boyce equations

Note: the $\%E_r$ variation determined when modelling all q/p stress ratios only uses either q/p = 1.0, 1.5 and 2.0 or q/p = 1.5, 2.0 and 2.5, to allow direct comparison of the results with those when only the limited q/p ratios were modelled.

FRENCH GNEISS MATERIAL:

Test ID	Parameter	γ = vary			γ = 1		
		Data for q/p			Data for q/p		
		All	1→2	1.5→2.5	All	1→2	1.5→2.5
DDR=96.8%	Ka	65.41	57.70	53.10	66.14	60.23	53.45
RMC=38%	Ga	143.14	131.4	123.03	110.5	93.24	88.82
SN 9-028-1a	n	0.307	0.234	0.194	0.448	0.394	0.362
	γ	1.393	1.563	1.726	1.000	1.000	1.000
	ρ	0.788	0.835	0.838	0.640	0.548	0.499
	E_{calc} (E_{meas} = 423)	**314**	278	246	451	437	**436**
	ν_{calc} (ν_{meas} = 0.02)	**0.04**	0.05	0.06	0.01	0.04	**0.00**
	% E (elastic) var	30.1	39.2		11.8	9.9	
		24.7		43.2	15.5		**9.2**
	E_v Boyce MPa	327	281	244	383	353	338
	ν Boyce	-0.03	-0.08	-0.10	0.05	0.09	0.06
DDR=96.8%	Ka	60.19	54.88	47.38	64.71	59.35	48.88
RMC=38%	Ga	147.22	149.0	124.59	102.9	87.29	78.66
SN 9-012-1a	n	0.236	0.190	0.145	0.469	0.422	0.362
	γ	1.765	2.027	2.285	1.000	1.000	1.000
	ρ	0.730	0.728	0.794	0.415	0.283	0.270
	E_{calc} (E_{meas} = 379)	**226**	195	166	414	396	**394**
	ν_{calc} (ν_{meas} = 0.04)	**0.07**	0.07	0.08	0.04	0.07	**0.02**
	% E (elastic) var	45.2	53.6		16.1	12.0	
		40.4		57.3	20.7		**11.4**
	E_v Boyce MPa	259	225	180	356	327	304
	ν Boyce	-0.08	-0.25	-0.24	0.06	0.10	0.08
DDR=97%	Ka	47.84	47.12	45.52	48.10	49.72	46.40
RMC=68%	Ga	62.19	67.98	60.69	61.61	64.36	59.16
SN 8-362-1a	n	0.335	0.270	0.280	0.347	0.352	0.326
	γ	1.026	1.189	1.108	1.000	1.000	1.000
	ρ	0.844	0.873	0.818	0.843	0.812	0.772
	E_{calc} (E_{meas} = 353)	**336**	299	317	345	355	**351**
	ν_{calc} (ν_{meas} = 0.13)	**0.14**	0.13	0.14	0.14	0.14	**0.15**
	% E (elastic) var	5.6	16.8		5.7	6.3	
		4.6		8.9	4.9		**4.5**
	E_v Boyce MPa	257	239	239	262	271	258
	ν Boyce	0.18	0.14	0.16	0.17	0.17	0.18
DDR=97%	Ka	55.41	55.70	52.12	54.05	55.58	52.05
RMC=67%	Ga	65.19	70.69	65.42	67.65	70.84	65.46
SN 9-007-1a	n	0.385	0.336	0.319	0.338	0.343	0.317
	γ	0.920	0.995	0.997	1.000	1.000	1.000
	ρ	0.884	0.895	0.856	0.874	0.896	0.857
	E_{calc} (E_{meas} = 401)	420	400	**395**	387	397	**394**
	ν_{calc} (ν_{meas} = 0.17)	0.18	0.16	**0.17**	0.17	0.16	**0.17**
	% E (elastic) var	10.8	3.3		3.4	3.2	
		10.7		**2.8**	3.4		**2.7**
	E_v Boyce MPa	309	304	290	293	303	290
	ν Boyce	0.17	0.16	0.17	0.18	0.18	0.19

Test ID	Parameter	γ = vary			γ = 1		
		Data for q/p			Data for q/p		
		All	1→2	1.5→2.5	All	1→2	1.5→2.5
DDR=97%	Ka	52.05	53.40	48.67	53.50	54.26	52.52
RMC=83%	Ga	48.47	53.30	42.79	53.42	58.73	49.24
SN 9-011-1a	n	0.446	0.440	0.451	0.358	0.365	0.328
	γ	0.837	0.862	0.776	1.000	1.000	1.000
	ρ	0.864	0.853	0.740	0.826	0.818	0.731
	E_{calc} (E_{meas} = 335)	**383**	388	416	318	335	**325**
	ν_{calc} (ν_{meas} = 0.18)	**0.21**	0.18	0.22	0.19	0.16	**0.20**
	% E (elastic) var	23.5	22.4		6.2	4.3	
		21.4		34.1	4.6		**3.3**
	E_v Boyce MPa	266	276	266	243	259	236
	ν Boyce	0.21	0.19	0.20	0.26	0.23	0.29
DDR=99.8%	Ka	60.18	57.19	55.25	60.29	58.71	57.31
RMC=66%	Ga	82.91	81.17	80.42	82.68	79.20	78.54
SN 9-025-1a	n	0.363	0.308	0.282	0.367	0.347	0.341
	γ	1.007	1.077	1.123	1.000	1.000	1.000
	ρ	0.877	0.899	0.879	0.877	0.871	0.813
	E_{calc} (E_{meas} = 450)	**432**	409	393	435	440	**441**
	ν_{calc} (ν_{meas} = 0.11)	**0.11**	0.12	0.11	0.11	0.12	**0.11**
	% E (elastic) var	4.7	6.8		4.6	4.6	
		4.6		10.5	4.7		**4.2**
	E_v Boyce MPa	335	314	300	336	331	328
	ν Boyce	0.14	0.14	0.14	0.14	0.15	0.15
DDR=95%	Ka	73.04	68.92	55.98	73.21	67.05	55.73
RMC=66%	Ga	105.60	110.8	82.68	87.23	81.58	70.43
SN 9-020-1a	n	0.389	0.328	0.275	0.527	0.479	0.410
	γ	1.295	1.436	1.381	1.000	1.000	1.000
	ρ	0.817	0.770	0.749	0.719	0.592	0.551
	E_{calc} (E_{meas} = 353)	**271**	249	250	351	354	**345**
	ν_{calc} (ν_{meas} = 0.12)	**0.13**	0.12	0.13	0.15	0.15	**0.14**
	% E (elastic) var	23.3	31.2		11.0	10.0	
		18.0		26.9	15.5		**8.8**
	E_v Boyce MPa	285	270	237	313	306	283
	ν Boyce	0.18	0.12	0.18	0.16	0.16	0.16

PORTUGUESE GRANITE MATERIAL:

Test ID	Parameter	γ = vary			γ = 1		
		Data for q/p			Data for q/p		
		All	1→2	1.5→2.5	All	1→2	1.5→2.5
DDR=96.8%	Ka	48.01	46.28	39.87	48.59	47.20	41.91
RMC=36.3	Ga	111.01	119.5	97.32	109.2	106.00	89.75
SN 191198-	n	0.316	0.290	0.241	0.330	0.331	0.299
	γ	1.029	1.118	1.154	1.000	1.000	1.000
	ρ	0.732	0.744	0.832	0.734	0.754	0.836
	E_{calc} (E_{meas} = 441)	**484**	430	392	500	484	**457**
	ν_{calc} (ν_{meas} = -0.05)	**-0.08**	-0.07	-0.03	-0.08	-0.08	**-0.06**
	% E (elastic) var	11.6	17.8		12.5	11.0	
		8.3		15.0	12.6		**3.9**
	E_v Boyce MPa	367	343	228	375	364	326
	ν Boyce	-0.07	-0.15	-0.11	-0.06	-0.06	-0.04
DDR=96.9%	Ka	67.46	65.73	57.77	67.96	66.69	60.01
RMC=54.2	Ga	79.05	85.08	65.22	90.70	93.42	74.01
SN 260998-	n	0.514	0.451	0.424	0.418	0.414	0.360
	γ	0.840	0.916	0.857	1.000	1.000	1.000
	ρ	0.769	0.816	0.804	0.725	0.791	0.767
	E_{calc} (E_{meas} = 421)	529	**490**	495	440	449	**423**
	ν_{calc} (ν_{meas} = 0.10)	0.09	**0.07**	0.10	0.08	0.06	**0.10**
	% E (elastic) var	25.5	**10.8**		11.7	11.3	
		31.2		20.1	7.9		**4.5**
	E_v Boyce MPa	378	367	333	352	358	313
	ν Boyce	0.13	0.11	0.15	0.14	0.12	0.18
DDR=97%	Ka	40.08	41.70	40.96	41.31	42.71	44.02
RMC=69.5	Ga	41.99	49.28	44.00	53.63	67.34	58.04
SN 021098-	n	0.464	0.447	0.467	0.280	0.300	0.293
	γ	0.669	0.711	0.683	1.000	1.000	1.000
	ρ	0.838	0.779	0.613	0.688	0.630	0.545
	E_{calc} (E_{meas} = 387)	579	573	566	366	400	**378**
	ν_{calc} (ν_{meas} = 0.01)	0.01	-0.03	0.01	0.04	-0.02	**0.05**
	% E (elastic) var	418.8	141.1		20.3	19.9	
		67.8		62.1	8.5		**8.2**
	E_v Boyce MPa	308	322	310	243	279	258
	ν Boyce	0.12	0.10	0.12	0.18	0.09	0.17
DDR=97.2%	Ka	60.77	58.46	54.14	63.14	62.61	65.15
RMC=65.6	Ga	68.78	66.65	52.85	78.64	84.91	82.17
SN 090199-	n	0.523	0.535	0.571	0.473	0.482	0.506
	γ	0.888	0.854	0.767	1.000	1.000	1.000
	ρ	0.784	0.718	0.428	0.756	0.680	0.382
	E_{calc} (E_{meas} = 341)	**390**	412	437	343	354	**336**
	ν_{calc} (ν_{meas} = 0.09)	**0.07**	0.05	0.09	0.07	0.04	**0.07**
	% E (elastic) var	23.9	34.7		11.3	11.7	
		24.2		44.4	12.3		**11.9**
	E_v Boyce MPa	301	306	292	293	305	294
	ν Boyce	0.15	0.14	0.16	0.15	0.12	0.14

Test ID	Parameter	γ = vary			γ = 1		
		Data for q/p			Data for q/p		
		All	1→2	1.5→2.5	All	1→2	1.5→2.5
DDR=95%	Ka	27.88	27.84	26.53	24.40	23.60	22.75
RMC=60%	Ga	29.10	31.73	27.80	35.57	36.02	29.05
SN 240599-	n	0.443	0.415	0.405	0.196	0.182	0.159
	γ	0.585	0.616	0.597	1.000	1.000	1.000
	ρ	0.902	0.902	0.850	0.683	0.696	0.792
	E_{calc} (E_{meas} = 344)	600	584	579	323	345	**344**
	ν_{calc} (ν_{meas} = 0.00)	-0.04	-0.08	-0.03	0.03	-0.01	**0.03**
	% E (elastic) var	136.1	147.5		28.0	18.1	
		100.8		92.2	11.9		4.4
	E_v Boyce MPa	267	268	253	170	172	152
	ν Boyce	0.10	0.09	0.11	0.15	0.13	0.21
DDR=95%	Ka	41.32	37.51	34.76	31.07	27.26	26.35
RMC=64.7	Ga	43.30	40.49	36.30	47.60	41.10	39.92
SN 090299-	n	0.466	0.422	0.404	0.194	0.169	0.164
	γ	0.669	0.674	0.659	1.000	1.000	1.000
	ρ	0.816	0.889	0.894	0.683	0.744	0.759
	E_{calc} (E_{meas} = 348)	465	444	436	**374**	365	362
	ν_{calc} (ν_{meas} = 0.13)	0.14	0.14	0.16	**0.12**	0.13	0.13
	% E (elastic) var	91.1	92.1		15.7	13.3	
		66.6		58.4	**5.7**		7.3
	E_v Boyce MPa	317	300	285	223	199	194
	ν Boyce	0.12	0.12	0.13	0.13	0.14	0.14
DDR=100%	Ka	69.69	62.48	54.24	71.07	63.31	58.05
RMC=62.7	Ga	82.12	72.40	70.13	74.62	67.27	62.80
SN 130599-	n	0.369	0.343	0.221	0.457	0.404	0.384
	γ	1.171	1.132	1.470	1.000	1.000	1.000
	ρ	0.815	0.804	0.803	0.782	0.786	0.700
	E_{calc} (E_{meas} = 330)	299	**307**	232	347	345	**335**
	ν_{calc} (ν_{meas} = 0.22)	0.19	**0.20**	0.18	0.22	0.22	**0.22**
	% E (elastic) var	16.7	**12.9**		10.2	8.6	
		10.0		31.8	13.5		**7.6**
	E_v Boyce MPa	278	267	208	298	283	269
	ν Boyce	0.25	0.27	0.33	0.22	0.23	0.23
DDR=100.1	Ka	64.77	55.70	48.55	65.01	55.75	49.43
RMC=63.4	Ga	104.57	89.39	77.92	101.6	86.84	73.59
SN 050299-	n	0.418	0.360	0.286	0.437	0.374	0.338
	γ	1.036	1.032	1.126	1.000	1.000	1.000
	ρ	0.712	0.736	0.771	0.713	0.738	0.766
	E_{calc} (E_{meas} = 379)	**411**	403	346	427	416	**391**
	ν_{calc} (ν_{meas} = 0.08)	**0.06**	0.06	0.08	0.06	0.06	**0.07**
	% E (elastic) var	**18.1**	16.1		18.4	15.7	
		12.8		11.5	16.4		**6.8**
	E_v Boyce MPa	355	326	274	361	330	296
	ν Boyce	0.07	0.08	0.10	0.07	0.09	0.11

SOLVENIAN LIMESTONE MATERIAL:

Test ID	Parameter	γ = vary			γ = 1		
		Data for q/p			Data for q/p		
		All	1→2	1.5→2.5	All	1→2	1.5→2.5
DDR=96.8%	Ka	71.55	76.74	73.85	65.79	66.03	58.97
RMC=67.3	Ga	83.88	94.91	74.47	90.54	95.13	80.78
SN	n	0.261	0.297	0.356	0.176	0.180	0.152
	γ	0.778	0.778	0.645	1.000	1.000	1.000
	ρ	0.846	0.846	0.866	0.826	0.831	0.736
	Ec (meas. = 824)	1067	1080	1270	**825**	834	839
	ν_{calc} (ν_{meas} = 0.13)	0.17	0.13	0.18	**0.15**	0.13	0.15
	% E (elastic) var	67.9	44.3		17.6	16.9	
		28.0		62.2	**8.7**		9.9
	Ev Boyce MPa	559	604	627	447	460	410
	ν Boyce	0.15	0.13	0.15	0.18	0.16	0.18
DDR=96.9%	Ka	75.80	79.26	74.73	70.66	68.87	62.81
RMC=67.3	Ga	68.30	79.16	60.91	84.27	87.99	69.06
SN	n	0.355	0.366	0.434	0.175	0.168	0.136
	γ	0.613	0.644	0.544	1.000	1.000	1.000
	ρ	0.849	0.857	0.864	0.748	0.761	0.717
	Ec (meas. = 860)	1380	1346	1530	824	870	**880**
	ν_{calc} (ν_{meas} = 0.13)	0.20	0.14	0.22	0.16	0.12	**0.15**
	% E (elastic) var	155.5	493.0		23.2	21.2	
		70.0		103.7	12.3		**10.9**
	Ev Boyce MPa	644	671	671	443	456	389
	ν Boyce	0.15	0.13	0.14	0.24	0.21	0.28
DDR=95.7%	Ka	74.36	76.51	76.20	71.40	73.85	72.30
RMC=57.1	Ga	103.02	115.8	109.60	108.3	120.37	111.71
SN	n	0.283	0.289	0.309	0.220	0.243	0.239
	γ	0.845	0.896	0.867	1.000	1.000	1.000
	ρ	0.799	0.839	0.867	0.784	0.819	0.847
	Ec (meas. = 777)	987	911	**905**	821	811	**780**
	ν_{calc} (ν_{meas} = 0.03)	0.02	0.01	**0.03**	0.04	0.02	**0.04**
	% E (elastic) var	31.6	17.9		11.6	15.0	
		28.4		**16.6**	4.2		**3.4**
	Ev Boyce MPa	571	571	565	495	522	497
	ν Boyce	0.11	0.08	0.09	0.13	0.09	0.12
DDR=96%	Ka	114.34	112.1	96.16	106.1	108.65	84.50
RMC=57.1	Ga	135.80	151.5	116.40	152.5	164.62	121.54
SN	n	0.445	0.395	0.382	0.310	0.329	0.254
	γ	0.802	0.886	0.803	1.000	1.000	1.000
	ρ	0.798	0.815	0.865	0.750	0.784	0.853
	Ec (meas. = 822)	1083	**982**	1030	864	871	**834**
	ν_{calc} (ν_{meas} = 0.13)	0.14	**0.11**	0.14	0.13	0.10	**0.14**
	% E (elastic) var	33.1	**12.9**		10.5	11.4	
		35.1		27.0	5.1		**3.6**
	Ev Boyce MPa	738	715	665	647	670	552
	ν Boyce	0.13	0.10	0.12	0.13	0.11	0.14

APPENDIX 6

Testing Results from Chapter 8

Material Description

Crushed Rock and Quarry Rubble Materials

Boral Para Hills

20mm sand/siltstone and quartzite blend, with the sand/siltstone essentially blended in at the –4.75mm sieve.

Boral Lobethal

20mm dolomitic meta-siltstone

Linwood

20mm dolomitic siltstone

Stonyfell

20mm sand/siltstone and quartzite blend

A6.1 Shear Strength Characterisation

Crushed Rock Quarry Materials

A6.1.1 Boral Para Hills

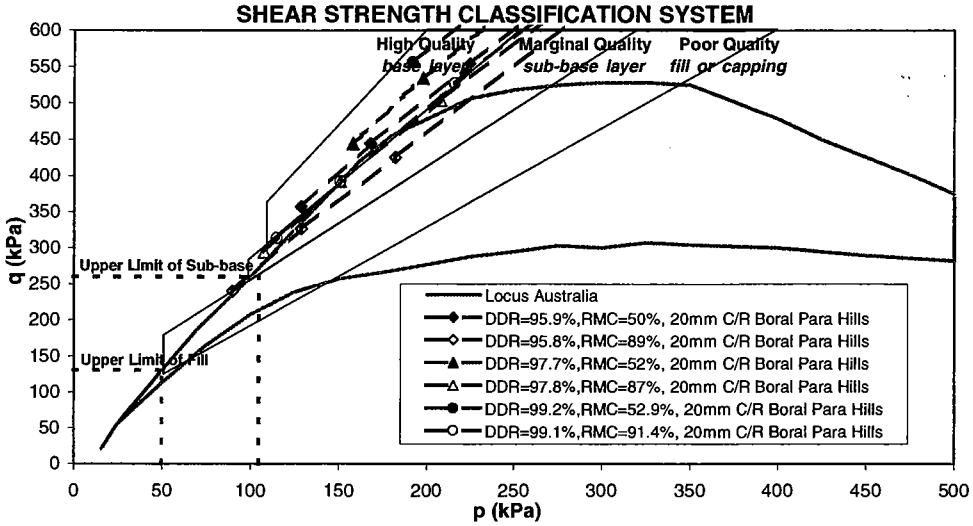

FIGURE A6.1: SHEAR STRENGTH, 20MM C/R BORAL PARA HILLS MATERIAL

A6.1.2 Boral Lobethal

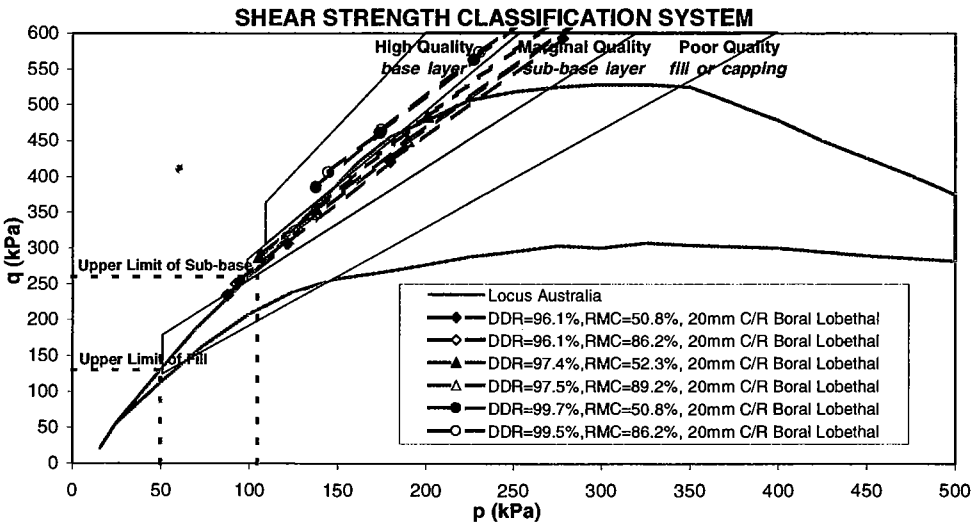

FIGURE A6.2: SHEAR STRENGTH, 20MM C/R BORAL LOBETHAL MATERIAL

A6.1.3 Linwood

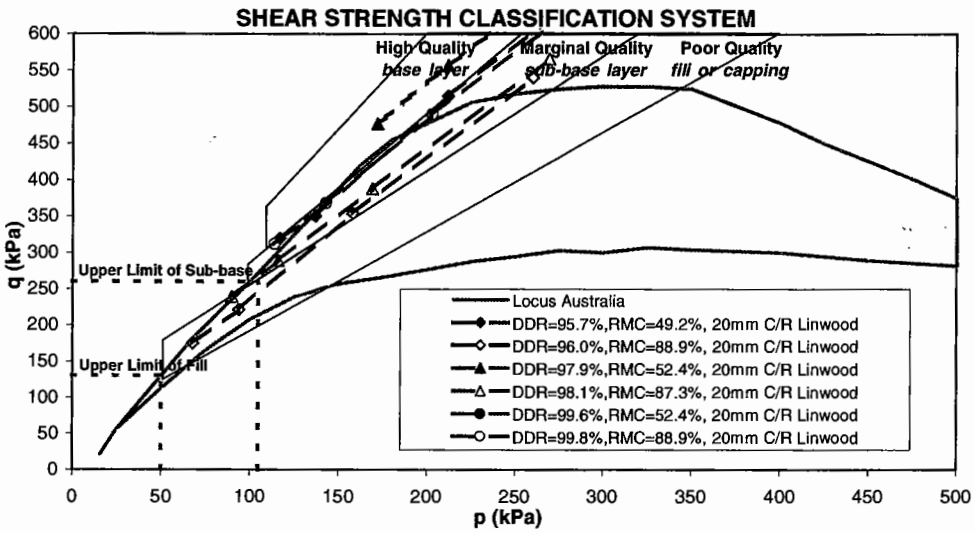

FIGURE A6.3: SHEAR STRENGTH, 20MM C/R LINWOOD MATERIAL

A6.1.4 Stonyfell

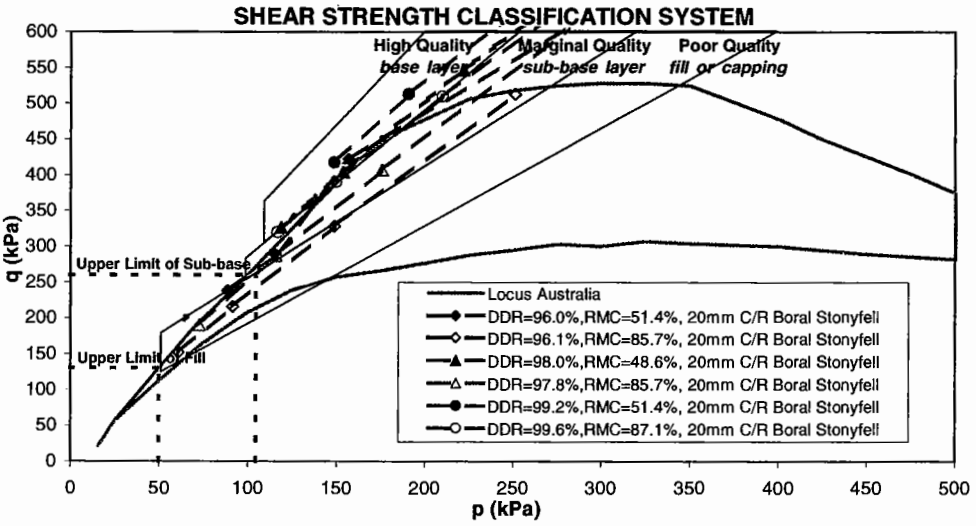

FIGURE A6.4: SHEAR STRENGTH, 20MM C/R STONYFELL MATERIAL

Quarry Rubble Materials

A6.1.5 Boral Para Hills

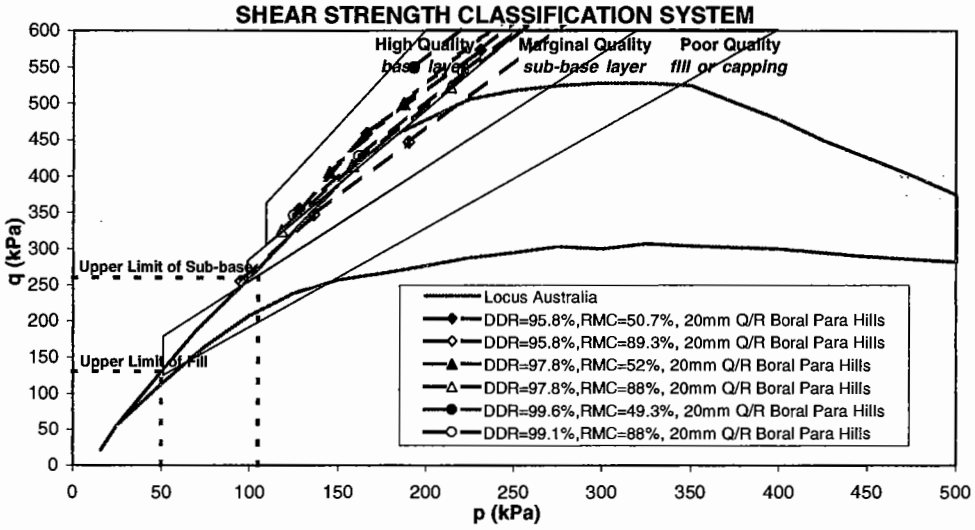

FIGURE A6.5: SHEAR STRENGTH, 20MM Q/R BORAL PARA HILLS MATERIAL

A6.1.6 Boral Lobethal

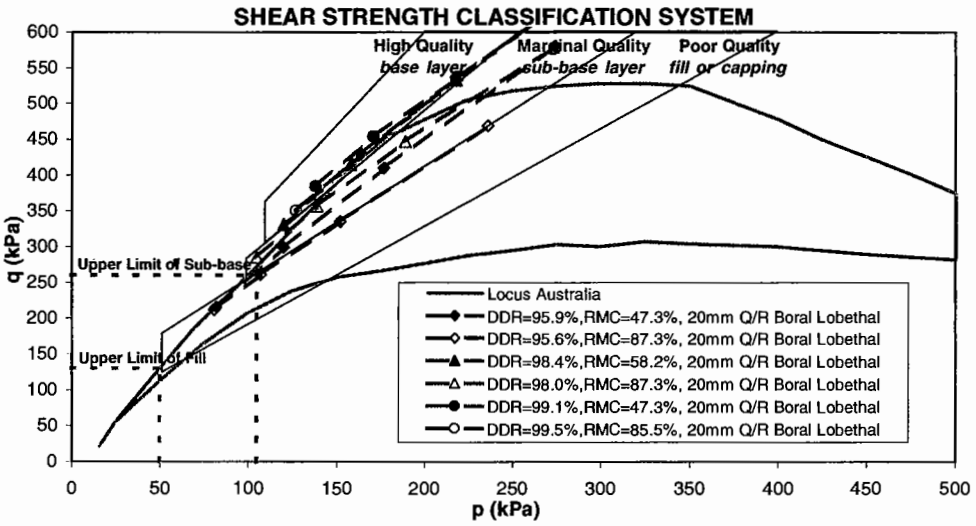

FIGURE A6.6: SHEAR STRENGTH, 20MM Q/R BORAL LOBETHAL MATERIAL

A6.2 Permanent Strain Rate

Crushed Rock Quarry Materials

A6.2.1 Boral Para Hills

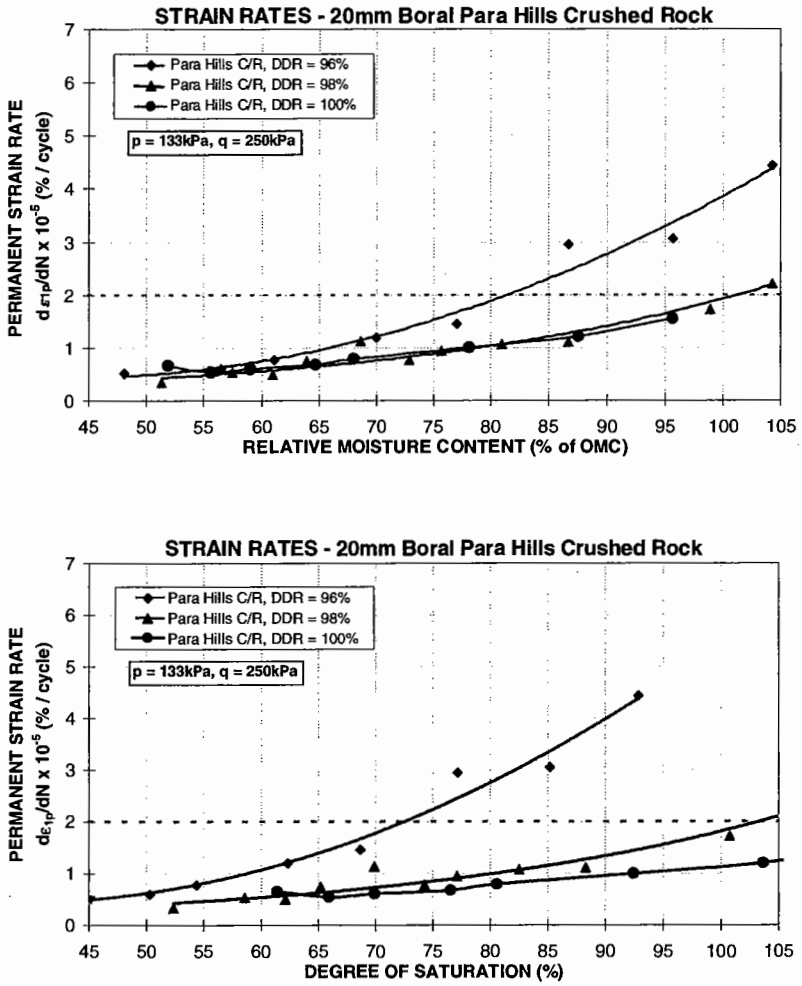

FIGURE A6.7A & B: PERMANENT STRAIN RATE, 20MM C/R BORAL PARA HILLS MATERIAL

A6.2.2 Boral Lobethal

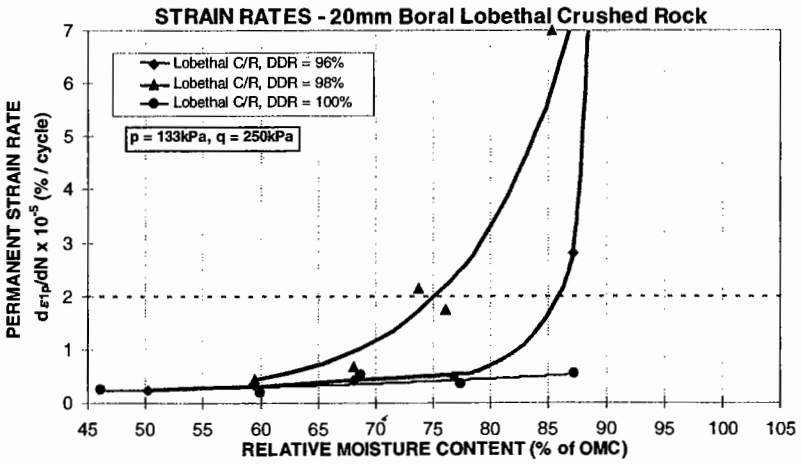

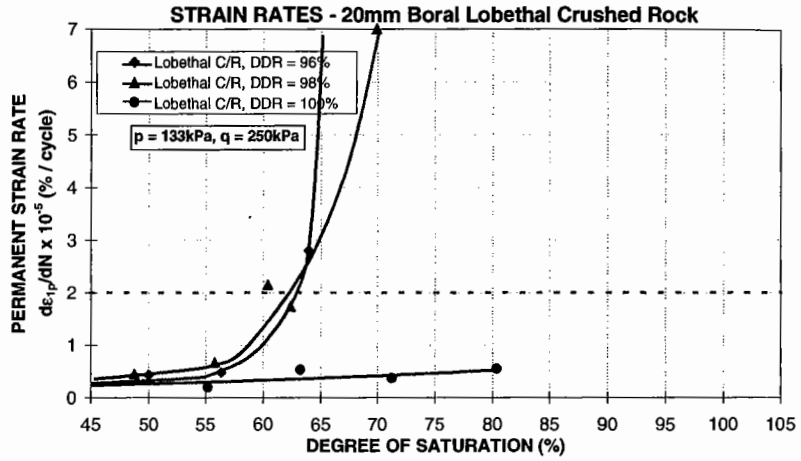

FIGURE A6.8 A & B: PERMANENT STRAIN RATE, 20MM C/R BORAL LOBETHAL MATERIAL

A6.2.3 Linwood

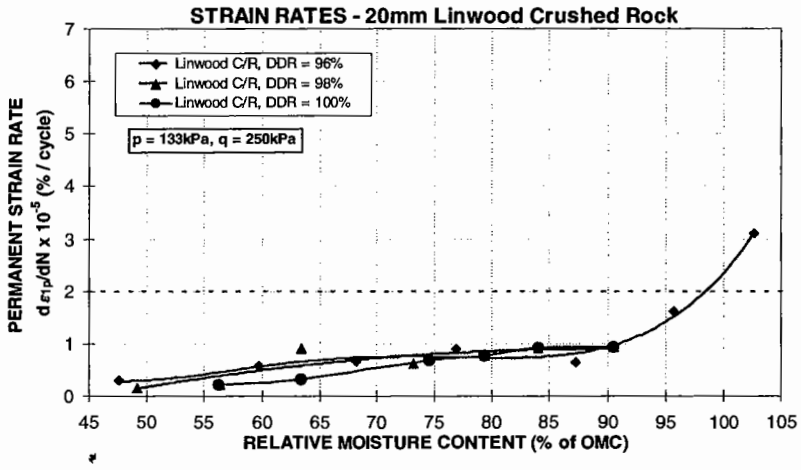

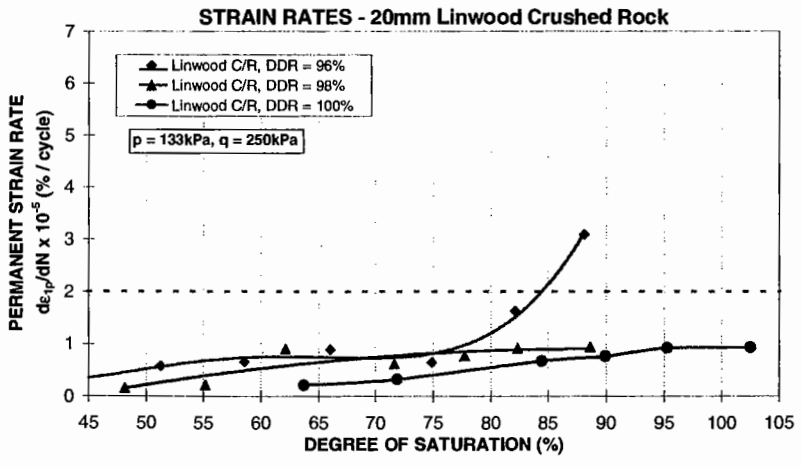

FIGURE A6.9 A & B: PERMANENT STRAIN RATE, 20MM C/R LINWOOD MATERIAL

A6.2.4 Stonyfell

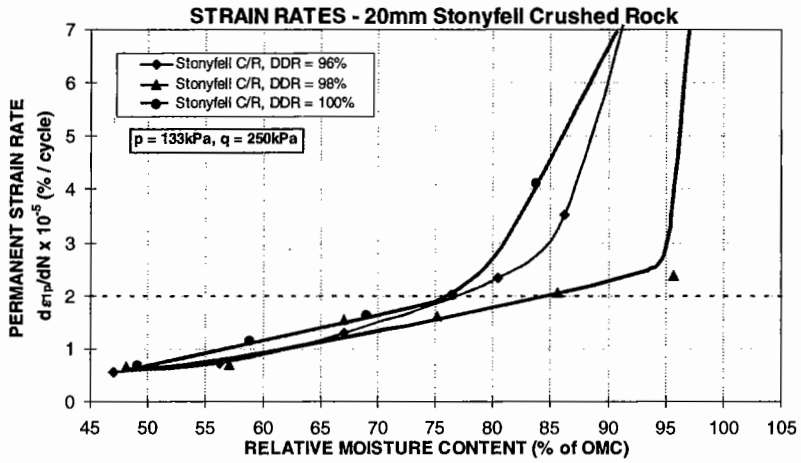

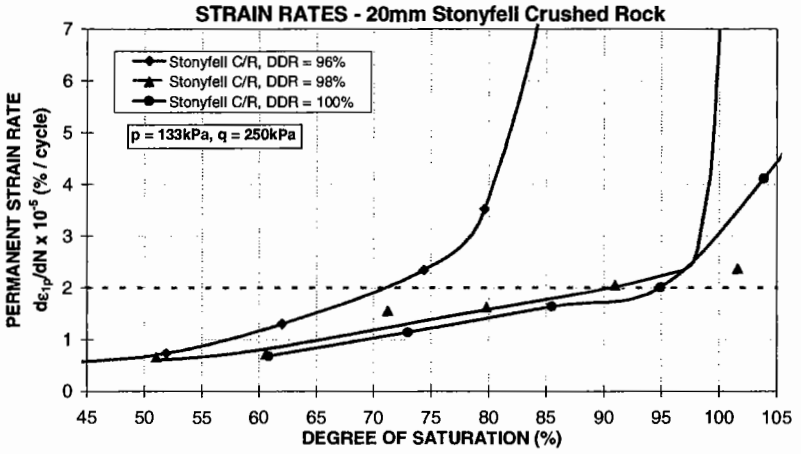

FIGURE A6.10 A & B: PERMANENT STRAIN RATE, 20MM C/R STONYFELL MATERIAL

Quarry Rubble Materials

A6.2.5 Boral Para Hills

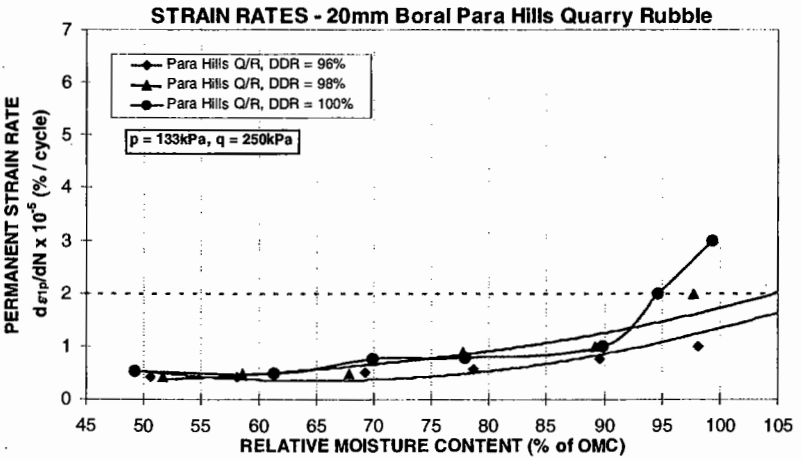

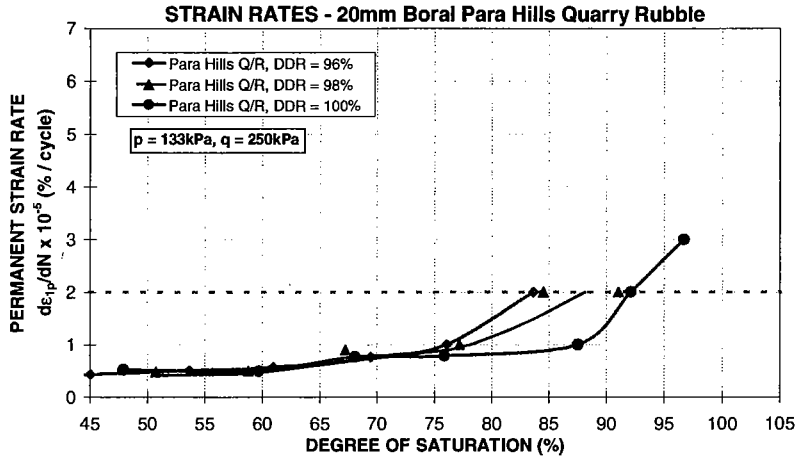

FIGURE A6.11 A & B: PERMANENT STRAIN RATE, 20MM Q/R BORAL PARA HILLS MATERIAL

A6.2.6 Boral Lobethal

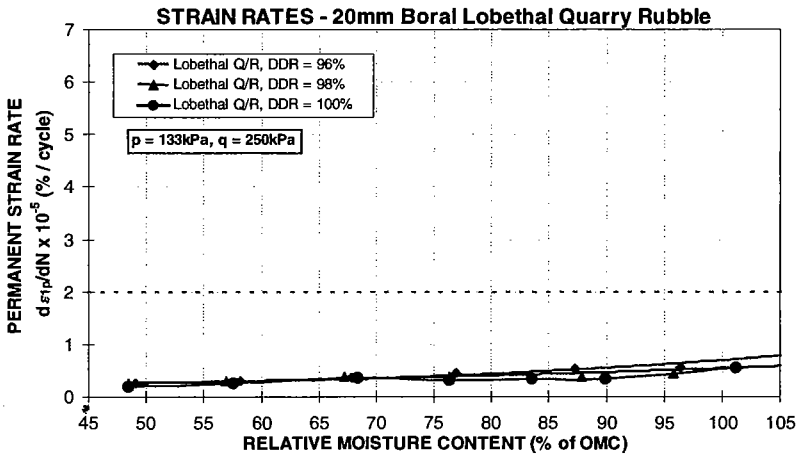

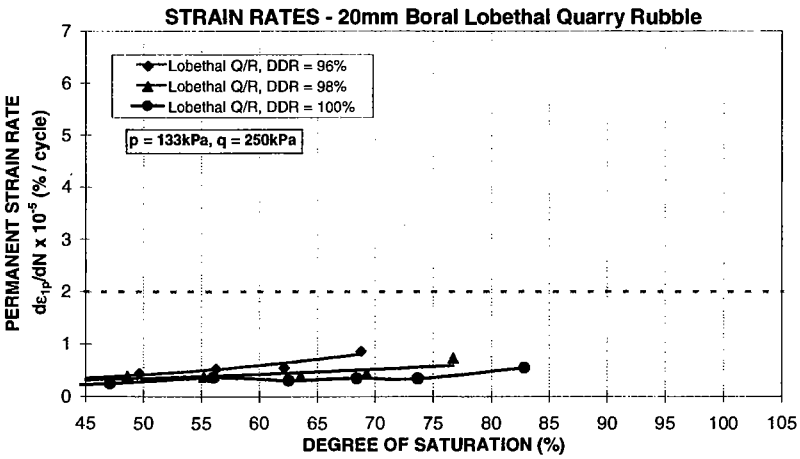

FIGURE A6.12 A & B: PERMANENT STRAIN RATE, 20MM Q/R BORAL LOBETHAL MATERIAL

A6.3 Resilient Modulus

Crushed Rock Quarry Materials

A6.3.1 Boral Para Hills

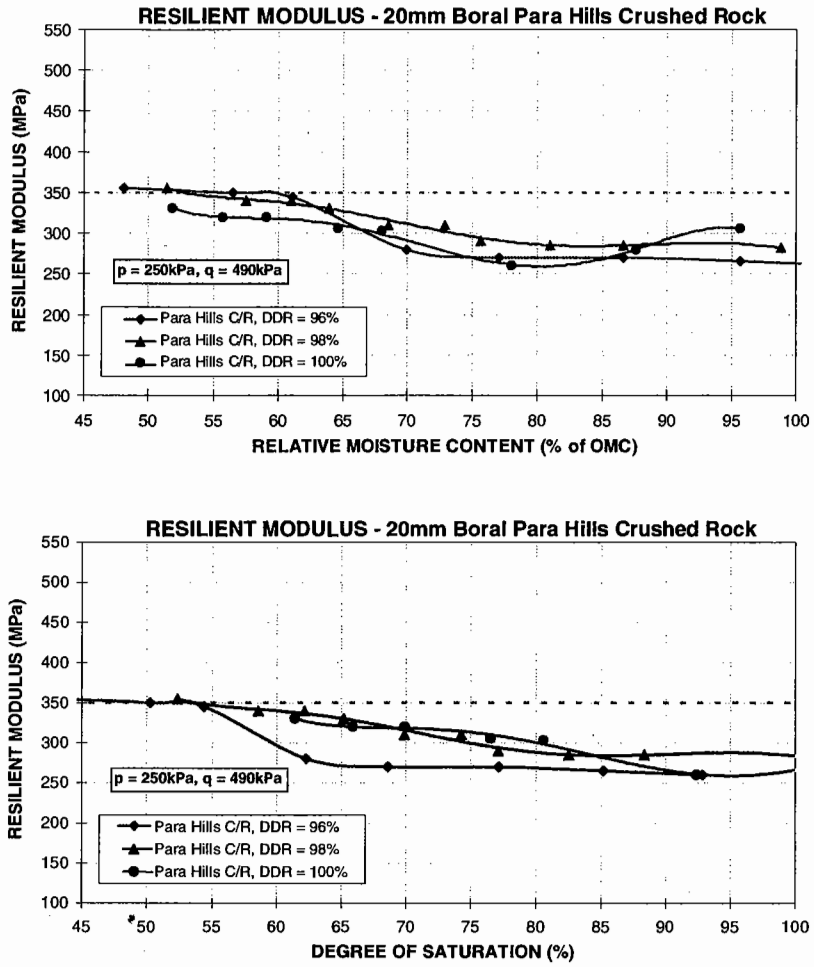

FIGURE A6.13 A & B: RESILIENT MODULUS, 20MM C/R BORAL PARA HILLS MATERIAL

A6.3.2 Boral Lobethal

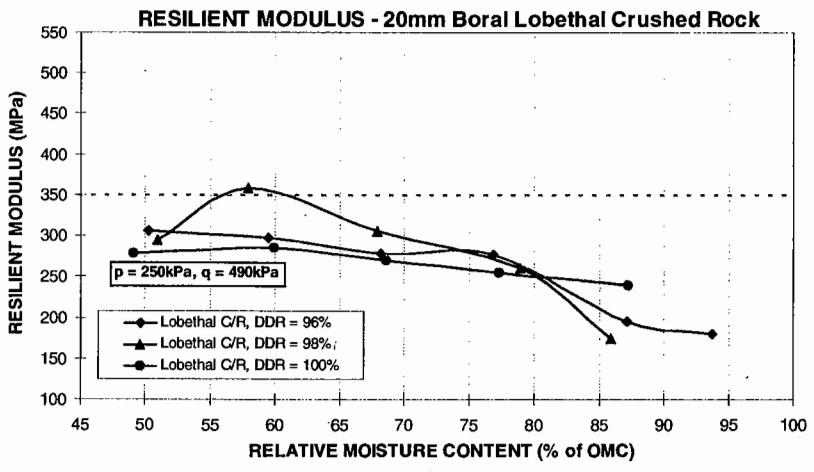

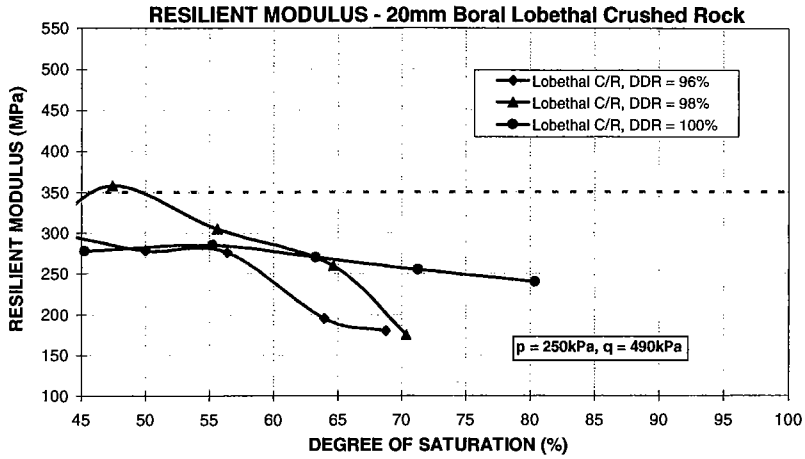

FIGURE A6.14 A & B: RESILIENT MODULUS, 20MM C/R BORAL LOBETHAL MATERIAL

A6.3.3 Linwood

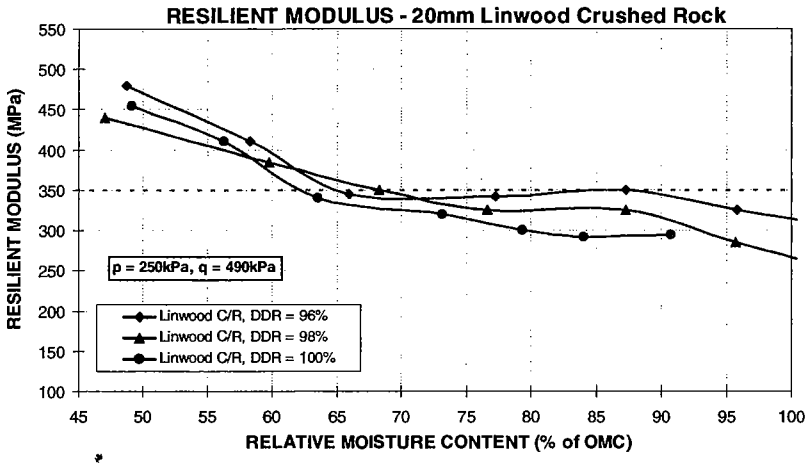

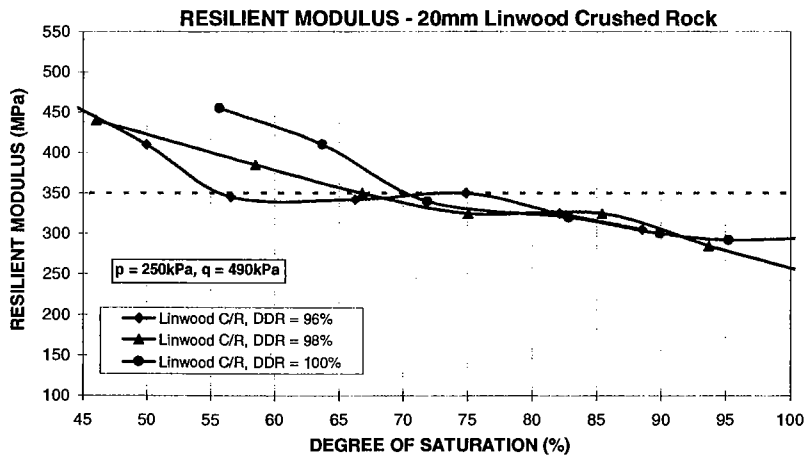

FIGURE A6.15 A & B: RESILIENT MODULUS, 20MM C/R LINWOOD MATERIAL

A6.3.4 Stonyfell

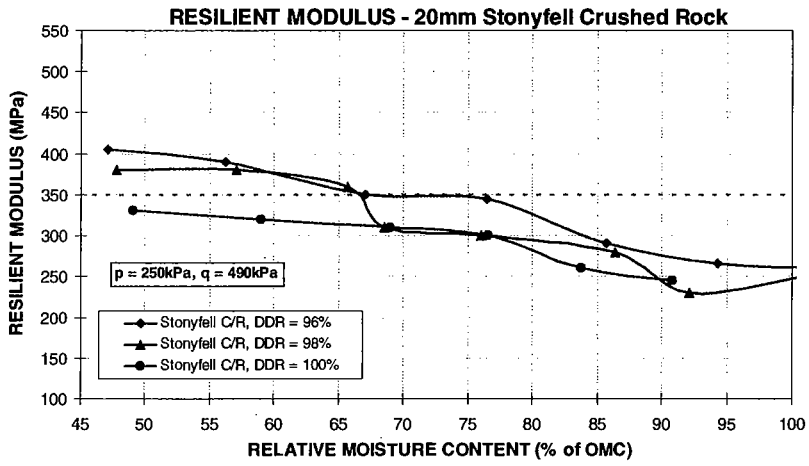

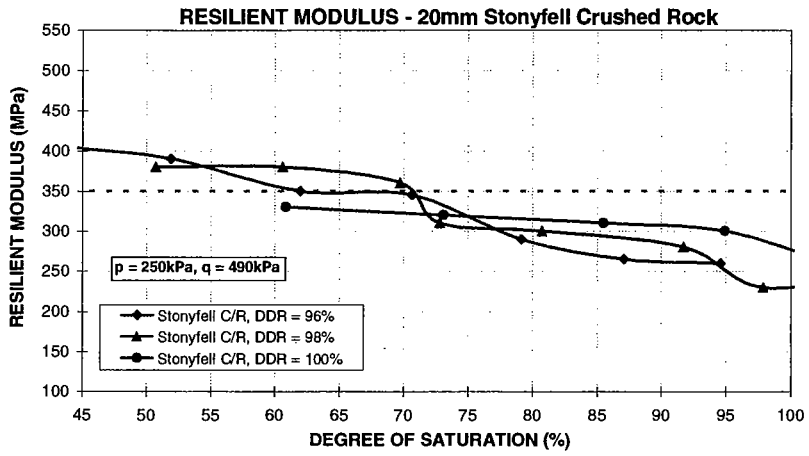

FIGURE A6.16 A & B: RESILIENT MODULUS, 20MM C/R STONYFELL MATERIAL

Quarry Rubble Materials

A6.3.5 Boral Para Hills

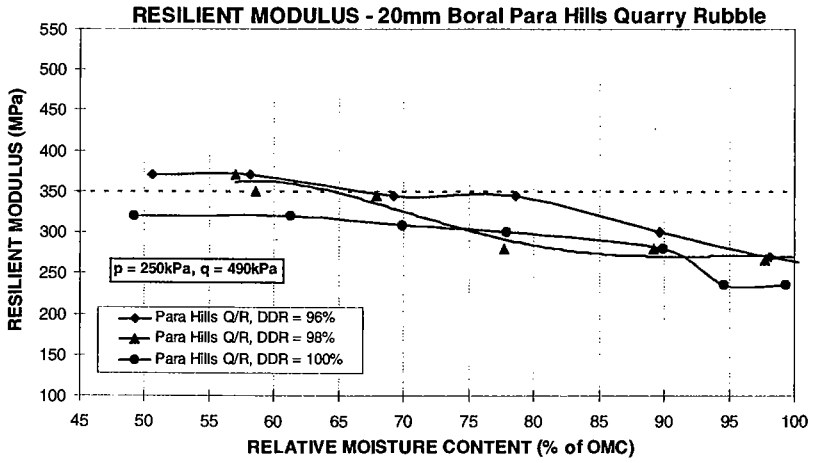

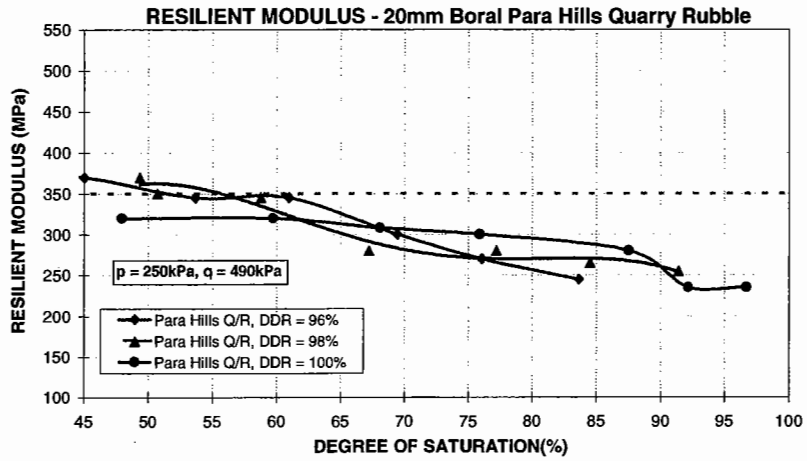

FIGURE A6.17 A & B: RESILIENT MODULUS, 20MM Q/R BORAL PARA HILLS MATERIAL

A6.3.6 Boral Lobethal

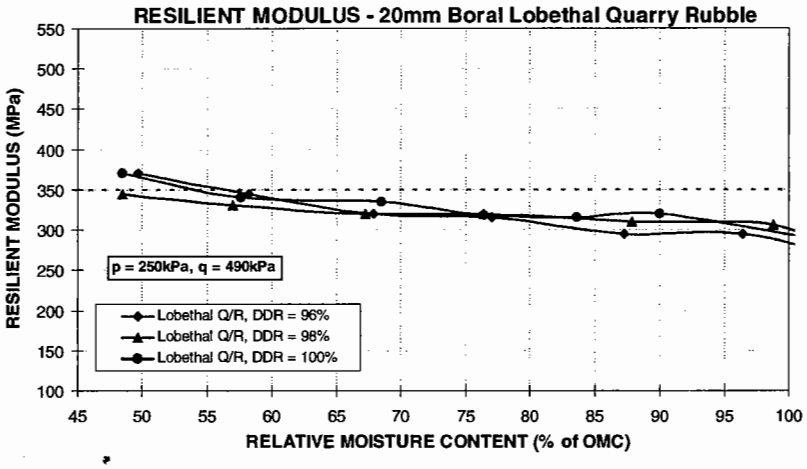

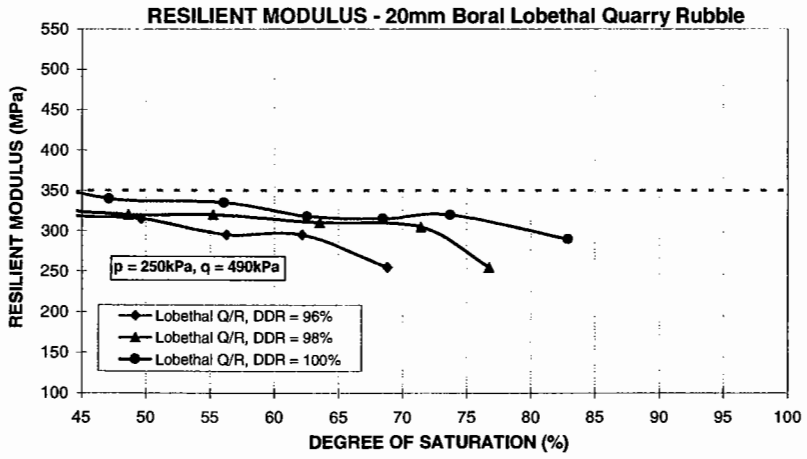

FIGURE A6.18 A & B: RESILIENT MODULUS, 20MM Q/R BORAL LOBETHAL MATERIAL

APPENDIX 7

A7.1 Solomon Crushing Contract (South Australia)

A7.1.1 History

In 1993, Transport SA established a material crushing contract at Solomon to supply material to a road construction project for a section of the Eyre Highway from Kimba (RRD 774km) to 20km west (RRD 794km). The material was intended for use as a basecourse layer of a 150mm granular overlay of an existing flexible granular pavement, founded on a moderate strength subgrade. A bituminous spray seal surfacing was used to seal the overlay.

The pavement is reported to be still performing well. In areas where the subgrade strength was low, the material was stabilised with 4% cement and laid. In these stabilised areas, poor compaction and layers of inadequate thickness has yielded poor performance.

The product, a 20mm granitic crushed rock won from an 'open pit', with materials extracted from different areas of the pits given different 'Lot' numbers. The material was required to meet the "Standard Specification for Supply and Delivery of Pavement Material" (Transport SA, 1997). The specification required the empirically based test, Los Angeles Abrasion, to meet an upper limit of 30%. Given that this material was unable to meet this limit, the specification was modified to 35%. At one stage well into the product process, the material reached a value of 45% which required further evaluation of the suitability or otherwise of the 'altered' non-conforming product.

The material with a Los Angeles Abrasion value of 35% (LA35%) was used as the granular overlay. This product seemed to be of marginal quality as determined by the testing conducted (see §A7.1.4), requiring 'dry-back' to at least 60% of OMC prior to spray sealing to ensure satisfactory performance. The study undertaken (Andrews and Mundy, 1993) aimed to determine the difference in the mechanical performance of the two products using specialised testing.

A7.1.2 Design Requirements

The design traffic loading in 1993 gave an AADT of approximately 650 vehicles / day with 40% commercial vehicles. Two classification counts, one positioned just east of the town of Kimba and one well east of the town of Kyancutta provides the following traffic data for the constructed section lying within:

East of Kimba (20/1/99)	AADT = 662, CV = 28.5%
East of Kyancutta (15/10/97)	AADT = 624, CV = 33.8%

From this and other traffic counting sites along this section of the Eyre Highway, a consistent volume of 650 vehicles / day and 32% commercial vehicles with little or no growth over the past six years, was evident. The predicted ten-year design traffic loading of ESAs, N_{10}, was:

$$N_{10} = 3.6 \times 10^6$$

A7.1.3 Field Assessment

A visual assessment of the pavement's surface reveals that the pavement is performing well with the LA35% material as a basecourse layer. The climate conditions at this site greatly assist in low moisture states within the granular layer, which in turn "maximises" performance. It is anticipated that in-service equilibrium moisture condition would be a value of approximately 50% of OMC.

A7.1.4 Materials Testing

The unbound granular material is a 20mm crushed rock. Modified Proctor compaction testing provided the following results for the Lot 199 material:

$$OMC = 6.5\%, MDD = 2160 kg/m^3$$

Repeated Load Triaxial Testing

To fully exploit the differences in product performance when used as a pavement basecourse layer at DDR = 98%, three levels of moisture content were tested for, namely 45, 70 and 90% of OMC. Samples were statically compacted to minimise particle breakdown and provide uniform test specimens.

The materials were preconditioned at $\sigma_{1\ max}$ = 300kPa and σ_3 = 50kPa, the combination used for comparing many different materials' plastic strain characteristics in South Australia. The strain rate variations of the two products are shown in Figure A7.1.

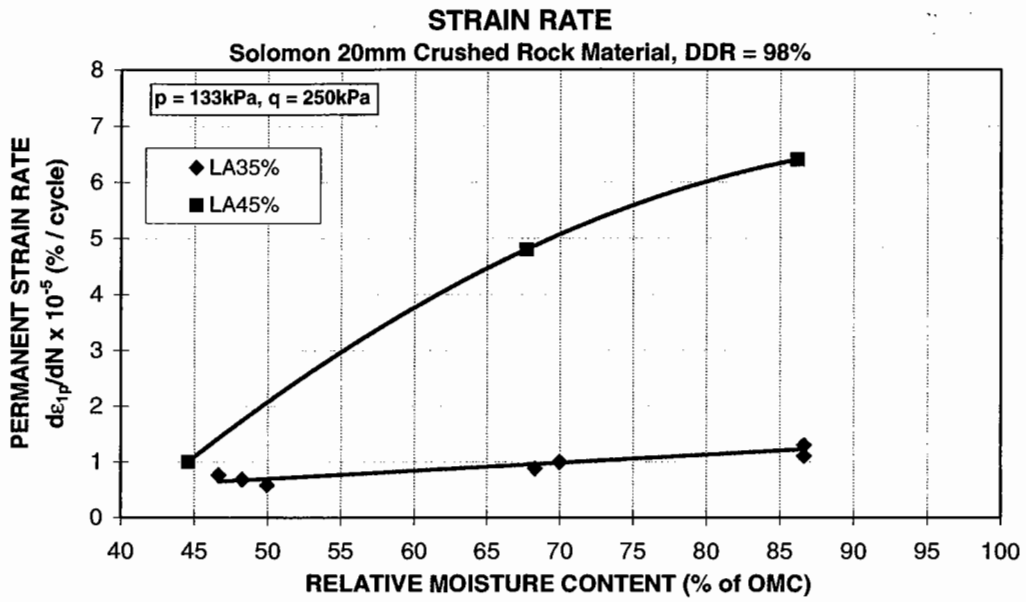

FIGURE A7.1: STRAIN RATE VARIATION FOR THE SOLOMON MATERIALS

The results show the much more rapid increase in strain development for the LA45% material, with a marked sensitivity to moisture. It is expected that this material would undergo considerable rutting if used as the upper basecourse layer at a high moisture condition. The LA35% material is considered to exhibit acceptable resistance to permanent strain or rutting, as can be seen by the low strain rate levels found from repeated load triaxial testing. Thus, this material has a low sensitivity to moisture content.

To compare resilient modulus, a stress condition of $\sigma_{1\ max}$ = 577kPa and σ_3 = 87kPa was used, as discussed in §8.5. It should be noted that a substantial reduction in resilient modulus is apparent for the "softer" LA45% material, which exhibits only very slightly increased moisture sensitivity compared to the LA35% rock. The LA35% material produces an acceptable level of resilient modulus at low moisture levels around 50% of OMC (refer to Figure A7.2).

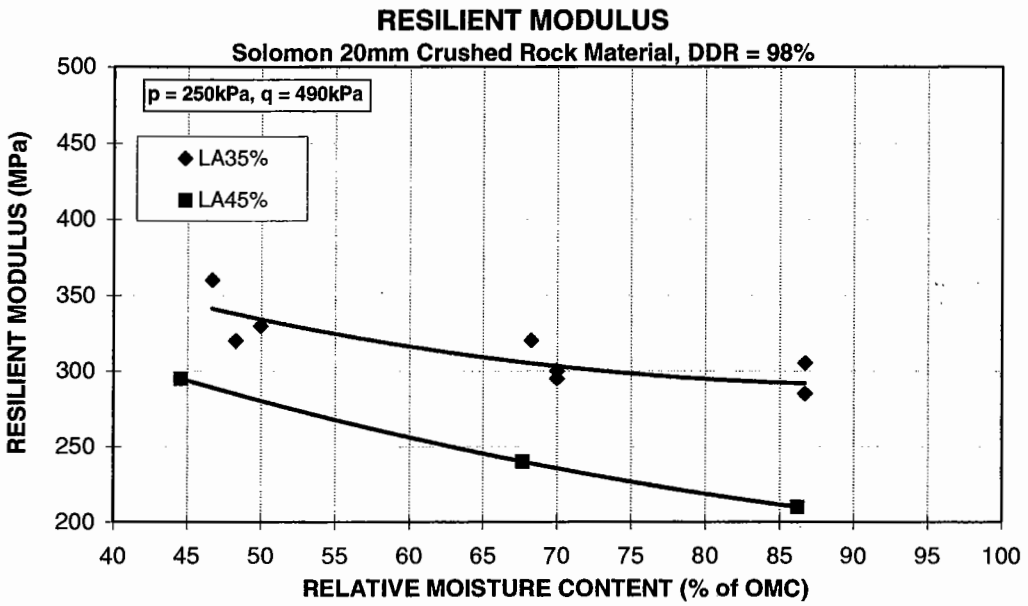

FIGURE A7.2: RESILIENT MODULUS VARIATION FOR THE SOLOMON MATERIALS

Due to the significant reduction in the performance of the LA45% product, determined through two key MPIs of strain rate and resilient modulus, the product was rejected for use as a basecourse layer material. It was however, used as a shoulder material.

A7.1.5 Summary

The Solomon crushed rock material, like the Lobethal material used in the Gawler Bypass Stage II pavement, was found to be highly variable in its permanent strain and resilient modulus properties. The only empirical test which differentiated the two different quality Solomon materials was the Los Angeles abrasion test. Whilst this test illustrated product variation in this case, it has been found to fail to do so in other instances. Quality control testing needs to involve performance-based testing to be sure to uncover any significant deficiencies in the consistency of the material during its production.

APPENDIX 8

Index of Spreadsheets

Austroads –	design Curvature and ESA data
CEN stress levels –	stress levels used for stress loci and RLT test procedures for CEN, TSA, Austroads, AWGRU, SHRP/AASHTO; newly proposed stress levels (Chapter 5, Appendix 3, Appendix 4)
Compact –	compaction stresses, Barksdale experiment (Chapter 4, Appendix 2)
Courage Results –	data and graphs for the materials testing for the EC COURAGE research project (Chapter 2)
Courage TXL –	COURAGE research project material failure envelopes (Chapter 5 and 6)
French -	Minimum required thickness of wearing course (Chapter 3)
Herner -	Vertical stress results from paper by Herner (Chapter 4)
Kings Rd -	Static triaxial test results for Kings Road pavement failure case study (Chapter 9)
King1-3 -	new RLT stress sequence test results (Chapter 7)
Lateral stress -	corrected lateral stresses data (Chapter 5)
MT79 strain -	vertical compressive strain data and graph for example of granular pavement with a basecourse layer of a low and high moisture content (Chapter 3)
Pave Stresses -	design examples computing stresses and moduli variations with depth into the pavement and stress paths graphed in p/q space (Chapter 5)
Permanent Strain -	permanent strain and modelled permanent strain result from one material preconditioning test (Chapter 2)
PM Spec TSA -	grading of PM32 crushed rock material within upper and lower limit specification envelopes (Chapter 7)
pq Design Charts -	resilient modulus design chart used by TSA plotted in p-q space (Chapter 5)
Seasonal Pave -	vertical compressive strain and stress profiles with depth into the pavement (Appendix 1)

Shear-vol graphs LS - volumetric shear and resilient strains for the limestone material tested under EC COURAGE research project (Chapter 6)

Shear-vol graphs - volumetric shear and resilient strains for the gneiss material tested under EC COURAGE research project (Chapter 6)

Solomon - permanent strain rate and resilient modulus results for the test results for Solomon crushing contract pavement material case study (Appendix 7)

Stats PS - statistical results for Boral Para Hills and Boral Lobethal materials permanent strain RLT testing (Chapter 7)

Stats RM - statistical results for Boral Para Hills and Boral Lobethal materials resilient modulus RLT testing (Chapter 7)

Stressco - vertical stress profiles with depth into pavement for varying subgrade stiffness conditions and lateral stress correction charts for material friction angle and cohesion variations (Chapter 5)

Tas - grading and static triaxial test results for Bass Highway pavement failure case study in Tasmania (Chapter 10)

TSA strain data - permanent strain rate data variation with RMC and degree of saturation for one material (Chapter 2)

TSA triaxial - static triaxial test results for a range of South Australian material products tested (Chapter 8)

Tsa_mats - data and graphs for permanent strain rate and resilient modulus test results for a range of South Australian material products tested (Chapter 8, Appendix 6)

VertLat Stress - vertical and lateral stress interaction under a loaded pavement (Chapter 5)

VT8kuvat - seasonal moisture variation with an unbound granular pavement monitored with TDR probes in Finland (Chapter 2)

WA - laboratory and field data for a number of pavement failure case studies in Western Australia (Chapter 10)